12-2009

Live Load Models for Long Span Bridges

Marta Lutomirska

mwolinska2@unl.edu

LIVE LOAD MODELS
FOR LONG SPAN BRIDGES

by

Marta Lutomirska

A DISSERTATION

Presented to the Faculty of

The Graduate College at the University of Nebraska

In Partial Fulfillment of the Requirements

For the Degree of Doctor of Philosophy

Major: Engineering

Under the Supervision of Professor Andrzej S. Nowak

Lincoln, Nebraska

December, 2009

LIVE LOAD MODELS

FOR LONG SPAN BRIDGES

Marta Lutomirska, PhD

University of Nebraska, 2009

Advisor: Andrzej S. Nowak

In the doctoral dissertation a live load model for long span structures was derived. The live load model is valid for spans between 600 ft and 5000 ft and it is intended to reflect current traffic patterns, quantities of trucks and their weights. The live load models available were developed for short and medium span bridges. Those models were not appropriate for long span bridges due to different types of structure and critical traffic patterns. Live load on long spans depends on traffic mix. One heavily overloaded truck does not have significant influence. Moreover, the continuous increase in the number of the trucks, their weights, and high percentage of overweight trucks led to a search for the newest traffic data. The database includes variety of sites within many different states. A numerical procedure was developed to process the database and simulate traffic jam situations. From the simulation the values of uniformly distributed load were derived. Trucks were kept in actual order, as recorded in the WIM surveys. Results of the simulations were plotted as a cumulative distribution function of uniformly distributed load for considered span lengths. For longer spans, uniformly distributed load decreases and is closer to the mean value. The bias factors were calculated for the heaviest 75-year combination of vehicles. The 75-year uniformly distributed loads were derived from

extrapolated distributions. It was stated that for most of the bridges current live load HL-93 is appropriate. It was also noticed that some bridges, characterized by high ADTT and increased percentage of overloaded loaded vehicles, require special attention and application of increased design live load. The developed live load model is recommended to be taken into consideration in the bridge design code.

DEDICATION

To My Family

ACKNOWLEDGMENTS

I wish to express my deepest gratitude to Professor Andrzej S. Nowak, my academic advisor and chairperson of my dissertation committee, for his support and guidance throughout my graduate study at the University of Nebraska. My appreciations also go to a member of my doctoral committee, Dr. George Morcous, who advised and encouraged me in my study. Special thanks go to Dr. Maria M. Szerszen and Dr. Elizabeth G. Jones, members of my reading committee for their effort and time spent on reviewing my dissertation and offering helpful suggestions.

The Department of Civil Engineering at the University of Nebraska-Lincoln is acknowledged for the study and research opportunities they provided.

I am deeply grateful to my husband, Tomasz, my parents, and whole family for their great support and encouragement.

TABLE OF CONTENTS

LIST OF FIGURES

LIST OF TABLES

CHAPTER 1

INTRODUCTION

1.1. PROBLEM STATEMENT

The live load models available were developed for short and medium span bridges. This doctoral dissertation deals with the development of a live load model for long span structures. The developed live load model is valid for spans between 600 ft and 5000 ft. In contrast to short and medium spans, a long span live load must include the possibility of multiple trucks being present.

The continuous increase in the number of the trucks and their weights led to a review of traffic data for live load. Observing traffic statistics helps to realize the rate of those changes, their importance, and to draw some conclusions regarding design. In the last 30 years, the number of the vehicle miles logged annually on American highways has increased 225%, with heavy truck traffic increasing 550%. Some percentage of trucks runs overweight, particularly if it is to their economic advantage. Therefore, a new live load model for long span bridges had to be developed and it had to be based on the newest traffic data obtained from highway and bridge administrators.

During the AASHTO LRD calibration, the live load model for short and medium span bridges was developed based on a set of truck weight and load effect statistics that were presumed to be valid for any typical bridge site in the U.S. The live load model may not represent the actual loading conditions at a particular bridge site or bridges in a state. Nowadays, several states are using Weigh-In-Motion (WIM) systems to collect vast

1

amounts of truck weight and traffic data that can be used to obtain site-specific and state-specific live load models for bridge design and load capacity evaluation. This could allow individual states to adjust the AASHTO live load factors to take into consideration the particular truck traffic conditions throughout a state, a region, or for a particular route. Site-specific or state-specific live load models may be developed based on actual truck weight and traffic data collected at the site or within the state. Traffic varies for different sites within each state. As a result, site specific models depending on average daily truck traffic and participation of heavily loaded vehicles seem to be more practical.

Since early publications by the American Association of State Highway Officials (AASHO), live load was modeled as an HS20 truck. As an addition to truck load, the uniformly distributed load of 0.64 kip/ft was introduced in 1944. Since then the original definition of HS-20 has been changed. The concentrated load was substituted with three axial forces representing a truck. In contrast, the uniformly distributed load has never been updated. It is still used in the current AASHTO LRFD Code as it was in 1944. The derivation of uniformly distributed load is not clear. To amend this, a new approach to model uniformly distributed load had to be developed and new value of uniformly distributed load had to be proposed. Current multilane reduction factors and dynamic allowance also may not be appropriate for long span bridges. Review of those topics was necessary.

1.2. OBJECTIVE AND BENEFITS OF THE STUDY

The objective in this study was to develop a live load model for long span bridges. The model is valid for spans between 600 ft and 5000 ft. It is intended to reflect current traffic patterns, quantities of trucks and their weights. The newest available traffic database from a variety of sites within many different states is used. Based on the analysis of traffic records (weigh-in-motion and videos) the design live load is developed and recommended to be taken into consideration in the bridge design code. Reliability analysis is used to verify the developed live load model.

In accordance with the stated objective, the first stage was to study previous research and current international codes' provisions on the topic. The second stage of the

research was the collection of state of the art traffic data from highway and bridge administrators. The data obtained had to be analyzed and filtered out from erroneous readings of measurement instruments. Then a new uniformly distributed load was derived. The value of the new live load is based on three models: an average 5-axle truck, legal load trucks and simulation of a traffic jam using WIM data. Such an extensive actual weigh in motion database has never been used in the derivation of live load for long span bridges. Most of the previous studies were based on measurements from limited numbers of sites within one state. The magnitude of the database obtained for the scope of this research has to be underlined. A derivation of uniformly distributed load from WIM data required developing a numerical procedure of calculation to process the extensive database. Cumulative distribution functions were plotted for all data, as well as for maximum daily and maximum weekly uniformly distributed load. New uniformly distributed load was proposed. Statistical parameters for live load (bias and coefficient of variation) are derived. Relationship between site characteristics (ADTT, percentage of overloaded loaded vehicles) and calculated values of uniformly distributed loads were studied. The problems of multilane reduction factors and the dynamic factor were also discussed.

The final step of this dissertation was reliability analysis. Reliability analysis was performed in order to assess how the increase in live load influences reliability indexes. An exemplary suspension bridge, the bridge component and a limit state function that are the most influenced by live load were selected. The calculations were performed for the current AASHTO LRFD design live load and increased load values obtained from real traffic data. For the scope of this study, new statistical parameters for uniformly distributed load were used and statistical parameters of resistance were derived based on the newest material, fabrication and professional factors.

The outcome of this research is the recommendation of a live load model for long span bridges. There is a recommended value of uniformly distributed load for bridges carrying low and average ADTT. In addition, there is a recommendation for an increase of the live load model for the long span bridges in heavily loaded urban and industrial areas.

3

1.3. ORGANIZATION OF THE DISSERTATION

Chapter 1 of this dissertation is an introduction to the research conducted. It presents a problem statement, objectives and the scope of the study, as well as the benefits and limitations of this research. The chapter also includes a review of prior research on the topic.

Chapter 2 reviews current international bridge design codes regarding live load, dynamic load and multiple presence factors provisions. Uniformly distributed load for wide range of spans is calculated and compared.

Chapter 3 presents the principals of the reliability theory that were applied in this study. Definitions of standard variables, probability distributions, limit state functions and reliability index are introduced. Methods of use of the normal probability paper and simulation techniques are described.

Chapter 4 describes the study of traffic data, regulations of truck types, truck sizes and weight limits, as well as the weight-in-motion technology and database to be used in this dissertation.

Chapter 5 describes development of the live load model. A model based on an average 5-axle truck, a model based on legal load trucks, and a model based on traffic jam simulation using WIM data are presented. New values of uniformly distributed load are derived and proposed to be applied in the code. New statistical parameters for live load are calculated.

In the Chapter 6, the problem of the presence of multiple trucks on a bridge is discussed. A short review of current studies, analysis of video recordings of traffic jam situations, and discussion on different approaches to the problem are presented.

Chapter 7 presents the problem of dynamic factor. Parameters affecting bridge dynamic response are discussed. Exemplary bridge-vehicle interaction is modeled and the dynamic factor is derived.

In the Chapter 8, the reliability procedures for a long span bridge are developed. The analysis is performed on a bridge tower of the selected suspension bridge. Reliability indexes for bridge loaded increasing values of live load are calculated.

Chapter 9 presents the summary and conclusions of research performed for the scope of this dissertation. As well, recommendations are specified.

1.4. PRIOR INVESTIGATIONS

1.4.1. Prior Investigations on Live Loading on Short and Medium Span Bridges

Live load models for short and medium span bridges were of interest to many researchers. Most of the studies performed on live load models were based on truck data obtained within programs carried out by the Ontario Ministry of Transportation since the early 1970s. This was the vastest database available until now.

Nowak and Hong (1991) formulated a procedure to calculate maximum moments and shears for various time periods. The maximum load effects for various time periods from one day to 75 years were derived from extrapolated distributions. Single and two lane bridges are considered. For one lane traffic a single truck governs for shorter spans, and two following trucks govern for longer spans. For two lanes of traffic, the maximum effect is obtained for two trucks with fully correlated weights, travelling side-by-side. It has also been concluded that the bias factor (ratio of the mean to nominal value) is larger for smaller spans.

Kim, Sokolik, and Nowak (1997) studied actual truck loads on selected bridges in the Detroit area. The measurements were taken by using a weight in motion system. It was observed that truck loads are strongly site specific. The observed truck weights were often heavier than legal limits. The maximum observed truck weights were up to 250 kips, causing maximum moments two times larger than AASHTO load and resistance factor design values. Gindy and Nassif (2006) formulated a similar conclusion based on data from New Jersey. It was found out that maximum gross vehicle weight reaches a value of 225 kips and it shows a steady increase at an annual growth rate is 1.2%.

Nowak, Laman, and Nassif (1994) published a research report on the effect of truck loading on bridges. The WIM measurements were taken on seven bridges in Michigan. The researchers developed procedures for evaluation of live load spectra on steel girder bridges with regard to fatigue. The deteriorating capacity of bridge was

evaluated as a function of the rate of corrosion. It has been proved that WIM measurements show the unbiased truck weights, which are 30-50 percent larger than extreme values obtained at weight stations. The WIM data is unbiased because the drivers are not aware of the measurements and they do not make an effort to avoid the scales. The WIM measurements from Michigan have also been used to study dynamic load, Nassif and Nowak (1995). It was found out that the dynamic load factor decreases with increased static loads, and that larger values of DLF are observed in exterior girders due to relatively smaller static load effect. Derivation of the dynamic load model is described by Hwang and Nowak (1991).

1.4.2. Prior Investigations on Live Loading on Long Span Bridges

The most widely known researcher in the field of live loading on long span brides is Peter G. Buckland (1978, 1980, and 1991). He concluded that traffic loading on long span bridges can be accurately represented in the traditional manner, by one set of uniform and concentrated loads. One of his findings was that uniform load per foot reduces as the load length is increased. However, unlike many other studies he found out that concentrated load increases as the loaded length increases. Four uniform loading curves were developed for different loading cases. The load cases were distinguished depending on the percentage of "heavy vehicles": 2.4, 7.4, 30.0, or 100 percent, where "heavy vehicles" are defined as trucks and buses over 12000 lb. These loading curves were recommended by the ASCE Committee as vehicle loading of long-span bridges, in 1981. They are known unofficially as the ASCE Loading. However, they have never been applied into the design codes.

Peter G. Buckland had also made a valuable observation regarding several loaded lanes. He stated that if a single lane has a certain load on it, than the additional lanes would increase the load in the lane closer to the curb, as trucks gravitate towards it. However, load in the additional lanes can be reduced.

In the paper by Buckland (1991) the comparison of North American and British live loads on long-span bridges is presented. The loads are compared as equivalent uniformly distributed loads, calculated as an equivalent shear and bending moment for

6

simply supported beams. This approach can be successfully used for short and medium span bridges. However, its application to long spans can be questioned, since long span bridges cannot be constructed as simply supported beams. This method of deriving the equivalent load can be used exclusively for comparison of codes.

1.4.3. Prior Investigations on Structural Reliability

The theory of structural reliability have been investigated and described by many researchers. Several books and publications provide available knowledge regarding reliability theory, for instance, Thorf-Christtensen and Baker (1982), Ang and Tang (1984), Madsen, Krenk and Lind (1986); Thorf-Christtensen and Murotsu (1986), Ayyub and McCuen (1997), Murzewski (1989), Nowak and Collins (2000) and Wolinski and Wrobel (2001). The application of reliability theory has resulted in the improvement of structural design in terms of safety, serviceability and durability. However, it was not until the late 70's when safety factors based on load and resistance uncertainties were proposed for introduction into the codes. In the United States, it was the building design code (Galambos and Ravindra 1978, and Ellingwood 1980, 1982), and in Canada, it was the Ontario highway bridge design code (Nowak and Lind 1979). Since then, reliability techniques have been increasingly used in modern design codes. Nowadays many researchers keep working on further development of new methods of structural reliability analysis, among them A.H.-S. Ang, O. Ditlevesen, R.E. Melchers, H. Nielsen- Faber, A.S. Nowak, R. Rackwitz, and P. Thoft-Christiansen.

For many years the random nature of various parameters influencing structural safety has been of interest to engineers. Until they gathered more knowledge about the laws of nature, they used to assure structural safety through 'trial and error' and intuition. Mathematical theories available nowadays describe material and structural behavior sufficiently enough to give a rational basis for structural safety evaluations (Nowak and Collins, 2000). Early publications that quantified and presented a mathematical formulation of structural safety problems were published by Mayer (1926) and Wierzbicki (1936). They recognized that load and resistance parameters have random characteristics, and that each structure has a finite and limited probability of failure. Their

7

concept of a structural reliability problem has been subsequently adopted in the precursory publication for that field by Freudenthal (1956). In the 1960s, a new trend in using probabilistic concepts in the analysis of limit capacity and structural resistance was developed. It was first presented by researchers Augusti and Baratta (1973, 1973). Subsequently, important work was done by Corotis and Nafday (1989) analyzing the limit capacity of beam-column frame structures using the principles of conditional probability.

The extensive development of practical tools and efficient methods for evaluating the probability of structural failure has been made in the last 30 decades. Initially, the probability of failure was defined by multidimensional integral functions of distributions and it was cumbersome to evaluate. Pioneering studies on the first practical application of reliability analysis were performed by Cornell and Lind in the late 1960s and early 1970s. Their approach estimated the limit state function at mean values of random parameters and used a linearized limit state function. A milestone was the estimation of the probability of failure proposed by Hasofer and Lind (1974). The simplified procedure involved a nonlinear mathematical programming problem with boundary conditions (an estimated limit state for all variables and a defined probability in the so called "design point"). The extension of the Hasofer and Lind approach and the transformation of uncorrelated random variables of various distributions into standardized normal distributions were proposed by Rackwitz and Fiessler (1978). The developed numerical procedure of the design point estimation used to be called the Rackwitz-Fiessler procedure. Hohenbichler and Rackwitz (1988) used the Rosenblatt (1952) transformation procedure for the transformation of dependent (correlated) random variables from and into standardized form, which is currently one of the major tools used in modern reliability analysis. Another commonly used transformation is Nataf's transformation, which was presented in work by Kiureghian and Liu (1986). Commonly used methods of reliability analysis are based on the approximation of the limit state function at the design point using first or second order functions (FORM and SORM). Advanced SORM have been elaborated by researchers such as Fiessler, Neumann and Rackwitz (1979), Breitung (1984), Nowak and Collins (2000). Adhikari (2004) systemized and published all of the earlier proposed SORM procedures. Simulation techniques are another approach to

8

estimating probability of failure. The most popular is the Monte Carlo Method simulation technique (Thoft-Christensen and Baker, 1982; Hart, 1982). Determination of the probability of structural failure with the use of simulation techniques has limited accuracy, and a huge number of numerical simulations are required to achieve a high accuracy of results. This method becomes very useful and an especially practical tool in cases where physical testing is expensive.

The structural system reliability is a field of interest for many researchers. Bridges usually consist of a combination of series and parallel systems. Identification of collapse mode and degree of correlation between members is very difficult or often even impossible to evaluate. Moses (1982) proposed incremental load approach and suggested a procedure for identifying collapse mode for both ductile and brittle components. The identification of collapse mode was also discussed by Rashedi and Moses (1988). Reliability models applied to bridge evaluation were addressed by Nowak and Tharmabala (1988). Moses and Verma (1987) used a load and resistance approach to evaluate the strength of bridges with reliability principles. Tantawi (1986) developed a grid nonlinear analysis program to calculate the moment-carrying capacity of a bridge. Than Zhou (1987) developed an integration sampling technique to calculate the system reliability of a bridge. Both Tantawi and Zhou, found that bridge system reliability is higher than girder reliability.

Practical procedures for system reliability analysis were suggested by Nowak and Zhou (1990), Zhou and Nowak (1990), and Tabsh and Nowak (1991). The procedures assumed that the ultimate load carrying capacity is equal to the weight of a truck which causes a collapse. A collapse was defined as an excessive, non-acceptable deflection. Estes and Frangopol (1999) assumed that failure occurs when failure occurs in three of five adjacent girders. Several major contributions were also made by researchers such as Ditlevsen (1982, 1996), Grigoriu (1982, 1983), and Rackwitz (1985). Ditlevsen used conditional probability to calculate bounds of the probability of failure, Grigoriu discussed a parallel system with brittle elements, and Rackwitz recognized the effect of correlation on system performance.

The present requirements for civil engineering structures primarily focus on structural safety. New structural design codes are calibrated using the limit state analysis

9

approach to assure safety standards and to provide the required reliability of new design structures. However, there is a major gap between the development of reliability techniques and their application to structural engineering design and evaluation. The system reliability analysis requires an efficient structural analysis procedure, as the calculations have to be repeated many times. Therefore, a more comprehensive method to assess the system reliability of a bridge needs to be developed.

CHAPTER 2

LIVE LOAD IN CURRENT DESIGN CODES

2.1. INTRODUCTION

While approaching the problem of live load for bridges it is necessary to review the current codes and perform a comparative analysis. The codes were selected with the objective to present various approaches to design live load, use of multilane factors, and dynamic impact allowance.

The live load for bridges can be represented in many ways, including a uniform load and a combination of truck(s), as for example in AASHTO LRFD Bridge Design Specifications (2007), CAN/CSA-S6-00 Canadian Highway Bridge Design Code (2000), and Eurocode 1 (2002). Non-uniform loading curves are used in the British Standard 5400 (2006) and ASCE Recommended Design Loads for Bridges (1981).

The design live loads specified in AASHTO LRFD Code (2007), OHBDC (1991), CAN/CSA-S6-00 [2000], Eurocode [2002], and ASCE (1981) were briefly summarized in the following paragraphs. The comparison of equivalent uniformly distributed loads for a variety of spans is presented in Paragraph 2.5.

11

2.2. INTERNATIONAL PROVISIONS FOR LIVE LOADING

2.2.1. AASHTO LRFD Code [2007]

The American Association of State Highway and Transportation Officials Standard Specifications for Highway Bridges define HL-93 live load as the extreme force effect taken as the larger of following:

1) The AASHTO LRFD 3-axle design truck, and uniformly distributed design lane load of 0.64 klf. Figure 2.1.

2) The AASHTO LRFD Design Tandem, and uniformly distributed design lane load of 0.64 klf. Figure 2.2.

3) For negative moment between points of contraflexure and reaction at interior piers, combination of two design trucks spaced at minimum of 50 ft, and uniformly distributed design lane load of 0.64 klf, should be considered. All of the forces reduced to 90 %. Figure 2.3.
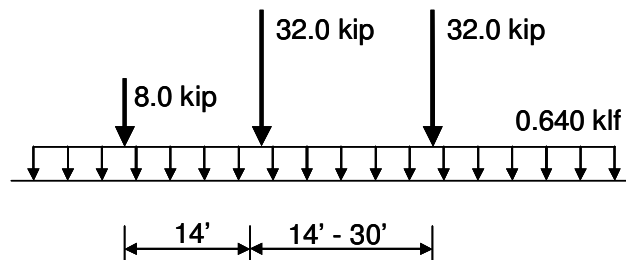
Figure 2.1. HL-93 Live Loading in AASHTO LRFD Code [2007].

Truck and Lane Load.
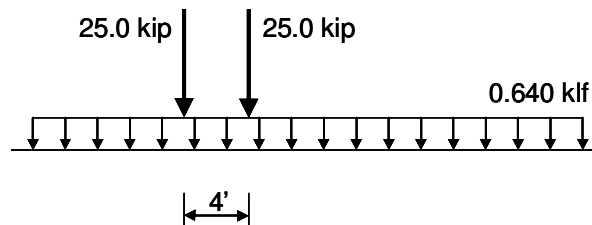
Figure 2.2. HL-93 Live Loading in AASHTO LRFD Code [2007].

Tandem and Lane Load.

12
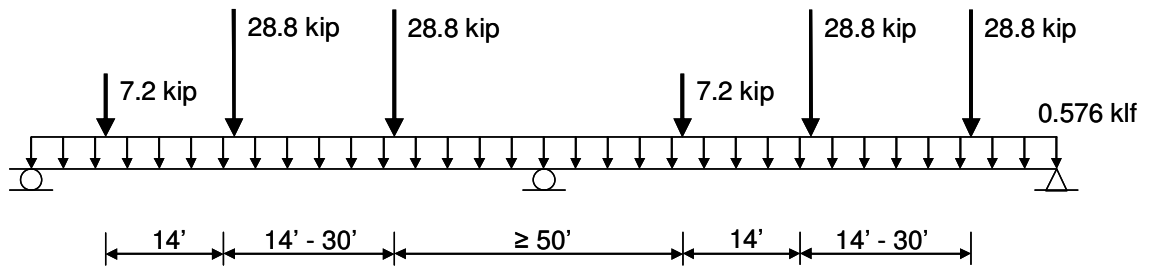
Figure 2.3. HL-93 Live Loading in AASHTO LRFD Code [2007].
Alternative Load for Negative Moment between points of contraflexure
and reaction at interior piers.

The loads shall occupy 10 ft transversally within a design lane. Truck wheels are assumed to be spaced 6.0 ft transversally.

2.2.2. **OHBDC [1991]**

The Ontario Highway Bridge Design Code (Third edition) determines live load as a truck or a combination of truck and lane load, whichever produces the maximum load effect:

1) The OHBD Truck, which is a 5-axle truck. Figure 2.4.
2) The OHBD Lane Load consists of an OHBD Truck with each axle reduced to 70%, and superimposed centrally within the width of a 3.0 m (10 ft) wide uniformly distributed load of 10.0 kN/m (0.685 kip/ft). Figure 2.5.
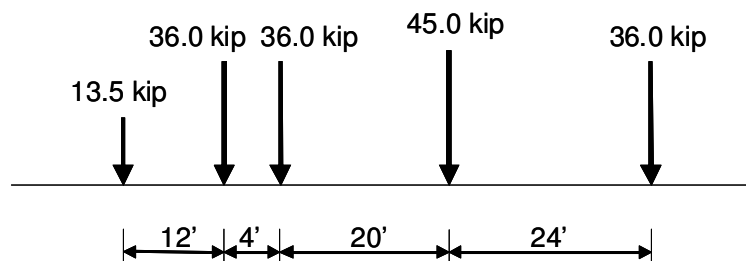
Figure 2.4. OHBD Live Loading [1991]. OHBD Truck.

13
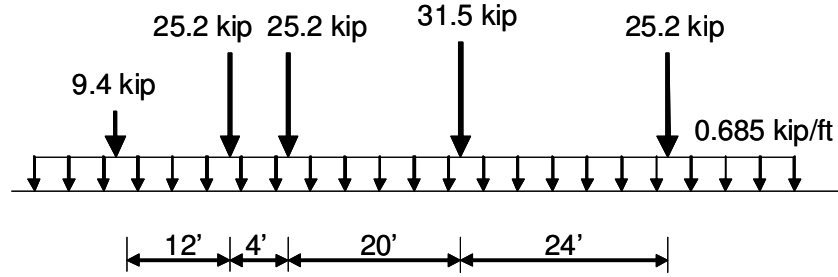
Figure 2.5. OHBD Live Loading [1991]. OHBD Truck and Lane Load.

Table 2.1. Number of design lanes vs. road width in OHBDC [1991]

Width	Number of lanes
Wc ≤ 6.0 m	1
6.0 m < Wc ≤ 10.0 m	2
10.0 m < Wc ≤ 13.5 m	3
13.5 m < Wc ≤ 17.0 m	4
17.0 m < Wc ≤ 20.5 m	5
20.5 m < Wc ≤ 24.0 m	6
24.0 m < Wc ≤ 27.5 m	7
27.5 m < Wc	8

2.2.3. CAN/CSA-S6-00 [2000]

The Canadian Highway Bridge Design Code applies CL-W loading, which consists of the truck or the lane load:

1) The CL-W Truck is 5-axle truck. The number "W" indicates the gross load of the truck in kN. For the design of a national highway network, loading not less than CL-625 shall be used. Figure 2.6.

2) The CL-W Lane Load consists of CL-W Truck with each axle reduced to 80%, and a superimposed uniformly distributed lane load of 9.0 kN/m (0.617 kip/ft), that is 3.0 m (10 ft) wide. Figure 2.7.

14
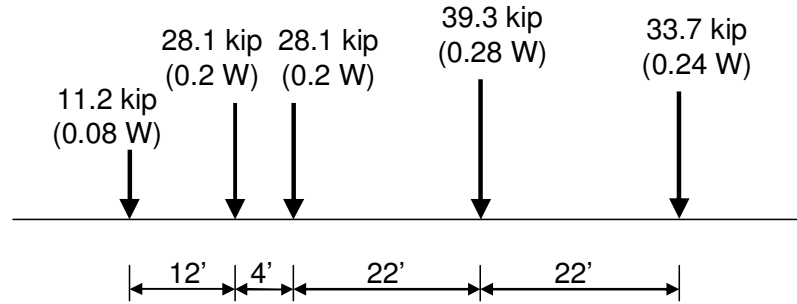
Figure 2.6. CAN/CSA-S6-00 Live Loading [2000]. CL-W Truck
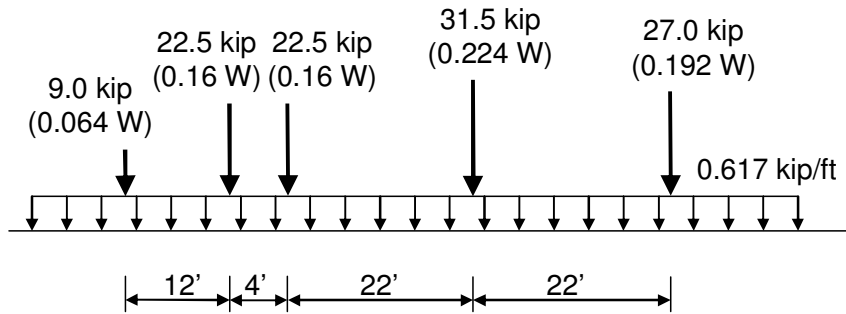
Figure 2.7. CAN/CSA-S6-00 Live Loading [2000]. CL-W Lane Load

Table 2.2. Number of design lanes vs. road width in CAN/CSA-S6-00

Width	Number of lanes
Wc ≤ 6.0 m	1
6.0 m < Wc ≤ 10.0 m	2
10.0 m < Wc ≤ 13.5 m	2 or 3 (check both)
13.5 m < Wc ≤ 17.0 m	4
17.0 m < Wc ≤ 20.5 m	5
20.5 m < Wc ≤ 24.0 m	6
24.0 m < Wc ≤ 27.5 m	7
27.5 m < Wc	8

2.2.4. **BS 5400 [2006]**

According to British Standard the structures and its elements shall be designed to resist the more severe effects of either design HA loading or design HA loading

15

combined with design HB loading. HA loading represents normal traffic in Great Britain. HB loading is an abnormal vehicle unit loading. Both loadings include impact.

HA loading consists of uniformly distributed load (UDL), and a knife edge load (KEL), or a single-wheel load. Live Loading curve HA UDL is shown in the Figure 2.8. Value of nominal uniformly distributed load (UDL) equal to:

- for loaded lengths up to and including 50 m:

$$W = 336 \ (1/L) \ 0.67 \ [kN]$$

- for loaded lengths in excess of 50 m but less than 160 0m:

$$W = 36 \ (1/L) \ 0.1 \ [kN]$$

- for loaded lengths above 1600 m, the UDL shall be in agree with the relevant authority.

The nominal knife edge load (KEL) per lane shall be taken as 120 kN (27 kip). The single nominal wheel load alternative to UDL and KEL is one 100 kN (22.5 kip) wheel placed on a carriageway and uniform distribution over a circular contact area assuming an effective pressure of 1.1 N/mm^2.
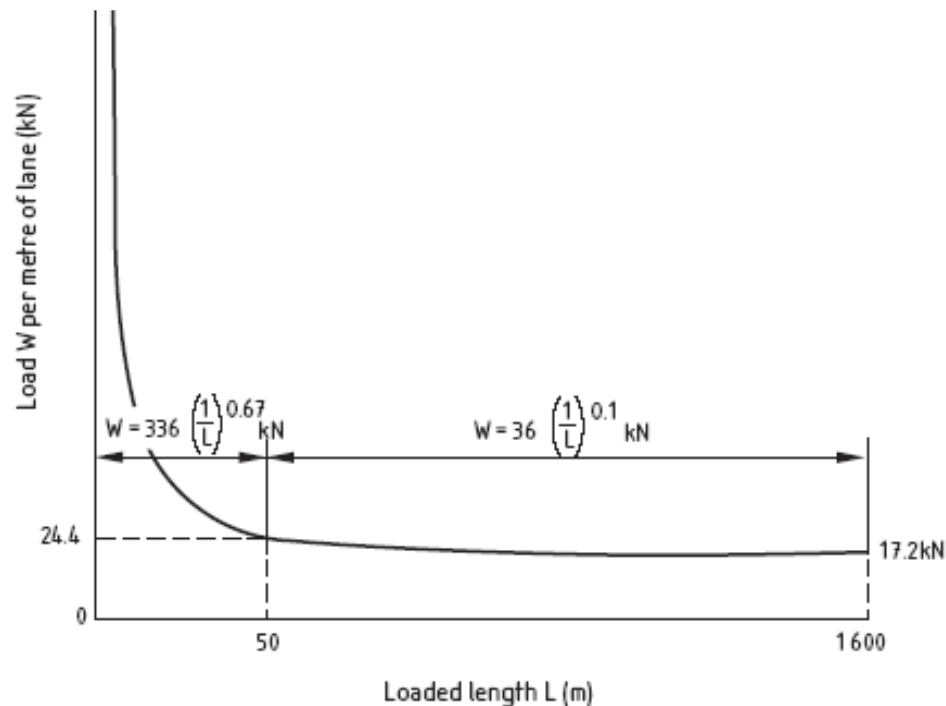
Figure 2.8. BS 5400 Live Loading curve HA UDL [2006]

HB loading defines the minimum number of HB loading units that shall be considered, which is 30. This number may be increased up to 45 if so directed by the relevant authority. Figure 2.9 below shows the plan and axle arrangement for one unit of HB loading. One axle is 10 kN (2.25 kip), i.e. 2.5 kN (0.56 kip) per wheel. The overall length of the HB vehicle shall be taken as 10, 15, 20, 25, or 30 m for inner axle spacing of 6, 11, 16, 21, or 26 m respectively. The effects of the most severe case shall be adopted.
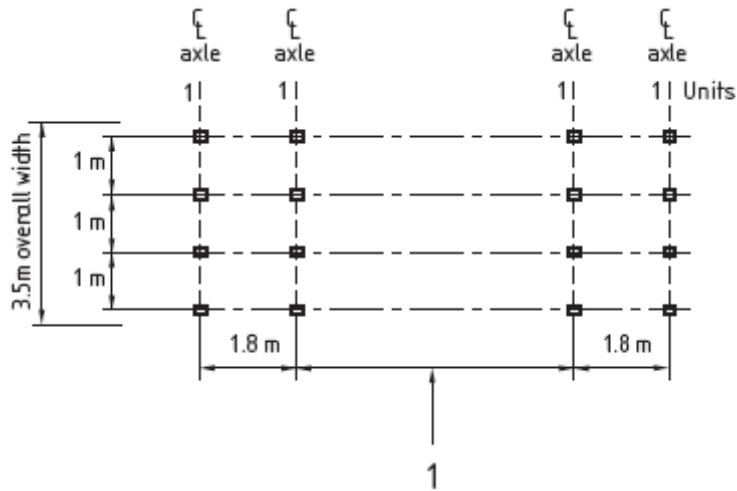
Figure 2.9. Dimensions of HB vehicle.

2.2.5. **Eurocode 1 [2002]**

The Eurocode 1 Part 2 is applicable to bridges with spans from 5 to 200 m (17 to 667 ft), and carriageway width up to 42 m (140 ft). It presents four models for determining the main vertical loads from traffic:

1) Load Model 1 (LM1) consists of concentrated and uniformly distributed loads (Figure 2.10) which cover most of the effects of the traffic of trucks and cars. The code specifies live load to be used on each traffic lane, therefore there is no need to introduce multilane factors. It is used for general and local verifications.

17

Table 2.3. Characteristic values of load for successive road lanes

Location	Axle load Q_{ik}	UDL q_{ik}
Lane number 1	300 kN (67.5 kip)	9 kN/m^2 (0.188 kip/ft^2)
Lane number 2	200 kN (45.0 kip)	2.5 kN/m^2 (0.052 kip/ft^2)
Lane number 3	100 kN (22.5 kip)	2.5 kN/m^2 (0.052 kip/ft^2)
Other lanes	0	2.5 kN/m^2 (0.052 kip/ft^2)
Remaining area	0	2.5 kN/m^2 (0.052 kip/ft^2)
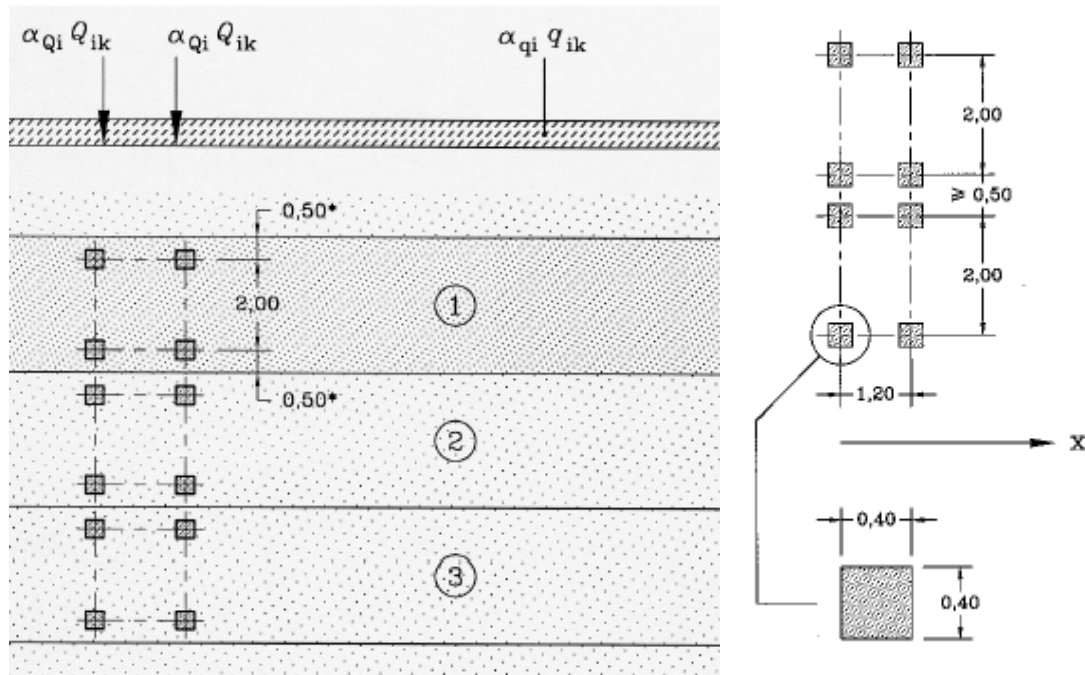
Figure 2.10. Eurocode 1 [2002]. Load Model 1

2) Load Model 2 (LM2) consists of a single axle load of 400 kN, which covers the dynamic effects of the normal traffic on short structural members. The distance between wheels is 2 m. The contact surface of each wheel should be taken as a rectangle of sides 0.35 m and 0.60 m. When relevant, only one wheel of 200 kN may be taken into account.

3) Load Model 3 (LM3) consists of sets of axle loads representing special (carrying heavy loads) vehicles, which can travel on routes permitted for abnormal loads. It is intended for general and local verifications.

18

4) Load Model 4 (LM4) represents crowd loading of 5.0 kN/m². It is intended only for general verifications and it is particularly relevant for bridges in or near town areas.

2.2.6. ASCE Loading [1981]

The live load known unofficially as the ASCE Loading is a result of the studies performed by Peter G. Buckland, which was recommended for long span bridge by the American Society of Civil Engineers Committee on Loads and Forces on Bridges. ASCE (1981) specifies three levels of live load for highway bridges depending on the average percentage of heavy vehicles in traffic flow: 7.5%, 30%, and 100% heavy vehicles of the total vehicle population. "Heavy vehicles" were defined as buses and trucks over 12 000 lbs. It has been proved that the loading can be represented by a uniform load and a concentrated load (Figure 2.11) to give moments and shears with a sufficient degree of accuracy.
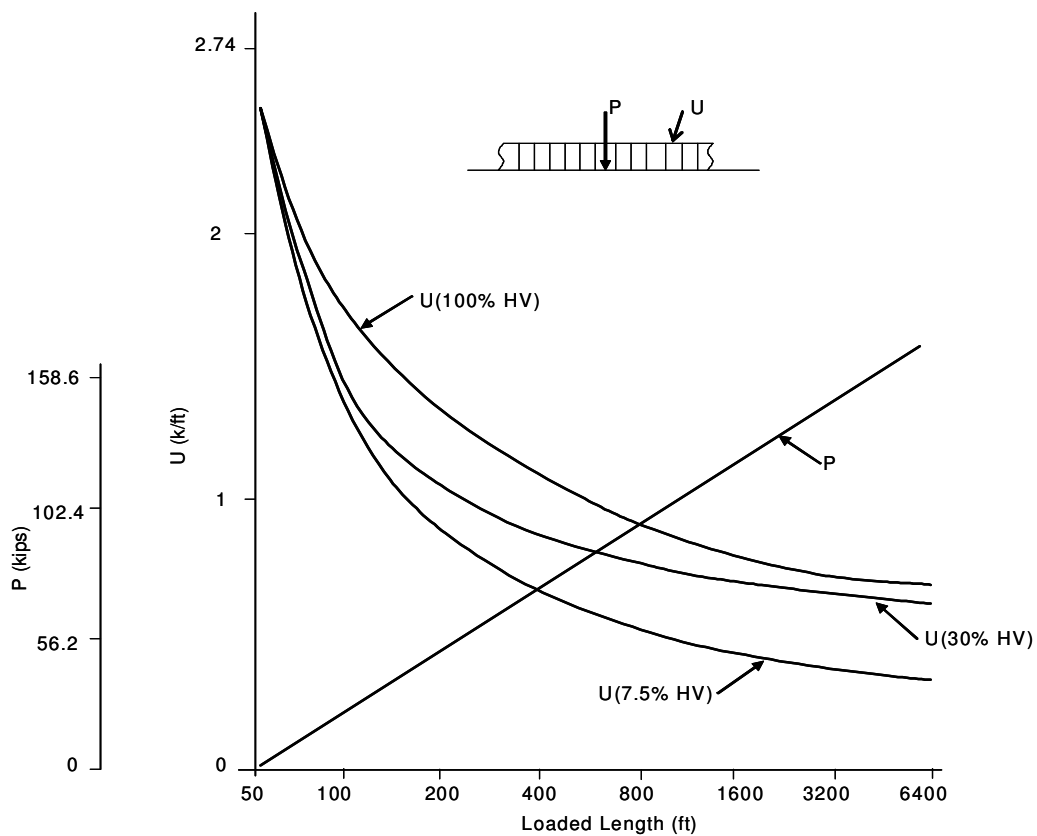
Figure 2.11. ASCE Loading on Log Scale

19

2.3. PROVISIONS FOR DYNAMIC LOAD FACTOR

There is considerable variation in the treatment of dynamic load effects by bridge design codes in different countries. The most common approach is to apply dynamic response as a fraction or multiple of the response that would be obtained if the same forces or loads were applied statically. The objective of this simple approach is to not increase complexity to the designer.

The American Association of State Highway and Transportation Officials Standard Specifications for Highway Bridges AASHTO LRFD [2007] define that dynamic load allowance shall be applied to static load effects of the truck or tandem, as a percentage specified in the table below. It shall not be applied to pedestrian loads or to the design lane load.

Table 2.4. Dynamic allowance in AASHTO LRFD [2007]

Component	Dynamic allowance, IM
Deck joints, all limit states	75%
All other components, fatigue and fracture limit states	15%
All other components, other limit states	33%

Until recently AASHTO Standard Specifications for Highway Bridges used to specify dynamic load effects in terms of an impact factor that is a function of bridge span. However relation between dynamic load factor and bridge span is a controversial issue between researchers (see Paragraph 7.2.).

The Canadian Highway Bridge Design Code CAN/CSA-S6-00 [2000] and OHBDC [1991] apply dynamic allowance as a percentage to static effects of the CL-W Truck for the number of axles considered in the design lane, as shown in the table below.

20

Table 2.5. Dynamic allowance in CAN/CSA-S6-00

for deck joints	0.50
1 axle of CL-W Truck	0.40
2 axles of CL-W Truck	0.30
3 or more axle of CL-W Truck	0.25

According to British Standard BS 5400 [2006] and the Eurocode 1 [2002] the effects of vibration due to live load are not required to be considered. Their effect has already been taken into consideration in definition of design loading.

The ASCE model (1981) does not have any allowance for dynamic load on the ground that the worst loading occurs with stationary bumper-to-bumper traffic.

2.4.   PROVISIONS FOR MULTILANE REDUCTION FACTORS

For multilane bridges, the multiple lane reduction factors are specified in most of the codes. The approaches to multilane factors vary significantly. They are shown in Table 2.6 and Table 2.7. The British Standard BS 5400 developed the most compound procedure of selection of multilane factor, which depend not only on the number of lanes, but also on loaded length, number and width of notional lanes (Table 2.7). Eurocode does not define multilane reduction factor, but it gives the load values to be applied on successive road lanes directly (Table 2.3). The multilane reduction factors are further discussed in CHAPTER 6 of this dissertation.

21

Table 2.6. Comparison of Multilane Reduction Factors

Code	Number of Lanes					
	1	2	3	4	5	6 or more
AASHTO LRFD (2007)	1.20	1.00	0.85	0.65	0.65	0.65
OHBDC (1983, 1991)	1.00	0.90	0.80	0.70	0.60	0.55
CAN/CSA-S6-00 (2000)	1.00	0.90	0.80	0.70	0.60	0.55
ASCE (1981)	1.00	0.70	0.40	0.40	0.40	0.40

Table 2.7. Multilane Reduction Factors for BS 5400

	Number of Lanes			
loaded length [m]	1	2	3	4 or more
$0<L\leq20$	α_1	α_1	0.6	$0.6\,\alpha_1$
$20<L\leq40$	α_2	α_2	0.6	$0.6\,\alpha_2$
$40<L\leq50$	1.0	1.0	0.6	0.6
$50<L\leq112, N<6$	1.0	$7.1/\sqrt{L}$	0.6	0.6
$50<L\leq112, N\geq6$	1.0	1.0	0.6	0.6
$L>112, N<6$	1.0	0.67	0.6	0.6
$L>112, N\geq6$	1.0	1.0	0.6	0.6

$\alpha_1 = 0.274\ b_L$

$\alpha_2 = 0.0137\{b_L(40-L)+3.65(L-20)\}$

where b_L is the notional lane width

N is total number of notional lanes on the bridge. For a bridge carrying one-way traffic only, the value N shall be multiplied by 2.

2.5.   COMPARISON OF EQUIVALENT UNIFORMLY DISTRIBUTED LOADS

In this paragraph, the resulting equivalent uniformly distributed loads for a variety of design codes and span lengths are plotted and compared. Figure 2.12 and Figure 2.14 compare the equivalent unfactored uniform loads. More valid comparison is to compare factored loads; these are shown in Figure 2.13 and Figure 2.15. For AASHTO LRFD (2007) live load factor is 1.75, for OHBDC (1991) it is 1.40, for CAN/CSA-S6-00 it is 1.70, for BS 5400 it is 1.50, and for Eurocode it is 1.35. ASCE studies made no reference to load factors to be used with its recommended loading, but since a factor of 1.80 has been used by (Buckland 1991), the same value has been adopted for this comparison.

Equivalent loads including dynamic loads are shown in Figure 2.14, Figure 2.15, and Figure 2.16. The design loads are increased by the dynamic load factor, DLF, which has a value as described for each code in the paragraphs above. Since live loadings in British Standards and Eurocode include dynamic load, they have been used only for comparison of loads including dynamic load.

Results of the comparison show that variation between the unfactored values of live load in different codes is significant. European values double those of North America. The application of load factors slightly reduces the differences. The comparison of four loaded lanes shows that the differences are reduced even more, Figure 2.16. The importance of load factors and multilane factors cannot be underestimated.

To obtain plots of UDL, the maximum bending moment (M_{max}) was calculated for simple spans from 400 through 5000 ft. Then, the equivalent uniformly distributed load UDL was determined from the following formula:

$$UDL = 8 \cdot (M_{max}) / L^2 \tag{2.1}$$

where: L is span length.

It should be noted that most of the codes are limited to certain lengths of span, and they are extrapolated beyond these points partially for interest and partially because these codes are also occasionally used for longer spans due to a lack of adequate guides.
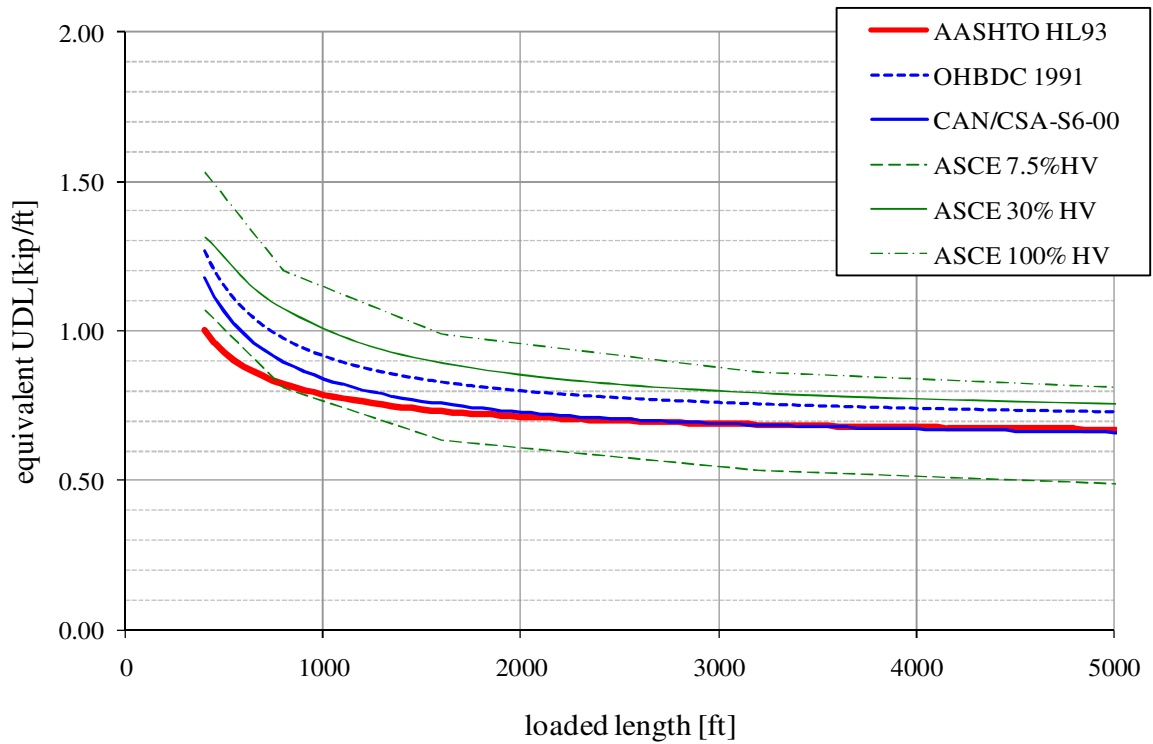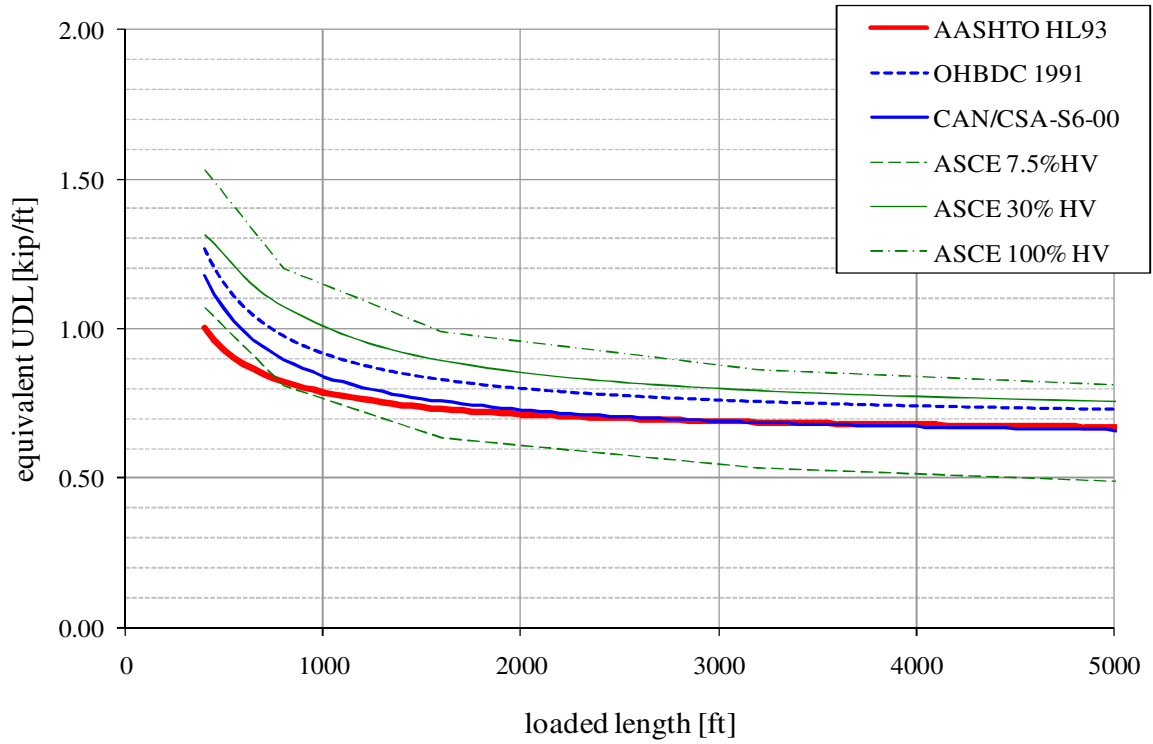
Figure 2.12. Equivalent Unfactored Loads, w/o IM, w/o multilane factors.

24
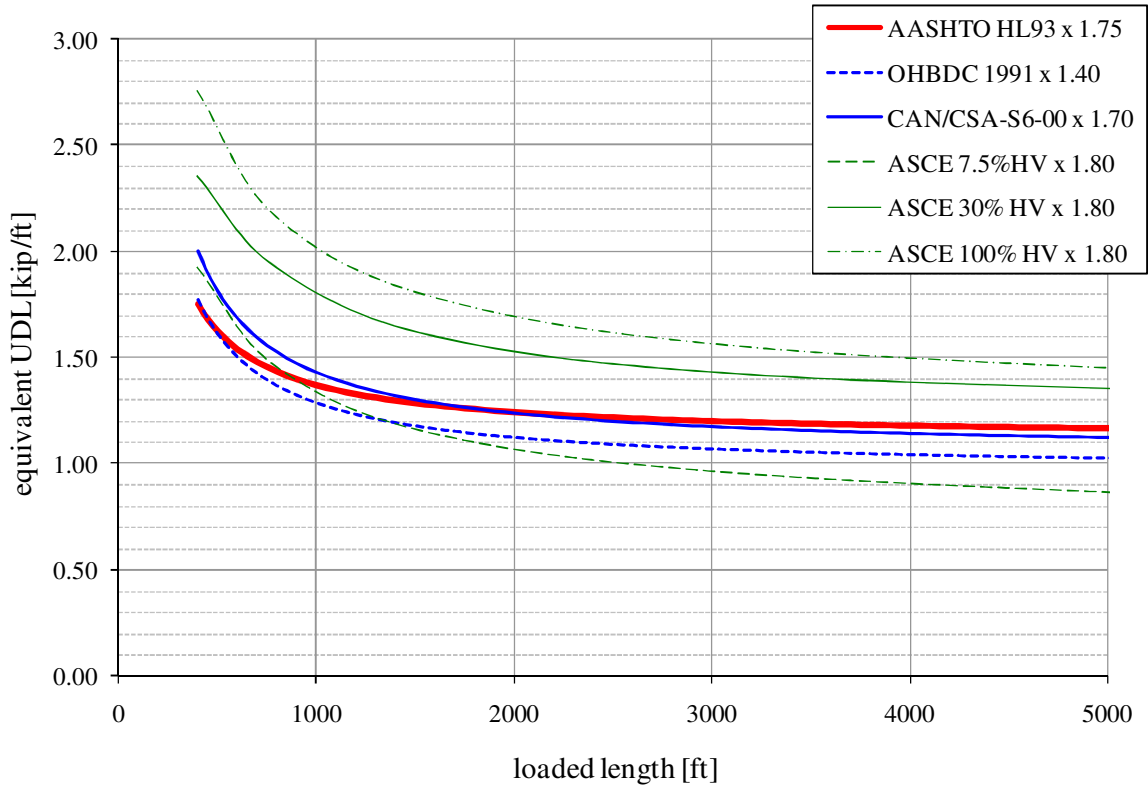
Figure 2.13. Equivalent Factored Loads, w/o IM, w/o multilane factors.
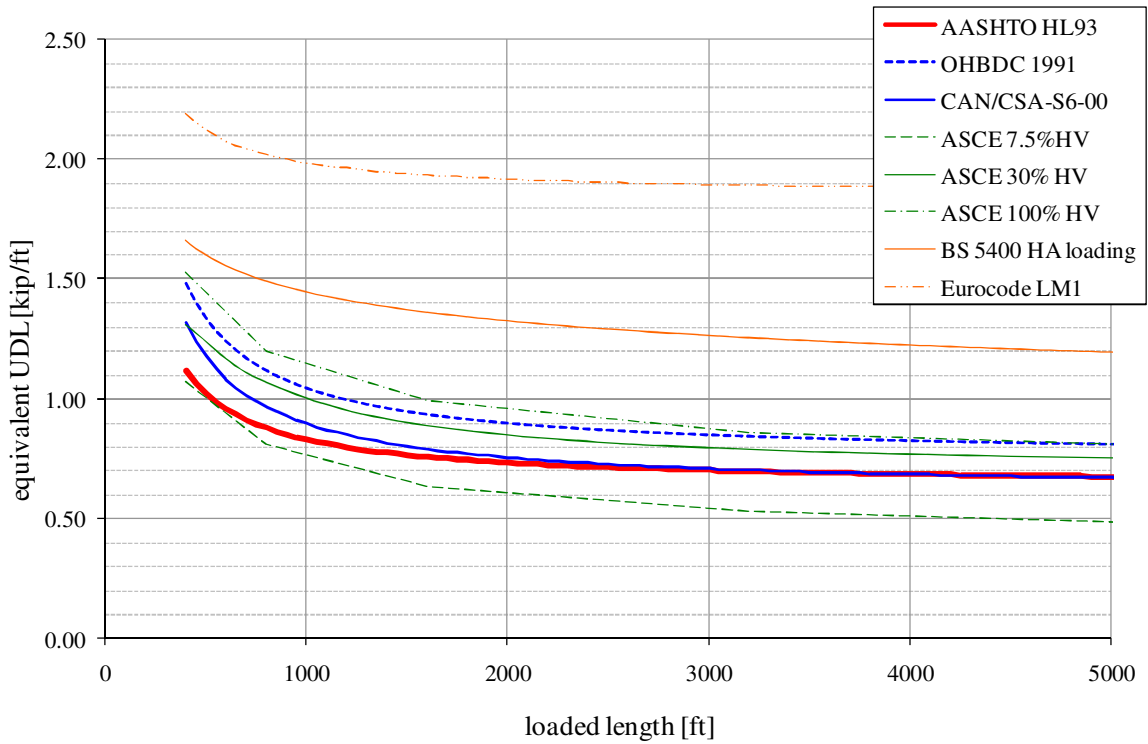
Figure 2.14. Equivalent Unfactored Loads, with IM, w/o multilane factors.

25
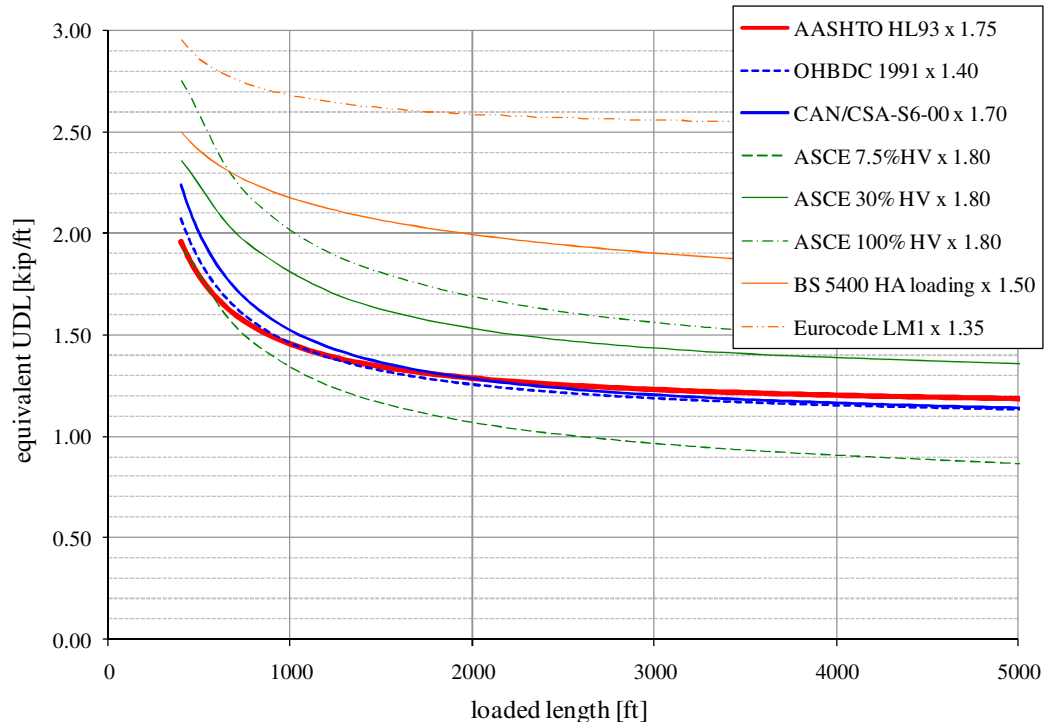
Figure 2.15. Equivalent Factored Loads, with IM, w/o multilane factors.
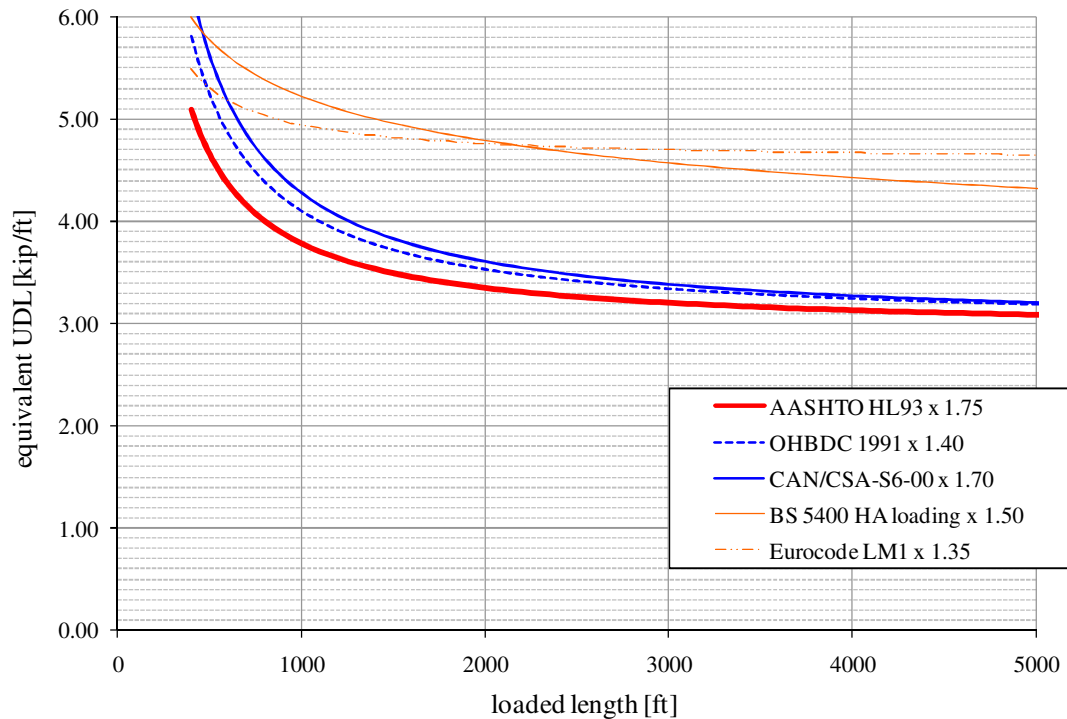
Figure 2.16. Equivalent Factored Loads, with IM, with multilane factors

for 4 traffic lanes.

Table 2.8. Values of Equivalent Unfactored Loads, w/o IM, w/o multilane factors.

length [ft]	OHBDC 1991	CAN/CSA-S6-00	HL-93
500	1.151	1.067	0.928
1000	0.918	0.842	0.784
1500	0.841	0.767	0.736
2000	0.802	0.729	0.712
2500	0.779	0.707	0.698
3000	0.763	0.692	0.688
3500	0.752	0.681	0.681
4000	0.744	0.673	0.676
4500	0.737	0.667	0.672
5000	0.732	0.662	0.669

Table 2.9. Values of Equivalent Factored Loads, w/o IM, w/o multilane factors.

length [ft]	OHBDC 1991	CAN/CSA-S6-00	HL-93
500	1.612	1.813	1.624
1000	1.286	1.431	1.372
1500	1.177	1.303	1.288
2000	1.123	1.240	1.246
2500	1.090	1.202	1.221
3000	1.068	1.176	1.204
3500	1.053	1.158	1.192
4000	1.041	1.144	1.183
4500	1.032	1.134	1.176
5000	1.025	1.125	1.170

Table 2.10. Values of Equivalent Unfactored Loads, with IM, w/o multilane factors.

length [ft]	OHBDC 1991	CAN/CSA-S6-00	HL-93	BS 5400	Eurocode
500	1.336	1.179	1.023	1.603	2.120
1000	1.045	0.898	0.832	1.449	1.985
1500	0.948	0.804	0.768	1.375	1.941
2000	0.900	0.757	0.736	1.328	1.918
2500	0.870	0.729	0.717	1.294	1.905
3000	0.851	0.711	0.704	1.268	1.896
3500	0.837	0.697	0.695	1.246	1.889
4000	0.827	0.687	0.688	1.228	1.884
4500	0.819	0.679	0.683	1.212	1.881
5000	0.812	0.673	0.678	1.198	1.878

Table 2.11. Values of Equivalent Factored Loads, with IM, w/o multilane factors.

	OHBDC 1991	CAN/CSA-S6-00	HL-93	BS 5400	Eurocode
500	1.871	2.004	1.790	2.404	2.862
1000	1.463	1.526	1.455	2.173	2.680
1500	1.327	1.367	1.343	2.063	2.620
2000	1.259	1.288	1.288	1.993	2.589
2500	1.219	1.240	1.254	1.942	2.571
3000	1.191	1.208	1.232	1.902	2.559
3500	1.172	1.185	1.216	1.869	2.550
4000	1.157	1.168	1.204	1.842	2.544
4500	1.146	1.155	1.194	1.818	2.539
5000	1.137	1.144	1.187	1.797	2.535

Table 2.12. Values of Equivalent Factored Loads, with multilane factors for 4 traffic lanes.

length [ft]	OHBDC 1991	CAN/CSA-S6-00	HL-93	BS 5400	Eurocode
500	5.238	5.612	4.655	5.771	5.309
1000	4.097	4.274	3.783	5.216	4.945
1500	3.716	3.828	3.493	4.952	4.823
2000	3.526	3.605	3.348	4.782	4.762
2500	3.412	3.471	3.261	4.660	4.726
3000	3.336	3.382	3.202	4.564	4.702
3500	3.282	3.318	3.161	4.486	4.684
4000	3.241	3.271	3.130	4.420	4.671
4500	3.209	3.234	3.106	4.364	4.661
5000	3.184	3.204	3.086	4.314	4.653

CHAPTER 3

STRUCTURAL RELIABILITY PROCEDURES

3.1. INTRODUCTION

The structures and their components should be designed to have a desirable level of reliability, which would assure their good performance to account for actions applied during construction and service. For this purpose civil engineering uses a probabilistic evaluation of reliability. The design of new structures as well as the evaluation of existing structures requires verification of limit states, which when exceeded lead to structural failure (ultimate limit states) or make use of the structure impossible (serviceability limit states).

The actions (loads, Q) and structural resistance (capacity, R) are the variables that decisively influence the state of a structure. They include uncertainties coming from mechanical material properties, geometry of a structure, loads, etc. Those uncertainties can be measured only with the use of probability. Therefore, the design of structures is a process in which decisions are made under uncertainty and limits. Their rational treatment, and agreement between real-input data and a mathematical model of phenomenon, is a concern of structural reliability.

Unreliability of a structure is a state in which a structure does not fulfill design requirements related to its function and desirable performance. It could be a collapse of a structure, failure or other deficiency in a structural resistance, unfulfilled service demands

29

of a structure, i.e. excessive deformations, excessive vibrations, etc. Structures usually have a number of possible failure scenarios. For most of the structures it is impossible to examine all their failure modes. Therefore, representative failure scenarios have to be chosen. The analysis usually includes an estimation of structural reliability with respect to specified failure modes. All modes must be treated separately. Thus, reliability of a structure is the probability that the system will not reach a specified failure mode related to a specified limit state during a specified period of time.

3.2. STANDARD VARIABLES AND PROBABILITY DISTRIBUTIONS

The key probabilistic characteristics of a random variable are described in terms of mean, variance and standard deviation. A distribution function would complete the description of the probabilistic characteristics of random variables, but sometimes it remains unknown. There are two types of random variables: discrete and continuous. A discrete random variable may take on only discrete values. Its probability is given by the probability mass function, $P_X(x_i)$. A continuous random variable can take on a continuous range of values, and its probability is defined by the probability density function (PDF), $f_X(x)$.

Mean

The mean (expected value) is an average of all observations on a random variable. It is also defined as the first moment about the origin. For the continuous random variables, the mean (μ) can be computed as:

$$\mu = \int\limits_{-\infty}^{+\infty} x \cdot f_X(x) \, dx \tag{3.1}$$

For the discrete random variables, the mean is given by:

$$\mu = \sum_{i=1}^{n} x_i \cdot P_X(x_i) \tag{3.2}$$

If all n observations are given equal weights ($P_X(x_i) = 1/n$), then the mean for a discrete random variable is given by:

30

$$\overline{X} = \frac{1}{n} \cdot \sum_{i=1}^{n} x_i \tag{3.3}$$

Variance

The variance (σ^2) is the second moment about the mean, and it is computed as follows:

$$\sigma^2 = \int_{-\infty}^{+\infty} (x - \mu)^2 \cdot f_X(x) dx \tag{3.4}$$

For the discrete variable, the variance is computed as:

$$\sigma^2 = \sum_{i=1}^{n} (x_i - \mu)^2 \cdot P_X(x_i) \tag{3.5}$$

If all n observations are given equal weights ($P_X(x_i) = 1/n$), the variance is as follows:

$$\sigma^2 = \frac{1}{n-1} \cdot \sum_{i=1}^{n} (x_i - \overline{X})^2 \tag{3.6}$$

Standard Deviation

The standard deviation (σ^2) of a probability distribution is defined as the square root of the variance.

Coefficient of Variation

The coefficient of variation (V) is a dimensionless quantity defined as:

$$V = \frac{\sigma}{\mu} \tag{3.7}$$

Probability distributions

There are many types of discrete and continuous distributions. The most commonly used are the continuous distributions: uniform, normal, lognormal, exponential, and gamma. In this section the normal distribution is presented, because this is the only distribution used in this dissertation. Further details about distributions can be found, for instance, in Nowak and Collins (2000).

Normal distribution (Gaussian distribution) is the most widely used probability distribution. It has a probability density function given by:

$$f_X(x) = \frac{1}{\sigma \cdot \sqrt{2 \cdot \pi}} \cdot \exp[-\frac{1}{2} \cdot (\frac{x-\mu}{\sigma})^2] \tag{3.8}$$

This function is graphically represented as shown in Figure 3.1.
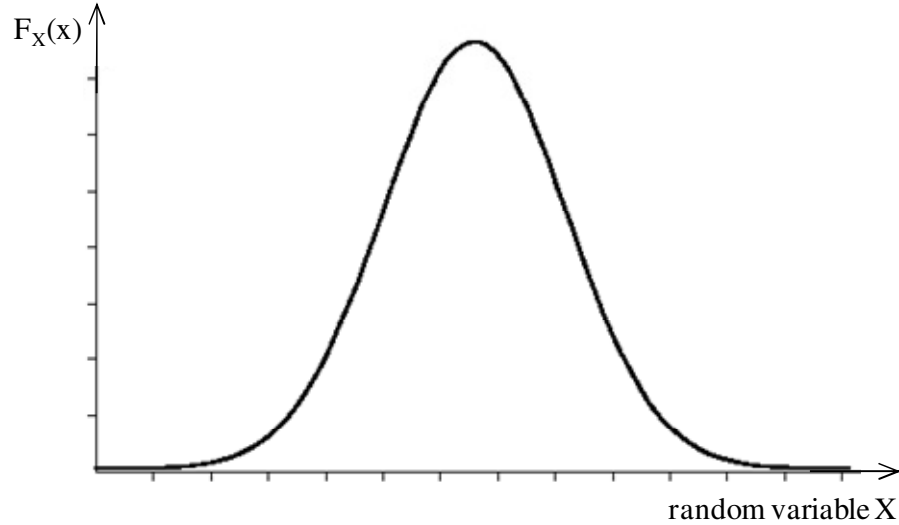
Figure 3.1 PDF and CDF of a normal random variable

The standard normal distribution is a special case of Gaussian distribution, with parameters $\mu_X = 0$ and $\sigma_X = 1.0$. Its PDF is denoted as $\phi(z)$, its CDF is denoted as $\Phi(z)$, and they are defined as follows:

$$\phi(z) = \frac{1}{\sqrt{2 \cdot \pi}} \cdot \exp(-\frac{1}{2} \cdot z^2) = f_Z(z) \tag{3.9}$$

$$\Phi(z) = \int_{-\infty}^{z} \frac{1}{\sqrt{2 \cdot \pi}} \cdot \exp(-\frac{1}{2} \cdot z^2)dz \tag{3.10}$$

Central limit theorem states that the sum of a large number of independent observations, without a dominating distribution type, approaches an approximate normal distribution. The higher the number of observations the better is the approximation. This theorem is one of the most important in probability theory. The sum of variables is often used to model total load acting on a structure, which can be approximated as a normal variable.

Mathematically it can be expressed that the sum of n random variables, $X_1, X_2,..., X_n$, is equal to function Y having normal distribution:

$$Y = X_1 + X_2 + ... + X_n \tag{3.11}$$

$$\mu_Y = \mu_{X_1} + \mu_{X_2} + ... + \mu_{X_n} \tag{3.12}$$

$$\sigma_Y{}^2 = \sigma_{X_1}{}^2 + \sigma_{X_2}{}^2 + ... + \sigma_{X_n}{}^2 \tag{3.13}$$

3.3.   LIMIT STATE FUNCTION

In most design codes, the structural design is based on the concept of limit states. The philosophy of limit state design assumes equilibrium between applied loads and structural response of the structure (capacity, resistance). Therefore, a specified set of load and resistance factors is required for each limit state formulated for different possible scenarios of structural behavior during construction as well as service life.

Three types of limit states are typically used with reference to structural reliability analysis:

1. Ultimate limit states (ULSs), which represents the loss of structural capacity.

2. Serviceability limit states (SLSs), which represents failure due to deterioration of functionality.

3. Fatigue limit states (FLSs), which represents the loss of strength for a structural component under the action of repeated loading.

The limit state defines the boundary between the desired and undesired performance of a structure, between situations when the structure is safe (a safety margin exists) and the structure is not safe (failure occurs). The probability of the desired performance of a structure is equal to the safety margin (P_S). The probability of an undesired performance of a structure is equal to the probability of failure (P_f). Failure and non-failure states fulfill the entire probabilistic sample space (Ω). Therefore, the probability of occurrence is $P(\Omega) = 1$, so:

33

$$P(\Omega) = P_f + P_s = 1 \quad \Rightarrow \quad P_s = 1 - P_f \tag{3.14}$$

Reliability analysis usually begins with the formulation of a limit state function (performance function). All loads are being incorporated into one variable (Q) and the resistance of the structure is being incorporated into one variable (R). In the general case, the performance function of a system can be related to any possible failure scenario or any limiting state and defined as a function of capacity and demand:

$$g(R,Q) = R - Q \tag{3.15}$$

where R is capacity representing resistance of a structural system or a structural element, and Q is demand representing load effect in a structure or a structural component.

Both R and Q are continuous random variables having a probability density function (PDF). The quantity $R - Q$ is also a random variable with its own PDF as shown in the Figure 3.2.
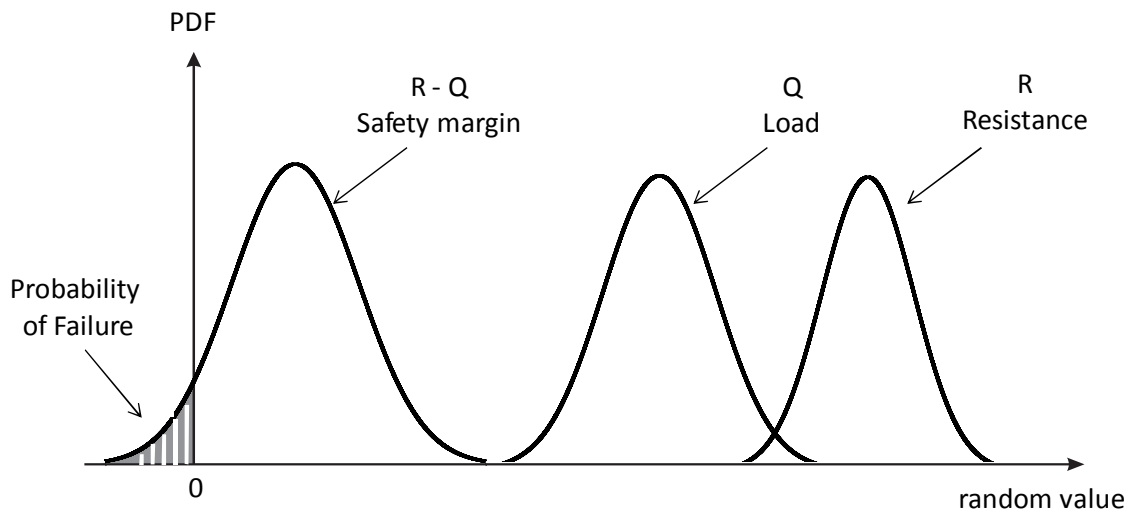
Figure 3.2 PDF's of load, resistance, and safety margin

The performance function usually is a function of capacity and demand variables ($X_1, X_2,...,X_n$), and it adopts a format:

$$g(X) = g(X_1, X_2,..., X_n) \tag{3.16}$$

where X_i is the collection of input parameters.

34

From the definition of the performance function, it can be derived that when $g(X) < 0$, it indicates failure and, when $g(X) \geq 0$, it indicates acceptable performance. The performance defined as $g(X) = 0$ is called the failure surface. The corresponding probability of failure can be defined as the integral of the joint density function of the variables over the negative domain of $g(X)$ (Thoft-Christensen and Baker 1982):

$$P_f = \int_{g(X)<0} .... \int f_{X_1, X_2,...,X_n}(x_1, x_2,...,x_n)dx_1 \cdot ... \cdot dx_n \tag{3.17}$$

where f_X is the joint probability density function of $X_1, X_2,...,X_n$

There is almost never sufficient data to define the joint probability density function for all basic variables, thus the equation (3.17) is very difficult to evaluate. Even knowing the joint density function, the necessary multi-dimensional integration may be extremely time-consuming. In practice, a direct calculation of the probability of failure becomes inefficient. Therefore, indirect procedures such as the reliability index are used.

3.4. RELIABILITY INDEX

The evaluation reliability index, also called safety index, is an effective measure of the probability of failure. There are several methods to calculate reliability of structural components: the first-order reliability methods (FORM), the advanced first-order second-moment methods (FOSM), simulation techniques, etc. In the late 1960s, the first-order second-moment formulation was developed and advanced by Cornell (1967) and Ang and Cornell (1974). Further advances in these methods were made by Hasofer and Lind (1974) and Rackwitz and Fiessler (1978). The FOSM methods can be used to solve many practical problems. The concept of second-moment is often used in practical quantification of safety and reliability. It has been extensively used in calibrations of structural design codes. The FOSM approach can be put into several categories with regard to accuracy of results, required input data, computing cost, or simplicity of formulation.

35

In 1974, Hasofer and Lind introduced the definition of the reliability index as the shortest distance from the origin to the limit state function in a system of reduced variables coordinates (Figure 3.3). Using geometry the reliability index can be calculated as:

$$\beta = \frac{\mu_R - \mu_Q}{\sqrt{\sigma_R^2 + \sigma_Q^2}} \tag{3.18}$$
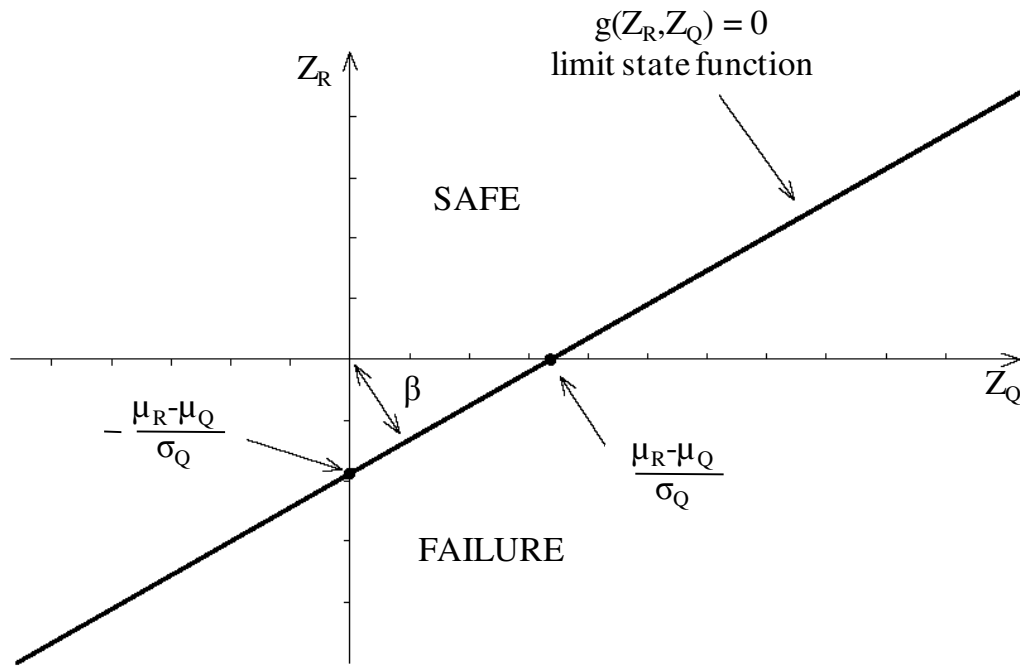
Figure 3.3 Reliability index defined as the shortest distance in the space of reduced variables

All the variables should be expressed in non-dimensional forms. Thus, the reduced variables (Z_R, Z_Q) have to be introduced:

$$Z_R = \frac{R - \mu_R}{\sigma_R}$$
$$Z_Q = \frac{R - \mu_Q}{\sigma_Q} \tag{3.19}$$

The resistance (R) and the load (Q) can also be expressed in the form of reduced variables:

36

$$R = \mu_R + Z_R \cdot \sigma_R$$
$$Q = \mu_Q + Z_Q \cdot \sigma_Q \tag{3.20}$$

Therefore the limit state function $g(R,Q) = R - Q$ in terms of reduced variables can be rewritten as:

$$g(Z_R, Z_Q) = \mu_R + Z_R \cdot \sigma_R - \mu_Q + Z_Q \cdot \sigma_Q \tag{3.21}$$

The reliability index recognizes the importance of uncertainty in load effects and strength. It incorporates the four key parameters, resistance and load with their mean values and standard deviations, μ_R, μ_Q and σ_R, σ_Q, respectively.

The limit state function used in this dissertation is linear. In case it was nonlinear, iteration would be required to find the design point in reduced variable space such that β corresponds to the shortest distance. Moreover, the Hasofer-Lind approach evaluates the reliability index for uncorrelated random variables. Thus, if the initial variables are correlated they must be transformed into uncorrelated random variables.

The probability of failure can be calculated using the formula (3.22). The calculation can give exact results, if the random variables are normally distributed and uncorrelated. Otherwise it provides only an approximation.

$$P_f = \Phi(-\beta) \tag{3.22}$$

where Φ is the standard normal distribution function.

3.5.   MONTE CARLO METHOD SIMULATION TECHNIQUE

Simulation is the process of replacing reality with theoretical and experimental models. Theoretical simulation is also called numerical or computer experimentation. It is a practical tool that allows obtaining data, either instead of or in addition to real-world data. Simulating a phenomenon numerically assumes events occur a finite number of times. The frequency of occurrence of an event in the entire set of simulations approximates its probability of occurrence. This relatively straightforward concept often requires complex procedures. The most commonly used simulation technique is the Monte Carlo Method (Thoft-Christensen and Baker, 1982; Hart, 1982). Many other

37

simulation techniques work similarly to the Monte Carlo Method. However instead of generating a large number of random values for variables, the values are arbitrary and selected according to specified rules.

The Monte Carlo Method is commonly used to predict the behavior of structural elements and systems from the probability point of view, and without physical testing. It is used to evaluate the probability of structural failure and, indirectly, the reliability index. A large amount of random numbers corresponding to random variables is numerically generated. This large number of repetitions is particularly valuable in solving problems involving rare events, where physical testing could be very expensive. This method may be used not only to study performance of a structural system for a prescribed set of design variables, but also to measure sensitivity in system performance due to variations of some parameters. Therefore, for engineering purpose, it can be used to determine optimal design.

The Monte Carlo simulation method consists of the following steps. In the first step a simulation of the uniformly distributed random numbers $u_1, u_2, ..., u_n$ between 0 and 1 is performed. They can be generated by computer programs using a built-in option. Then, the standard normal random values can be calculated using generated numbers and information about the types of distributions and statistical parameters of distributions (mean value and standard deviation) of each design variable. The standard normal random number z_i is calculated using the equation:

$$z_i = \Phi^{-1}(u_i) \tag{3.23}$$

where:

Φ^{-1} is the inverse of the standard normal cumulative distribution function

Using standard random values (mean value μ_X and standard deviation σ_X), the values x_i of sample random numbers can be generated for the random normal variable X, as:

$$x_i = \mu_X + z_i \cdot \sigma_X \tag{3.24}$$

38

It is important to simulate an efficient number of sets, such that the variation of the design parameters in a single simulation will not influence the solution of the entire process of simulations.

Performed Monte Carlo simulations allow for estimation of the probability of failure. The probability of failure is defined as the ratio between the numbers of times the criterion for the failure is achieved (n), to the total number of simulations (N). Each simulated value has the same weight.

$$\overline{P}_f = \frac{n}{N} = \frac{\text{total number of simulations when } g(\overline{X}) < 0}{\text{total number of simulations of } g(\overline{X})} \qquad (3.25)$$

where:

$g(\overline{X})$ defines the performance function with the limit state $g(\overline{X}) = 0$

$g(\overline{X}) < 0$ defines the state of failure

3.6. NORMAL PROBABILITY PAPER

Normal probability paper is used to present cumulative distribution functions (CDF) in a convenient way. Cumulative distribution functions for the normal distribution are "S-shape" function. Normal probability paper redefines the vertical scale so that the normal CDF can be plotted as a straight line and allows for an easy evaluation of the most important statistical parameters as well as type of distribution function. More detailed information about normal probability paper can be found in textbooks (Nowak and Collins 2000, Benjamin and Cornell 1970). The basic variable is presented on the horizontal. The vertical axis, being the standard normal variable, represents the distance from the mean value in terms of standard deviations. It can also be implied as the corresponding probability of being exceeded. The relationship between the standard normal variable and probability is given in Table 3.1.

Table 3.1. Relationship between vertical scale on Normal Probability Paper
and Probability

Distance from the mean value in terms of standard deviations	Corresponding probability
4	0.9999683
3	0.99865
2	0.9772
1	0.841
0	0.5
-1	0.159
-2	0.0228
-3	0.00135
-4	0.0000317

The shape of the resulting curve representing CDF allows for analysis of the test data plotted on the normal probability paper.

The basic properties of the normal probability paper:

- A straight line represents a normal distribution function.
- The mean value and standard deviation read directly from the graph.
- The mean value is at the intersection of the normal CDF and horizontal axis.
- The standard deviation can also be read as shown in Figure 3.4.
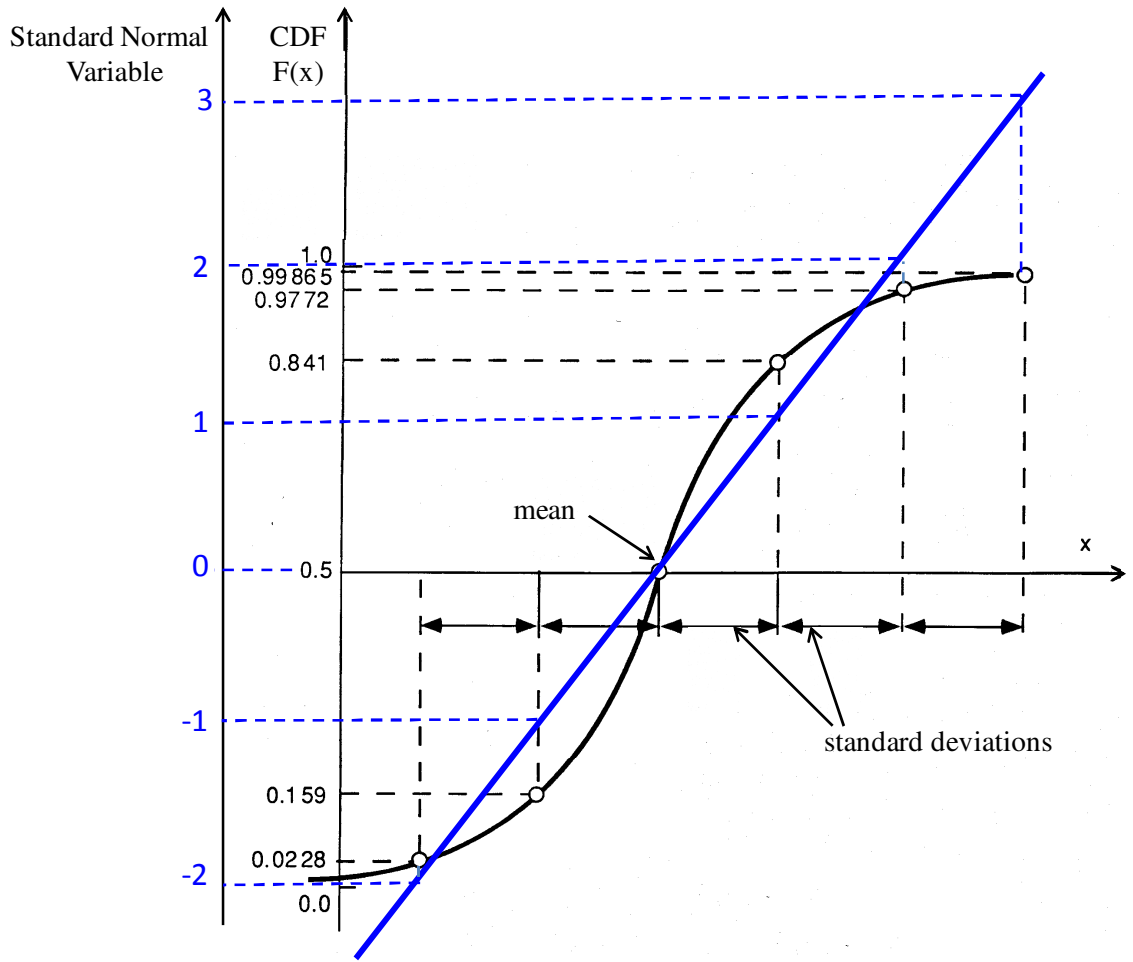
Figure 3.4 Normal Distribution Function on the Normal Probability Paper.

CHAPTER 4

TRAFFIC DATA

4.1. REGULATIONS OF TRUCK TYPES, TRUCK SIZES AND WEIGHT LIMITS

Federal and state regulations limit the weight and dimensions of vehicles on U.S. highways. These restrictions have important impacts on highway construction costs, maintenance costs, and highway safety issues. Current Federal law includes the following limits:

- 20 000 pounds - maximum gross weight upon any one axle
- 34 000 pounds - maximum gross weight on tandem axles
- 80 000 pounds - maximum gross vehicle weight
- 102 inches - maximum vehicle width
- 48-feet - minimum vehicle length for a semi-trailer in a truck-tractor/semi-trailer combination
- 28 feet - minimum vehicle length for a semi-trailer or trailer operating in a truck-tractor/semi-trailer/trailer combination.

The types of the vehicles in use on American roads are classified by FHWA into 13-categories, as show in Figure 4.1. Classes 1-3 are passenger vehicles, classes 4-7 are single unit trucks and buses, classes 8-10 are combination trucks, classes 11-13 are multi-trailer trucks.

42

Figure 4.1. FHWA 13-category scheme

Table 4.1. Conversion chart for vehicles' class and number of axles

Vehicle Class	Average Number of Axles per Vehicle
1	2
2	2
3	2
4	2.2
5	2
6	3
7	4
8	4
9	5
10	6
11	4
12	6
13	7

Several states issue overweight permits and allow higher truck loads. For example the state of Michigan, from where some publications on field test results are used in this study, allows trucks up to 164,000 pounds. The states which allow various longer combination vehicles are presented in Figure 4.3. Types of longer combination vehicles (Figure 4.2) are:

- Rocky Mountain Double (common maximum weight – 105,500 - 137,800 lbs)

- Turnpike Double (common maximum weight – 105,500 - 129,000 lbs)

- B-train Double Trailer Combination (common maximum weight – 105,500 - 147,000 lbs)

- Triple Trailer Combination (common maximum weight – 105,500 - 131,000 lbs)

44

Rocky Mountain Double

Turnpike Double

8-Axle B-Train Double Trailer Combination

Triple Trailer Combination

Figure 4.2. Longer Combination Vehicles (LCV's)

States Allowing LCVs'

States Allowing Triples

States Allowing Turnpike Doubles

States Allowing Rocky Mountain Doubles

Figure 4.3. States allowing various Longer Combination Vehicles

Federal size and weight studies were established in 1982, and since then no significant changes have been made. However, several proposals to make changes in these regulations were presented. The most recent studies are the TRB Special Report 267 "Regulation of Weights, Lengths, and Widths of Commercial Motor Vehicles" and the U.S. Department of Transportation "Comprehensive Truck Size and Weight Study: Volume I Summary Report". Both documents discuss existing regulations and give recommendations on their improvement. Elimination of the federal 80 000 pounds weight limit on Interstate highways is recommended. It is proposed that the gross weight should be governed by appropriate axle weight limits and the bridge formula (Figure 4.4). The maximum weight (in pounds) carried on a group of two or more consecutive axles would not exceed that given by the following formulas:

- $W = 1000*(2L+26)$ for L≤24 ft

- $W = 1000*(L/2+62)$ for L>24 ft
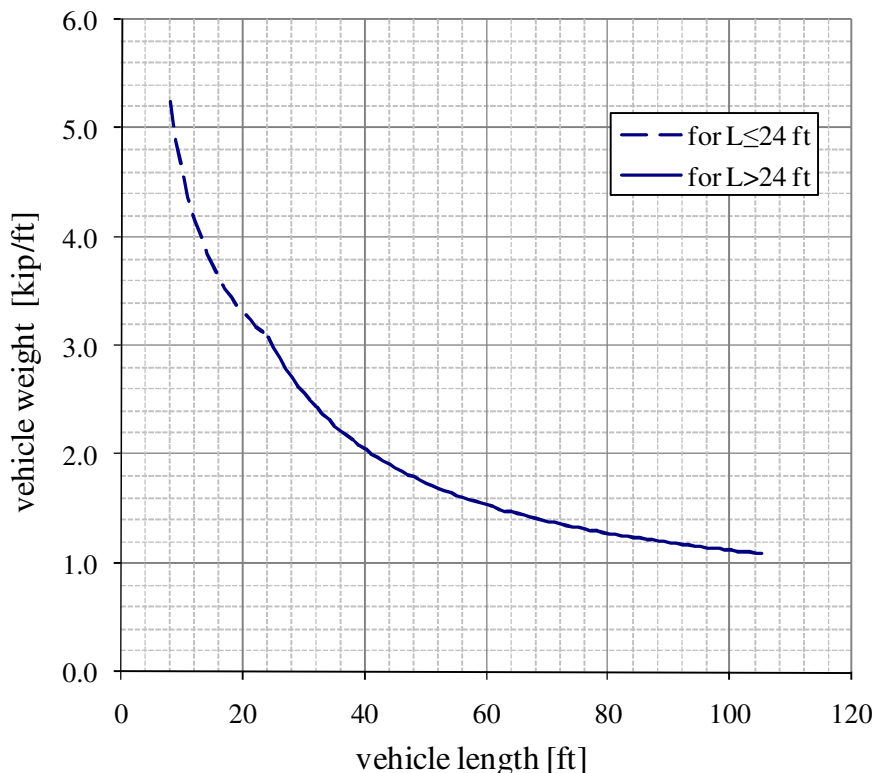
Figure 4.4. New Bridge Formula - regulation of vehicles' length and weight

In the Figure 4.5, the data from the Transportation Statistics Annual Report December 2006 of U.S. Department of Transportation is shown. As can be observed, the number of trucks has a trend of rapid growth. The number of heavy trucks is growing faster than number of light trucks. The number of light trucks (under 10 000 pounds) increased 73 percent between 1992 and 2005, and the number of heavy trucks (greater than 10 000 pounds) increased 112 percent. In 2005 heavy trucks constituted 8% of the volume of trucks, while in the 1990's they were only 4% of the volume. In 2005, 95.3 million light trucks traveled 1.060 trillion vehicle-miles, and 8.5 million heavy trucks traveled 222.29 billion vehicle-miles.
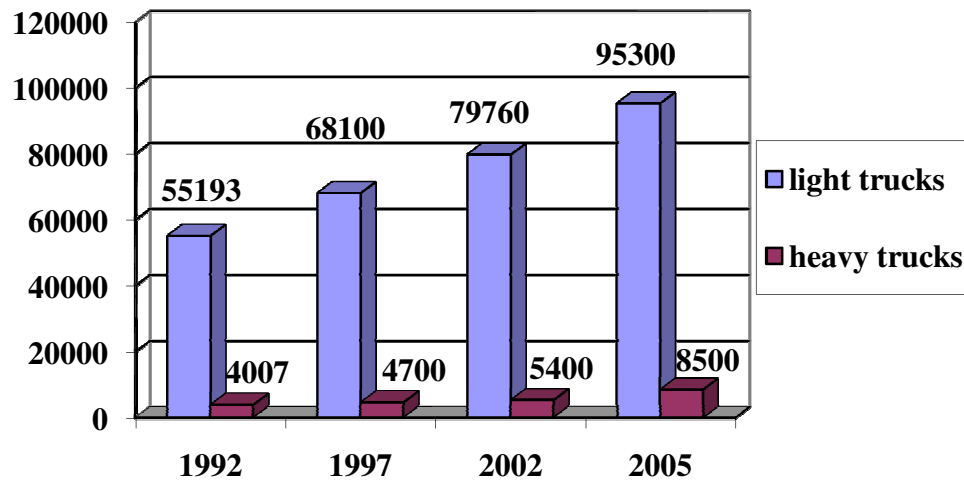
Figure 4.5. Number of trucks by weight (in thousands of trucks).
Transportation statistics annual report, December 2006.

According to Texas Transportation Institute "Over the next 20 years, truck tonnage is expected to increase at a rate more than five times that of population growth."
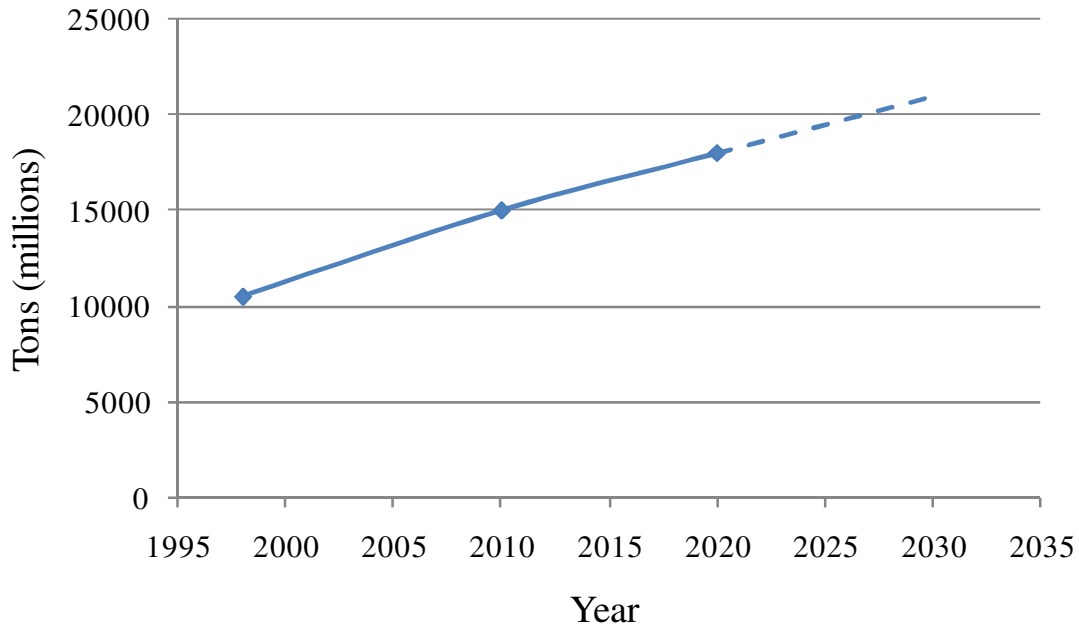
Figure 4.6. Freight Tonnage Moved by Truck (FHWA)

Figure 4.7 presents time variation of total truck weight statistic between the years 1993 and 2003. The data is expressed as: mean value (μ), 95th percentile (W95, 95 percent of the trucks weigh less), and maximum observed total truck weight (Max). The study was made for the state of New Jersey, which has lower limits than the state of Michigan. However, the observed maximum gross vehicle weight is high, and it reaches a value of 225 kips (1000 kN). The maximum truck weight shows steady increase at an annual growth rate of 1.2%.
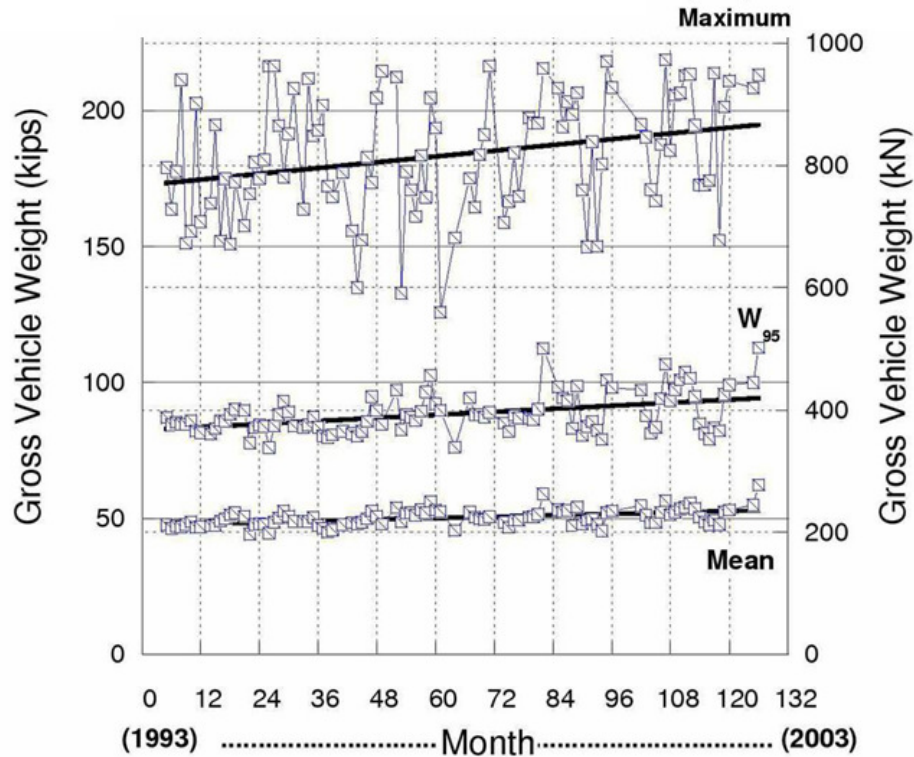
Figure 4.7. Time variation of total truck weight statistic.

(Gindy, M., Nassif, H.H., 2006)

4.2. DATA COLLECTION METHODOLOGY (WIM)

Weigh in Motion (WIM) Technology had its beginnings in the early 1950s when the U.S. Bureau of Public Roads, the Virginia State Department of Highways, and the Williams Construction Company installed a load cell WIM system on the Henry G. Shirley Memorial Highway. From these early beginnings, WIM technology and application continued to advance and spread across the nation. In 1990, the American Society for Testing and Materials (ASTM) published the first Standard Specification for Highway Weigh-in-Motion (WIM) Systems with User Requirements and Test Methods (Designation: E 1318-90). This document was revised in 1994, and again in 2002 to the version (Designation: E 1318-02) that is used today.

ASTM Designation: E 1318-02 defines WIM as "the process of measuring the dynamic tire forces of a moving vehicle and estimating the corresponding tire loads of the

49

static vehicle". In addition to the collection of dynamic tire forces, a variety of ancillary traffic data can also be obtained through the use of WIM systems: traffic volume, speed, directional distribution, lane distribution, date and time of passage, axle spacing, axle weight, and vehicle classification. Of all data collection methodologies, WIM data collection requires the most sophisticated technology for data collection sensors, the most controlled operating environment (smooth, level pavement), as well as the highest equipment set-up and calibration costs. The primary reason for sophistication in technology and its high costs comes from a need to determine static weight from a dynamic measurement. In standard weigh scale application, vehicles are stopped on a static scale and are measured without any interaction between the vehicle and the roadway. In WIM applications, a variety of forces are acting on the vehicle, including the force of gravity as well as dynamic effects of influences such as: roadway roughness, vehicle speed, vehicle acceleration and deceleration, out of balance tires and wheels, tire inflation pressure, suspension, aerodynamics and wind; and other dynamic factors.

Several different technologies are available for WIM data collection systems. The most commonly used are: piezoelectric cables, bending plate, load cell, quartz cables, and Bridge WIM systems. ASTM Standard Designation: E 1318-02 distinguishes four types of WIM systems (Type I, II, III, and IV) based on application and performance requirements for data collection. Each type of WIM system has been specified to perform its indicated functions within specific tolerances. The piezoelectric sensors, which are the most common, offer acceptable accuracy ±15%. Strain based and load cell WIM systems are much more expensive, but they provide more accuracy. Recently, piezo-quartz sensors were introduced in the United States. They are less sensitive to temperature changes and generally more accurate. The majority of WIM data collection is done with permanently installed weight sensors, although the data is not always collected continuously.

In order to assure unbiased data, WIM sites should be localized away from weight stations and be unknown to truck drivers'. WIM equipment should be subject to a regular maintenance and calibration. To limit erroneous data, it is recommended to avoid sites with numerous traffic stoppages (speed >10 mph), close to exits, and with rough surfaces.

Highway agencies have recognized the advantages of having automated data collection systems that can provide information on truck weights and truck traffic patterns for economic analysis, traffic management and various other purposes. Therefore, the quality and quantity of WIM data has greatly improved in recent years, and new WIM technologies continue to be developed. Due to the weigh-in-motion technologies, unbiased truckloads are being collected at normal highway speeds, in large quantity, and without truck driver's knowledge (Figure 4.8).
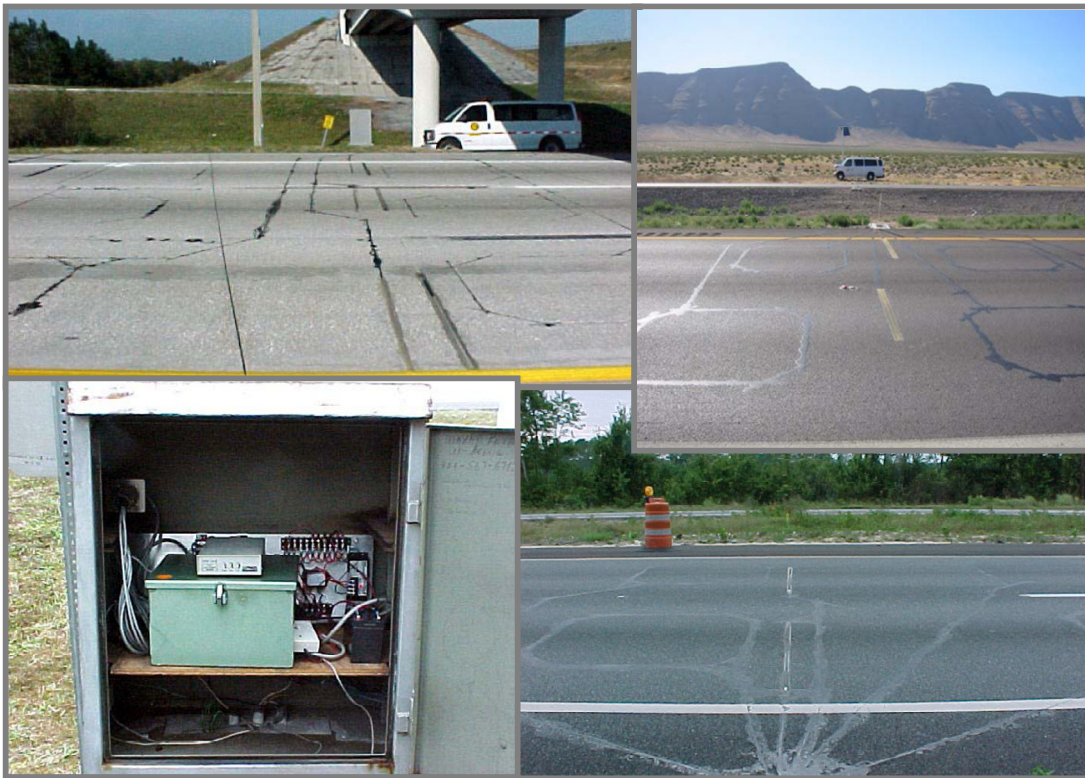
Figure 4.8. WIM data collection

4.3. WEIGH IN MOTION DATABASE

For the scope of this research, the weigh in motion database was obtained from the project NCHRP 12-76 and measurements on the Throggs Neck Bridge in New York. The database includes newest (2001-2006) WIM database for a variety of sites: California (6), Florida (5), Indiana (6), Mississippi (5), New York (7+2), Oklahoma (16),

and Oregon (4). The variety of sites is important, because the truck traffic changes depending on the site location: interstate or non-interstate highways, rural or urban areas, and state. Traffic data varies also depending on time of day, day of the week, season of the year, and direction. Therefore, it is important that the WIM database is collected continuously (mostly one-year data), on many traffic lanes and in both directions (usually). The database contains date and time, lane, number of axles, spacing between axles, axle weight, speed, and vehicle category. A summary of WIM data, including site localizations, number of lanes, and types of sensors used is presented in Table 4.2. Distribution of vehicles by axles and traffic lanes are presented in Table 4.3 - Table 4.10. The statistics is presented for four states selected for simulations: Oregon, Indiana, Florida, and New York. Cumulative distribution functions of gross vehicle weights by axles (GVW) were plotted in Figure 4.9-Figure 4.11. It can be noticed, that for New York I-495, the heaviest vehicles are 6-axles. Those are construction debris, gravel and garbage haulers. They often drive overloaded above 150 kips and occasionally above 200 kips, while NYSDOT routine permit trucks that are legal up to 120 kips.

The WIM technology is known to have certain traffic data quality problems. The errors are due to physical and software-related failures of equipment and transmission, the difference between the dynamic weight measured and the actual static scale weight, as well as the effect of tire pressure, size and configuration of the WIM results. Therefore, the data quality checks have to be implemented to detect and fix/eliminate erroneous data before processing. A standardized procedure to filter out errors is applied to WIM data from various sites. According to Traffic Monitoring Guide (2001), reasonableness checks were performed on the axle weights and spacing. The limits were 200 to 20,000 kilograms (0.44 to 4.41 kips) for axle weights and 0.5 to 15 meters (1.6 to 49.2 feet) for axle spacing. Moreover, all obvious errors such as zero readings for number of axles or speed were eliminated. The percentage of filtered out data varies for different sites, which depends on condition of equipment, its regular maintenance and recalibration.

Table 4.2. Summary of WIM Data

State	Site ID	Route	# of Traffic Lanes	# of WIM Lanes	Both Dir	WIM Type
CA	0001	Lodi				
CA	0003	Antelope				
CA	0004	Antelope				
CA	0059	LA710				
CA	0060	LA710				
CA	0072	Bowman				
FL	9916	US-29	4	4	Y	P
FL	9919	I-95	4	4	Y	P
FL	9926	I-75	6	4	Y	BP
FL	9927	SR-546	4	4	Y	BP
FL	9936	I-10	4	4	Y	P
IN	9511	I-65	4	4	Y	P
IN	9512	I-74	4	4	Y	SLC
IN	9532	US-31	4	4	Y	P
IN	9534	I-65	6	6	Y	P
IN	9544	I-80/I-94	6	6	Y	P
IN	9552	US-50	2	2	Y	P
MS	2606	I-55	4	4	Y	P
MS	3015	I-10	4	4	Y	P
MS	4506	I-55	4	4	Y	P
MS	6104	US-49	2	2	Y	P
MS	7900	US-61	4	4	Y	P
NY	8280	I-84	4	4	Y	P
NY	8382	I-84	4	4	Y	P
OR	Woodburn	I-5	3	2	N	SLC
OR	Emigrant Hill	I-84	2	1	N	SLC
OR	Lowell	OR 58	2	2	N	SLC
OR	Bend	US 97	2	1	N	SLC
NY	9121	I-81	2	2	Y	P
NY	2680	8	4	4	Y	P
NY		I-495			Y	

P – Piezo, BP – Bending Plate, SLC – Single Load Cell

Table 4.3. Vehicles by axle in Oregon

axles	total		I-5 Woodburn (NB)		I-84 Emigrant Hill (WB)		OR 58 Lowell (WB)		US 97 Bend (NB)	
2	44507	4.6%	36959	6.04%	3333	1.56%	2273	2.48%	1942	3.28%
3	71365	7.3%	42009	6.87%	9242	4.34%	9807	10.70%	10307	17.40%
4	62025	6.4%	31066	5.08%	14728	6.91%	8032	8.76%	8199	13.84%
5	575846	59.0%	350107	57.22%	140520	65.97%	57123	62.30%	28096	47.44%
6	70639	7.2%	46792	7.65%	14441	6.78%	3789	4.13%	5617	9.48%
7	85658	8.8%	58407	9.55%	19003	8.92%	5725	6.24%	2523	4.26%
8	60907	6.2%	43947	7.18%	10041	4.71%	4764	5.20%	2155	3.64%
9	3500	0.4%	2253	0.37%	894	0.42%	131	0.14%	222	0.37%
10	697	0.1%	210	0.03%	404	0.19%	26	0.03%	57	0.10%
11	345	0.0%	46	0.01%	239	0.11%	20	0.02%	40	0.07%
12	277	0.0%	34	0.01%	172	0.08%	6	0.01%	65	0.11%
sum	975766		611830		213017		91696		59223	

Table 4.4. Vehicles by traffic lane in Oregon

lane	I-5 Woodburn (NB)		I-84 Emigrant Hill (WB)		OR 58 Lowell (WB)		US 97 Bend (NB)	
1	552388	90.28%	213017	100.00%	51404	56.06%	59223	100.00%
2	59442	9.72%			40292	43.94%		
3								
4								
sum	611830		213017		91696		59223	

Table 4.5. Vehicles by axle in Florida

axles	total		Florida 9916		Florida 9919		Florida 9926		Florida 9927		Florida 9936	
2	2400362	25.9%	482051	65.98%	229680	10.11%	1408095	36.45%	127986	19.70%	152550	8.37%
3	779456	8.4%	67058	9.18%	124347	5.47%	402640	10.42%	115466	17.77%	69945	4.12%
4	747991	8.1%	24388	3.34%	156406	6.88%	430324	11.14%	74984	11.54%	61889	3.50%
5	5156752	55.6%	148424	20.31%	1720367	75.69%	1554039	40.23%	297593	45.81%	1436329	82.08%
6	143470	1.5%	7011	0.96%	37909	1.67%	56038	1.45%	11271	1.74%	31241	1.76%
7	18988	0.2%	888	0.12%	2847	0.13%	6990	0.18%	6296	0.97%	1967	0.11%
8	8495	0.1%	410	0.06%	867	0.04%	2475	0.06%	4051	0.62%	692	0.03%
9	15755	0.2%	422	0.06%	405	0.02%	2533	0.07%	11977	1.84%	418	0.02%
10												
11												
12												
sum	9271269		730652		2272828		3863134		649624		1755031	

Table 4.6. Vehicles by traffic lane in Florida

lane	Florida 9916		Florida 9919		Florida 9926		Florida 9927		Florida 9936	
1	249213	34.11%	915451	40.28%	897806	23.24%	229181	35.28%	818460	46.64%
2	74085	10.14%	237260	10.44%	1119347	28.98%	88830	13.67%	114341	6.52%
3	407354	55.75%	181535	7.99%	0	0.00%	62778	9.66%	112767	6.43%
4			938583	41.30%	0	0.00%	268830	41.38%	709463	40.42%
5					1044850	27.05%				
6					801070	20.74%				
sum	730652		2272829		3863073		649619		1755031	

Table 4.7. Vehicles by axle in Indiana

axles	total		Indiana 9511		Indiana 9512		Indiana 9532		Indiana 9534		Indiana 9544		Indiana 9552	
2	2527382	27.0%	44867	10.11%	16938	8.38%	738274	57.08%	1509944	24.18%	82330	9.91%	135029	37.48%
3	513522	5.5%	15135	3.41%	7400	3.66%	91398	7.07%	353721	5.67%	26523	3.19%	19345	5.37%
4	571231	6.1%	12517	2.82%	3170	1.57%	120486	9.31%	385840	6.18%	26400	3.18%	22818	6.33%
5	5654115	60.3%	364519	82.13%	171368	84.79%	334457	25.86%	3928062	62.91%	675794	81.38%	179915	49.93%
6	95770	1.0%	6534	1.47%	2993	1.48%	7359	0.57%	60292	0.97%	15688	1.89%	2904	0.81%
7	7547	0.1%	193	0.04%	159	0.08%	836	0.06%	3740	0.06%	2381	0.29%	238	0.07%
8	2967	0.0%	59	0.01%	54	0.03%	486	0.04%	1501	0.02%	829	0.10%	38	0.01%
9	945	0.0%	10	0.00%	14	0.01%	100	0.01%	396	0.01%	414	0.05%	11	0.00%
10	355	0.0%	8	0.00%	18	0.01%	46	0.00%	225	0.00%	52	0.01%	6	0.00%
11	131	0.0%	4	0.00%	6	0.00%	20	0.00%	89	0.00%	12	0.00%	0	0.00%
12	88	0.0%	0	0.00%	0	0.00%	21	0.00%	67	0.00%		0.00%	0	0.00%
sum	9374053		443846		202120		1293483		6243877		830423		360304	

Table 4.8. Vehicles by traffic lane in Indiana

lane	Indiana 9511		Indiana 9512		Indiana 9532		Indiana 9534		Indiana 9544		Indiana 9552	
1	375357	84.57%	185645	91.85%	823175	63.64%	3232127	51.76%	412695	49.70%	360304	100.00%
2	68489	15.43%	16475	8.15%	470308	36.36%	2657717	42.57%	393046	47.33%	0	0.00%
3	0	0.00%	0	0.00%			354033	5.67%	24682	2.97%	0	
4	0	0.00%	0	0.00%					0	0.00%	0	
sum	443846		202120		1293483		6243877		830423		360304	

Table 4.9. Vehicles by axle in New York

axles	total		I-495 EB		I-495 WB		NY 9121		NY 2680	
2	114115	41.6%	56459	38.58%	57656	45.02%	108563	7.88%	34752	25.34%
3	40359	14.7%	21102	14.42%	19257	15.04%	135919	9.87%	23644	17.24%
4	19297	7.0%	10605	7.25%	8692	6.79%	74822	5.43%	14154	10.32%
5	82959	30.2%	47294	32.32%	35665	27.85%	1010780	73.39%	52845	38.54%
6	17426	6.4%	10716	7.32%	6710	5.24%	44357	3.22%	9720	7.09%
7	217	0.1%	131	0.09%	86	0.07%	1758	0.13%	1113	0.81%
8	27	0.0%	20	0.01%	7	0.01%	542	0.04%	560	0.41%
9	20	0.0%	19	0.01%	1	0.00%	335	0.02%	212	0.15%
10	0	0.0%	0	0.00%		0.00%	182	0.01%	98	0.07%
11	0	0.0%		0.00%		0.00%	18	0.00%	25	0.02%
12	0	0.0%		0.00%		0.00%	8	0.00%	4	0.00%
13		0.0%		0.00%		0.00%	2	0.00%	1	0.00%
sum	274420		146346		128074		1377284		137127	

Table 4.10. Vehicles by traffic lane in New York

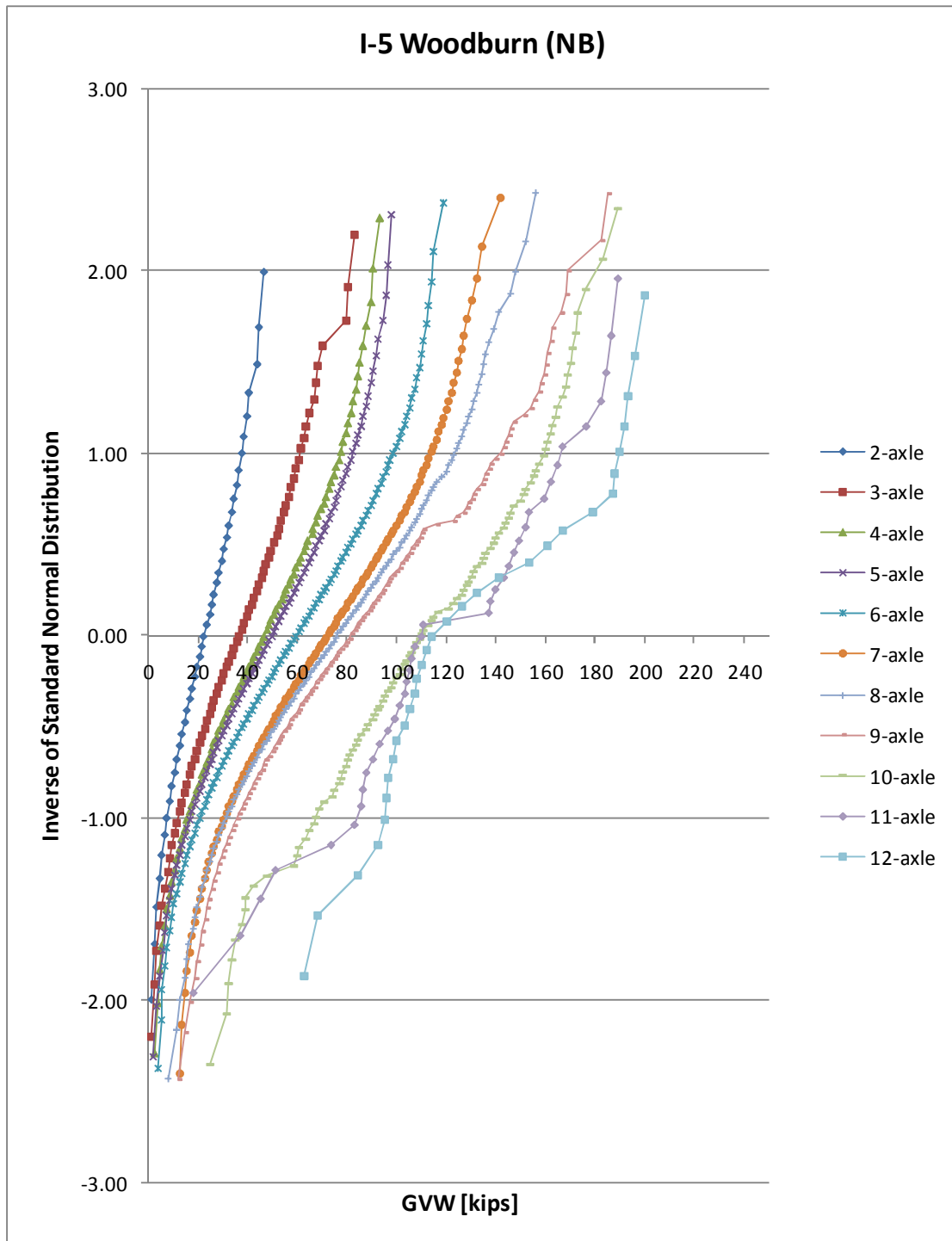| lane	I-495 EB		I-495 WB		NY 9121		NY 2680	
1	52703	36.01%	43278	33.79%	618289	44.89%	46008	33.55%
2	90625	61.93%	78891	61.60%	88037	6.39%	3148	2.30%
3	3018	2.06%	5905	4.61%	74831	5.43%	8298	6.05%
4	0	0.00%		0.00%	596129	43.28%	79677	58.10%
sum	146346		128074		1377286		137131	

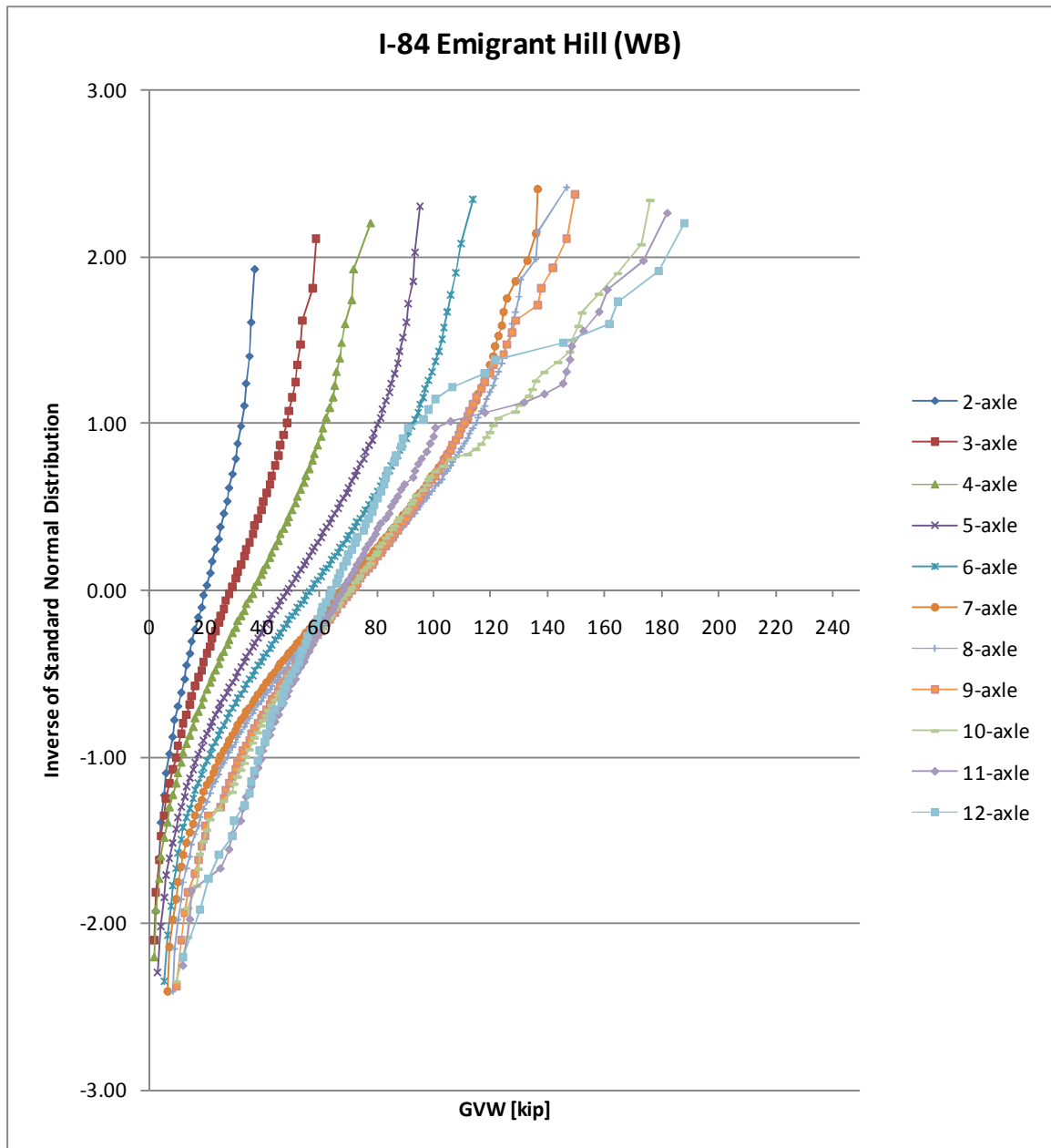Figure 4.9. CDF's of GVW by axles Oregon I-5 Woodburn

Figure 4.10. CDF's of GVW by axles Oregon I-84 Emigrant Hill
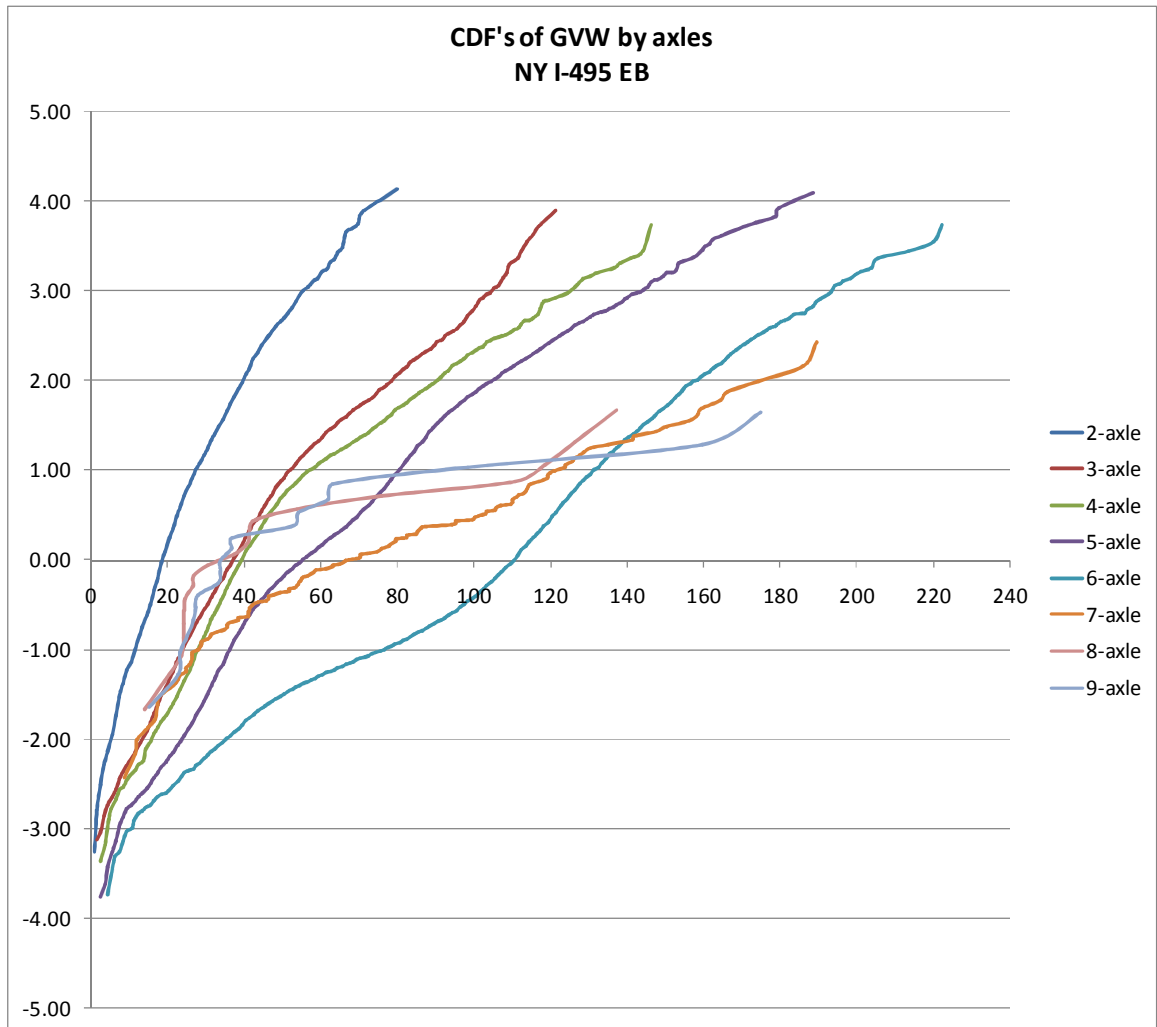
Figure 4.11. CDF's of GVW by axles NY I-495 EB

CHAPTER 5

DEVELOPMENT OF LIVE LOAD MODEL

5.1.   INTRODUCTION

For long span bridges, the extreme live load is governed by the traffic jam scenario. The live load is modeled as the uniformly distributed lane load and additional axle load or single truck for deck components. Development of live load model is based on three approaches. Two of them can be classified as initial studies. The first of them is based on a 5-axle average truck and the second one is based on AASHTO LRFD legal load trucks. The third approach is detailed study based on truck WIM Data.

5.2.   MODEL BASED ON AVERAGE 5-AXLE TRUCK

For computation of the live load on the most loaded lane, the following traffic model has been assumed:

- Traffic jam situation, Figure 5.1.
- Left lane loaded only with average trucks.
- Average trucks are 5-axle trucks, which are the most popular among truck types, Figure 5.4 and Figure 5.5. In the FHWA WIM Data, vehicle categories 1-3 FHWA are omitted, therefore the percentage of 2-axle vehicles is relatively low.

61

- An average 5-axle truck:

    - is 45 ft long

    - weights 55 kips, Figure 5.2 and Figure 5.3.

- Clearance distance is 10 to 15 ft, therefore spacing between the last axle of one truck and first axle of the following truck is 20-25 ft.

Live load due to such a combination of vehicles is equal to:

55 kip / 70 ft = 0.79 kip/ft for clearance distance of 15 ft

55 kip / 65 ft = 0.85 kip/ft for clearance distance of 10 ft
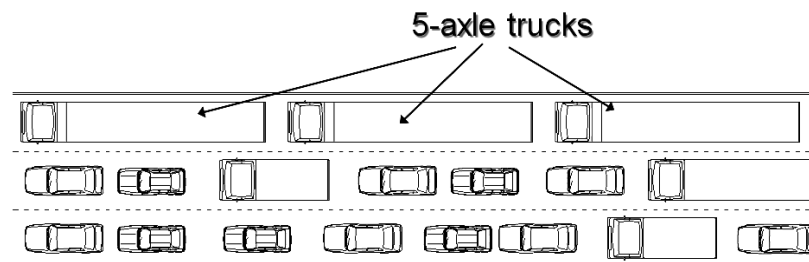
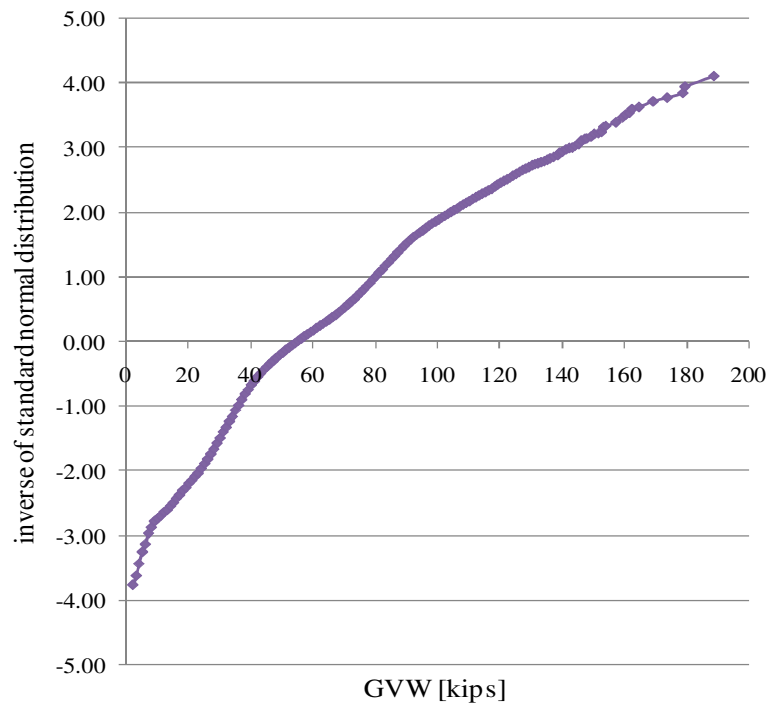Figure 5.1. Critical loading. Traffic jam scenario.

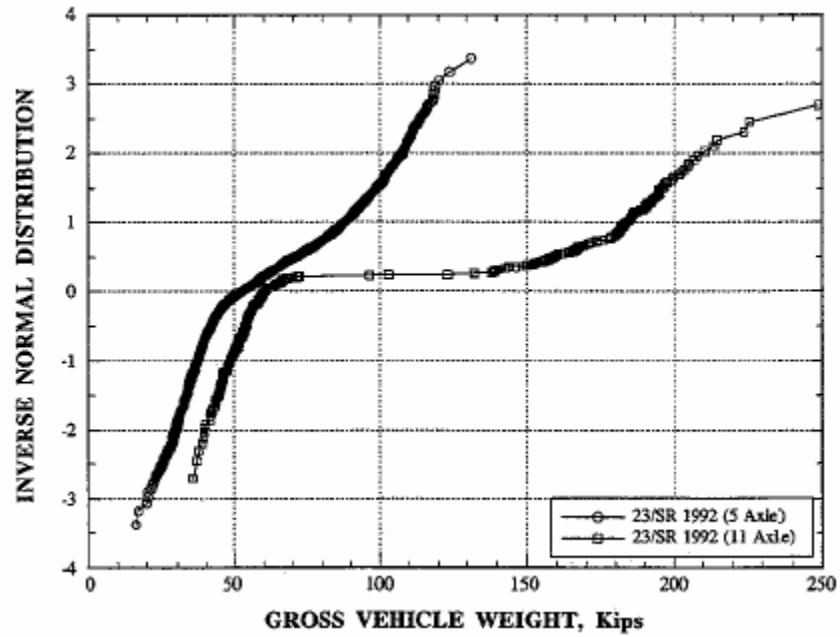Figure 5.2. CDF's of GVW for 5-axle trucks. New York WIM Data.

62

Figure 5.3. CDF of GVW for 5-axle and 11-axle trucks

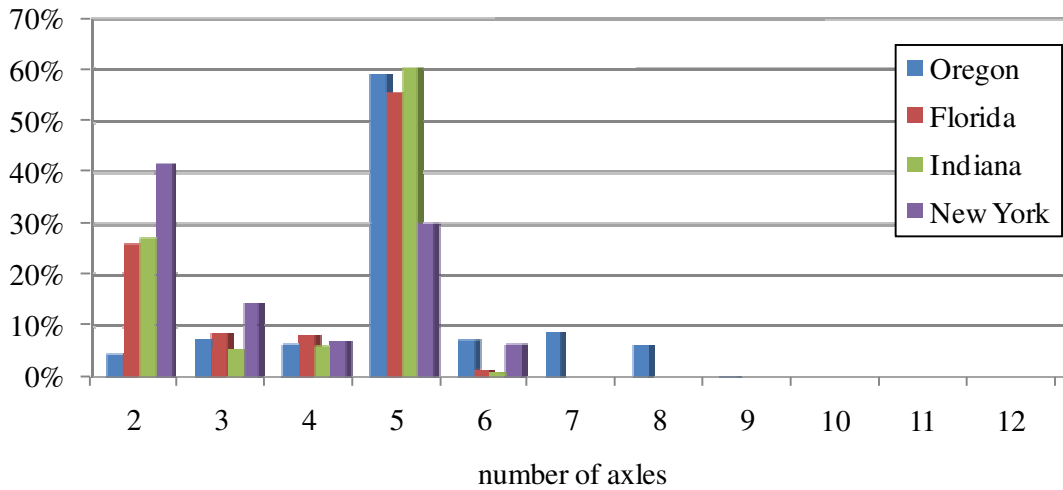(Nowak, A.S., Laman, J. and Nassif, H., 1994)

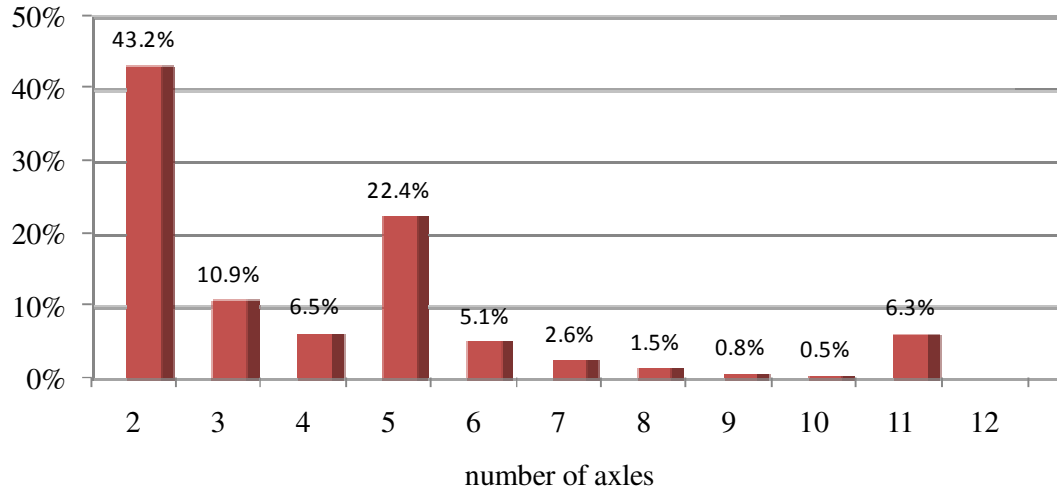Figure 5.4. Percentage of vehicles by number of axles. FHWA WIM Data.

Figure 5.5. Percentage of vehicles by number of axles.

(Kim, S-J., Sokolik, A.F., and Nowak, A.S., 1997)

If we would like to consider all types of trucks, not only 5-axles, the result would be similar. The mean value of GVW is above 50 kips, Figure 5.6.
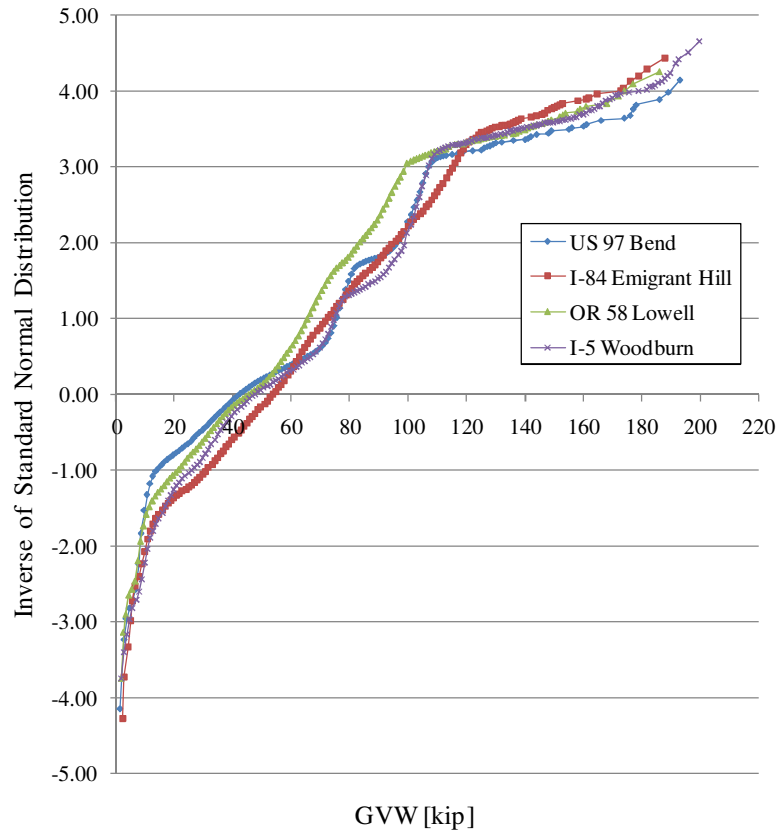

Figure 5.6. CDF's of GVW for all types of vehicles in Oregon.

64

5.3. MODEL BASED ON LEGAL LOAD TRUCKS

The second approach to model live load is based on vehicles called "legal load types", which are developed in AASHTO. Some of the states use them for rating instead of the traditional HS-20 load. These vehicles were selected to match the federal bridge formula (known as Formula B) for vehicles up to 80 000 lb. While HS-20 was intended to be appropriate for all span ranges, three legal AASHTO vehicles (Type 3 Unit, Type 3S2 Unit, Type 3-3 Unit) are supposed to adequately model short vehicles and a combination of vehicles for short, medium and long spans respectively.

To model traffic jam situations on long span bridge the Type 3-3 Units have been placed in a lane with the clearance distance of 10 to 15 ft. Therefore spacing between the last axle of one truck and first axle of the following truck is 20-25 ft. Figure 5.7. Gross Vehicle Weight of a Type 3-3 Unit is 80 kips and total length of a Type 3-3 Unit is 54 ft, therefore:

$$80 \text{ kips} / (54+25) \text{ ft} = 1.01 \text{ kip/ft for clearance distance of 15 ft}$$
$$80 \text{ kips} / (54+20) \text{ ft} = 1.08 \text{ kip/ft for clearance distance of 10 ft}$$

Since the value obtained in this way is based on heavy trucks and it is very conservative, its value can be multiplied by factor 0.75. This approach derives from basic philosophy used to develop lane load of 0.64 kip/ft.

$$0.75 \times 1.01 \text{ kip/ft} = 0.76 \text{ kip/ft}$$
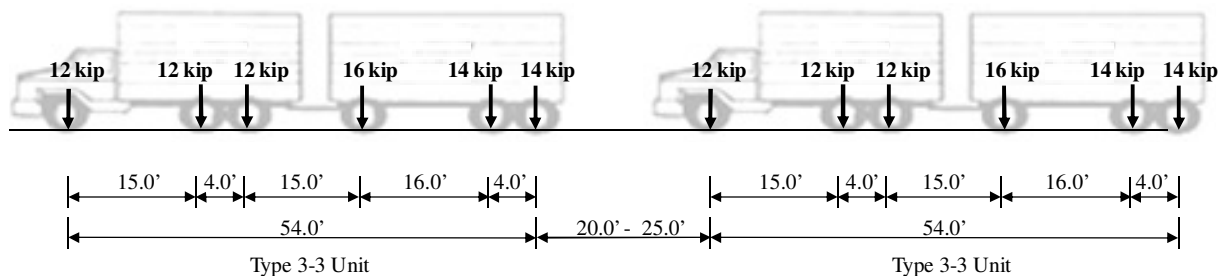$$0.75 \times 1.08 \text{ kip/ft} = 0.81 \text{ kip/ft}$$

Figure 5.7. AASHTO LRFD legal load trucks, Type 3-3 Units.

5.4.   MODEL BASED ON TRAFFIC JAM SIMULATION USING WIM DATA

The considered WIM data was obtained from NCHRP 12-76, described in CHAPTER 4. The available data served as a basis for simulation of a traffic jam situation. Starting with the first truck, all consecutive trucks were added with a fixed clearance distance between them until the total length reached the span length (Figure 5.8). Then, the total load of all trucks was calculated and divided by the span length to obtain the first value of the average uniformly distributed load. Next, the first truck was deleted, and one or more trucks were added so that the total length of trucks covers the full span length and the new value of the average uniformly distributed load was calculated. The calculations were performed for span lengths 600, 1000, 2000, 3000, 4000, and 5000 ft. Trucks were kept in actual order, as recorded in the WIM surveys. Clearance distance is assumed to be about 15 ft, while spacing between the last axle of one truck and first axle of the following truck is 25 ft. Clearance concept is as defined as in Figure 5.9, and according to literature it varies between 6 and 21 ft. Spacing between the last axle of one truck and first axle of the following truck is clearance plus distance from first and last axles to corresponding bumpers, based on the most common 5-axle truck WB-20 defined in *"AASHTO Geometric Design of Highways and Streets*. Only the most loaded lane was considered. It was assumed that in a traffic jam situation, light vehicles are using faster lanes, therefore, vehicles of the 1-3 FHWA category were omitted.
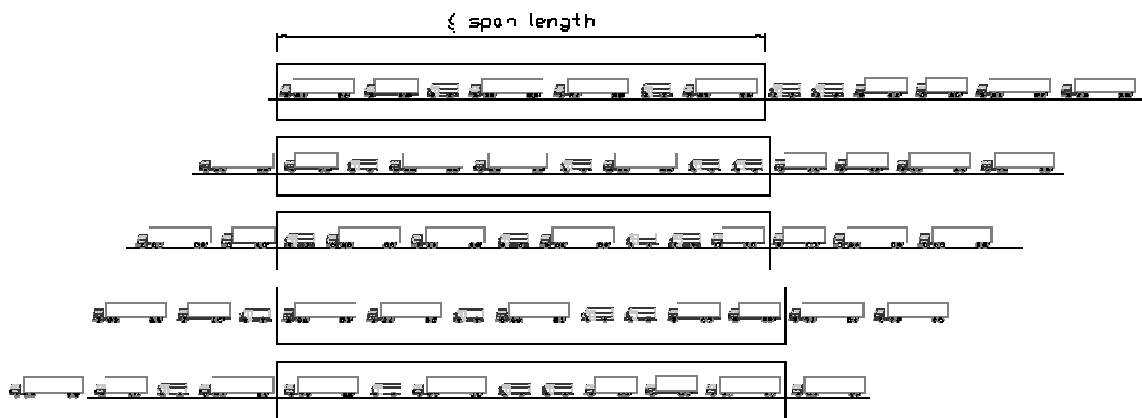

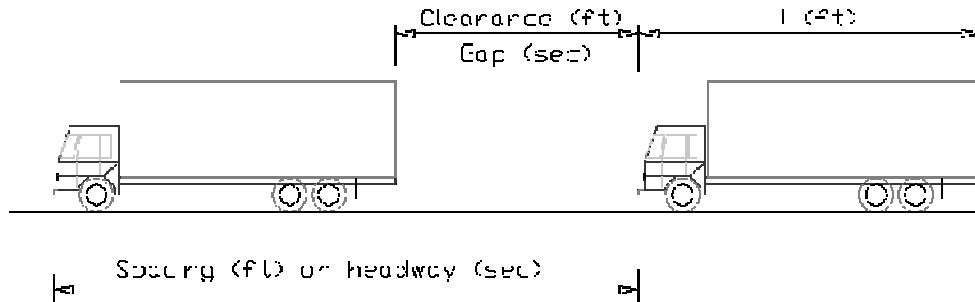Figure 5.8. Simulation of trucks moving throughout span length

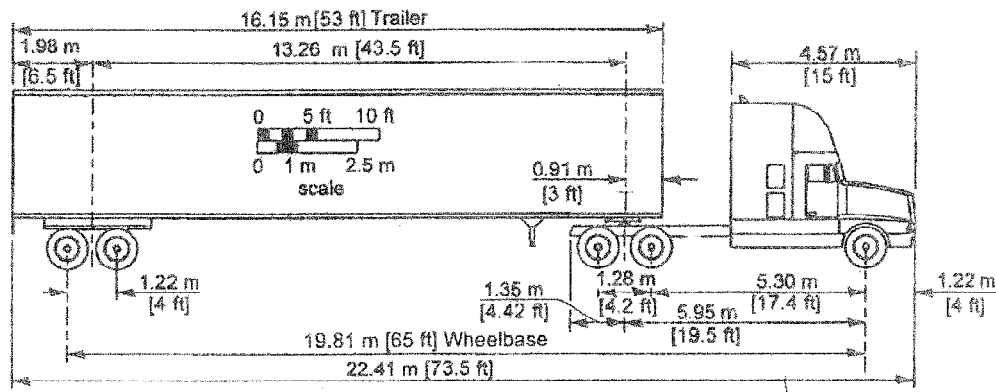Figure 5.9. Clearance - Gap and Spacing - Headway Concepts

Figure 5.10. Interstate semitrailer WB-20
(AASHTO Geometric Design of Highways and Streets)

To perform an extensive number of simulations on the huge databases for each site and different span lengths, a numerical procedure based on Visual Basic coding were developed. WIM data, such as weight and length of the trucks in actual order, had to be inputted to the program. The desired clearance distance was added automatically before computation. Running the computation was an extremely time consuming process.

Results of the simulations were plotted as a cumulative distribution function (CDF) of uniformly distributed load for considered span lengths. The CDF's for all simulated data are presented in Appendix A, CDF's of daily maximum combinations in Appendix B, and CDF's of weekly maximum combination in Appendix C.

Calculations were performed for one month, three, four, six, nine months or one year data depending on localization. Even though it is a long period of time, it is small compared to the actual life time of the structure. The uniformly distributed loads

67

corresponding to longer period of time, 75 years, were calculated by extrapolation of simulated results. The extrapolated distributions are shown for maximum daily and weekly combinations (Appendix B and Appendix C). Let N be the number of truck combinations in time period T and assume that the traffic will remain the same. For T = 75 years, N will be larger 900 times for one month data, 300 times for 3 month, 75 times for one year data etc. For example, for a site with 400,000 truck combinations monthly, this will result in N = 360 million truck combinations. The probability corresponding to N is 1/N. For 360 million, it is $1/360,000,000 = 2.8 \times 10^{-9}$, which is 5.83 on the vertical scale of CDF plot. Probability corresponding to extrapolated maximum daily truck is 3.65×10^{-5}, and to maximum weekly truck is 2.56×10^{-4}. The number of truck combinations N, probabilities 1/N, and inverse normal distribution corresponding to 75 years periods are shown in Table 5.2.

From the results of simulations, the statistical parameters of live load were obtained. It was noticed that mean value of uniformly distributed load oscillates between value 0.50 and 0.75 k/ft (Figure 5.12). The value 0.75 k/ft is close to those obtained in two previous models. The mean daily and weekly maximum can be found in Figure 5.12 and Figure 5.13. For longer spans uniformly distributed load decreases and is closer to mean value. This observation confirms that for a long loaded span, one heavily overloaded truck does not have significant influence. This is because the load depends on a mix of traffic. The bias factors (ratio of mean to nominal) were calculated for the heaviest 75-year combination of vehicles. The 75-year uniformly distributed loads were derived from extrapolated distributions. In Figure 5.16, it can be noticed that the bias factor values for some sites do not exceed 1.25, which is similar as for short and medium spans, as shown in the NCHRP Report 368 (1999). It is recommended to use HL-93 also for those long spans (Figure 5.11). To keep bias value below 1.0, it would be necessary to increase design value of uniformly distributed load to 0.85 k/ft (Figure 5.17). Brides in localizations with high ADDT and high percentage of overloaded trucks, such as those in New York, will require development of site specific models. For some sites with very heavy traffic, the bias factor reaches value 2.0 (Figure 5.16). Therefore, for those bridges the uniformly distributed load should be higher. It was found that to not exceed bias 1.25, the uniformly distributed load should be 1.2 kip/ft (Figure 5.18). The heaviest truck

68

combinations were observed on I-475, Throggs Neck Bridge in New York. They have been presented in Table 5.3.

The coefficient of variation is calculated from the slope of transformed CDF. Figure 5.19 and Figure 5.20 present coefficient of variation of daily and weekly maximum uniformly distributed load. Daily maximum uniformly distributed load has more variation due to weekends. Lighter traffic during weekends can be observed in lower tail of CDF's. Estimated coefficients of variation were derived from weekly maximum values, excluding sites from Yew York. Calculated statistical parameters for uniformly distributed load are summarized in Table 5.1.
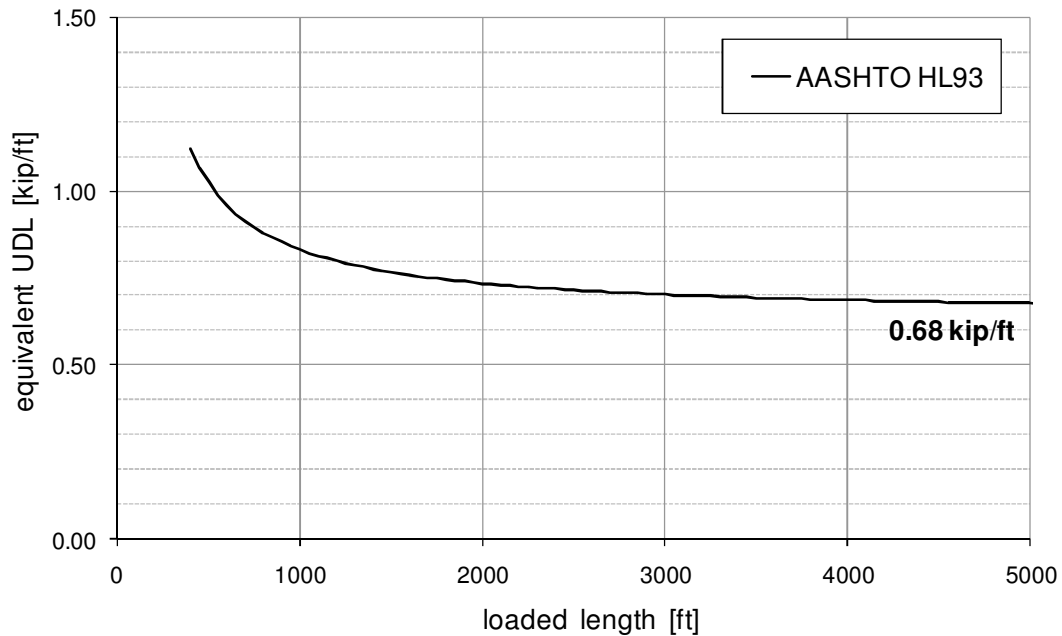

Figure 5.11. HL-93 proposed for long span bridges

Table 5.1. Statistical parameter for proposed uniformly distributes live load

span length	Bias	CoV
600 – 1000 ft	1.25	0.10
> 1000 ft	1.20	0.08

Table 5.2. Summary of simulated data

State	Site ID	Route	Number of truck combinations	Time period	75-years probability
FL	9916	US-29	247,449	1 year	5.39×10^{-8}
FL	9919	I-95	222,368	3 months	1.50×10^{-8}
FL	9927	SR-546	225,868	1 year	5.90×10^{-8}
FL	9936	I-10	188,990	1 year	7.05×10^{-8}
IN	9512	I-74	167,630	1 month	6.63×10^{-9}
IN	9534	I-65	266,333	1 month	4.17×10^{-9}
IN	9544	I-80/I-94	406,418	1 month	2.73×10^{-9}
OR	Woodburn	I-5	552,390	4 months	8.04×10^{-9}
OR	Emigrant Hill	I-84	213,019	4 months	2.09×10^{-8}
OR	Lowell	OR 58	51,406	4 months	8.65×10^{-8}
OR	Bend	US 97	59,225	3 months	7.50×10^{-8}
NY	9121	I-81	300,500	6 months	2.22×10^{-8}
NY	2680	8	45,030	9 months	2.23×10^{-7}
NY		I-495WB	43,200	1 month	2.57×10^{-8}
NY		I-495EB	52,618	1 month	2.11×10^{-8}
		sum	**3,042,444**		

Table 5.3. Heaviest truck combinations for 600 ft on I-495 WB

| number of axles	W	L	W	L	W	L	W	L	W	L	W	Total length	GVW		
	[kip]	[ft]	[kip]	[ft]	[kip]	[ft]	[kip]	[ft]	[kip]	[ft]	[kip]	[ft]	[kip]		
5	20.04	17.39	41.41	4.27	35.68	22.31	38.77	4.27	37.44	0.00	0.00	73.3	173.3		
2	27.97	19.69	32.82	0.00	0.00	0.00	0.00	0.00	0.00	0.00	0.00	44.7	60.8		
5	33.26	17.72	36.12	4.27	33.04	23.62	25.11	3.94	28.41	0.00	0.00	74.6	155.9		
3	30.40	16.08	26.87	4.27	27.75	0.00	0.00	0.00	0.00	0.00	0.00	45.4	85.0		
2	28.19	22.97	42.73	0.00	0.00	0.00	0.00	0.00	0.00	0.00	0.00	48.0	70.9		
5	35.68	15.42	37.44	4.27	38.55	34.45	33.04	3.94	32.38	0.00	0.00	83.2	177.1		
5	33.48	12.14	43.83	3.94	38.99	28.87	43.61	3.94	39.87	0.00	0.00	74.0	199.8		
5	38.11	13.12	25.33	4.27	20.48	31.50	19.60	3.94	23.57	0.00	0.00	77.9	127.1		
2	33.26	15.75	39.87	0.00	0.00	0.00	0.00	0.00	0.00	0.00	0.00	40.8	73.1		
												561.9	1123.1	2.00	k/ft
2	11.23	18.70	21.15	0.00	0.00	0.00	0.00	0.00	0.00	0.00	0.00	43.7	32.4		
5	20.04	17.39	41.41	4.27	35.68	22.31	38.77	4.27	37.44	0.00	0.00	73.3	173.3		
2	27.97	19.69	32.82	0.00	0.00	0.00	0.00	0.00	0.00	0.00	0.00	44.7	60.8		
5	33.26	17.72	36.12	4.27	33.04	23.62	25.11	3.94	28.41	0.00	0.00	74.6	155.9		
3	30.40	16.08	26.87	4.27	27.75	0.00	0.00	0.00	0.00	0.00	0.00	45.4	85.0		
2	28.19	22.97	42.73	0.00	0.00	0.00	0.00	0.00	0.00	0.00	0.00	48.0	70.9		
5	35.68	15.42	37.44	4.27	38.55	34.45	33.04	3.94	32.38	0.00	0.00	83.2	177.1		
5	33.48	12.14	43.83	3.94	38.99	28.87	43.61	3.94	39.87	0.00	0.00	74.0	199.8		
5	38.11	13.12	25.33	4.27	20.48	31.50	19.60	3.94	23.57	0.00	0.00	77.9	127.1		
												564.9	1082.4	1.92	k/ft
5	38.99	14.11	35.68	4.27	31.94	17.39	28.85	3.94	31.28	0.00	0.00	64.8	166.7		
5	37.00	12.14	40.09	4.27	33.04	32.48	30.84	3.94	37.22	0.00	0.00	77.9	178.2		
5	37.67	10.50	22.47	4.27	24.01	26.57	15.42	10.17	18.28	0.00	0.00	76.6	117.8		
2	29.07	16.08	38.11	0.00	0.00	0.00	0.00	0.00	0.00	0.00	0.00	41.1	67.2		
3	43.61	18.70	21.37	4.59	27.53	0.00	0.00	0.00	0.00	0.00	0.00	48.3	92.5		
2	34.14	21.33	26.21	0.00	0.00	0.00	0.00	0.00	0.00	0.00	0.00	46.4	60.4		
5	40.75	13.45	30.62	4.27	25.33	30.51	22.03	3.94	22.47	0.00	0.00	77.3	141.2		
5	35.46	10.50	22.03	4.27	20.70	22.64	20.04	4.27	20.48	0.00	0.00	66.7	118.7		
3	36.56	19.69	37.00	4.27	31.06	0.00	0.00	0.00	0.00	0.00	0.00	49.0	104.6		
												548.1	1047.4	1.91	k/ft
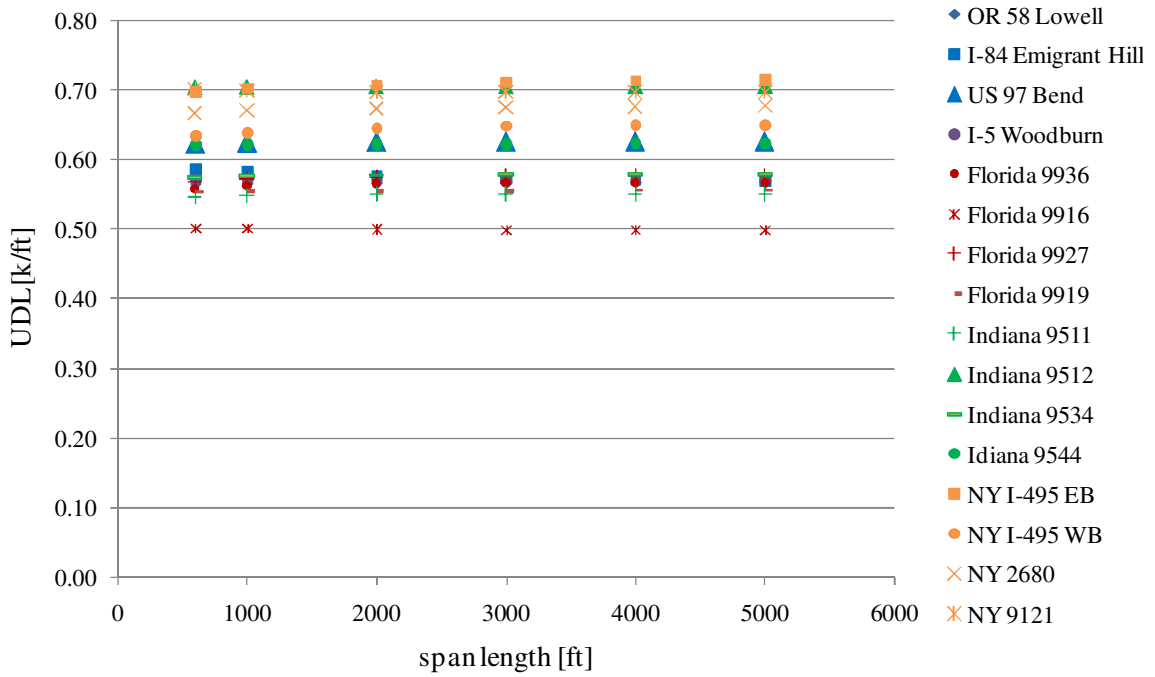
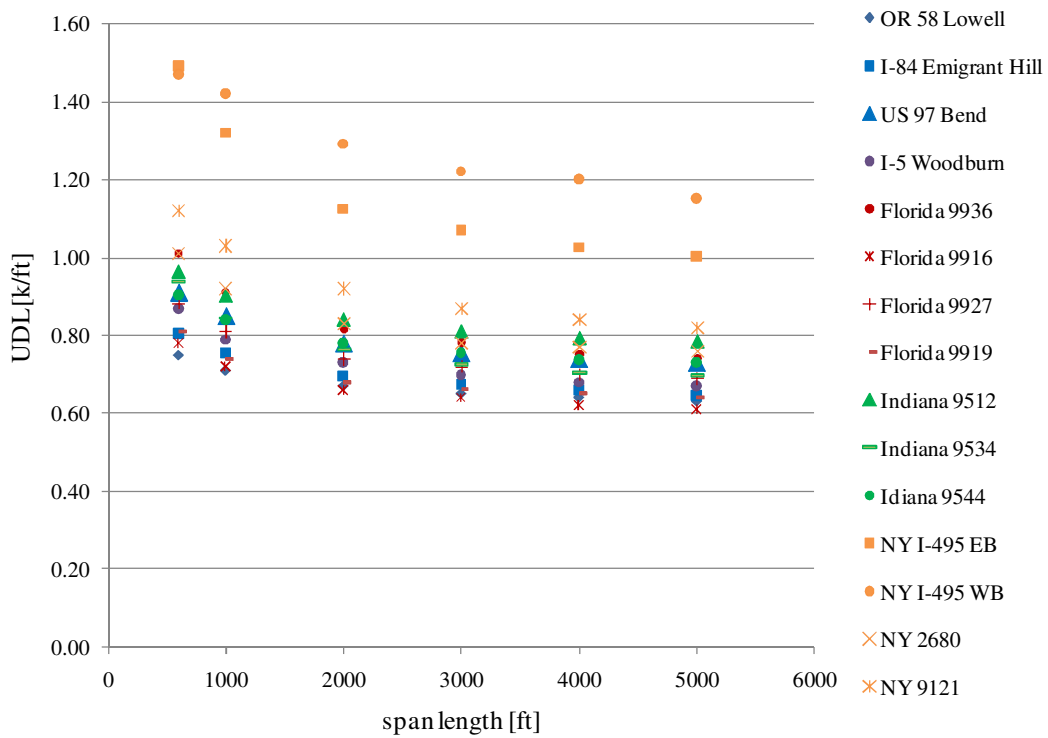Figure 5.12. Mean value of uniformly distributed load

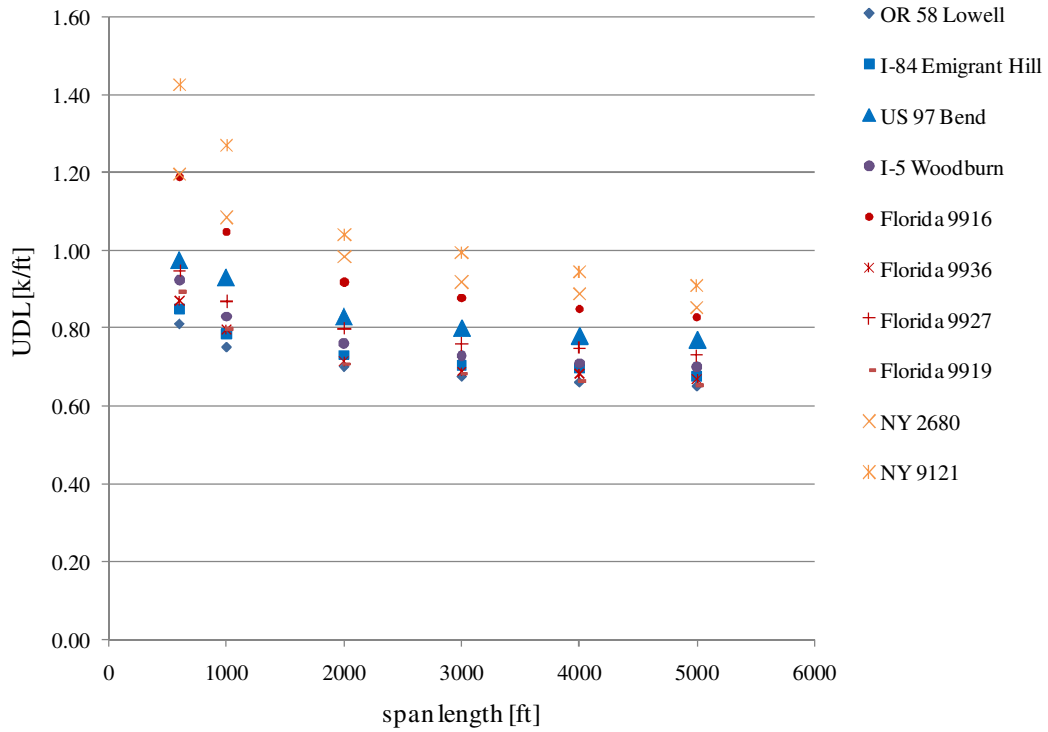Figure 5.13. Daily maximum mean value of uniformly distributed load

72

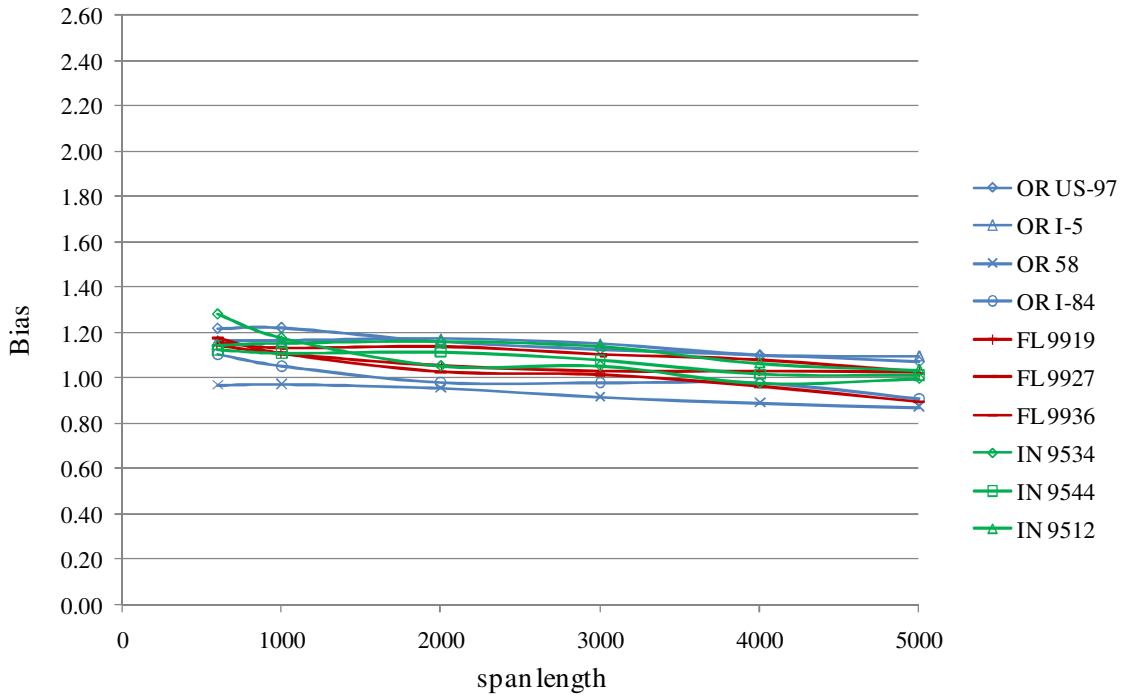Figure 5.14. Weekly maximum mean value of uniformly distributed load

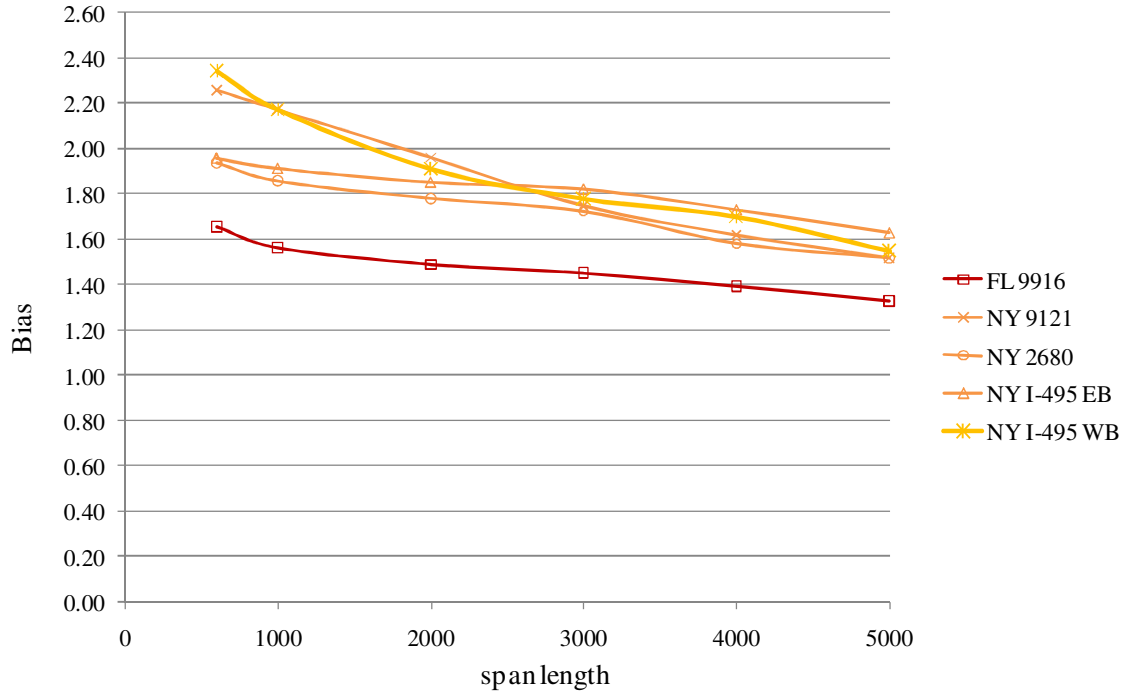Figure 5.15. Bias (mean max 75 year to nominal value of UDL)

73

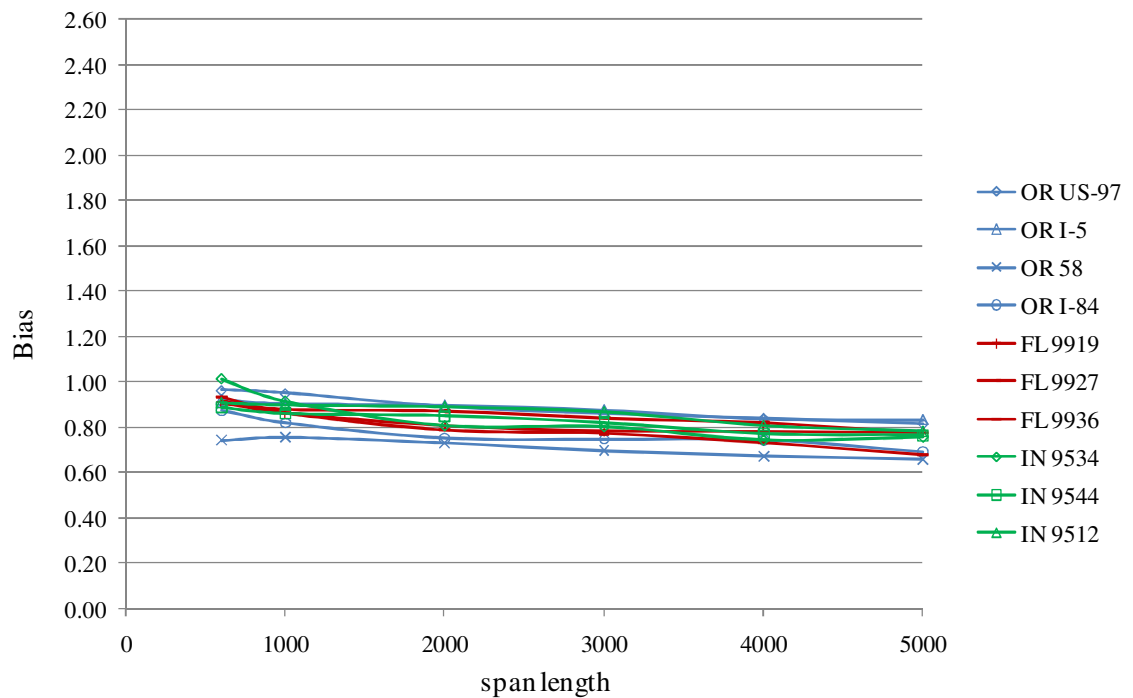Figure 5.16. Bias (mean max 75 year to nominal value of UDL)

Figure 5.17. Bias (mean max 75 year to nominal value of UDL)
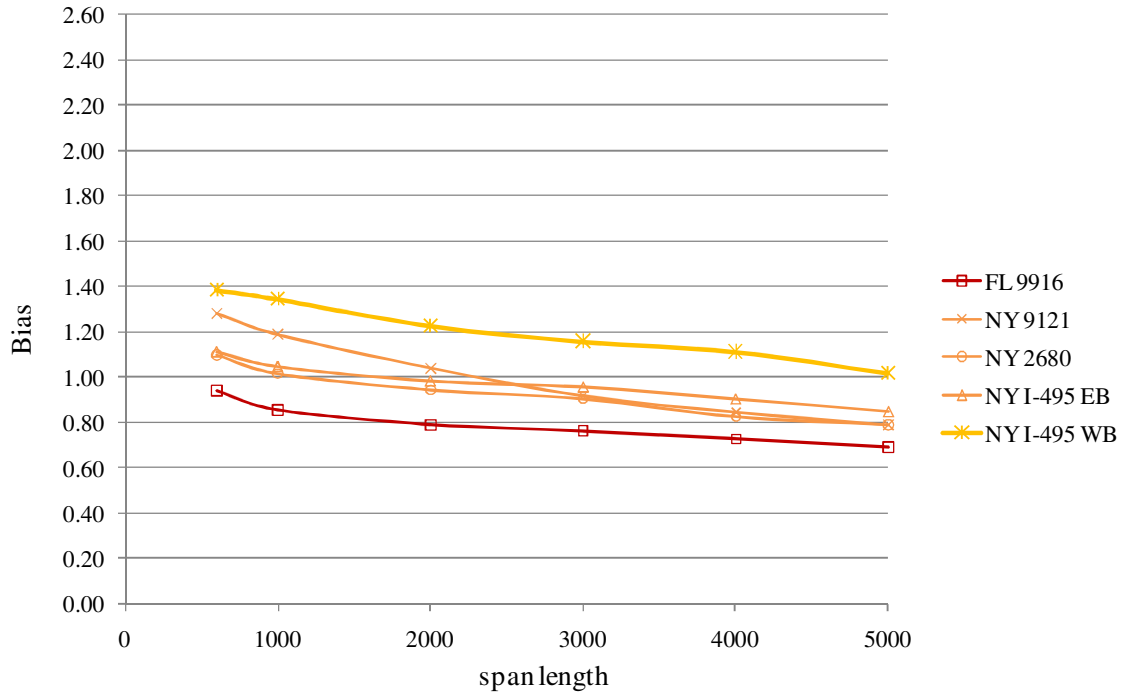
assumed designed UDL of 0.85 k/ft

74

Figure 5.18. Bias for heavily loaded localizations, assumed designed UDL of 1.25 k/ft
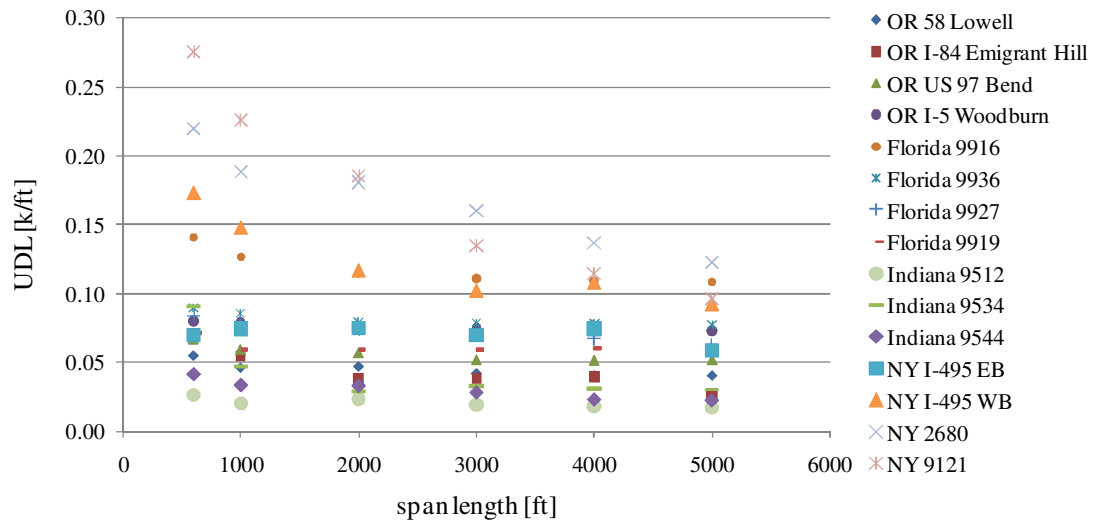
Figure 5.19. Coefficient of variation of daily maximum uniformly distributed load
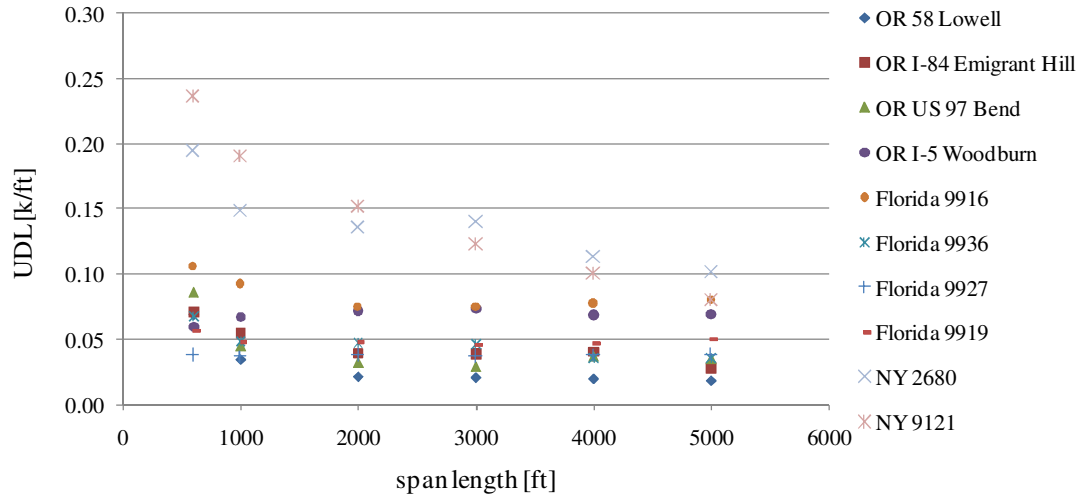
Figure 5.20. Coefficient of variation of weekly maximum uniformly distributed load
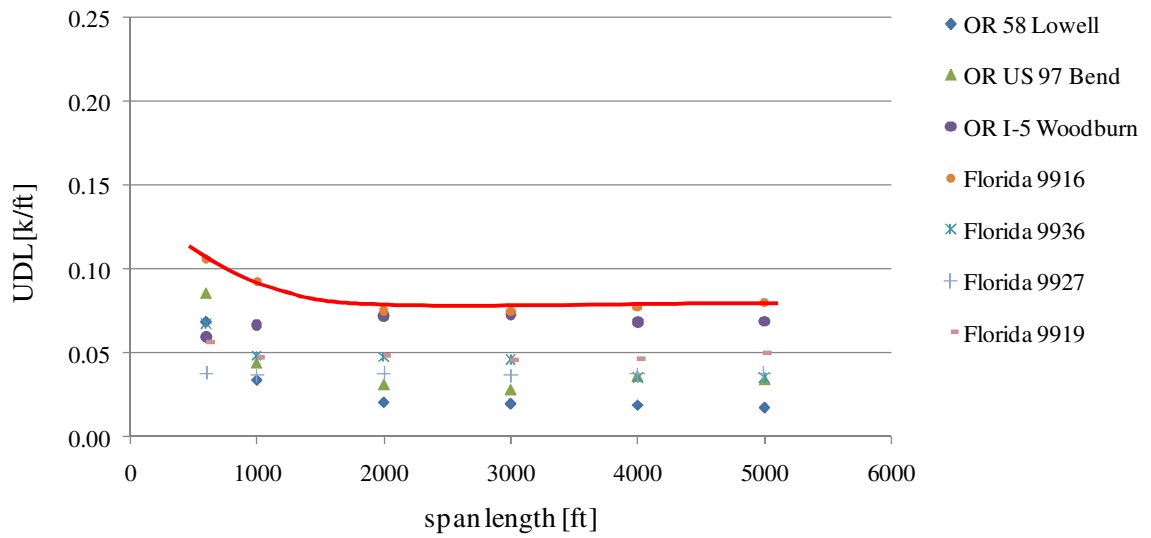
Figure 5.21. Proposed coefficient of variation of uniformly distributed load

76

CHAPTER 6

MULTIPLE PRESENCE

6.1.   INTRODUCTION

Determination of live loading for multiple traffic lanes is very important for appropriate bridge design. Each traffic lane can be loaded with different live load. The more traffic lanes the more difference in distribution of loading. Trucks tend to use right lanes loading them heavily, while passenger cars use faster left lanes. Structural components are strongly influenced by the location of trucks on the bridge. Those carrying the right lane of traffic are usually subjected to more load cycles and fatigue than the components closer the left lane. However, it has to be remembered that traffic can be deviated and truck can be directed to left lanes, for example during maintenance works on bridge. Presence of truck on multiple traffic lanes at the same time is critical from the bridge design point of view.

In this chapter, a short review of current studies on presence of multiple trucks, study of video recording of traffic jam situations, and discussion on different approaches to multilane reduction factors are presented. Multiple presence factors applied in international codes are discussed in CHAPTER 2.

77

6.2. STUDIES ON PRESENCE OF MULTIPLE TRUCKS

In 1993 Andrzej S. Nowak, Hani Nassif, and Leo DeFrain performed a study on the occupation of road lanes and presence of multiple truck. For the study, the database of over 600 000 trucks on two lanes in each direction was collected using weigh-in-motion equipment. It was found that 70-90% of trucks use the right lane (Table 6.1), and 65-70 percent of trucks are 5-axle trucks. The researchers had also found out that less than 2% of trucks appear simultaneously with another truck in the lane, 4-8% side by side in tandem or behind, with distance between front axles less than 50 ft (Table 6.1).

Table 6.1. Presence of multiple trucks and their location on the road lanes

Interstate highway	Eastbound					Westbound				
	right	left	in lane	side by side		right	left	in lane	side by side	
				tandem	behind				tandem	behind
I-94	1582 91,3%	151 8,7%	14 0,8%	28 1,6%	48 2,8%	2073 85,6%	349 14,4%	14 0,6%	86 3,6%	93 3,8%
U.S.-23	1685 82,0%	371 18,0%	24 1,2%	40 1,9%	76 3,7%	1247 67,5%	601 32,5%	2 0,1%	38 2,1%	34 1,8%

The results were later confirmed by the investigation by Gindy and Nassif (2006). Data used in this study was collected over an 11-year period between 1993 and 2003 by the New Jersey Department of Transportation. The study gives detailed analysis of the relation between multiple presences of trucks and four parameters: truck volume, area type, road type, and bridge span length. An increase in truck volume results in an increase of all multiple presence cases and a decrease in the frequency of single loading events (Figure 6.2). The area (urban or rural) and vicinity of industry affect the frequency of multiple truck presence. Heavier volume sites tend to be located in urban areas, and as a consequence more cases of multiple trucks can be observed. Increasing bridge spans also gives more opportunities for trucks to occur simultaneously (Figure 6.3). The frequency of staggered events increases faster for shorter spans and at a steadier pace for longer spans. Span length has almost no influence on the frequency of side-by-side trucks.

78

Assumptions of traffic patterns made for multiple presence analysis following (see Figure 6.1):

- single – only one truck is present on the bridge
- following – two trucks on the same lane with a varying clearance distance
- side-by-side – two trucks in adjacent lanes with an overlap at least one-half the body length of the leading truck
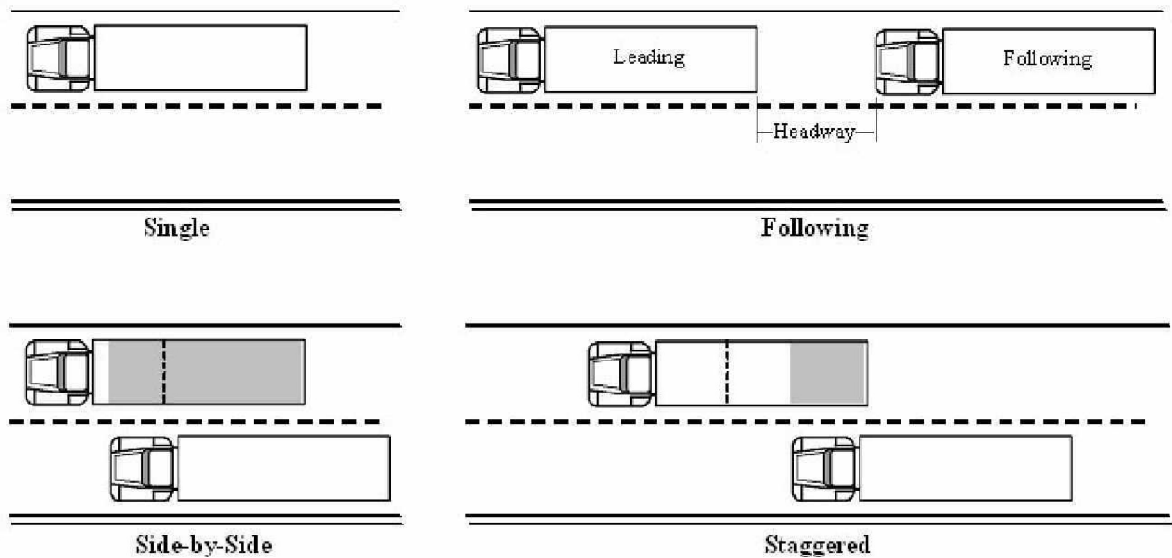- staggered – two trucks in adjacent lanes with an overlap at less than one-half the body length of the leading truck

Figure 6.1. Traffic loading pattern used for multiple truck presence statistics.

Comparing results of the study made by Andrzej S. Nowak, Hani Nassif, and Leo DeFrain in 1993 and the study made by Mayrai Gindy and Hani H. Nassif in 2006, some divergences can be observed. Some of them can be caused by the differences in the definition of "side-by-side" and "staggered" cases. Trucks which are considered "staggered" in one case can be considered as "side by side" in the other. However, joining those two cases and making a sum of those two values, we obtain relatively close results, 7.3 % for the study from 1993 and 6% for study from 2006. Regarding the occurrence of following trucks, values obtained in 1993 vary between 0.1 and 1.2%, and values obtained in 2006 vary between 1 and 8%. Those values cannot be compared

79

because of differences in the assumptions and definition of "following" trucks. Furthermore, the bridges taken into consideration in the study from 2006 were longer, which increases the probability of this occurring. The probability that the trucks will occur as following trucks increases with the span length.

In the report NCHRP 12-76 (2008), it is stated that multi-presence probabilities for permit trucks are different from those for normal traffic. The likelihood of permit trucks exceeding the authorized weight as well as the likelihood of the presence of multiple permit trucks is reduced.
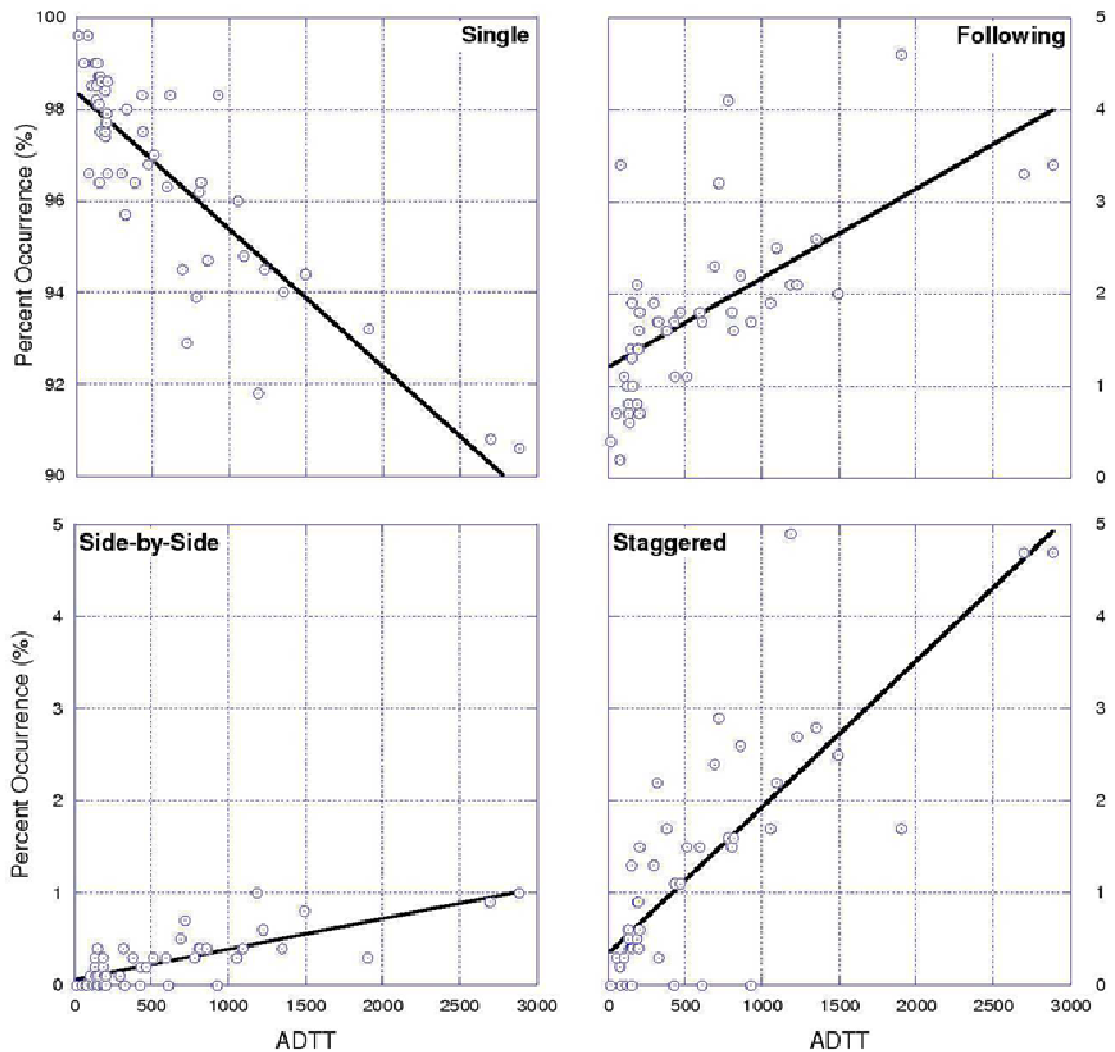
Figure 6.2. Variation of multiple truck presence statistics with respect to truck volume.
Gindy and Nassif (2006).
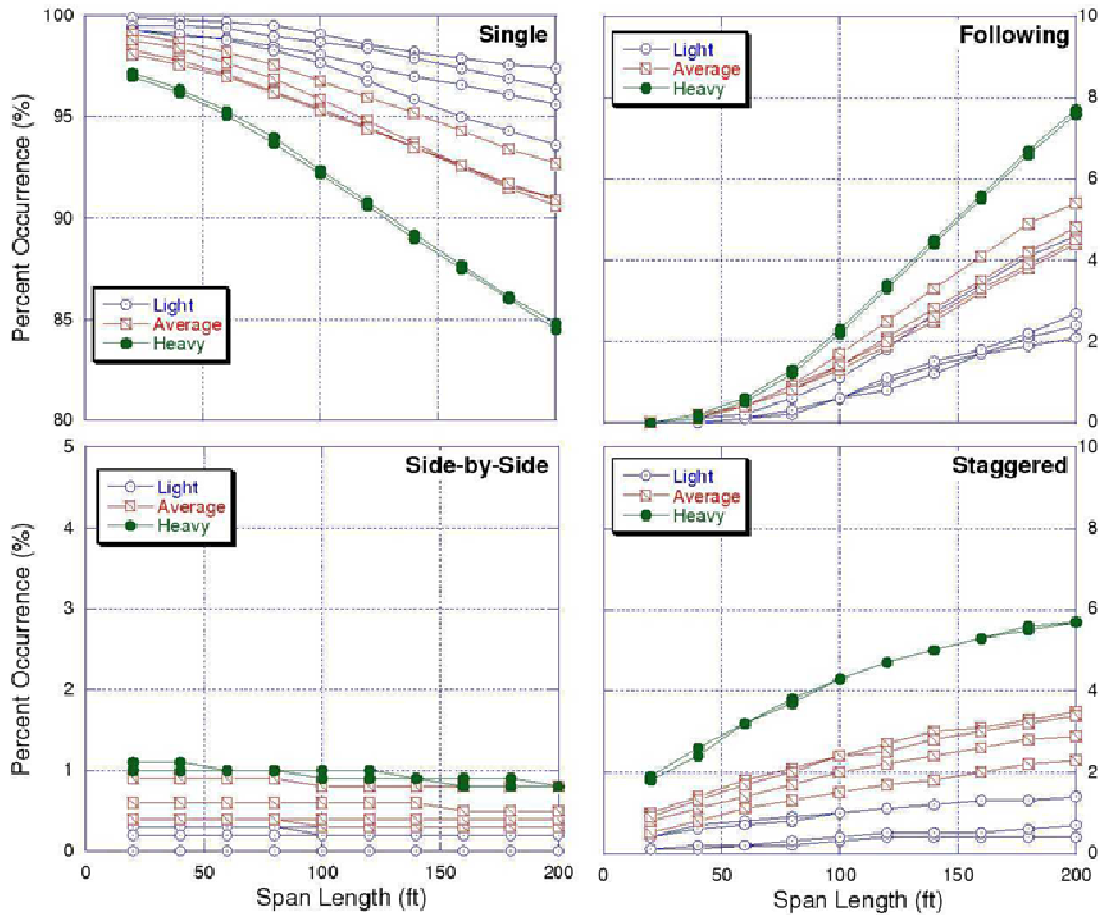
Figure 6.3. Variation of multiple truck presence statistics with respect to bridge span length. Gindy and Nassif (2006).

6.3. MULTIPLE PRESENCE OF TRUCKS BASED ON THE VIDEO FILES OF TRAFFIC

FHWA has provided a DVD including video files monitoring seven traffic situations in different sites, at different times and days of the week. The localization of the sites was not specified. Total time of all sixteen video recordings is 2 hours 6 minutes and 30 seconds. The list of video recordings is following:

- (1) 05.30.2008, Friday, 12.17 pm (33min44sec)
- (2) 05.29.2008, Thursday, 6.08pm (4min43sec)

81

- (3) 05.22.2008, Thursday, 11.22am (0min22sec)

- (4) 05.22.2008, Thursday, 11.20am (0min22sec)

- (5) 05.14.2008, Wednesday, 12.52pm (4min51sec)

- (6) 05.14.2008, Wednesday, 12.50pm *(2min26sec)*

- (7) 05.14.2008, Wednesday, 12.48pm *(1min47sec)*

- (8) 05.14.2008, Wednesday, 12.44pm *(3min59sec)*

- (9) 05.06.2008, Tuesday, 7.59am *(3min49sec)*

- (10) 05.01.2008, Thursday, 12.20pm *(1min04sec)*

- (11) 04.04.2008, Friday, 4.42pm *(9min28sec)*

- (12) 04.04.2008, Friday, 4.43pm *(8min54sec)*

- (13) 04.04.2008, Friday, 4.43pm *(0min36sec)*

- (14) 04.04.2008, Friday, 4.43pm *(19min26sec)*

- (15) 04.04.2008, Friday, 4.43pm *(22min53sec)*

- (16) 04.04.2008, Friday, 4.43pm *(8min06sec)*

The recordings show dense traffic jam situations, some of them being the result of traffic accidents. They allow for making some observations and conclusions regarding traffic patterns and the presence of multiple trucks moving at a crawling speed. This is the critical case from the point of view of live loading on bridges. Despite the fact the recordings are taken on highways, the recorded situations can be related to bridges as well. One of the most important observations is that even in very dense traffic it is very common to observe cars or pick-up among heavy vehicles (Figure 6.4).

Figure 6.4. Video 10, time: 00:00:58

The video file number 1 contains the longest and the most interesting material. It has a registered traffic accident on a highway having four lanes in one direction. The accident takes place on the second lane (counting from the external side). The second and the third lanes remain completely stopped by crushed cars and emergency vehicles for approximately half an hour. Passing cars are using the first and the fourth lanes. For a short period of time three lanes are blocked, and the passing cars can use only the fourth lane, that intensifies jam-packed traffic. For the majority of time we can observe that the moving lanes contain a mixture of trucks and cars. However, we can also observe some situations with multiple-presence of trucks occupying three or four lanes at the same time (Figure 6.5 and Figure 6.6). We can also observe a situation when one lane is almost exclusive occupied by trucks (Figure 6.6). Those cases should also be taken into consideration during the evaluation of design live load. There is no information about trucks' weight. However, it can be assumed that only a limited number of the trucks are correlated, and while some of them are fully loaded some percentage of them can be empty.

Figure 6.5. Video 1, time: 00:05:28
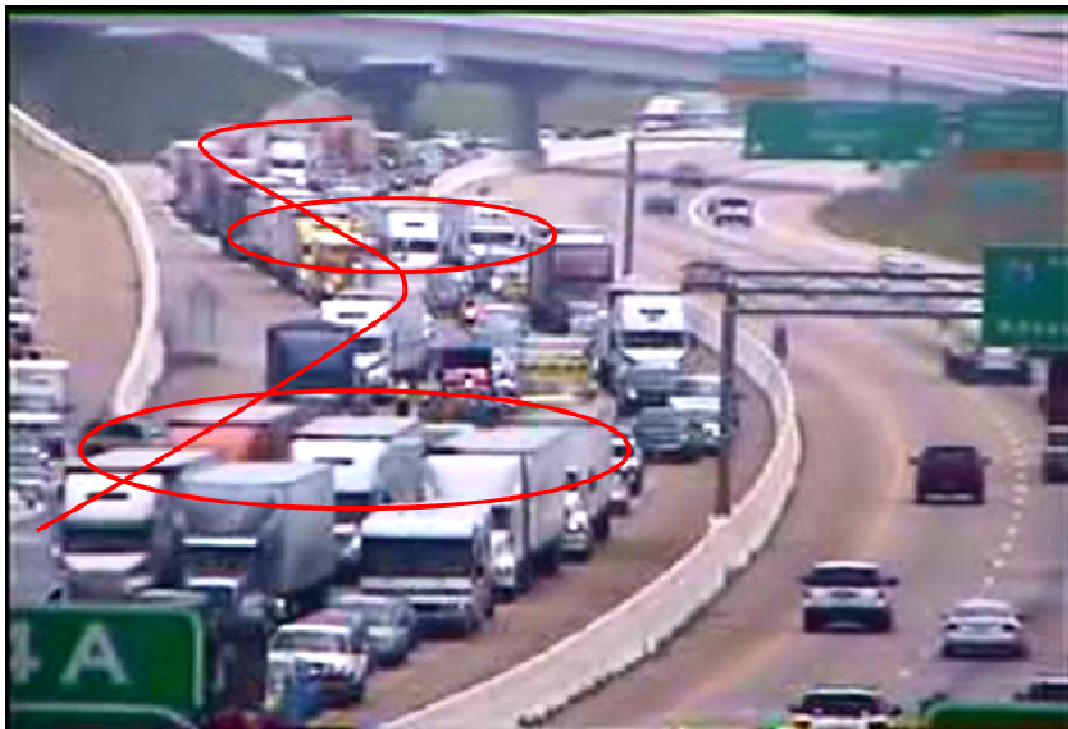
Figure 6.6. Video 1, time: 00:18:36

Some of the video files show traffic jam situations at roads junction that cannot be representative. The number of cars among trucks is increased because some of them are entering or exiting the highway (Figure 6.7 and Figure 6.8). This observation calls our attention to the importance of the appropriate selection of sites.

Figure 6.7. Video 2, time: 00:00:15

Figure 6.8. Video 8, time: 00:00:16

Video recordings from 11 to 16 show traffic situation caused by the same accident. Three lanes are blocked and the moving vehicles are using only one lane. However, warning signs posted adequately ahead result in the vehicles forming one lane and do not cause multilane traffic jam situation in the vicinity of the place of the accident. An ordered one lane of traffic is a mixture of trucks and cars. This situation does not allow for the observation of multiple truck presence situations.

6.4. APPROACHES TO MULTILANE REDUCTION FACTORS

There are many approaches to multilane reduction factors. International codes vary significantly in this matter (see CHAPTER 2), and all of them are much more simplified than actual situation.

Most of the design codes decrease the value of uniformly distributed load as the number of traffic lanes increases. The load value is the same on all traffic lanes, Figure 6.9.

86
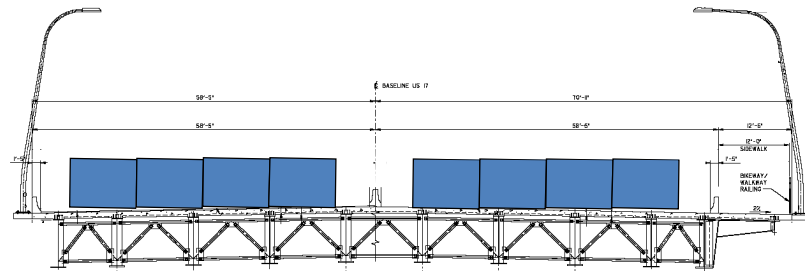
Figure 6.9. Multilane load in design codes AASHTO LRFD Code (2007), OHBDC (1991), CAN/CSA-S6-00 [2000], and ASCE (1981).

According to the Eurocode one of the lanes is loaded more than the others, Figure 6.10.
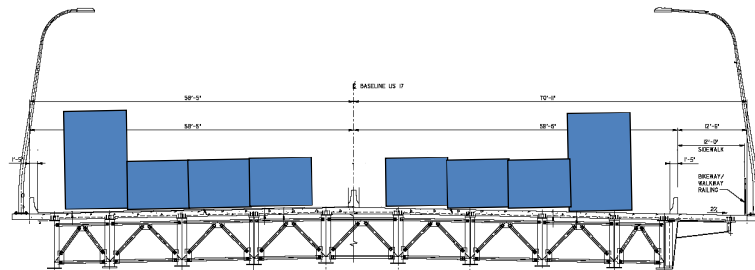
Figure 6.10. Multilane load in Eurocode 1.

The observations indicate that the actual traffic is distributed differently for each lane of traffic, Figure 6.11.
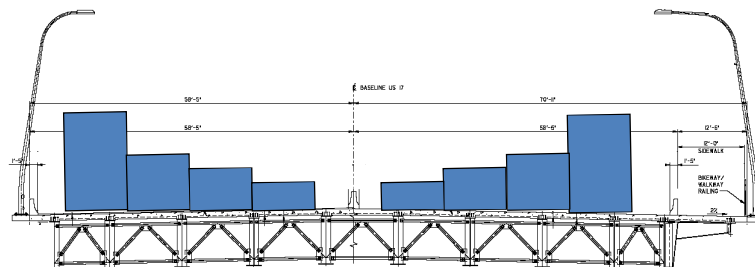
Figure 6.11. Multilane load in actual observation.

87

To reflect actual traffic situation would be very difficult and time consuming for designers. Therefore, the approach applied in the Eurocode seems the most practical one. Each of the lanes should be considered as the most loaded one, while the other lanes carry equal loading.

6.5. CONCLUSIONS

Presence of multiple trucks depend on factors such as: truck volume (light, average, heavy) area type (urban/rural), road type (major/minor), bridge span length, law enforcement, and traffic flow control, which can cause heavy truck queues. Therefore, multilane reduction factors could be very site specific.

Based on video recordings of traffic it was confirmed that for the majority of time we can observe that the moving lanes contain a mixture of trucks and cars. However, situations when one lane is almost exclusively occupied by trucks or trucks occupy three or four lanes at the same time are also possible. Multiple reduction factors for design live load should account for those the most critical loading cases.

In the available WIM database, the vehicles of 1-3 categories have not been registered. Therefore, it does not allow for simulations and derivation of multilane factors for all traffic lanes. Simulation of the traffic on the most loaded lane was possible with assumption, that it is occupied exclusively by trucks. In the traffic jam situations, the passenger vehicles are assumed to move to faster lanes.

It was concluded that the multilane reduction factors have to be an object of additional extensive studies. They have to account for intensive traffic jam situations, as those registered in the video recordings. As well, different distribution of loading on multiple traffic lanes has to be considered.

Since no new multilane reduction factors were proposed, those from the current AASHTO Code are used in this dissertation.

CHAPTER 7

DYNAMIC FACTOR

7.1. INTRODUCTION

The scope of this chapter is studying the origin and adequacy of the application of the dynamic load factor in bridge design. There is considerable variation in the treatment of dynamic load effects by bridge design codes in different countries (see CHAPTER 2). The most common approach is to apply dynamic response as a fraction or multiple of the response that would be obtained if the same forces or loads were applied statically. The objective of this simple approach is to not increase complexity for the designer. This is the approach specified in the current AASHTO Code. The live load model itself does not account for dynamics, but the dynamic amplification is added additionally as a percentage to static effects.

In this chapter there is a short review of the research studies. As well, a developed exemplary vehicle-bridge interaction model and the derivation of dynamic factor is presented. In the modeling a finite element software ABAQUS was used. Three-axle AASHTO truck HS-20 travelling over a 120 ft steel girder bridge is modeled. The truck is assumed to travel with the velocity of 40 miles per hour and with the crawling speed. The final result is comparison of the static the dynamic deflections, and derivation of dynamic factor for this specific case.

89

7.2. STUDIES ON PARAMETERS AFFECTING DYNAMIC BRIDGE RESPONSE

The dynamic response of a bridge to a crossing vehicle is a complex problem affected by the dynamic characteristics of the bridge, the vehicle, and by the bridge surface conditions. Many of the parameters interact with one another, further complicating the issue. Consequently, many research studies have reported seemingly conflicting conclusions. Based on the review of past research, the effects of various parameters on the dynamic response of bridges to vehicular loading are discussed in this paragraph.

Bridge Fundamental Frequency

The fundamental frequency of vibration for a bridge due to vertical loading has a significant effect on the dynamic response. If the frequencies of the bridge and vehicle converge, the dynamic response induced may be large. A majority of the fundamental frequencies for typical bridges are in the range of 2 to 5 Hz (Figure 7.1), which corresponds to the body bounce response frequency range of a truck.
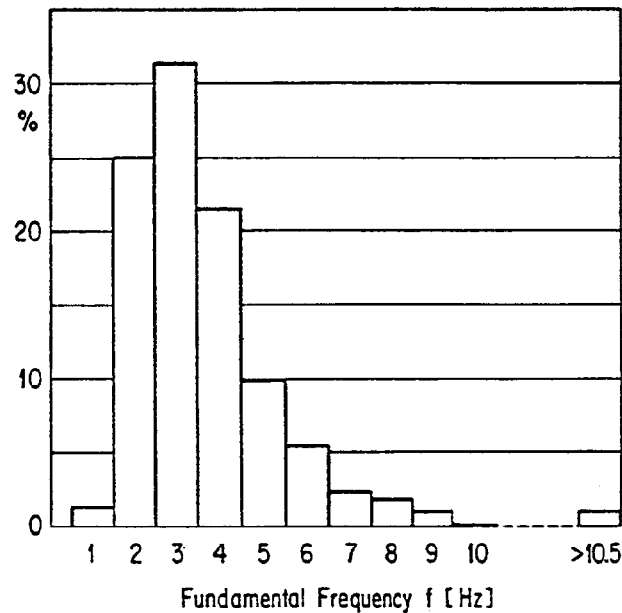
Figure 7.1. Distribution of fundamental bridge frequencies

(Cantieni 1984)

Field measurements and values obtained from analytical modeling show relation between frequencies and bridge span (Figure 7.2 and Figure 7.3).
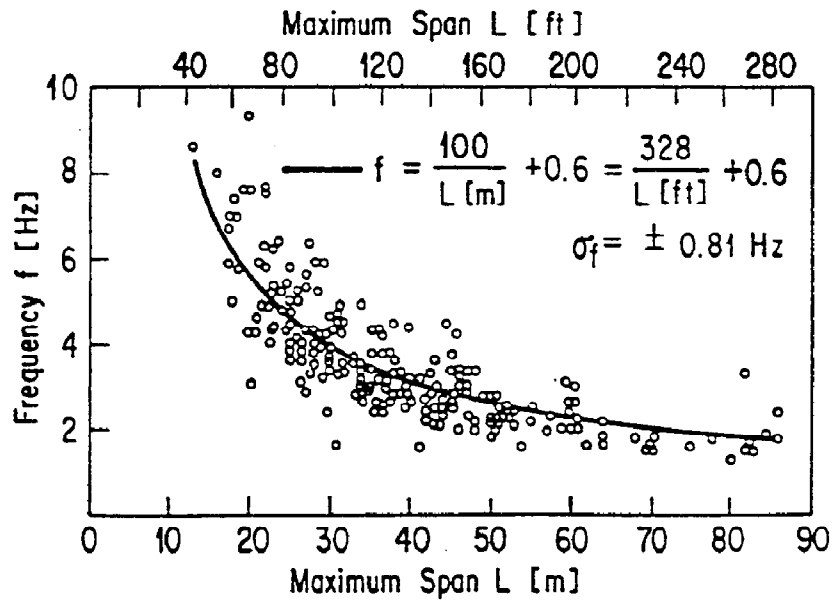
Figure 7.2. Fundamental frequency versus span length

(Cantieni 1984)
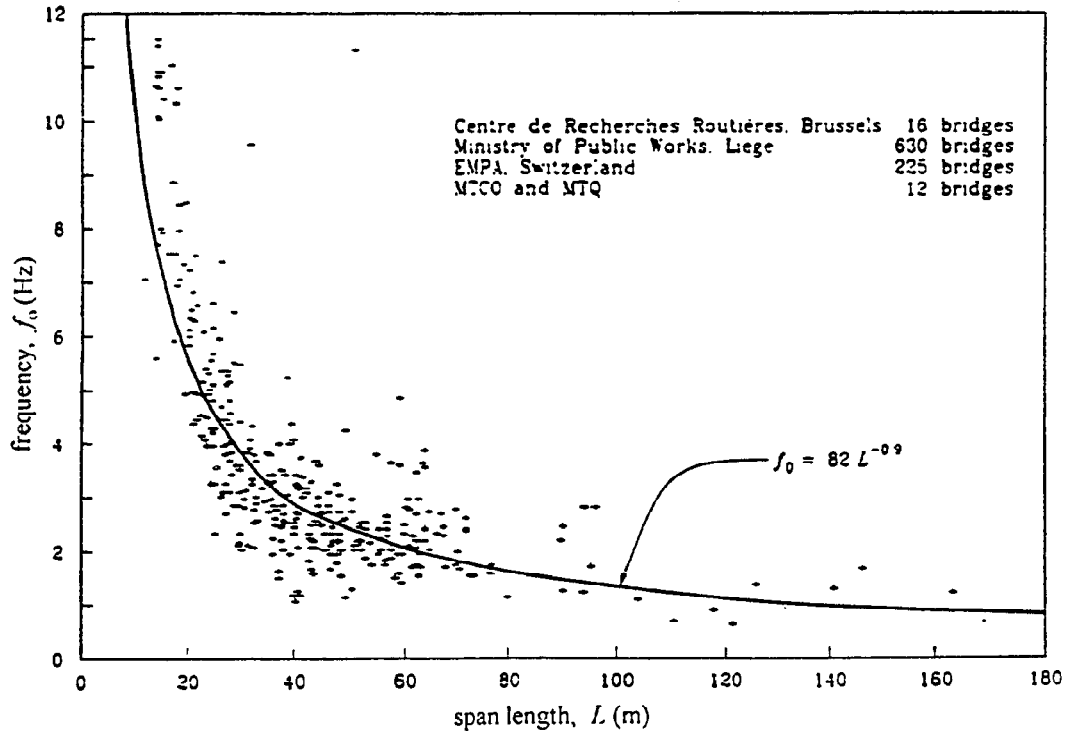
Figure 7.3. Fundamental frequency versus span length

(Paultre 1992)

From basic dynamic principles, higher levels of damping reduce the dynamic response in bridges and low levels of damping in a bridge are expected to result in high dynamic amplification. However, damping affects impact differently at different locations within the bridge as a result of varying modal contributions (Huang, Wang, and Shahawy, 1992). Damping values for bridges obtained from field testing can also vary considerably based on the method of testing, level of loading, and different methods used for evaluating damping. Reported values of damping for different types of bridges are as follows:

- concrete bridges - 2 to 10 % (Tilly, 1978)

- steel bridges - 2 to 6 %(Tilly, 1978), 0.4 to 1.3 % (Billing, 1984)

- composite steel-concrete bridges - 5 to 10 % (Tilly, 1978)

- prestressed concrete bridges - 1 to 2.2 % (Billing, 1984)

- timber bridges - 3 to 4 % (Ritter, 1995)

Roadway Roughness and Approach Condition

The bridge approaches and roughness of the roadway surface have a significant influence on the magnitude of the dynamic response. Not only do the impact forces increase for increased roughness, but also vehicle speed affects the influence of roughness. The faster vehicle speed has greater impact on rougher surfaces than on better maintained ones. The results of the study by Wang, Shahawy, and Huang (1993) can be seen in Figure 7.4.
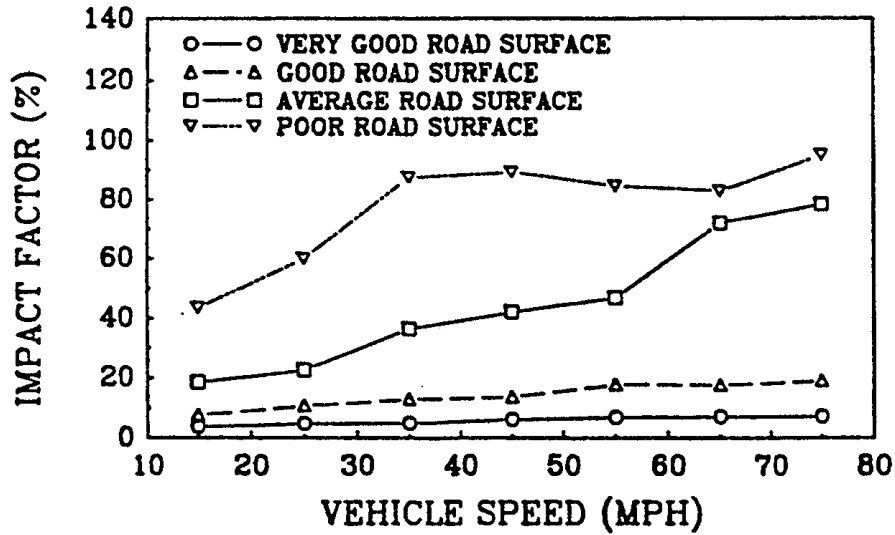
Figure 7.4. Impact factor versus vehicle speed and road surface condition
(Wang, Shahawy, and Huang 1993)

Experimental tests have also shown that the most severe wheel impact forces are likely to occur adjacent to the bridge approaches, i.e., shortly after a vehicle enters the bridge (Tilly 1978). In many experimental investigations, wooden planks were placed in the path of the test vehicle. It was supposed to represent surface irregularities such as dropped objects or packed snow on the roadway. Dynamic response was higher with the planks and the planks were exciting wheel hop in the test vehicles, although excitation of the higher vibration mode associated with wheel hop is also speed dependent.

Vehicle Speed

For most heavy trucks, natural frequencies of the vehicle typically occur in two frequency ranges: between approximately 2 and 5 Hz for the "body bounce" response and between approximately 10 and 15 Hz for the "wheel hop" response. However, depending on vehicle speed, roadway surface irregularities may be effective in exciting both modes of response (Cantieni 1983).

Weight of Vehicles

Many studies have shown that as the weight of the crossing vehicle increases, the magnitude of the dynamic response expressed as a percentage of the static load decreases. The explanation of this fact is that when the dynamic forces increase with increasing vehicle weight, the static load increases more rapidly with increasing weight. Thus, the impact ratio of dynamic force to live load decreases with increasing vehicle weight and impact factors obtained from the measured dynamic response of lightly loaded vehicles will be relatively large.

Number of Vehicles

The dynamic load factors associated with multiple vehicles are lower than those for single vehicles. This is most likely because the total static load is larger (similar to having a heavier vehicle) compared to the associated dynamic load, and the dynamic responses from the two individual vehicles are likely to be at least somewhat out of phase with each other.

Vehicle suspension

The vehicle frequency ranges are a function of the suspension systems. The body bounce frequencies in vehicles with air suspensions are lower than those for steel leaf-spring suspensions, with measured frequencies in the 1.5 to 2 Hz range. Worn dampers in the suspension systems also dramatically increased the dynamic wheel forces.

In Figure 7.5 the influence of suspension is presented. On one deflection trace the vehicle had its normal suspension characteristics, in the other the springs were blocked so that the truck rode directly on the axles. The increase in response is evident for the unsprung condition.

94
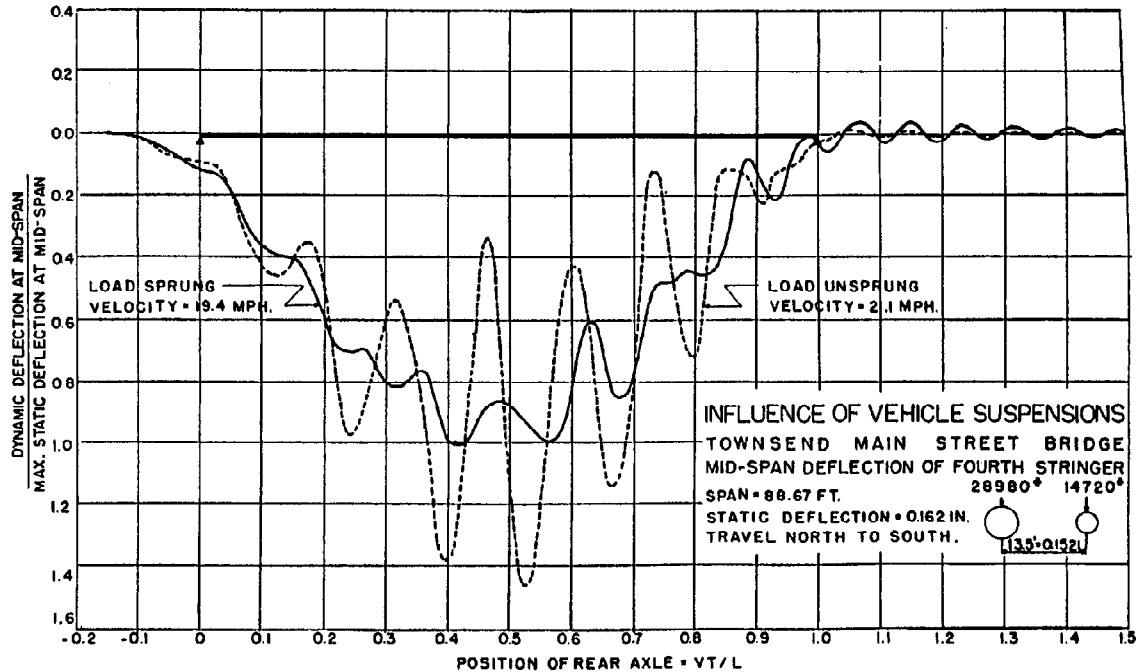
Figure 7.5. Effects of vehicle suspension on the measured bridge response

(Biggs and Suer 1955)

Bridge Span

There are conflicting opinions regarding dynamic response and bridge span. While some investigations have shown a general trend of decreasing impact in conjunction with increasing span (Figure 7.6, Fleming and Romualdi 1961), other investigations have concluded that considerable scatter exists in the results and there is poor correlation of impact and span (Figure 7.7, Cantieni 1983). Some researchers have concluded that impact is not a function of bridge span (Coussy et al. 1989). However, it should be concluded that as span length influences bridge fundamental frequency, it also indirectly influences bridge dynamics.
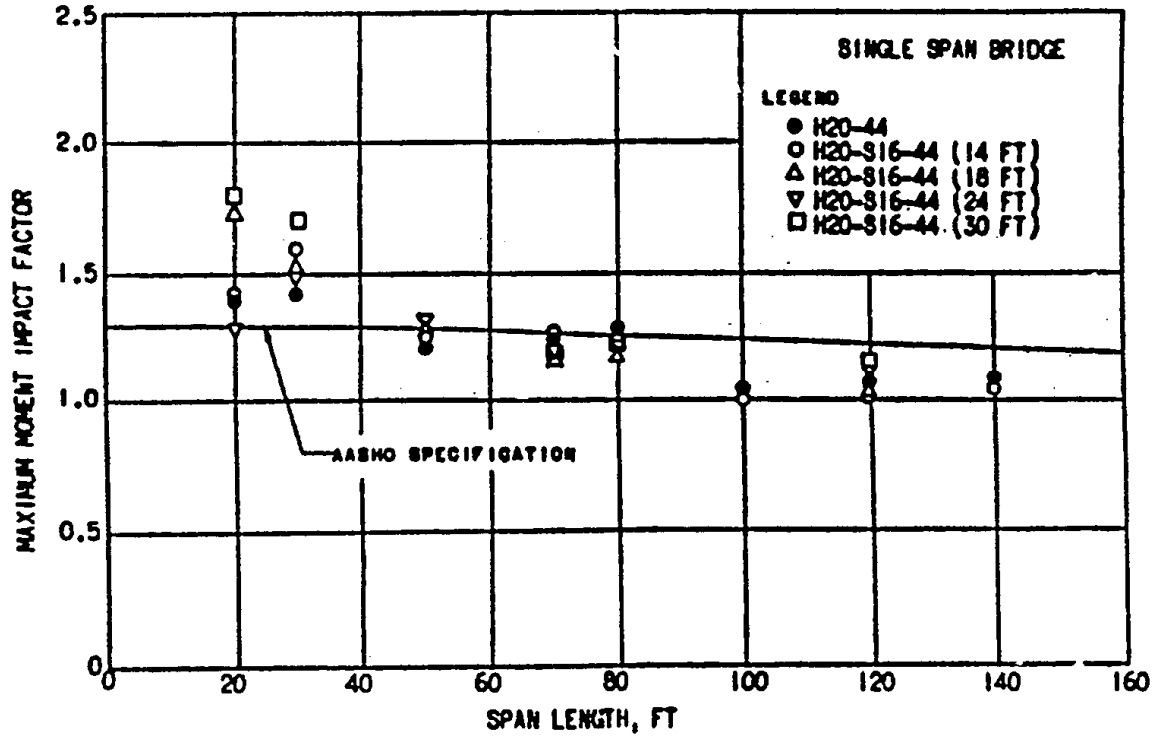
Figure 7.6. Impact versus span length (Fleming and Romualdi 1961)
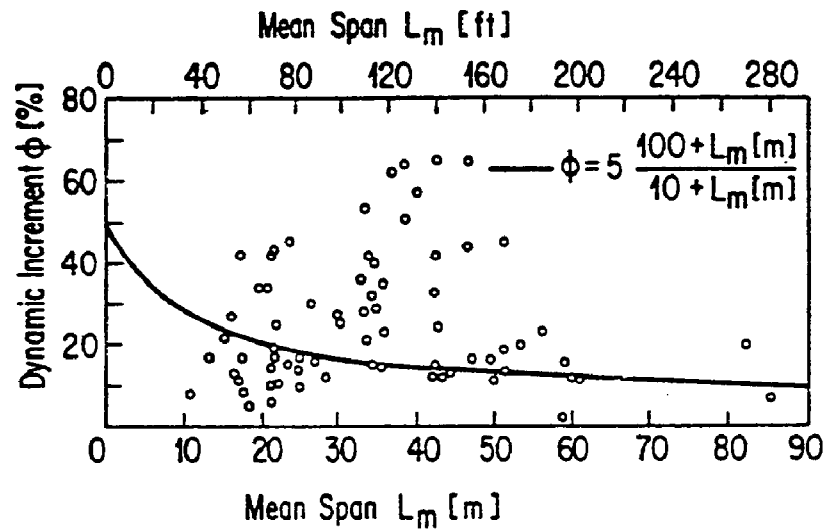
Figure 7.7. Impact versus span length (Cantieni 1984)

96

Bridge Type and Geometry

Most of the studies on dynamic response were performed on simple-span multi-girder bridges. The investigations concluded that the total number of girders has little influence on the maximum impact factors for each girder and that the impact at the interior supports was larger than at external locations. The dynamic response of simple-span bridges is higher than that for similar continuous bridges.

Cable-stayed and suspension bridges are more complicated to assess than for beam/girder bridges, mostly due to the influence of cables' dynamics. Dynamic response quantities are sensitive to damping, which is difficult to determinate in these types of bridges, and may be different for different vibration modes. In analytical investigations it was found that, with a good road surface, impact factors were generally less than 0.20. However, for rough surfaces, impact forces increased dramatically. (Khalifa 1992)

Dynamic response of continuous and cantilever thin-walled box girder bridges under multi-vehicle loading was analytically investigated by Wang, Huang, and Shahawy (1996) and Huang, Wang, and Shahawy (1995a). It was found that the vibration characteristics of the continuous and cantilever box girder bridges are quite different. For cantilever bridges, the most important factor affecting impact is the vehicle speed, and they are much more susceptible to vibration than continuous bridges. This is due to the abrupt change in loading due to span discontinuities, when no support exists between cantilevers. For continuous bridges, both vehicle speed and surface roughness are significant. End diaphragms were found to provide lateral support and significantly reduce the response of the box girder bridges. The beneficial effect of a midspan diaphragm is relatively small.

Dynamic behavior depends on curvature of the bridge. It was found that the dynamic response in horizontally curved bridges is influenced by centrifugal accelerations, thus, vehicle speed is particularly important. Impact forces are higher in the outer elements of the curved bridges. Impact forces are insensitive to curvature for radii greater than 4 000 ft (1219

97

m) and markedly influenced by curvature for radii less than 800 ft (244 m). Research done by Galdos et al. (1993) and Schilling et al. (1992) and Huang, Wang, and Shahawy (1995b).

7.1. BRIDGE-VEHICLE INTERACTION MODEL AND DERIVATION OF DYNAMIC FACTOR

7.1.1. Bridge and Vehicle Model

To study vehicle-bridge interaction, with the use of ABAQUS 6.6.1 software a finite element model of bridge and vehicle has been developed.

The bridge chosen for the analysis is a 120 ft steel girder bridge. It is modeled with 3D shell elements:

Steel girders:

- five steel W40x264 (profile properties: area A = 77.60 in2, depth of the section d=40 in, web thickness: tw = 0.96 in, flange width bf = 11.93 in, flange thickness tf =: 1.73 in, moment of inertia Ix-x=19400 in4)
- spaced 64 in
- fy = 60 ksi
- steel diaphragms every 30 ft
- 2360 elements, 2715 nodes

Concrete slab:

- thickness: 7.5 in
- width:312 in
- f_c'=:8 ksi
- 4464 elements, 4640 nodes

Supports:

- left support - pinned
- right support - roller

Connection between girders and slab: tied (compatibility of all degrees of freedom)

Bridge model meshed with S4R elements is shown in Figure 7.8.
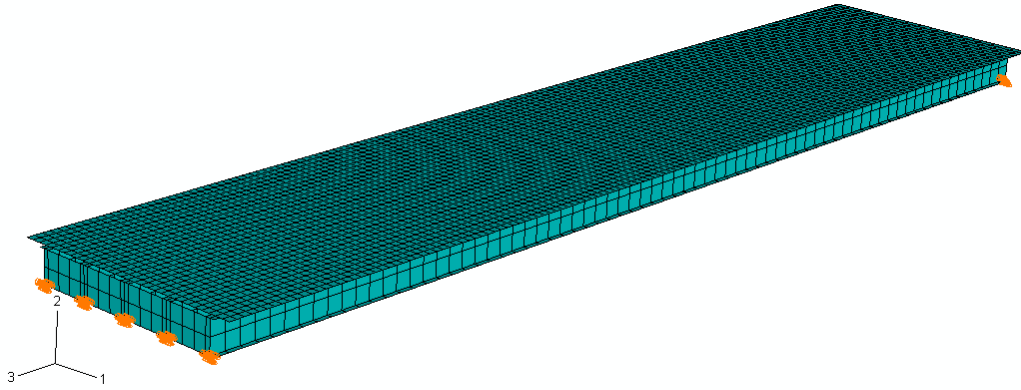
Figure 7.8. Meshed model of the bridge

A vehicle model was developed based on three-axle AASHTO HS-20 truck, which is the design vehicle in the AASHTO Specifications. Two cases are considered, the truck HS-20 is assumed to travel with the velocity of 40 miles per hour and with the crawling speed. Figure 7.9, shows FEM model of moving masses. To simplify the analysis each wheel is modeled with one DOF in the vertical direction. Detailed model would include a seven degree of freedom system. Tractor and semitrailer would have individually assigned two DOFs corresponding to: vertical displacement (y_i) and rotation about the transverse axis (θ_i). Moreover each wheel-axle set would be provided with one DOF in the vertical direction (y_i). Five sprung masses would be: the tractor, semitrailer, steer wheel-axle set, tractor wheel-axle set, and trailer wheel axle set. A more detailed model could include rotations about longitudinal axis (Φ_i).In this case the total independent DOFs would be eleven.
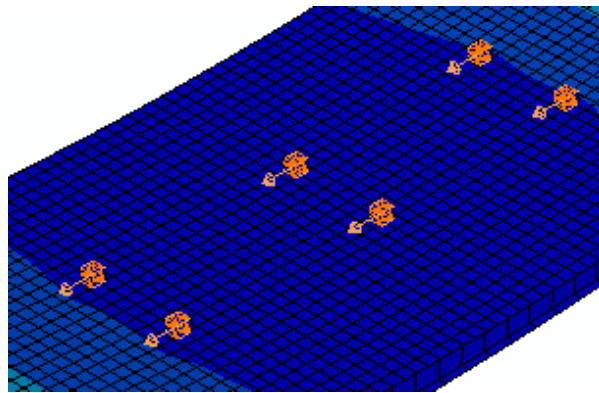
Figure 7.9. Truck model in FEM

99

7.1.1. Bridge-Vehicle Interaction Model

There are two main sources of vibrations induced by the vehicle into the bridge. One of them is the settling of the approach slab of the bridge. The bump at the bridge entrance causes so called "wheel hop" that could be approximated by impulse loading. A vehicle vibrates with a frequency between 10 and 15 Hz. Transmitted force is significant, however it fades relatively fast converging into "body bounce" that occurs at lower frequencies. The other source of vibrations is an undulating roadway surface. The condition of driving a vehicle over an undulating roadway surface can be approximately idealized as an SDOF system under harmonic loading provided the roadway varies as a sine wave. These kinds of vibrations are called "body bounce" and usually occur at frequencies between 2 and 5 Hz. The loading is characterized by the roughness amplitude, roughness wavelength, and vehicle speed. If the shock-absorbing elements of the vehicle suspension system are worn, then the vehicle's damping is fairly low and the response is quite large. Under such conditions, nearly resonant response can develop.

Since the truck model is simplified and the scope of the project requires comparison of the deflections in the middle of the span, the interaction model includes only "body bounce", which depends on the relation between suspension system and the truck. Tire stiffness and "wheel hop" response are neglected.

The vertical interaction force acting on a bridge consists of the static interaction force F_w and the variation of the interaction force ΔF_w.

$$F_b = F_w + \Delta F_w.$$

$$F_w = M\,g$$

$$\Delta F = c_i \cdot \left(\frac{dy(t)}{dt} - \frac{dy_1}{dt} \right) + k_i \cdot (y(t) - y_1(t))$$

The interaction force is approximated by a sinusoidal shape, as shown in the Figure 7.10. The force F_w transmitted by the rear wheels is 16 kips and its variation ΔF_w is equal to ±10%. The front wheels carrying 4 kips each are also assumed to produce force variation ±10%. The effects of damping are small, and they will be neglected in the analysis.

100
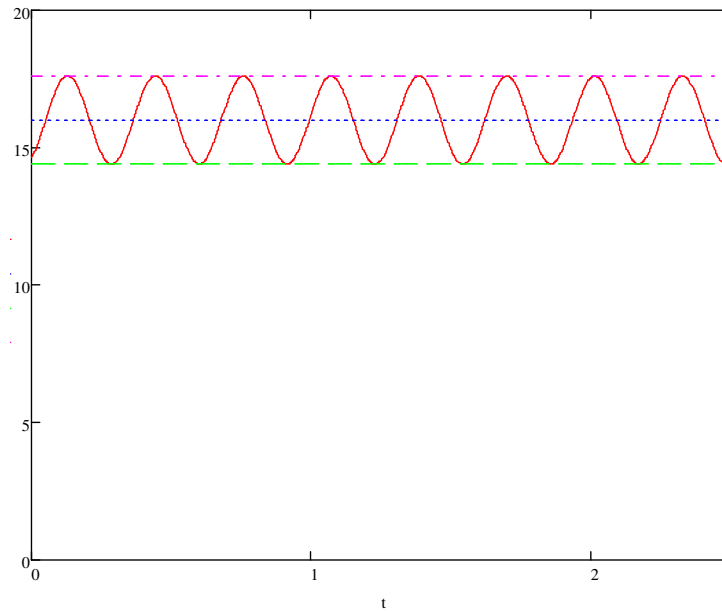
Figure 7.10. Vehicle-bridge interacting force.

Figure 7.11 is a plot from ABAQUS that shows forces being applied to the bridge versus time. It can be noticed when the following truck axes are entering and leaving the bridge. Their amplitudes are interfering and adding to each other. Those forces could also be canceling each other. Such a situation of adding amplitudes was simulated on purpose, to obtain the maximum dynamic deflections in the middle span.
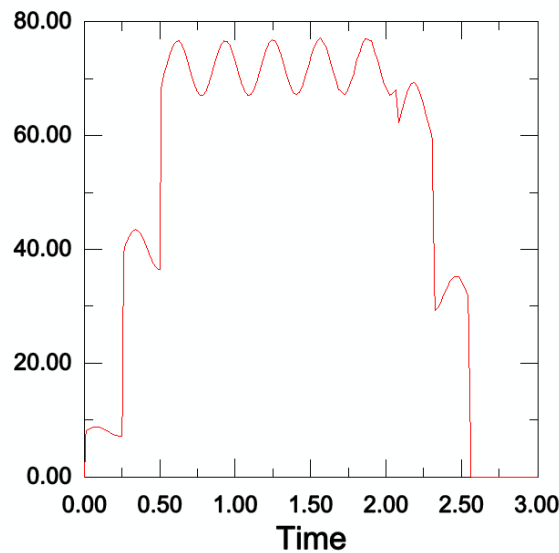
Figure 7.11. Force due to moving truck versus time. Plot from ABAQUS.

101

7.1.1. Results of analysis

Mode shapes obtained in the analysis are shown in Figure 7.12 (bending modes) and Figure 7.13 (torsion modes). The natural frequencies are following:

- first bending mode 2.12 Hz

- second bending mode: 8.19 Hz

- third bending mode: 17.10 Hz

- first torsion mode: 3.17 Hz

- second torsion modes: 9.09 Hz
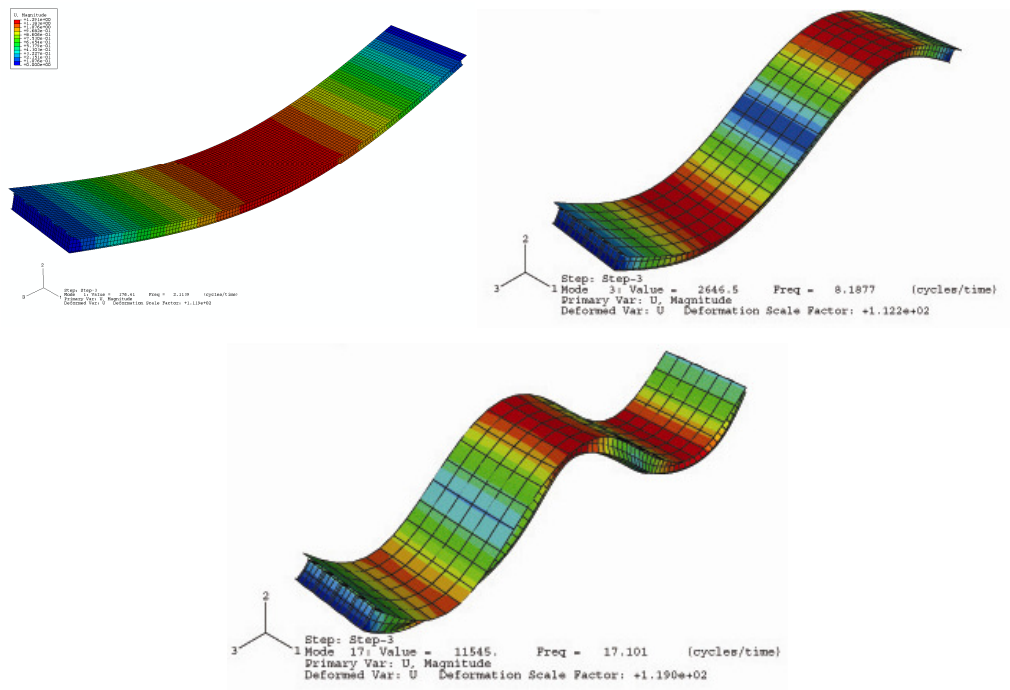
Figure 7.12. Bending modes
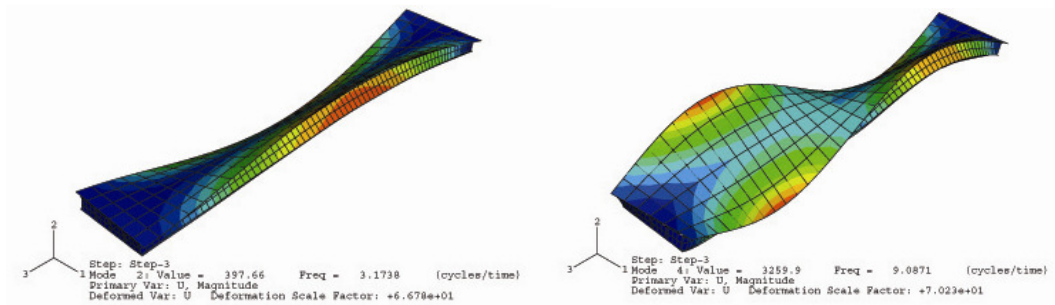
Figure 7.13. Torsion modes.

The deflection due to dead load, weight of the concrete slab and the steel profiles, is 2.74 in. Maximal deflection due to moving truck is 0.69 in (Figure 7.14). It corresponds to the truck being located almost, but not in the span center.
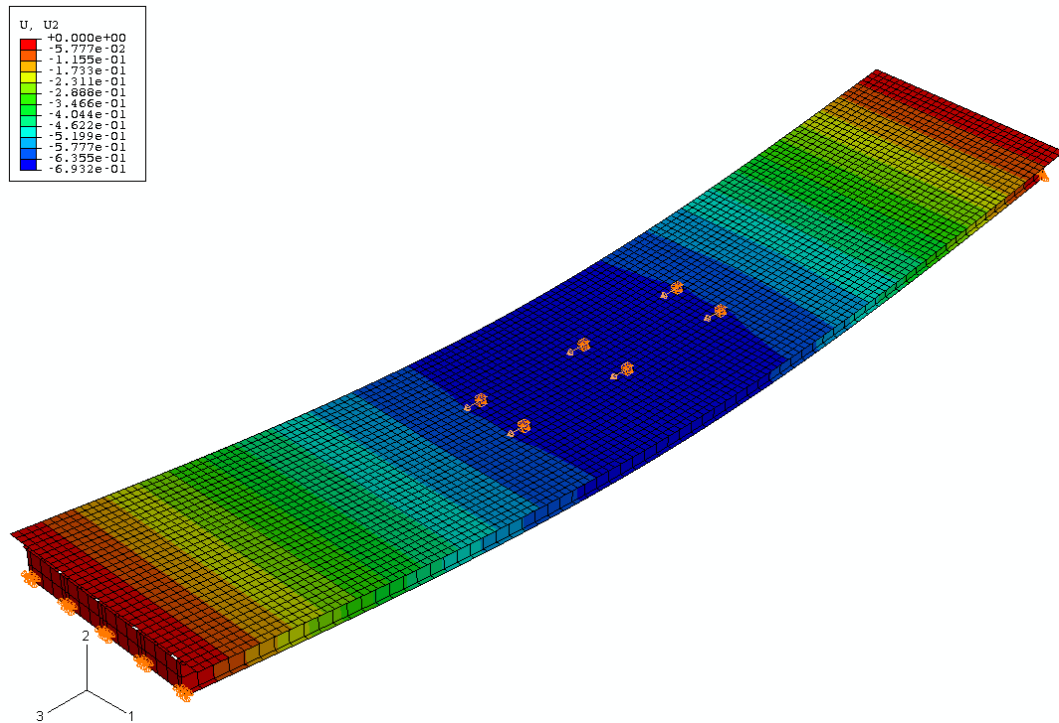
Figure 7.14. Maximal deflection due to moving truck

Figure 7.15 and Figure 7.16 show deflections in the middle of the span due to moving and stationary trucks. Maximum deflection due to moving truck (0.69 in) versus maximum deflection due to stationary truck (0.65 in) shows 6% difference.
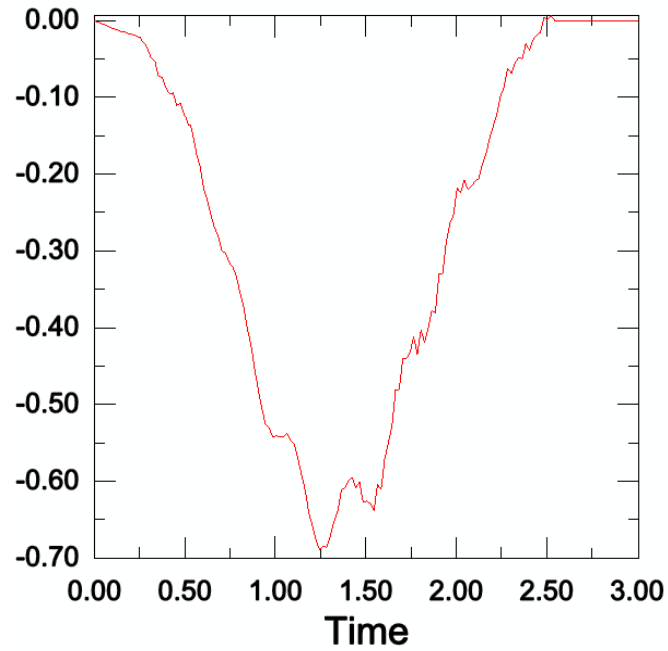
Figure 7.15. Deflection due to a truck moving 40mil/hr versus time.
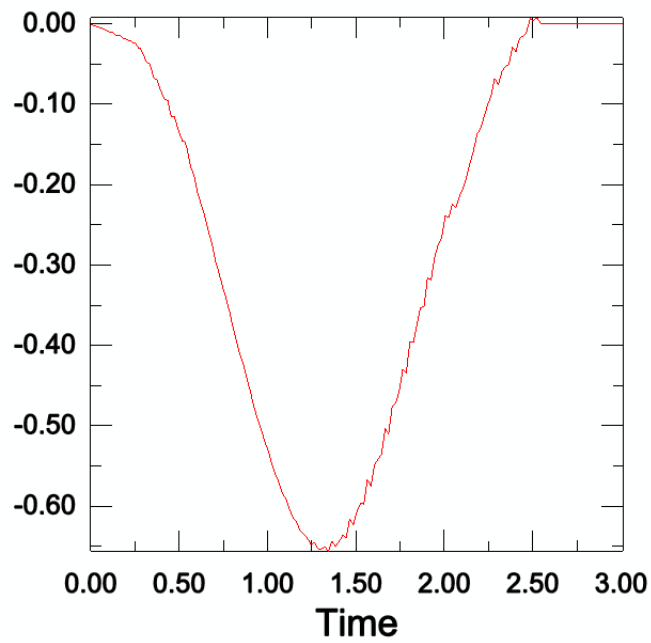
Figure 7.16. Deflection due to a truck moving at crawling speed versus time.

104

7.2.   CONCLUSIONS

The study of the topic and the developed FEM model allowed for estimating the magnitude of the dynamic load factor and to draw some conclusions. It was concluded that the current dynamic load factor of 0.33 is too high for bridges with longer spans. It may be applicable in short bridges, when vibration due to "wheel hop" on the approach slab is significant. However, for longer bridges where the influence of the approach slab decreases and vibrations of many vehicles interfere with each other, the dynamic load factor could be smaller. Even for the exemplary case of medium span bridge presented in this thesis the dynamic load factor is only 6%. The FEM model was built using ABAQUS 6.6.1 software. Finite element problem modeling, including moving load and defined interaction between surfaces, are non linear and very time demanding. To be adequate and draw more conclusions further studies should be performed, including a wide range of bridge types, spans and roadway conditions. Also, a more elaborate truck model should be performed, accounting for both "body bounce" as well as "wheel hop". Moreover, analytical studies should be confirmed with field tests on the representative structures.

In this dissertation, a traffic jam situation was assumed to develop the live load model. Therefore there is no allowance for dynamic. However, to not introduce confusion among designers it is recommended do keep dynamic factor as it is for short and medium span bridges, which results in very small value for long span bridges.

CHAPTER 8

RELIABILTY ANALYSIS OF SUSPENSION BRIDGE

8.1.   RELIABILITY ANALYSIS PROCEDURE

Reliability analysis was performed to verify the live load model for long span bridges. The reliability procedure includes the following steps:

1. Selection of a representative bridge and its component
    A representative suspension bridge and the structural element that is the most influenced by live load were selected.
2. Limit state function
    The limit state function was defined as the exceeding of the ultimate bending moment capacity by the cross-section and Strength I combination.
3. Nominal resistance model
    In order to find nominal resistance, software for the tower cross section was developed.
4. Reliability resistance models
    The material, fabrication and professional factors were established. Evaluation of material, fabrication and professional factors was based on the database available in the literature of and described by Nowak et al. (2008) and Ellingwood et al. (1980). Based on the developed software for nominal

106

resistance and the Monte Carlo simulation method, the statistical parameters for resistance were obtained.

5. Load model

   The three-dimensional FEM model of a bridge was created using Robot Millennium software. The model was based on the actual Cooper Bridge design made by PB World. Cross sectional axial force and bending moment along the tower height due to dead load and live load were derived. The statistical models for load components are defined.

6. Reliability Indices

   Reliability indices were calculated in order to assess how they are influenced by the increase in the values of live load. Reliability analysis was performed for the several forces possible and moment in the bridge tower due to live load cases.

8.2.   SELECTION OF REPRESENTATIVE STRUCTURE, ELEMENT AND LIMIT STATE FUNCTION

The Cooper River Bridge in South Carolina was chosen to be a representative long span bridge for this analysis. It is a suspension bridge designed by PB Word in 2001.

For long span bridges dead load is the main loading. Dead load is also critical for most of the structural components, such as the deck and cables. For the scope of this dissertation, the bridge component that is the most influenced by live loading had to be selected. The bridge tower was chosen to be such an element. Live load from all spans is transferred through cables to the bridge tower. When not all spans are loaded evenly, the bending moment due to live load is much higher than the bending moment due to dead load. The bending moment due to dead load of opposite spans almost negate each other.

The limit state function was defined as the exceeding of the ultimate bending moment capacity by the cross-section. The tower cross-section just above the deck level was selected.

8.3. NOMINAL RESISTANCE

The nominal resistance can be represented by interaction diagram of force and moment for the eccentric loaded bridge tower. To plot interaction diagram, representing all possible cases of force and bending moment combinations, a MathCad software was used. The mathematical description of the behavior for the exemplary bridge tower was developed based on procedure for columns described by Lutomirski (2009). The assumptions are based on linear strains in a distribution over the cross section and the mechanical behavior of reinforcement. The procedure takes into account the geometry of the tower, all layers of the reinforcement in the cross-section and the characteristics of the materials (steel and concrete).

The first step in the procedure is the calculation of the initial compression block. The initial compression block represents the compression over the full cross-section and the lowest layer of the reinforcement yields due to compression. It means that strains in concrete at the top of cross section reach value of $\varepsilon_m = 0.003$, while the strains in the lowest reinforcement bar represent yielding strains due to compression in steel $\varepsilon_s = \varepsilon_y = 0.00207$ (Figure 8.2). The position of the neutral axis can be calculated based on the linear strain distribution and strain compatibility assumptions. As a result of the first step the size of the compression block is much bigger than the size of the cross-section. The size of the initial compression block can be calculated as follows:

$$a_I = \beta_1 \frac{\varepsilon_m \cdot d_I}{\varepsilon_m - \varepsilon_y} \tag{8.1}$$

where:

d_I is the distance of the lowest layer of the reinforcement to the top of the cross-section.

The position of the neutral axis in the initial step can be calculated from:

$$c_I = \frac{a_I}{\beta_1} \tag{8.2}$$

108
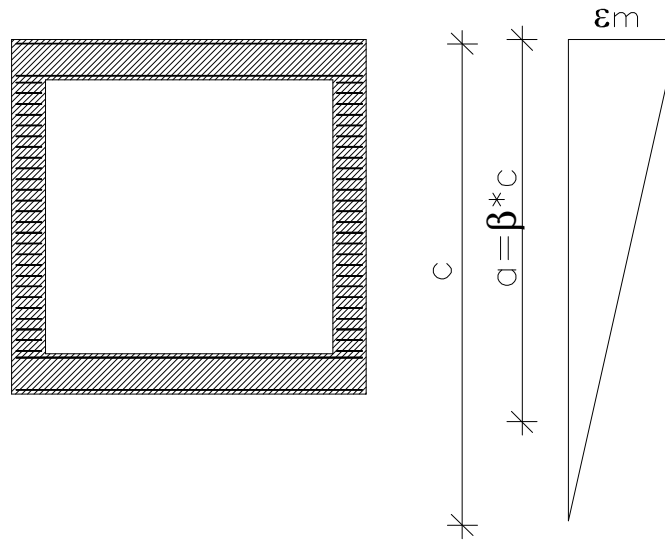
Figure 8.1 Distribution of strains for the pure axial loading

The characteristic point of end of compression control zone and beginning of tension control zone call balance failure point can be derived. It happens when the strains in the bottom layer of reinforcement reaches the yielding strains for the steel $\varepsilon_s=\varepsilon_y$ (Figure 8.2). The size of the compression block in balance failure is represented:

$$a_B = \beta_1 \frac{\varepsilon_m \cdot d_I}{\varepsilon_m + \varepsilon_y} \tag{8.3}$$
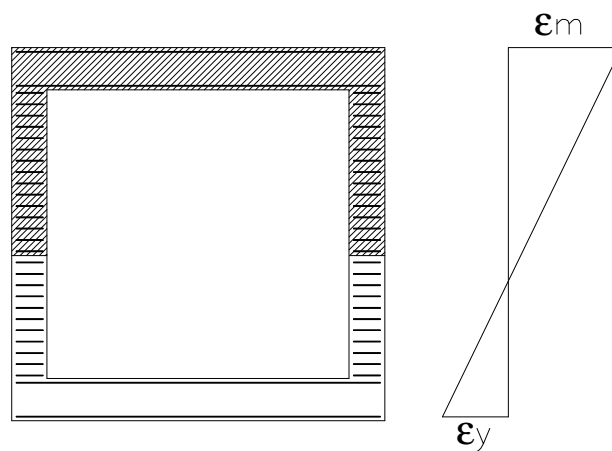
Figure 8.2 Distribution of strains distribution for the balance failure point B, the end of the compression control zone

109

The entire force and moment interaction diagram is calculated using the decreasing size of the compression block of concrete, from the initial a_I up to the point when the compression block does not exist ($a = 0$). For each reinforcement layer and for each size of the compression block the strains in reinforcement are computed from the equation:

$$\varepsilon_s(i,a) = \varepsilon_m \cdot \left(1 - \frac{d_i}{c(a)}\right) \qquad (8.4)$$

where:

i	number of ith reinforcement bar in cross-section
a	size of compression block of concrete
ε_m	extreme compressive strain in concrete equal to 0.003
d_i	distance of ith reinforcement layer for the top of cross-section
$c(a)$	position of neutral axis due to changing size of compression block

In the procedure, four characteristic cases there can be distinguished. The first case is when the position of neutral axis is outside of the cross section (Figure 8.1). The second case is when the end of compression block of concrete is in the bottom flange of the cross section (Figure 8.3). Two next cases correspond to the end of compression block of concrete localized in the webs and in the top flange (Figure 8.4 and Figure 8.5).
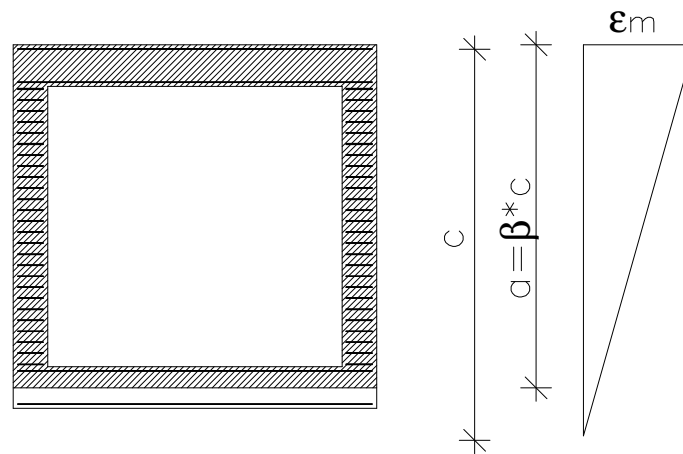
Figure 8.3 End of compression block of concrete in the bottom flange
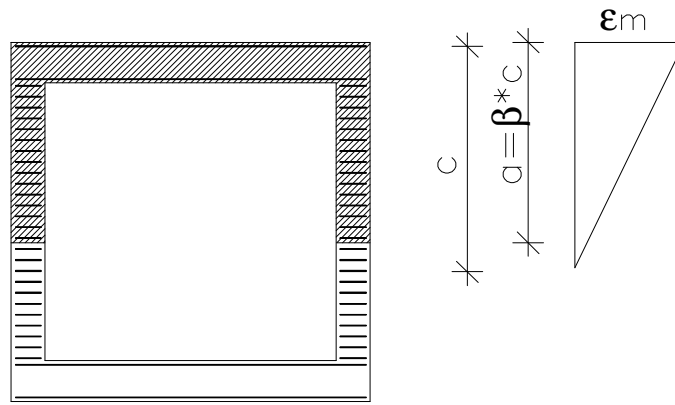
Figure 8.4 End of compression block of concrete in the web.
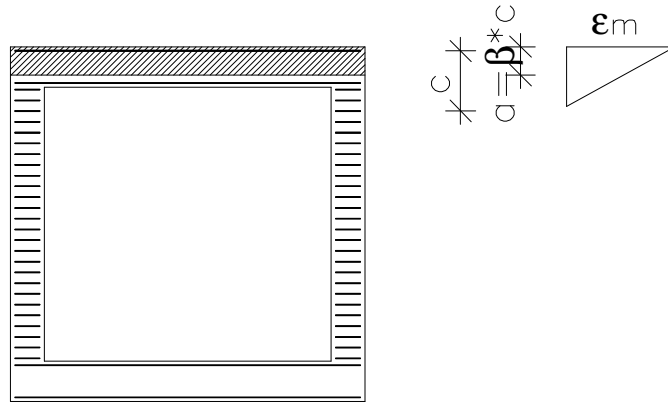
Figure 8.5 End of compression block of concrete in the top flange.

Figure 8.6 shows material behavior of reinforcing steel, and it is described by the following equation:

$$f_s = \begin{cases} -f_y & for & \varepsilon_s < -\varepsilon_y \\ E_s \cdot \varepsilon_s & for & -\varepsilon_y \leq \varepsilon_s \leq \varepsilon_y \\ f_y & for & \varepsilon_y < \varepsilon_s \leq \varepsilon_m \\ 0 & for & \varepsilon_s > \varepsilon_m \end{cases} \tag{8.5}$$

where:

$$E_s = \frac{f_y}{\varepsilon_y} \tag{8.6}$$

111
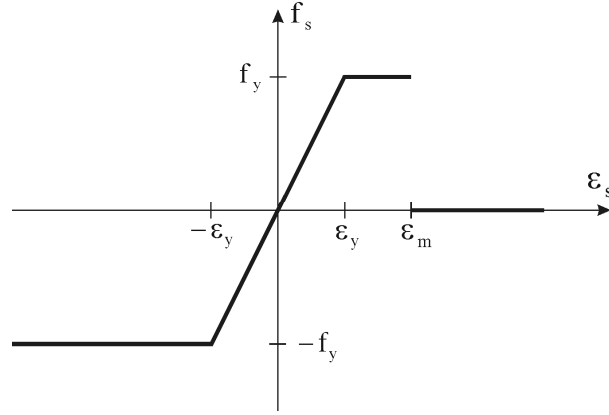
Figure 8.6 Stress - Strain Relationship for Reinforcing Steel

Having calculated strains in every reinforcement bar, it is possible to evaluate forces for each reinforcement layer.

$$P(i,a) = \begin{cases} A_s \cdot f_y & for & \varepsilon_s(i,a) \geq \varepsilon_y \\ A_s \cdot E_s \cdot \varepsilon_s(i,a) & for & -\varepsilon_y \leq \varepsilon_s(i,a) \leq \varepsilon_y \\ -A_s \cdot f_y & for & \varepsilon_s(i,a) < -\varepsilon_y \end{cases}$$ (8.7)

where:

i   number of ith reinforcement bar in cross-section

a   size of compression block of concrete

The resultant reinforcement force is calculated using:

$$P_{steel}(a) = \sum_i P(i,a)$$ (8.8)

The force in concrete is based on the size of compression block of concrete.

$$P_C(a) = 0.85 \cdot A(a) \cdot f_c'$$ (8.9)

For each size of the compression block, the resistance force of the cross section is expressed by the sum of all forces acting in the cross-section:

$$P_{Total}(a) = \sum_i P(i,a) + P_c(a)$$ (8.10)

112

For each size of the compression block, the bending moment resistance is equal to sum of all the forces in the section multiplied by the corresponding force arm to the centroid of the cross-section:

$$M_{Total}(a) = \sum_i \left[P(i,a) \cdot \left(\frac{h}{2} - d_i \right) \right] + 0.85 \cdot A(a) \cdot f'_c \cdot Y_C(a) \qquad (8.11)$$

8.4. LOAD MODEL

For the scope of this dissertation Cooper River Bridge was modeled using Robot Millennium software. The three dimensional model was based on the actual design made by PB World. Shell elements were used to model concrete slab in the bridge. 840 3-D beam elements were used - with 12 degrees of freedom $u1_x$, $u1_y$, $u1_z$, $\phi1_x$, $\phi1_y$, $\phi1_z$, $u2_x$, $u2_y$, $u2_z$, $\phi2_x$, $\phi2_y$, $\phi2_z$ - to represent all others members: towers leg, tower, girders and the diaphragms. The cables elements were used to model suspension cables.

Total length of the structure is 3296 ft. Main span is 1546 ft long, two spans are 650 ft and two spans are 225 ft long. Geometry of the bridge is shown in Figure 8.7.

Bridge towers are 568 ft high, both of them have 368 ft above deck level.
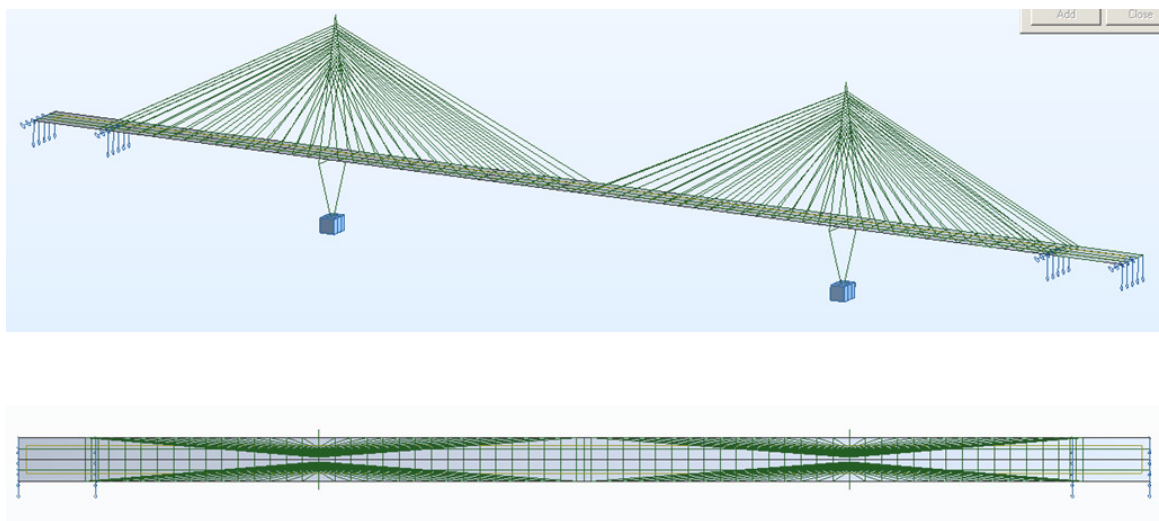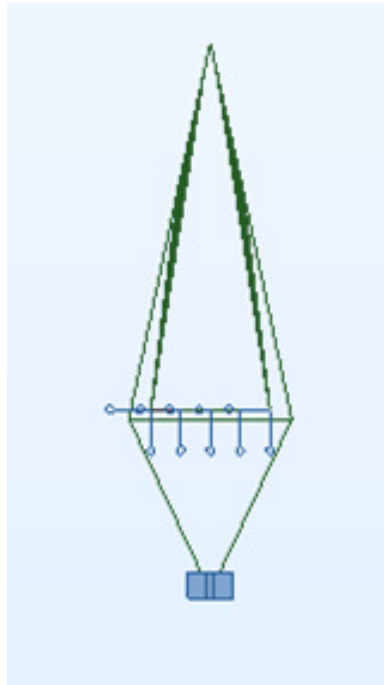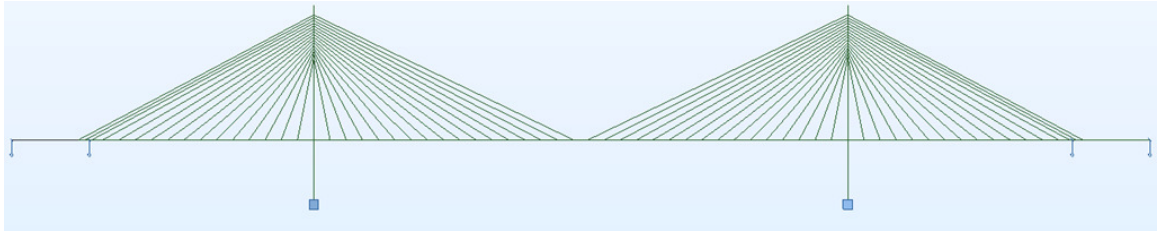
Figure 8.7. Geometry of Cooper River Bridge

In the analysis all loading cases have been considered. For five spans, there are 31 loading combinations. They are shown in Figure 8.8.

All of the live load combinations were used to calculate load effect on the bridge tower. The 31 combinations were used four times; for the different value of loading: 0.64 k/ft, 0.80 k/ft, 1.00 k/ft and 1.20 k/ft as a value of lane live load loading.

The resulting envelopes of bending moments due to various combinations of live load for bridge tower are shown in Figure 8.9 - Figure 8.12.

114
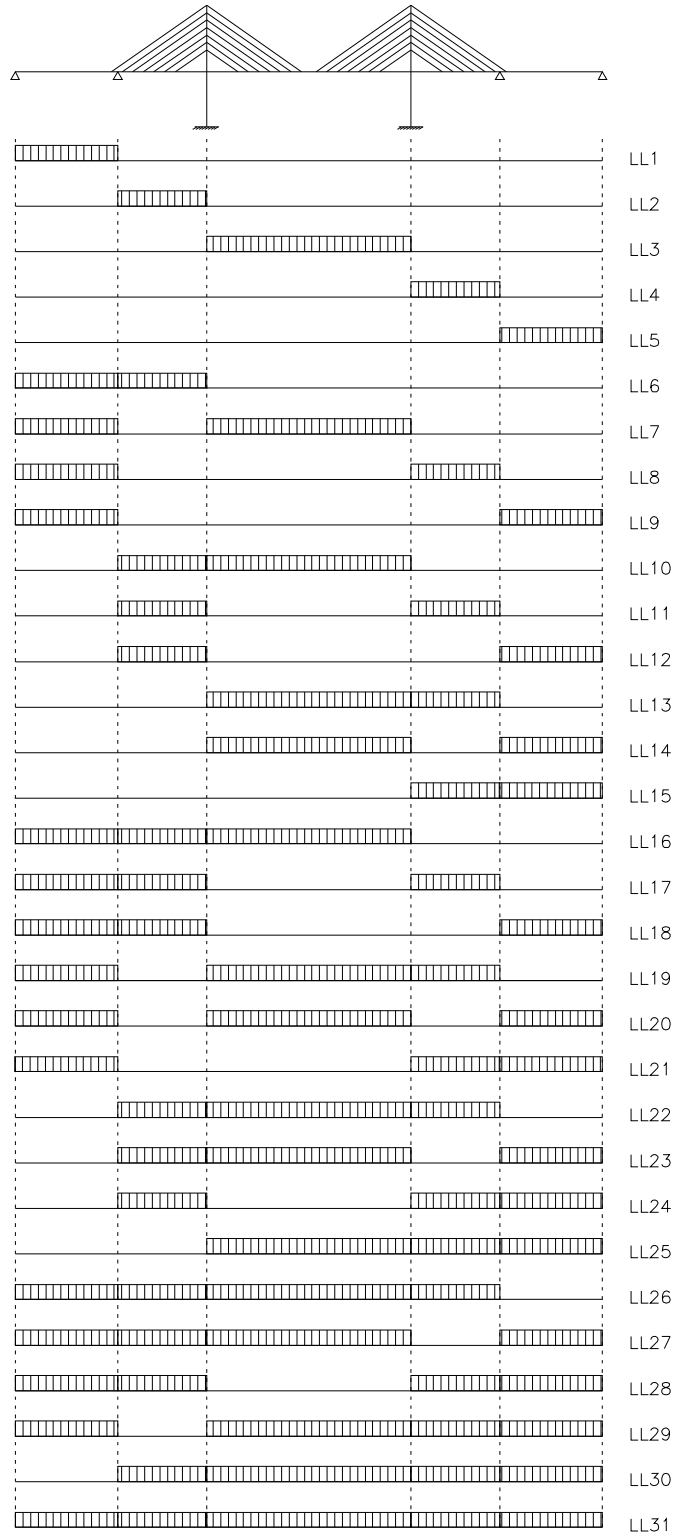
Figure 8.8. Load combinations
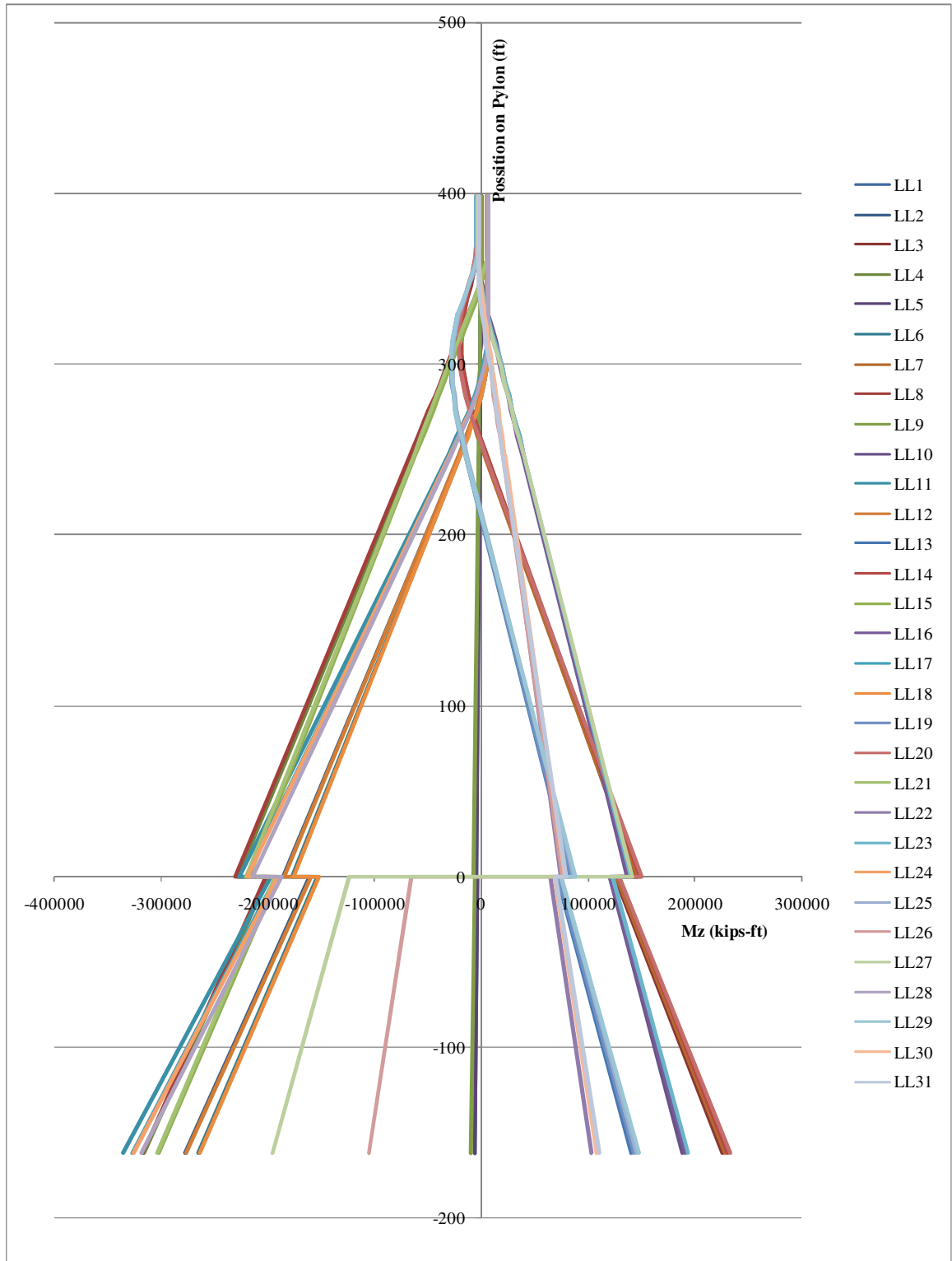
Figure 8.9. Envelope of bending moments for bridge tower for w=0.64k/ft

116
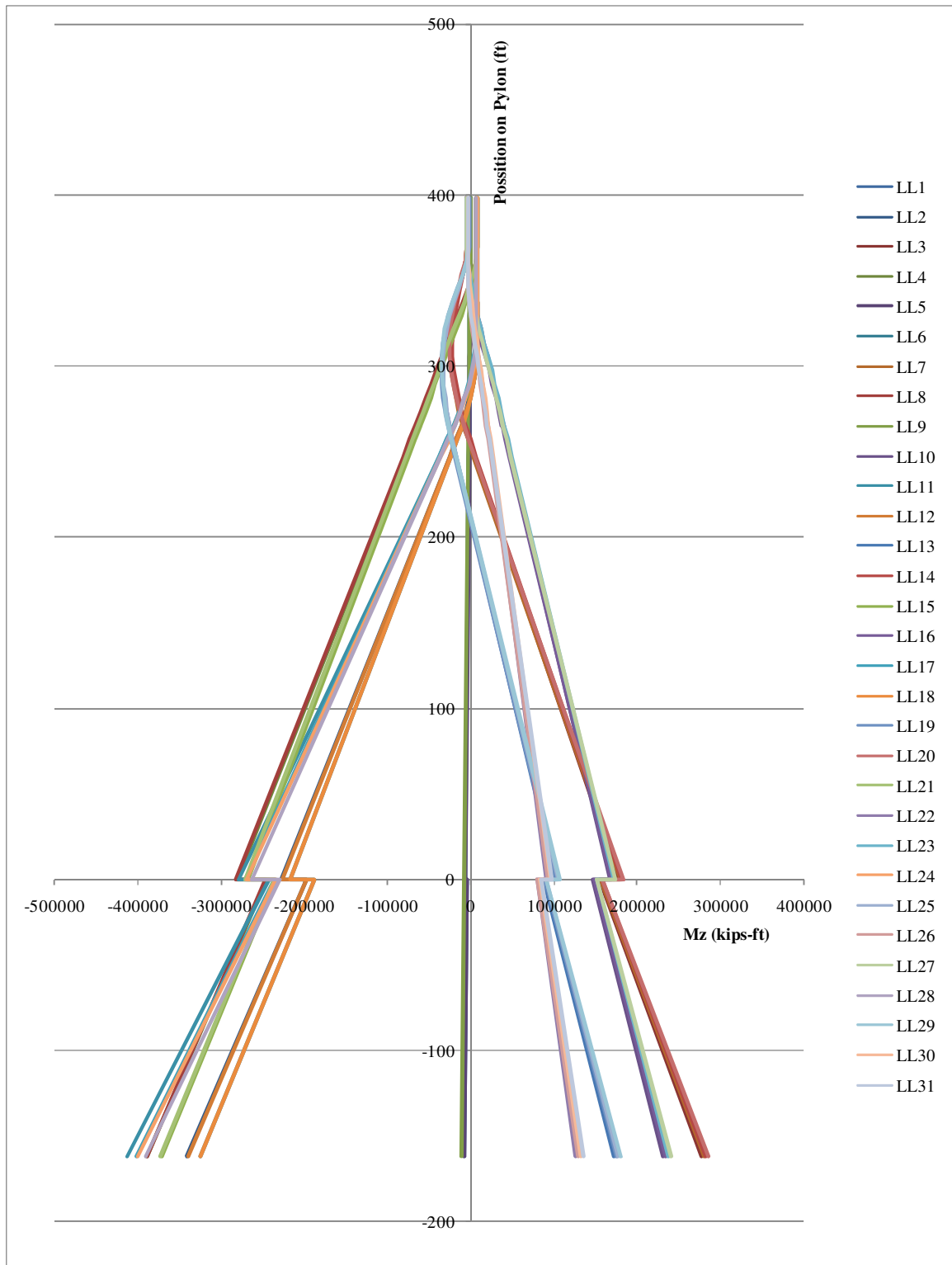
Figure 8.10. Envelope of bending moments for bridge tower for w=0.80 k/ft

117
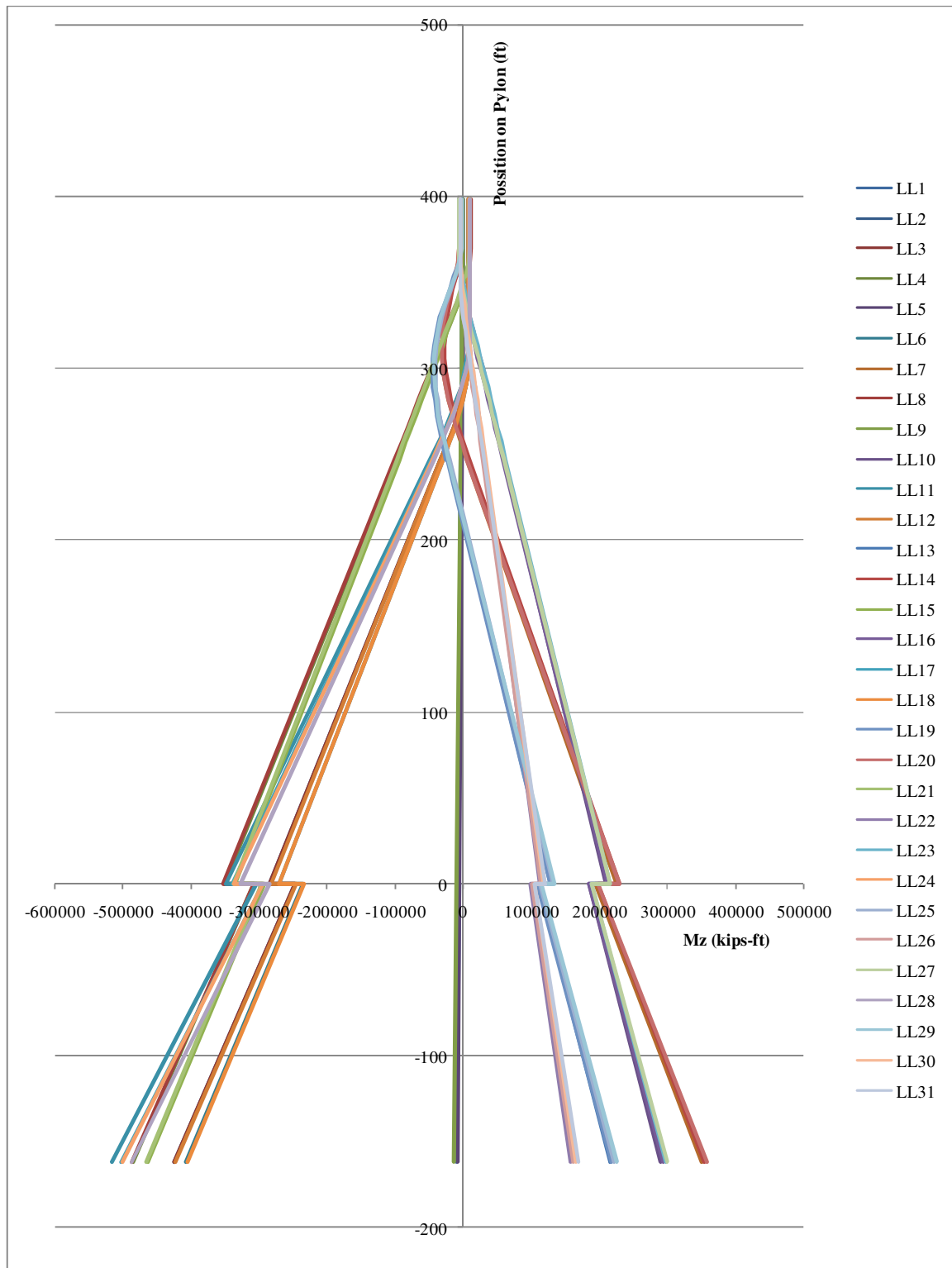
Figure 8.11. Envelope of bending moments for bridge tower for w=1.00 k/ft
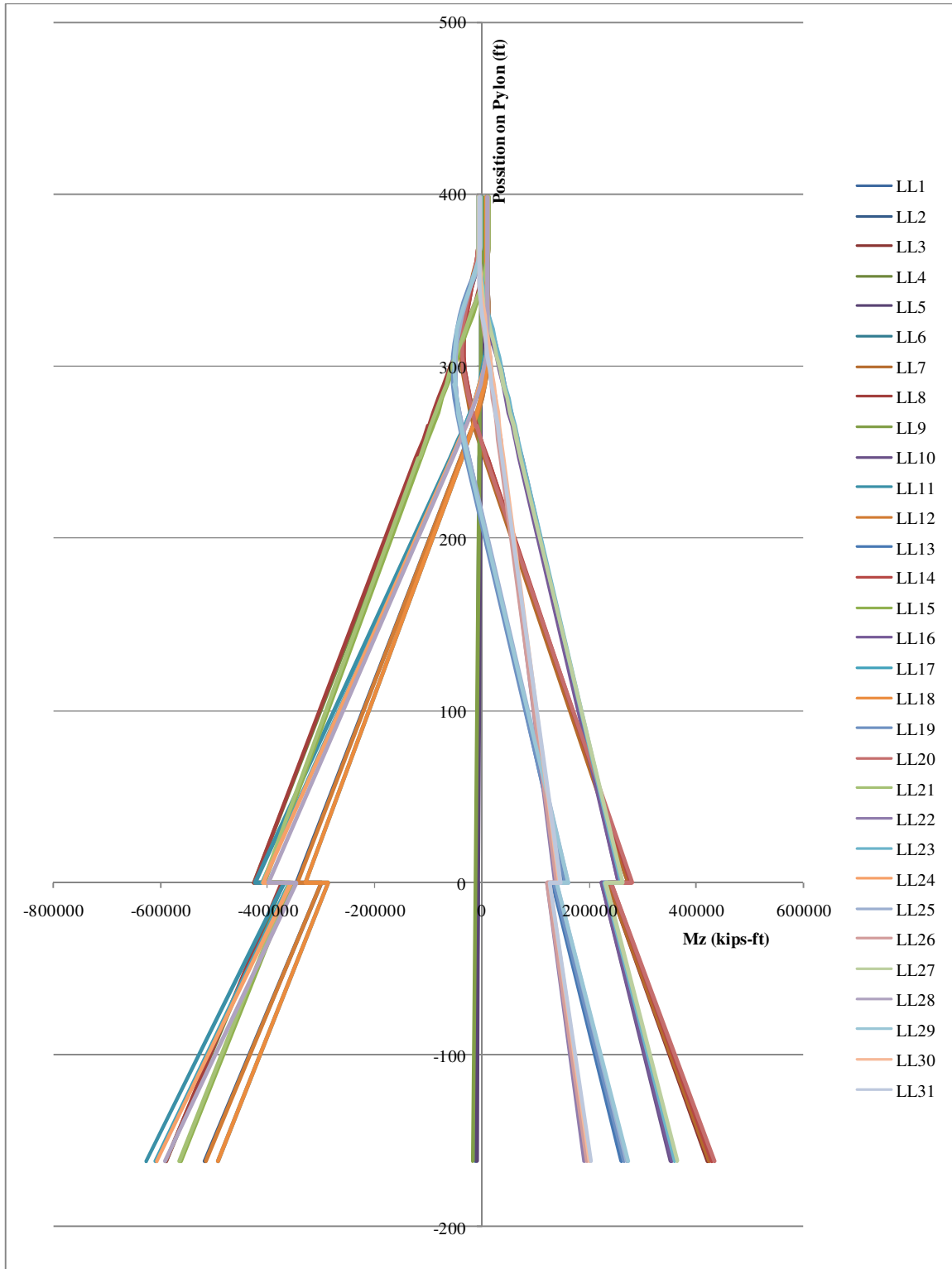
Figure 8.12. Envelope of bending moments for bridge tower for w=1.20 k/ft

8.5. RELIABILITY RESISTANCE MODELS

Due to various categories of uncertainties, the resistance of a structural component R, can be considered as a random variable being a product of nominal resistance R_n and three factors: the materials factor, fabrication factor and professional factor:

$$R = R_n M F P \qquad (8.12)$$

The materials factor represents material properties, in particular strength and modulus of elasticity. The fabrication factor represents the dimensions and geometry of the component, including cross-sectional area, moment of inertia, and section modulus. The professional factor represents the approximations involved in the structural analysis and idealized stress/strain distribution models. The professional factor is defined as the ratio of the test capacity to analytically predicted capacity (the actual in-situ performance to the model used in calculations).

The statistical parameters for material factors used in this dissertation were based on the project "Reliability-Based Calibration for Structural Concrete" (Nowak A.S. et al., 2008). Because the quality of materials such as reinforcing steel and concrete has improved over the years, the materials factors have been updated based on a new test database. There is no new information regarding two other factors, F and P. Therefore, in most cases, statistical parameters for F and P are taken from the previous study (Ellingwood et al. 1980).

8.5.1. Material Factor

The material factors for concrete were based on the study within the project "Reliability-Based Calibration for Structural Concrete" (Nowak A.S. et al., 2008). Figure 8.13 and Figure 8.14 show the bias factor and coefficients of variation for all types of concrete and all nominal compressive strengths of concrete. In both figures there is a trend line of changing parameter with respect to concrete compressive strength f_c'.

120

Recommended values are summarized in Table 8.1. In this dissertation, the concrete compressive strength of bridge tower is 7000 psi. Statistical parameters assumed are: bias factor $\lambda = 1.13$ and coefficient of variation $V = 0.12$.
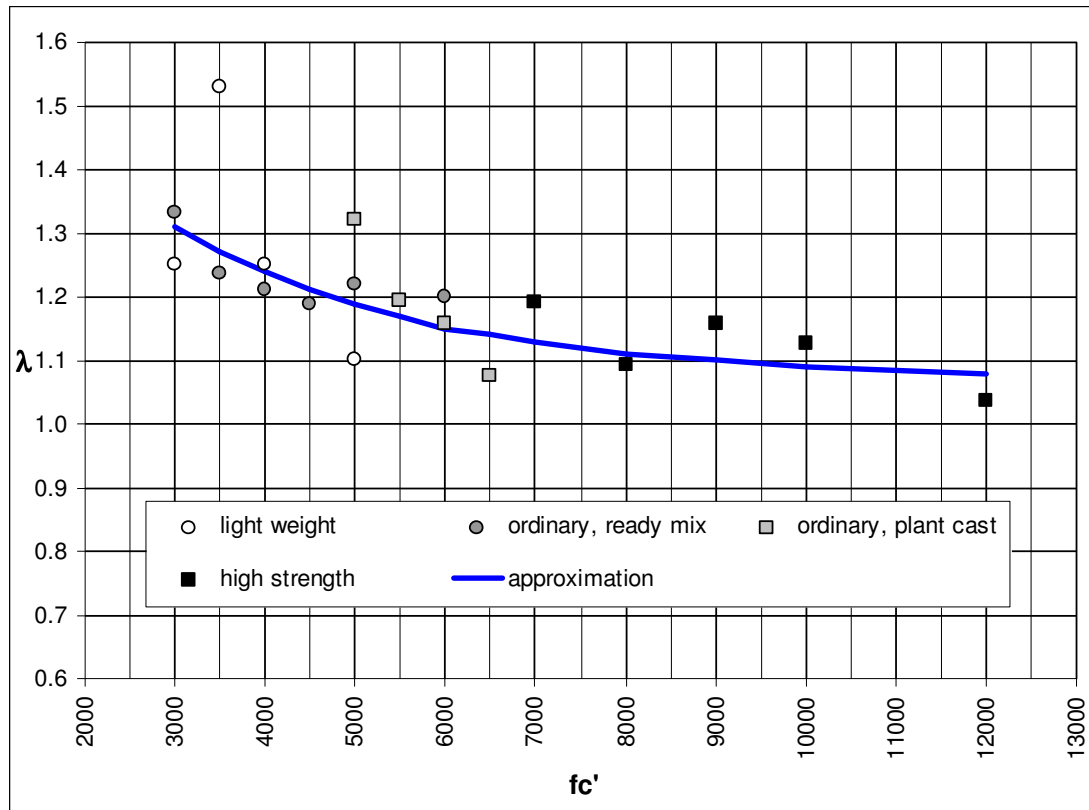
Figure 8.13 Bias factor for compressive strength of concrete
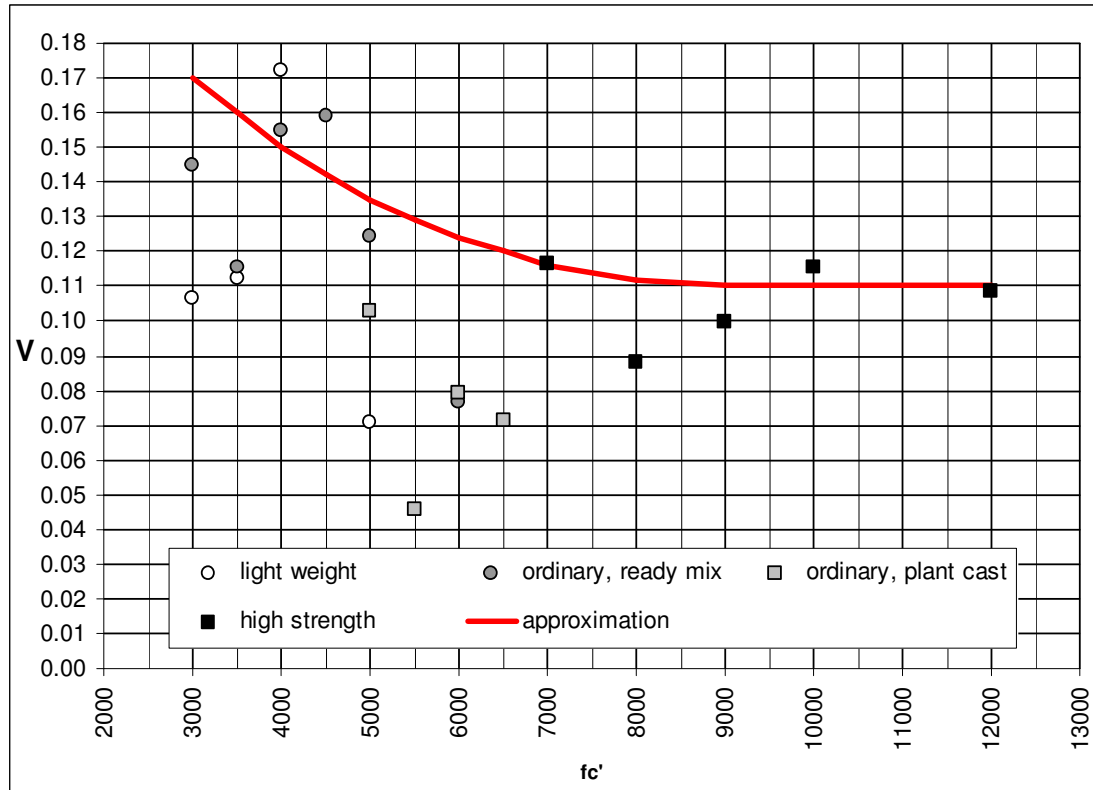
(Nowak A.S. et al., 2008)

Figure 8.14 Coefficient of variation for compressive strength of concrete

(Nowak A.S. et al., 2008)

Table 8.1 Recommended Statistical Parameters for Compressive Strength, f_c'

(Nowak A.S. et al., 2008)

Concrete Grade	f_c'	
f_c' (psi)	λ	V
4000	1.24	0.15
6000	1.15	0.125
8000	1.11	0.11
12,000	1.08	0.11

The material factors for reinforcement steel were based on the study within the project "Reliability-Based Calibration for Structural Concrete" (Nowak A.S., Szerszen

122

M.M., et al., 2008). Data included the yield strength for the reinforcing steel bars with the nominal yield strength of 60 ksi, and different bar sizes from No.3 to No.14. The recommended values of statistical parameters are: bias factor $\lambda = 1.13$ and coefficient of variation $V = 0.03$. Those recommended values have been used in this dissertation for the bar sizes No.9 and No.11, which were used in the calculations. Plots of the cumulative distribution functions (CDF) of yield strength of every reinforcement size and recommended parameters are shown in Figure 8.15 and Figure 8.16.
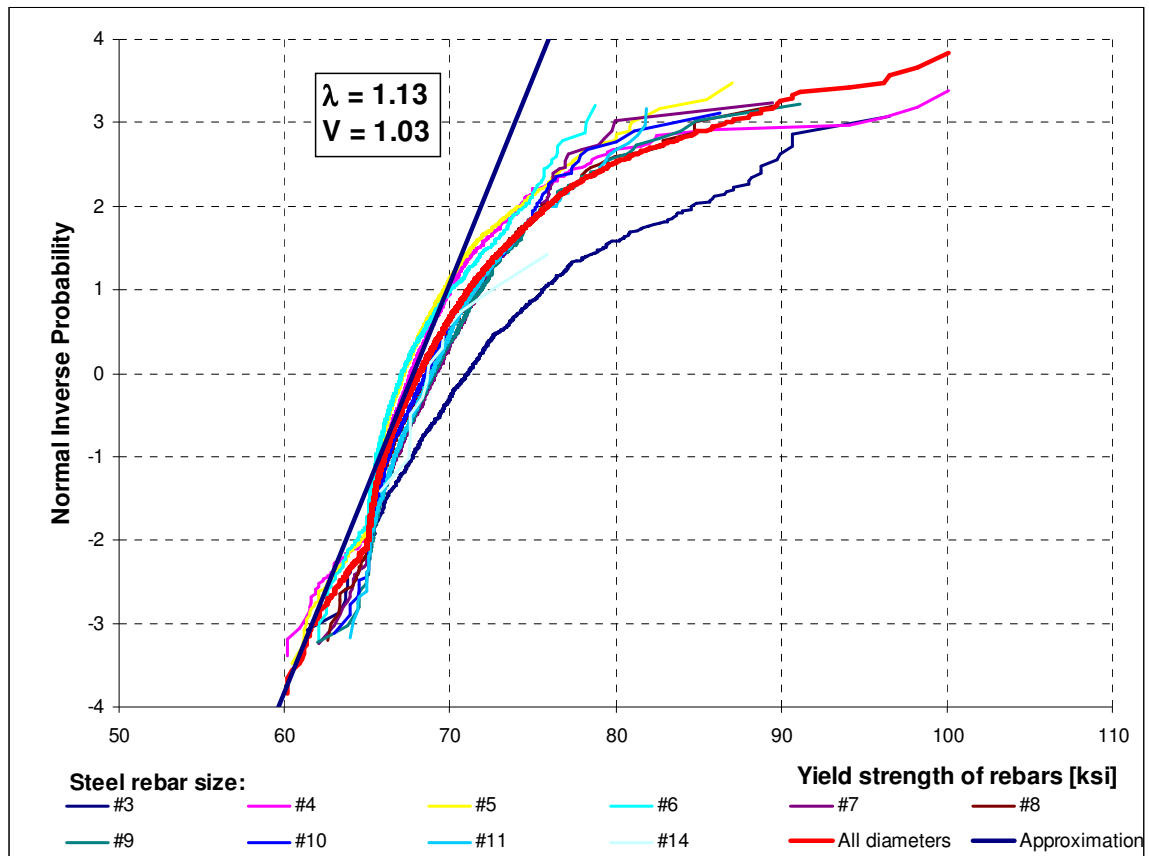
Figure 8.15 CDF's of yield strength for Reinforcing Steel Bars, Grade 60 ksi

(Nowak A.S. et al., 2008)

123
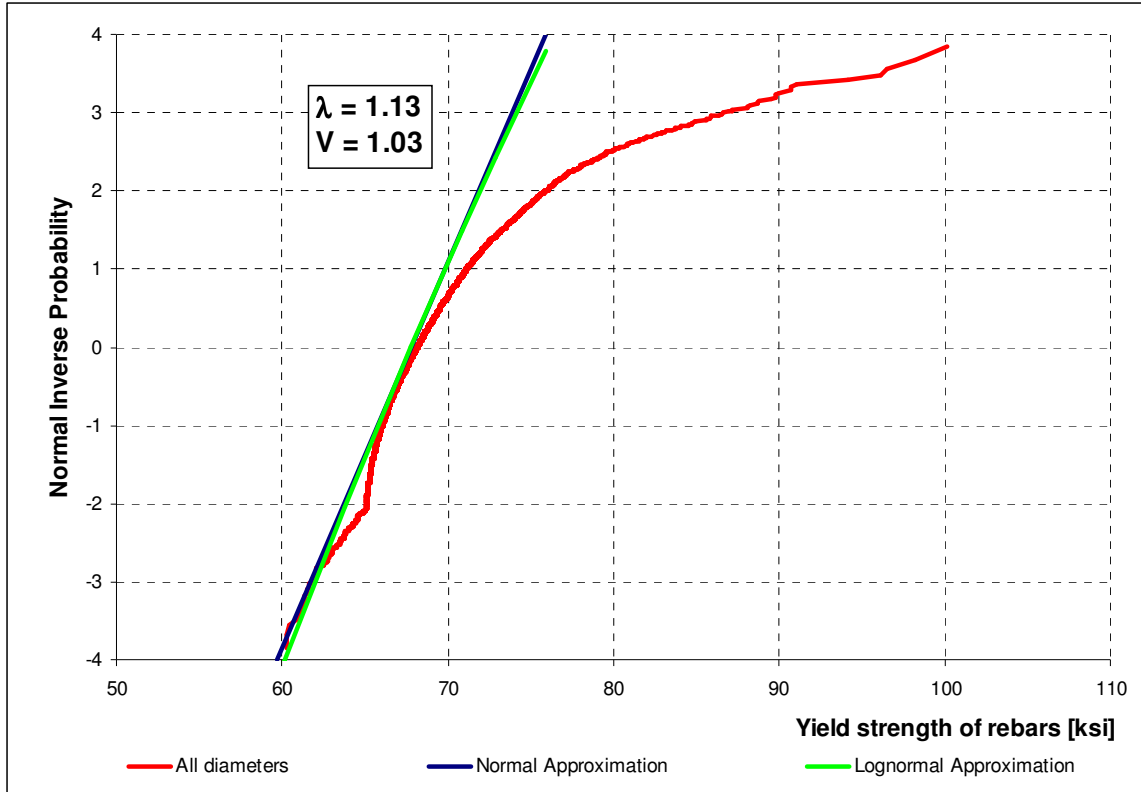
Figure 8.16 Recommended material parameters for reinforcing steel bars, Grade 60 ksi
(Nowak A.S. et al., 2008)

8.5.1. **Fabrication Factor**

The statistical parameters of fabrication factor are based on previous studies by Ellingwood et al., 1980. Due to lack of data for bridge towers, the parameters for columns were assumed. They are summarized in Table 8.2.

Table 8.2 Statistical Parameters of Fabrication Factor.

Material	Item	Bias factor	V
Concrete	Radius of column	1.005	0.04
	Reinforcement cover		
Steel	Reinforcement area	1.00	0.015
	Reinforcement diameter		

124

8.5.1. **Professional Factor**

The statistical parameters of professional factor are based on the previous study performed by Ellingwood et al. (1980). The bridge tower behaves as an eccentrically loaded column. Therefore, the statistical parameters of professional factors for columns were used in this dissertation. The professional factors were chosen for tied columns: bias factor is $\lambda = 1.00$ and coefficient of variation is $V=0.08$.

8.5.1. **Statistical Parameters of Resistance**

Statistical parameters of resistance were obtained by 10000 Monte Carlo Simulation: coefficient of variation $V=0.16$ and bias factor $\lambda=1.17$.
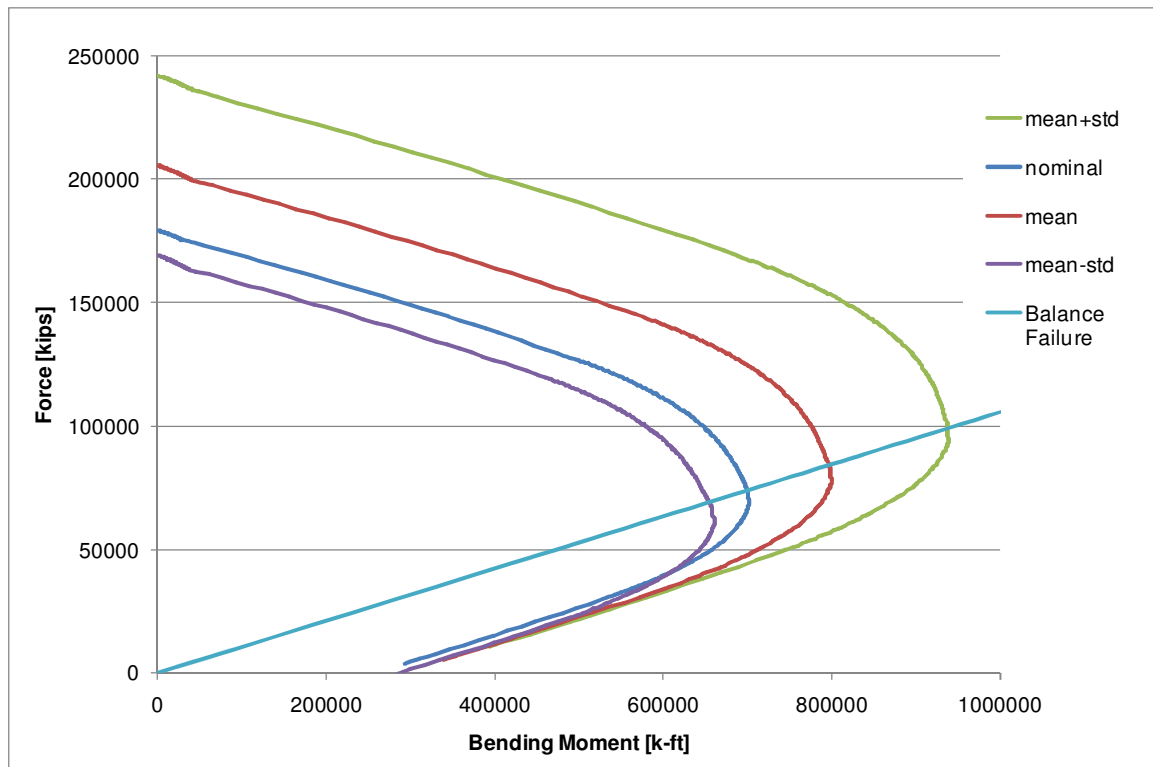
Figure 8.17 Statistical Parameters of Resistance

8.6. LOAD MODEL

The case considered in this study is combination Strength I, which is combination of dead load and live load. This combination has the highest load factor for live load.

For time varying loads two random variables for arbitrary-point-in-time and maximum 50-year load components can be considered. In this study live load is the only varying load and it is assumed to reach the maximum 50-year load value. Therefore there is no need to use Turkstra's rule.

Variation in the dead load, which is caused by variation of the weight of materials (concrete and steel), variation of dimensions, and idealization of analytical models affects statistical parameters of resistance. The assumed statistical parameters for dead load are based on the data available in literature (Ellingwood et al. 1980; Nowak 1999). They include for cast-in-place concrete elements a bias factor of 1.05 and coefficient of variation of 0.10.

Variation of live load is derived in Paragraph 5.4 of this dissertation.

8.7. RELIABILITY ANALYSIS

Reliability analysis was performed for the considered bridge. The element selected for the analysis was the bridge tower subjected to the bending moment and the axial force. The bridge was design by the PB World for the design live load specified in AASHTO LRFD CODE. The limit state function was selected as the Strength I load combination according to AASHTO LRFD Code. There are only two major load components: dead load and live load. However, on the real structure in a specific localization other loads, such as wind load, influence the bridge behavior, the selected limits state was chosen to demonstrate the sensitivity of reliability index on long span bridges due to change of live load.

Reliability indexes were calculated for bridge loaded with AASHTO design live load 0.64 k/f t and three other possible load cases of 0.80, 1.00 and 1.20 k/ft. For every value of lane load the 31 load cases were analyzed according to paragraph 8.4. Each load case, Figure 8.8, generates separate loading case to the bridge tower with different

126

eccentricity condition. The results vary depending on eccentricity. None of them exceeds the balance failure zone, Figure 8.18 . It means that all the cases are in the compression control and the strength reduction factor is φ=0.75, specified in AASHTO LRFD Section 5.
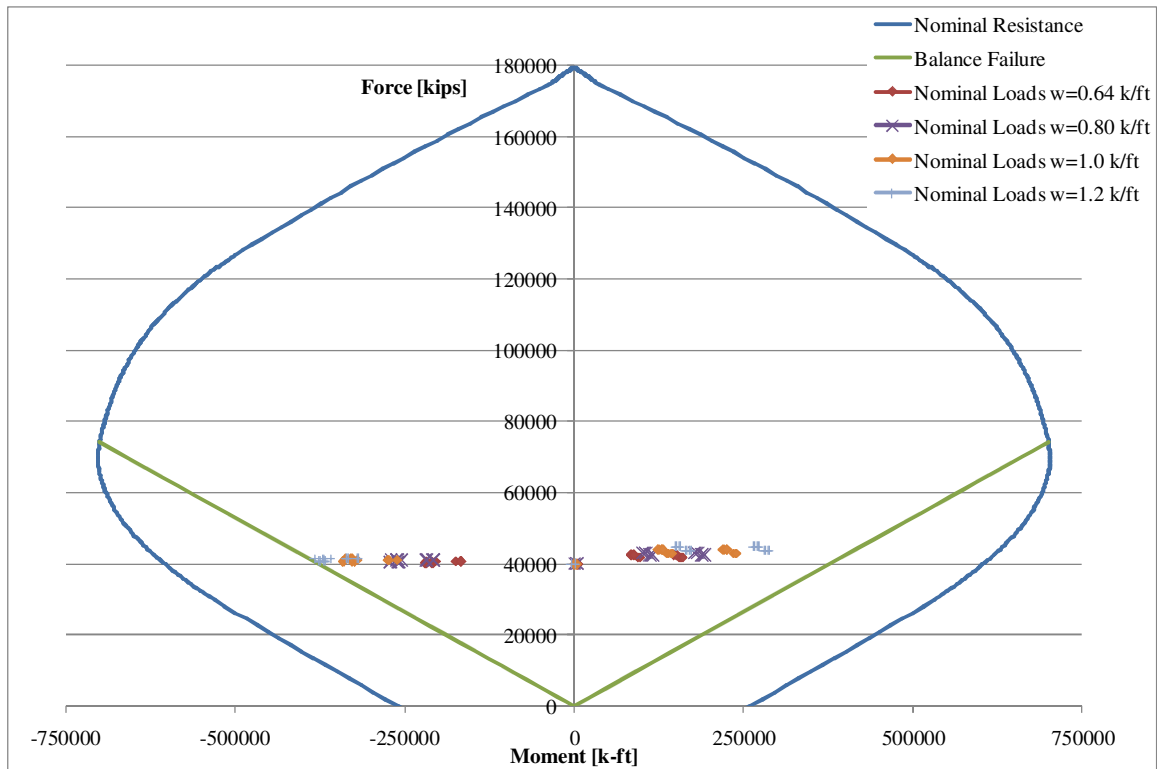
Figure 8.18 Force and Moment results on the bridge tower for different live loads

Figure 8.19 shows the results of reliability indexes due to different live loads. It can be noticed that values of β are in high range for the cases with the eccentricity of loads very small for all possible loading conditions. For the cases with the eccentricities approaching the balance failure the reliability indexes are decreasing with the increase of the actual loading.
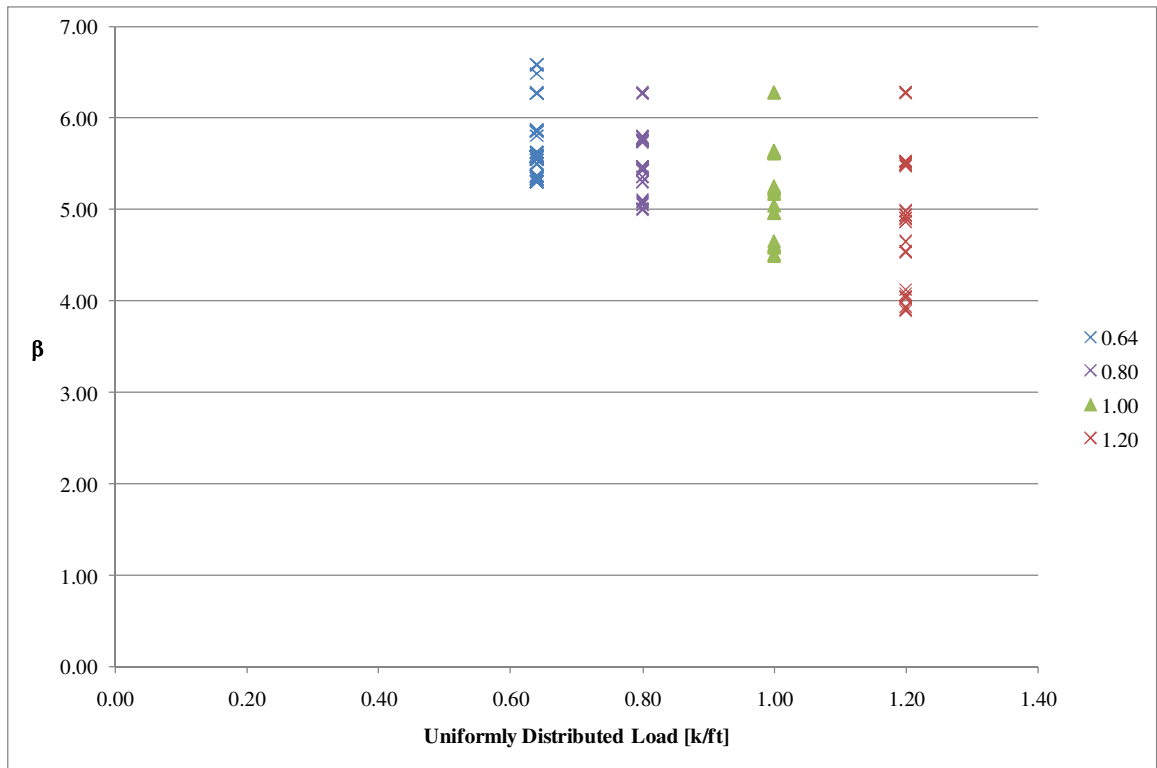
Figure 8.19 Reliability indexes due to different live load

CHAPTER 9

SUMMARY & CONCLUSIONS

In the study, a live load model for long span structures was derived. The live load model is valid for spans between 600 ft and 5000 ft and it is intended to reflect current traffic patterns, quantities of trucks and their weights. The developed live load model is recommended to be taken into consideration in the bridge design code.

Preliminary study was performed by reviewing previous research and current provisions of international codes on the topic. Equivalent uniformly distributed load is calculated and compared. The new live load was developed based on three models: an average 5-axle truck, legal load trucks and simulation of a traffic jam using WIM data. The newest available traffic database from a variety of sites within many different states was obtained. The magnitude of the database has to be underlined, because such an extensive actual weigh in motion database has never been used in the derivation of live load for any kind bridges. A numerical procedure was developed to filtered out WIM data from erroneous readings and to simulate traffic jam situations. From the simulation the values of uniformly distributed load were derived for a variety of span lengths and site localizations. In the developed procedure, starting with the first truck, all consecutive trucks were added with a fixed clearance distance between them until the total length reached the span length. Then, the total load of all trucks was calculated and divided by the span length to obtain the first value of the average uniformly distributed load. Next, the first truck was deleted, and one or more trucks were added so that the total length of trucks covers the full span length and the new value of the average uniformly distributed

129

load was calculated. Trucks were kept in actual order, as recorded in the WIM surveys. Results of the simulations were plotted as a cumulative distribution function of uniformly distributed load for considered span lengths. The obtained mean value oscillates between values of 0.50 and 0.75 k/ft. Cumulative distribution functions were also plotted for maximum daily and maximum weekly combinations of trucks. For longer spans, uniformly distributed load decreases and is closer to the mean value. This observation confirms that for a long loaded span, one heavily overloaded truck does not have significant influence. This is because the load depends on a mix of traffic. The bias factors (ratio of mean to nominal) were calculated for the heaviest 75-year combination of vehicles. The 75-year uniformly distributed loads were derived from extrapolated distributions. It was noticed that the bias factor values for most of the sites do not exceed 1.25, which is similar as in short and medium spans, as shown in the NCHRP Report 368 (1999). It is recommended to use HL-93 also for those long spans. Two other models, an average 5-axle truck and a legal load trucks model led to similar conclusion. It was noticed that for some sites, with very heavy traffic, the bias factor reaches a value of 2.0. Those sites are characterized by high ADTT (usually over 3000) or increased percentage of overloaded loaded vehicles (over about 10%). Bridges located in such sites require special attention and application of increased design live load. The value of the design load should be agreed with the owner of the structure. For some bridges considered, for example in the area of New York, it was found that the uniformly distributed load should be 1.25 kip/ft in order to obtain bias lower than 1.25. Statistical parameters for live load are: for spans 600-1000 ft bias 1.25 and coefficient of variation 0.10, for spans longer than 1000 ft bias 1.20 and coefficient of variation 0.08.

In this dissertation, the problem of multilane reduction factors was discussed. Multilane factors were found to be very site specific, as with the live load. Video recordings of traffic confirmed that for the majority of the time we can observe that the moving lanes contain a mixture of trucks and cars. However, situations when one lane is almost exclusively occupied by trucks or trucks occupy three or four lanes at the same time are also possible. Multiple reduction factors for design live load should account for those most critical loading cases. In the WIM database available, the vehicles of 1-3 categories 1-3 have not been registered. Therefore, it did not allow for simulations and

derivation of multilane factors for all traffic lanes. Simulation of the traffic on the most loaded lane was possible with an assumption, that in traffic jam situations passenger vehicles merge to the left and the right lane remains occupied exclusively by trucks. It was stated that equal reduction of load on all traffic lane does not reflect the actual situation. At least one of the lanes should be loaded more than the others. It was concluded that the multilane reduction factors have to be an objective of additional extensive studies.

The study of dynamic factor was performed for the research. It was concluded that the current dynamic load factor of 0.33 is too high for bridges with longer spans. It may be applicable in short bridges, when vibration due to "wheel hop" on the approach slab is significant. For longer bridges, where the influence of the approach slab decreases and vibrations of many vehicles interfere with each other, the dynamic load factor could be smaller. The assumption of a traffic jam situation to develop live load model induces no dynamic allowance. However, to not introduce confusion among designers it is recommended do keep dynamic factor as it is for short and medium span bridges, which results in very small value for long span bridges.

CHAPTER 10

RECCOMENDATIONS

1. The developed live load model is valid for long spans between 600 ft and 5000 ft.

2. For long spans it is recommended to use HL-93 load, specified in AASHTO LRFD Code (2007), uniformly distributed load of 0.64 k/ft plus design truck or tandem. The bias factor calculated for the heaviest 75-year combination of vehicles did not exceed 1.25, which is similar as in short and medium spans, as shown in the NCHRP Report 368 (1999).

3. For some sites characterized by high ADTT or increased percentage of overloaded vehicles (over 10%) bias factor reaches a value of 2.0. Those bridges require application of increased site specific design live load, which should be agreed with the owner of the structure.

4. It was proposed to use dynamic factor as specified in AASHTO LRFD Code (2007). Developed live load model assumes traffic jam situation and does not allow for dynamic. However, to not introduce confusion among designers it is recommended do keep dynamic factor as it is for short and medium span bridges, which results in very small value for long span bridges.

5. It was proposed to use multilane reduction factors as specified in AASHTO LRFD Code (2007). It is recommended to perform further studies in this field.

6.   Statistical parameters for live load are:

- for spans 600-1000 ft: bias 1.25 and coefficient of variation 0.10,

- for spans longer than 1000 ft: bias 1.20 and coefficient of variation 0.08.

The developed live load model is recommended to be taken into consideration in the AASHTO LRFD Bridge Design Specifications.

REFERENCES

[1]. AASHTO LRFD Bridge Design Specifications. (2007). American Association of State Highway and Transportation Officials, Washington, D.C.

[2]. AASHTO Geometric Design of Highways and Streets (2001). American Association of State Highway and Transportation Officials, Washington, D.C.

[3]. CAN/CSA-S6-00 Canadian Highway Bridge Design Code, CSA International, Toronto, Canada.

[4]. Manual for Condition Evaluation and load and Resistance Factor Rating (LRFD) of Highway Bridges. 2003. American Association of State Highway and Transportation Officials, Washington, D.C.

[5]. OHBDC (1991), Ontario Highway Bridge Design Code, Ontario Ministry of Transportation, Downsview, Ontario.

[6]. ASCE Committee on Loads and Forces on Bridges (1981). "Recommended Design Loads for Bridges", ASCE Journal of Structural Engineering, Vol. 107, No. 7, December 1981, pp. 1161-1213.

[7]. Ang, A. H-S., and Tang, W.H., *"Probability Concepts in Engineering Planning and Design,"* Volume I: Basic Principles, John Wiley & Sons, new York, 1975

[8]. Ang, A. H-S., and Tang, W.H., *"Probability Concepts in Engineering Planning and Design,"* Volume II: Decision, Risk, and Reliability, John Wiley & Sons, New York, 1984

[9]. Augusti G., Barrata B. "Limit and Shakedown Analysis of Structures with Stochastic Strengths," Proceedings of the Second SMiRT Conference, Berlin, 1973

[10]. Augusti G., Barrata B. "Plastic Shakedown of Structures with Stochastic Local Strengths," Proceedings of the Symposium on Resistance Ultimate Deformability of Structures, IABSE, Lisbon, 1973

[11]. Ayyub B.M., Halder A. "Practical Structural Reliability Techniques," Journal of Structural Engineering, ASCE, Vol. 110, No. 8, 1984, pp. 1707-1724

134

[12]. Ayyub B.M., McCuen R.H. "Probability, Statistics, & Reliability for Engineers," CRC Press Boca Raton, New York, 1997

[13]. Benjamin J.R., Cornell C.A. "Probability, Statistics and Decision for Civil Engineers," McGraw-Hill, New York, 1970

[14]. Biggs, J.M., Suer, H.S. 1955. "Vibration Measurements on Simple-Span Bridges", Highway Research Board, Bulletin 124.

[15]. Breitung K. "Asymptotic Approximations for Multinormal Integrals," Journal of Engineering Mechanics, ASCE, Vol. 110, 1984, pp. 357-366

[16]. Buckland, P.G., Navin, F.P.D, Zidek, J.V., and McBryde, J.P, 1978, "Traffic loading of long-span bridges", Transportation Research Record, Vol. 665, pp. 146-154.

[17]. Buckland, P.G., Navin, F.P.D, Zidek, J.V., and McBryde, J.P., 1980, "Proposed Vehicle Loading of Long-Span Bridges", Journal of Structural Division, ASCE, Vol. 106, pp. 915-932.

[18]. Buckland, P.G., 1991, "North American and British Long-Span Bridge Loads", Journal of Structural Division, ASCE, Vol. 117, pp. 2972-2987.

[19]. Cantieni, R. 1984. "Dynamic Load Testing of Highway Bridges", Transportation Research Record No 950, pp. 141-148.

[20]. Cebon, D. 1999. "Handbook of vehicle-road interaction", Department of Engineering, University of Cambridge. London.

[21]. Cebon, D. 1993. "Interaction between heavy vehicles and roads", Department of Engineering, University of Cambridge. London.

[22]. Cornell, C. A., *"Bounds on the Reliability of Structural Systems,"* Journal of the Structural Division, ASCE, 93 (ST1), 171-200, 1967

[23]. Corotis R.B., Nafday A.M. "Structural Systems Reliability using Linear Programming and Simulations," Journal of Structural Engineering, ASCE, Vol. 115, No. 10, 1989, pp. 2435-2447

[24]. Ellingwood, B.; Galambos, T.V.; MacGregor, J.G., and Cornell, C.A., "Development of a Probability Based Load Criterion for American National Standard A58," NBS Special Publication 577, Washington, DC, National Bureau of Standards, 1980

[25]. Ellingwood, B., MacGregor, J.G., Galambos, T.V., and Cornell, C.A., *"Probability Based Load Criteria: Load factors and Load Combinations,"* Journal of Structural Engineering, ASCE, Vol. 108, No. ST5, 1982

[26]. Fiessler B., Naumann H-J., Rackwitz R. "Quadratic Limit States in Structural Reliability," Journal of Engineering Mechanics, ASCe, Vol. 105, 1979, pp. 661-676

[27]. Fleming, F.J., Romualdi, J.P. 1961. "Dynamic Response of Highway Bridges", Journal of the Structural Division, Vol. 87.

[28]. Fraudenthal A.M. "Safety and Probability of Structural Failure," Transactions, ASCE, Vol. 121, 1956, pp. 1337-1375

[29]. Galambos, T.V., and Ravindra, M.K., *"Load and Resistance Factor Design,"* Journal of Structural Devision, ASCE, ST9, Proc. Paper 14008, Sep. 1978

[30]. Galdos, N.H., Schelling, D.R., Sahin, M.A. 1993. "Methodology for Impact Factor of Horizontally Curved Box Bridges", Journal of Structural Engineering, Vol. 119, No. 6, pp. 1917-1934.

[31]. Gindy, M., Nassif, H.H., 2006, "Multiple Presence Statistics for Bridge Live Load Based on Weigh-in-Motion Data", TRB annual meeting

[32]. Hasofer A.M., Lind N.C. "An Exact and Invariant First Order Reliability Format," Journal of Structural Mechanics Division, ASCE, Vol. 100, No. 1, 1974

[33]. Hohenbichler M., Rackwitz R. "Improvement of Second-Order Reliability Estimates by Importance Sampling," Journal of the Engineering Mechanics, ASCE, Vol. 114, 1988, pp. 2195-2199

[34]. Hwang, E-S. and Nowak, A.S., "Simulation of Dynamic Load for Bridges", ASCE Journal of Structural Engineering, Vol. 117, No. 5, May 1991, pp. 1413-1434.

[35]. Khalifa, M.A. 1992. "Parametric Study of Cable-Stayed Bridge Response Due to Traffic-induced Vibration", Computers & Science, Vol. 47, No. 2, pp. 321-339.

[36]. Khisty, C.J. Prentice Hall, Englewood Cliffs, New Jersey, "Transportation Engineering", 1990.

[37]. Kim, S-J., Sokolik, A.F., and Nowak, A.S., 1997, "Measurement of Truck Load on Bridges in the Detroit Area", Transportation Research Record, No.1541, pp. 58-63.

[38]. Kiureghian A., Liu P-L. "Structural Reliability under Incomplete Probability Information," Journal of Engineering Mechanics, ASCE, Vol. 112, 1986, pp. 85-104

[39]. Kulicki J.M., Prucz Z., Clancy C.M., Mertz D.R., Nowak A.S., "Updating the calibration report for AASHO LRFD", NCHRP 20-7/186, January 2007

[40]. Lutomirski, T.A., "Reliability models for circular concrete columns", Doctoral Dissertation, 2009.

[41]. MacAdam, C.C., Fancher, P.S., Hu, G.T., Gillespie, T.D. 1980. "A computerized model for simulating the breaking and steering dynamics of trucks, tractor-semitrailers, doubles, and triples combinations", MVMA Project 1197.

[42]. McLean, D.I., Marsh, M.L. 1998. "Dynamic Impact Factors for bridges", NCHRP Synthesis 266.

[43]. Nassif, H.H., and Nowak, A.S., 1995, "Dynamic Load Spectra for Girder Bridges", Transportation Research Record, No. 1476, pp. 69-83.

[44]. Navin, FPD, 1982, "Road vehicles on bridges", Canadian Journal of Civil Engineering, Vol. 9, pp. 468-476.

137

[45]. Nowak, A.S., "Calibration of LRFD Bridge Design Code," NCHRP Report 368, Transportation Research Board, Washington, D.C., USA, 1999

[46]. Nowak, A.S., and Lind , N.D., *"Practical Bridge Code Calibration,"* Journal of Structural Division, ASCE, pp. 2497-2510, December 1979

[47]. Nowak, A.S., 1993, "Live Load Model for Highway Bridges", Journal of Structural Safety, Vol. 13, Nos. 1+2, December, pp. 53-66.

[48]. Nowak, A.S., "Calibration of LRFD Bridge Design Code", Final Report, NCHRP Project 12-33, December 1993.

[49]. Nowak, A.S., 1994, "Load Model for Bridge Design Code", Canadian Journal of Civil Engineering, Vol. 21, pp. 36-49.

[50]. Nowak, A.S., 1995, "Calibration of LRFD Bridge Code", ASCE Journal of Structural Engineering, Vol. 121, No. 8, pp. 1245-1251.

[51]. Nowak, A.S. and Hong, Y-K., "Bridge Live Load Models", ASCE Journal of Structural Engineering, Vol. 117, No. 9, Sept. 1991, pp. 2757-2767.

[52]. Nowak, A.S., Hong, Y-K and Hwang, E-S., "Modeling Live Load and Dynamic Load for Bridges", Transportation Research Record, No. 1289, 1991, pp. 110-118.

[53]. Nowak, A.S., Kim, S-J., Laman, J., Saraf, V. and Sokolik, A.F., "Truck Loads on Selected Bridges in the Detroit Area", Final Report submitted to MDOT, November 1994.

[54]. Nowak, A.S., Laman, J. and Nassif, H., "Effect of Truck Loading on Bridges", Final Report submitted to MDOT, December 1994.

[55]. Nowak, A.S. and Collins, K.R., "Reliability of Structures," McGraw-Hill New York, New York, USA, 2000

[56]. MacGregor J.G., Mirza S.A., Ellingwood B., "Statistical Analysis of Resistance of Reinforced and Prestressed Concrete Members", ACI Structural Journal, Title no.80-16, May-June, 1983, pages 167 to 176.

[57]. Madsen H.O., Krenk S., Lind N.C. "Methods of Structural Safety," Prentice-Hall, 1986

[58]. Murzewski J. "Reliability of Engineering Structures" (in Polish), Arkady, Warsaw, Poland, 1989

[59]. Paultre, P., Chaallal, O., Proulx, J. 1992. "Bridge Dynamics and Dynamic Amplification Factors: A Review of Analytical and Experimental Findings", Canadian Journal of Civil Engineering, Vol. 19, No. 2, pp. 260-278.

[60]. Rackwitz, R., Fiessler, B. "Structural Reliability under Combined Random Load Sentences," Computers & Structures, Vol. 9, 1978, pp. 489-494

[61]. Rosenblatt, M. "Remarks on Multivariate Transformations," The Annuals of Mathematical Statistics, Vol. 23, 1952, pp. 470-472

[62]. Schelling, D.R., Galdos, N.H., Sahin, M.A. 1992. "Evaluation of Impact Factors for Horizontally Curved Steel Box Bridges", Journal of Structural Engineering, Vol. 118, No. 11, pp. 3203-3221.

[63]. Sivakumar, B., Ghosn, M., Moses, F., "Protocols for Collecting and Using Traffic Data in Bridge Design," Final Report, NCHRP Project 12-76, July 2008.

[64]. Thoft-Christiansen, P., Baker, M.J. "Structural Reliability Theory and Its Applications," Springer-Verlag, Berlin, Heidelberg, New York, 1982

[65]. Thoft-Christiansen, P., Murotsu, Y. "Application of Structural Systems Reliability Theory," Springer-Verlag, Berlin, Heidelberg, New York, Tokio, 1986

[66]. Wang, T.L., Shahawy, M., Huang, D.Z. 1993. Dynamic Response of Highway Truck Due to Road Surface Roughness. Computers and Structures, Vol. 49, No. 6, pp. 1055-1067.

[67]. Wang, T.L, Hunag, D.Z. 1992. "Cable-stayed Bridge Vibration Due to Road Surface Roughness", Journal of Structural Engineering, Vol. 188, No. 5, pp. 1354-1374.

[68]. Wang, T.L., Huang, D.Z., Shahawy, M. 1996. "Dynamic Behavior of Continuous and Cantilever Thin-Walled Box Girder Bridges", Journal of Bridge Engineering, Vol. 1, No. 2, pp. 67-75.

[69]. Winkler, C.B., Fancher, P.S., MacAdam, C.B. 1983. "Parametric Analysis of heavy duty truck dynamic stability", UMTRI-83-13.

[70]. Wolinski Sz., Wrobel K. "Reliability of Engineering Structures" (in Polish), Publishers of Rzeszow Technical University (Oficyna Wydawnicza Politechniki Rzeszowskiej), 2001

[71]. Zhu, X.Q., Law, S.S. 2002. "Dynamic Load on Continuous Multi-lane Bridge Deck from moving vehicles", Journal of Sound and Vibration, Vol. 251, No. 4, pp. 697-716.

[72]. Transportation Statistics Annual Report, December 2006, U.S. Department of Transportation.

[73]. "Regulation of Weights, Lengths, and Widths of Commercial Motor Vehicles". Special Report 267. TRB, National Research Council, Washington, DC, 2002.

[74]. "Comprehensive Truck Size and Weight Study. Volume I: Summary Report". Publication FHWA-PL-00-029. FHWA, U.S. Department of Transportation, Washington, DC, 2000.

[75]. Truck Driver's Guidebook, Michigan Center for Tuck Safety, 2008.

[76]. "Model for Highway Bridge Impact", Journal of Structural Engineering, Vol. 116, No. 7, pp. 1772-1793.

[77]. Traffic Monitoring Guide, U.S. Department of Transportation, Federal Highway Administration, 2001.

APPENDIX A

CDF OF UDL FOR ALL TRUCK COMBINATIONS
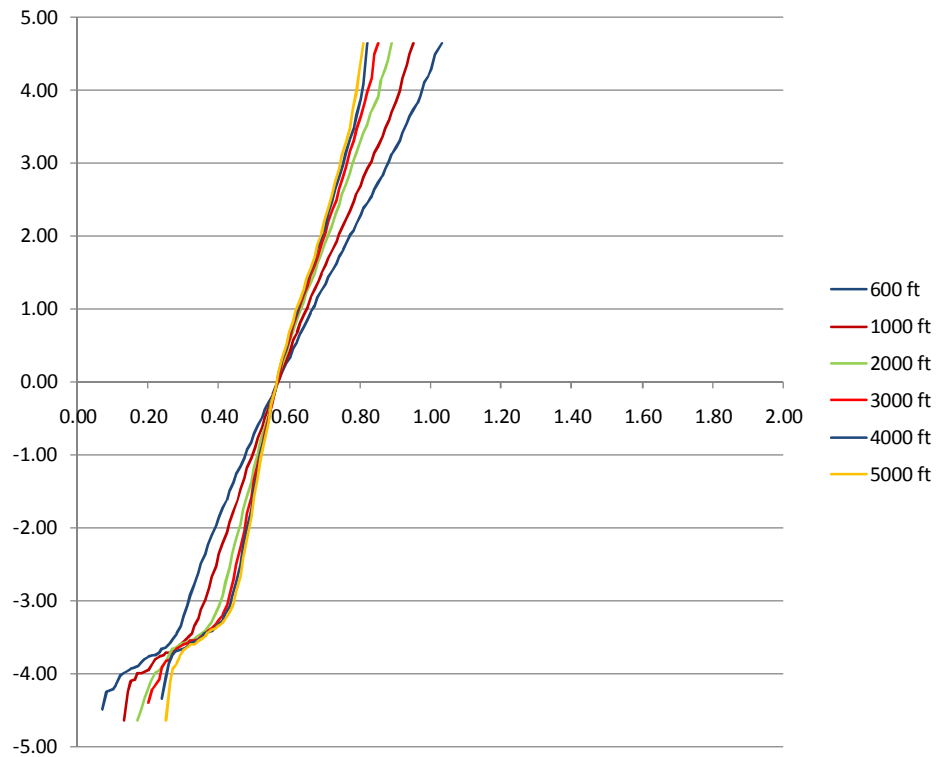
Figure A.1. CDF of UDL for Oregon I-5 Woodburn, lane 1
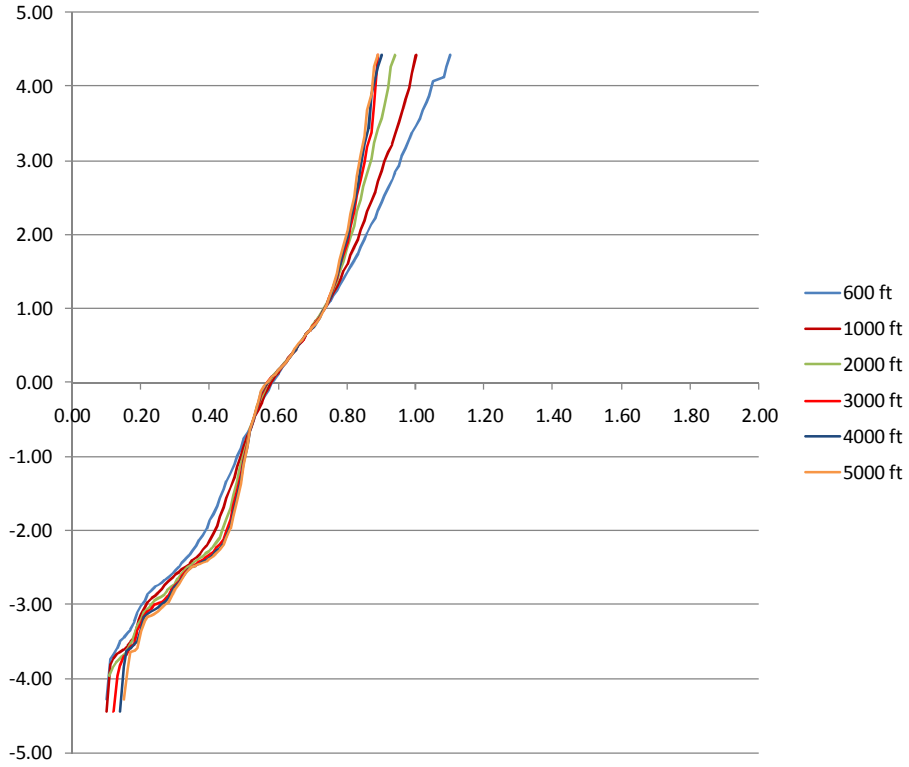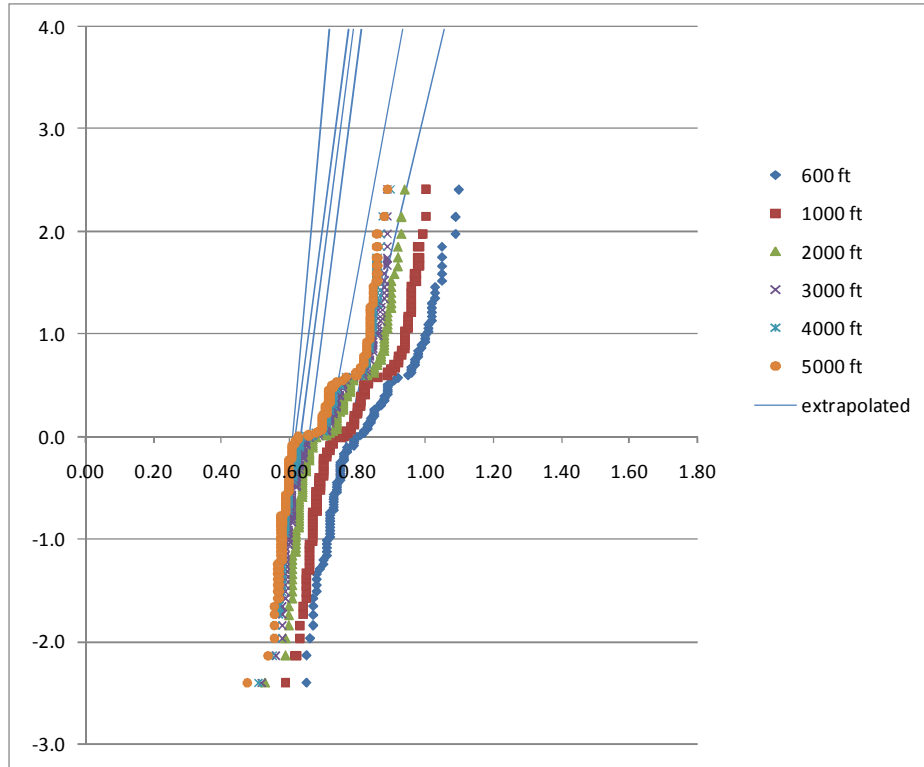
Figure A.2. CDF of UDL for Oregon I-84 Emigrant Hill, lane 1
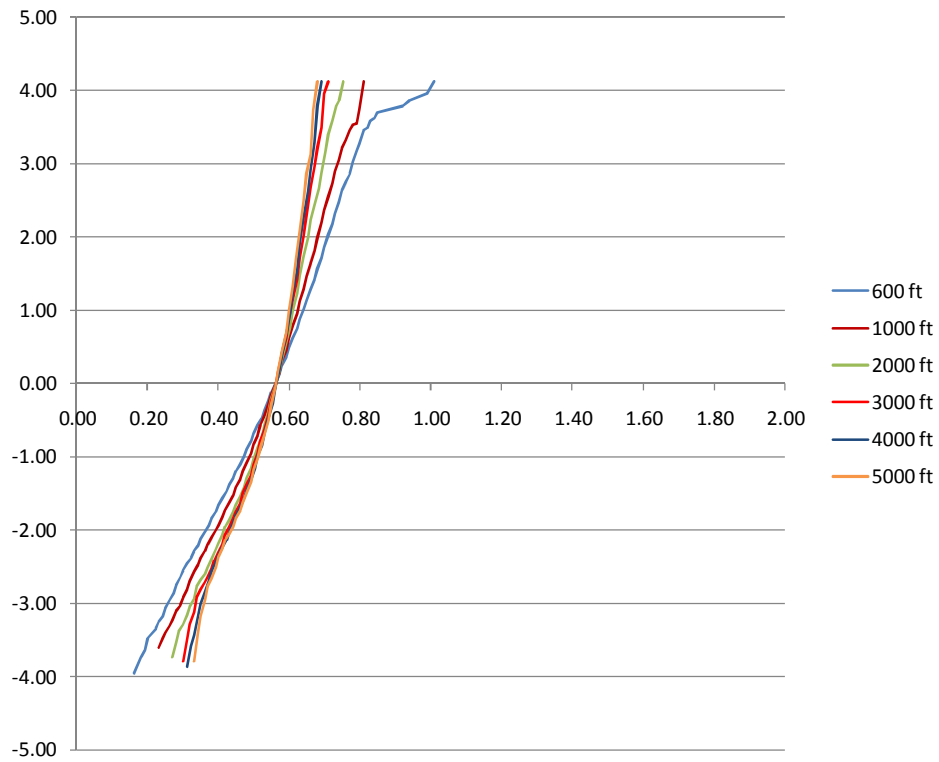
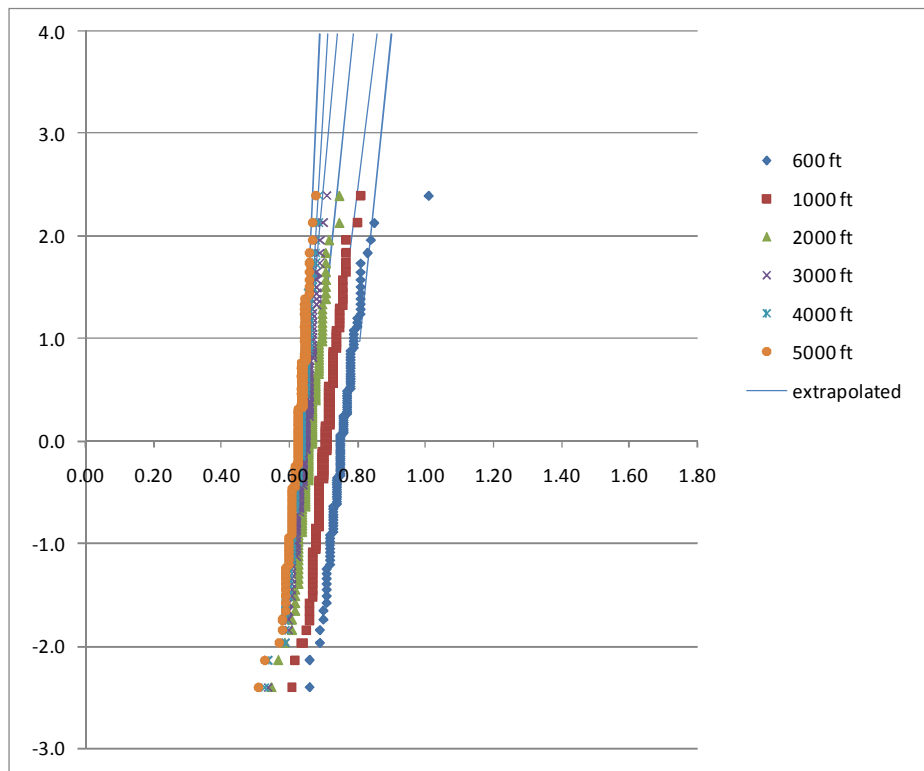Figure A.3. CDF of UDL for Oregon OR 58 Lowell, lane 1
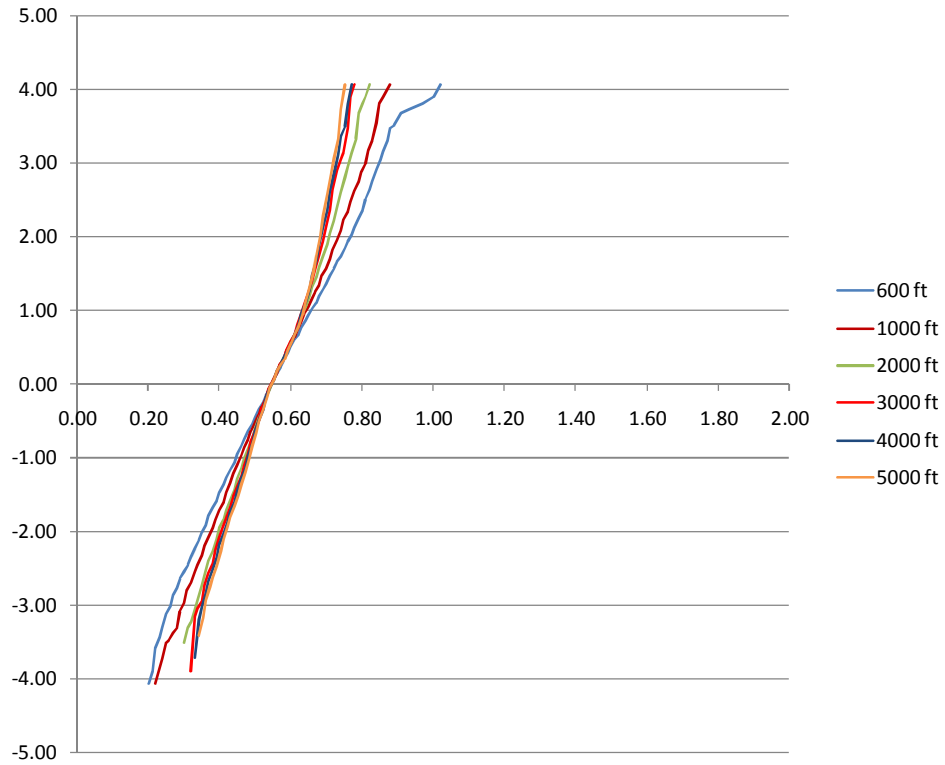
Figure A.4. CDF of UDL for Oregon OR 58 Lowell, lane 2
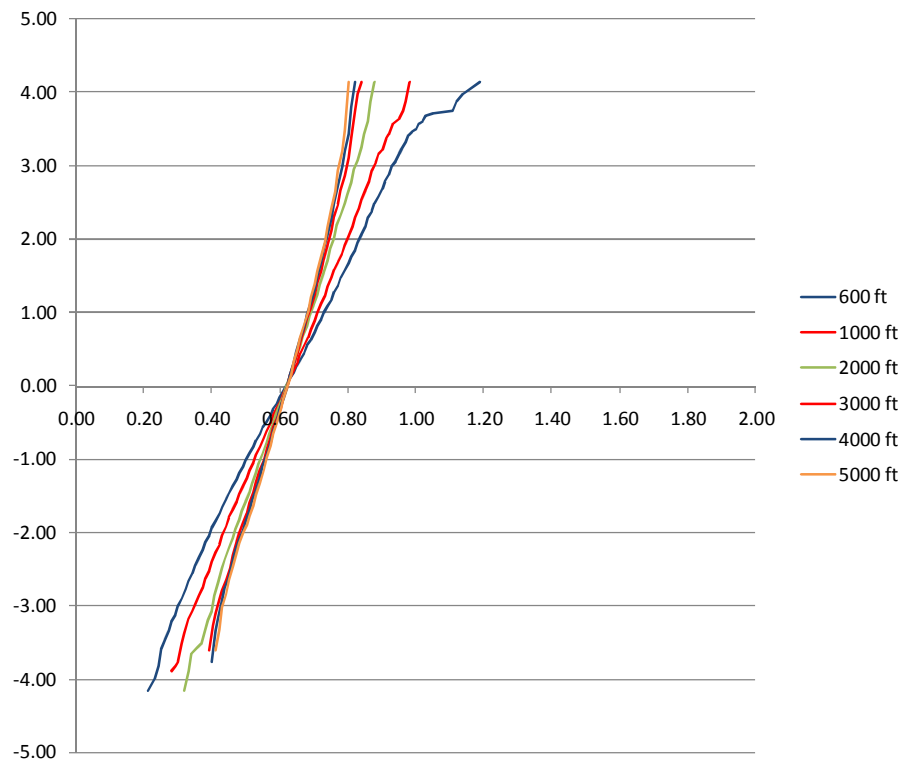
Figure A.5. CDF of UDL for Oregon US 97 Bend, lane 1

143
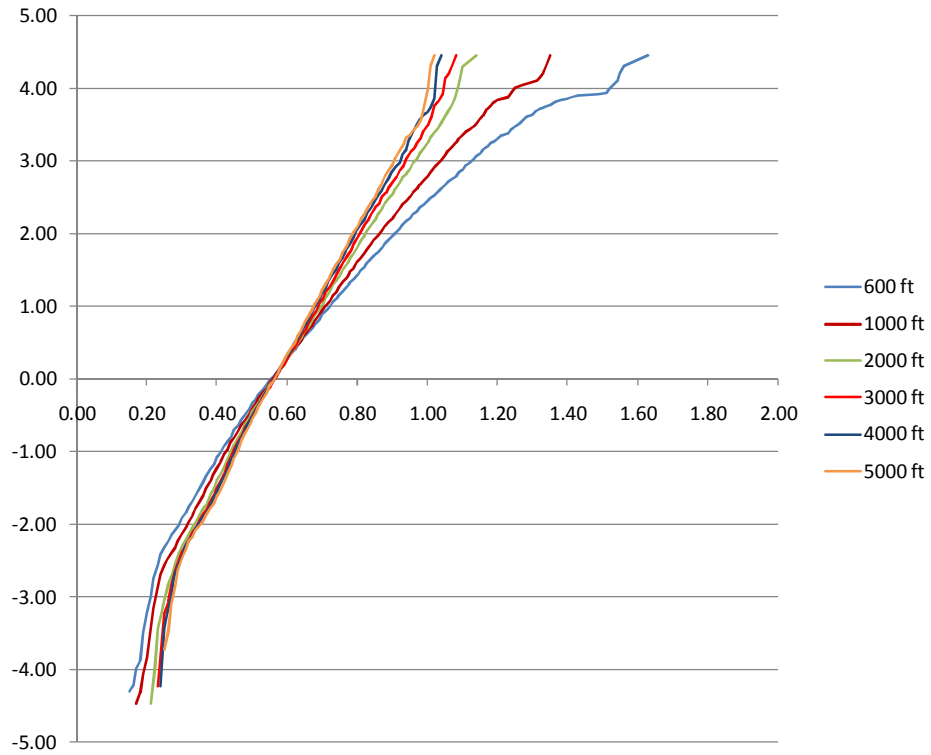
Figure A.6. CDF of UDL for Florida 9916, lane 1
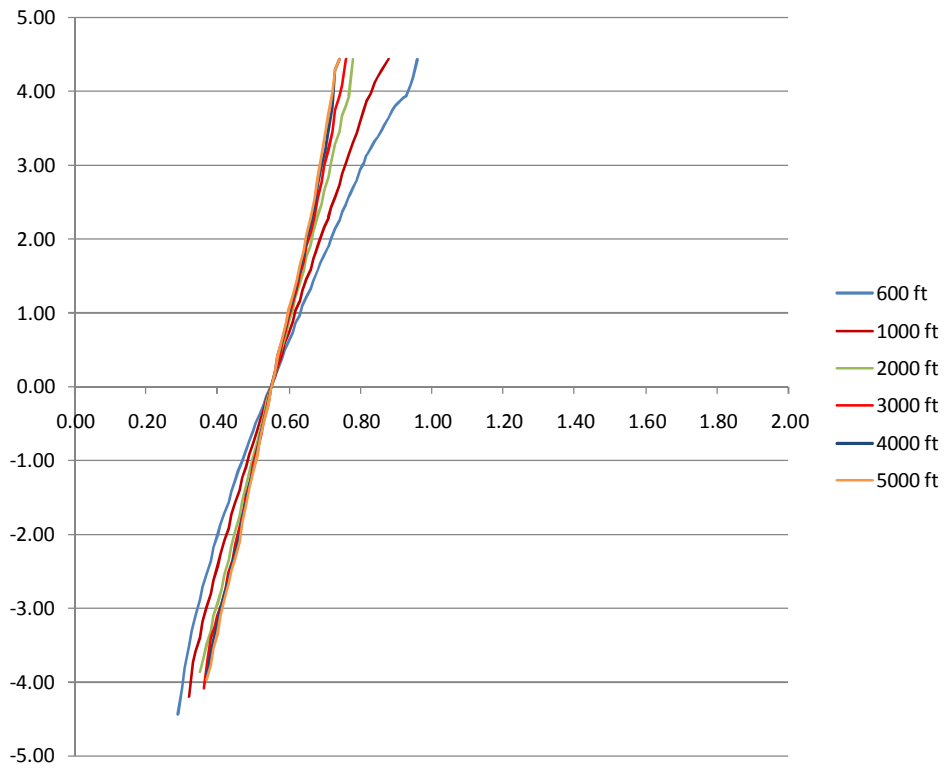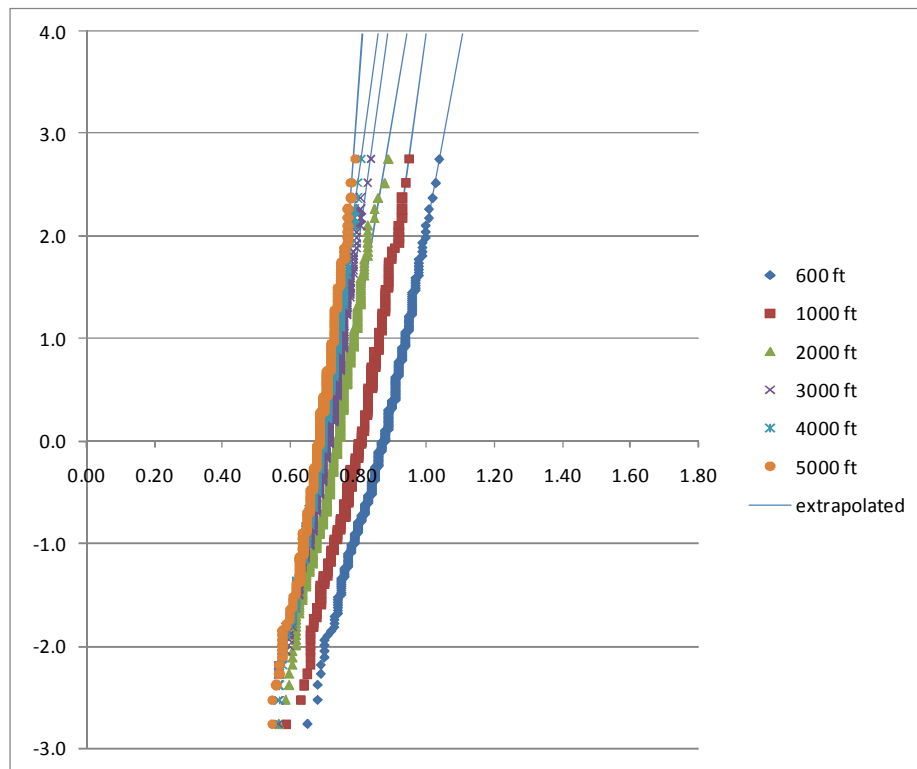

Figure A.7. CDF of UDL for Florida 9919, lane 1

144
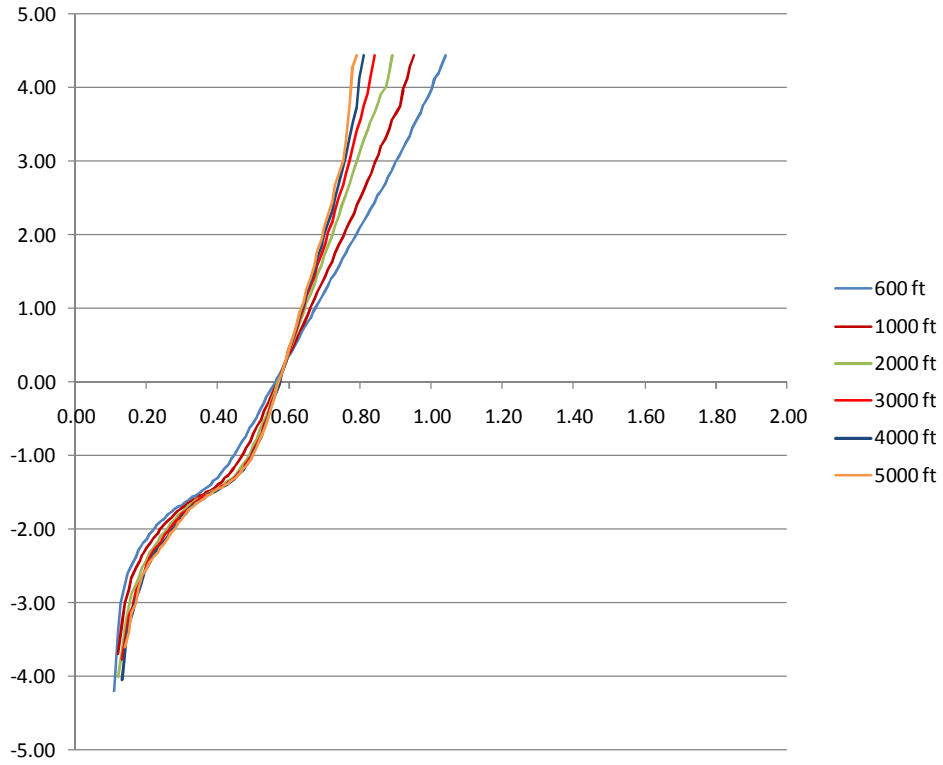
Figure A.8. CDF of UDL for Florida 9927, lane 1
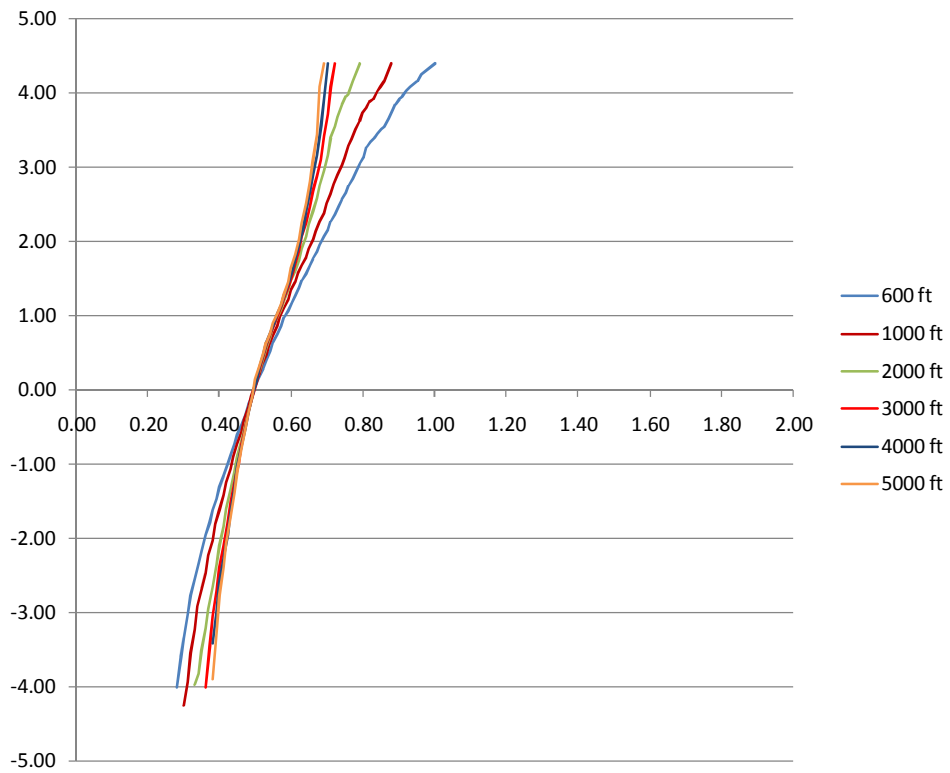
Figure A.9. CDF of UDL for Florida 9936, lane 1

145
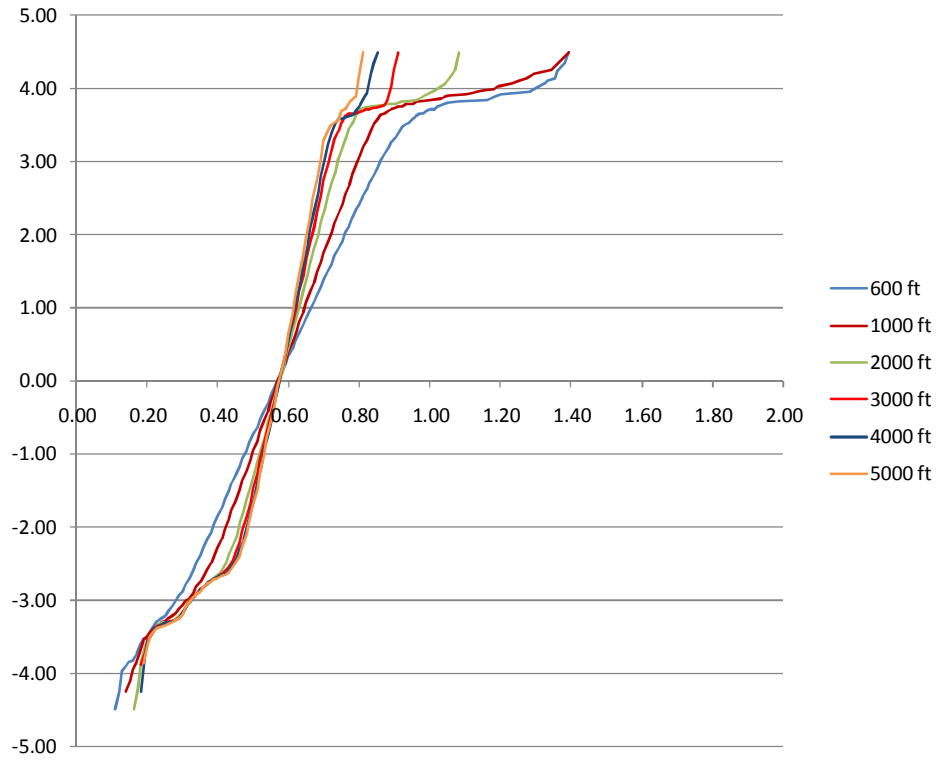
Figure A.10. CDF of UDL for Indiana 9534, lane 1
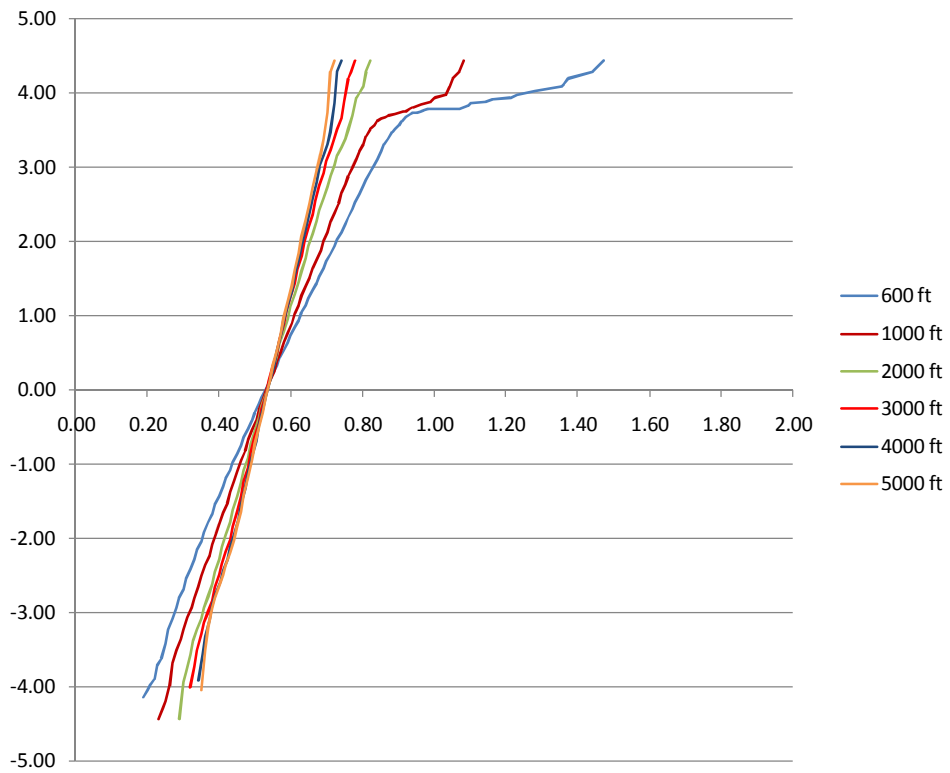
Figure A.11. CDF of UDL for Indiana 9534, lane 2

146
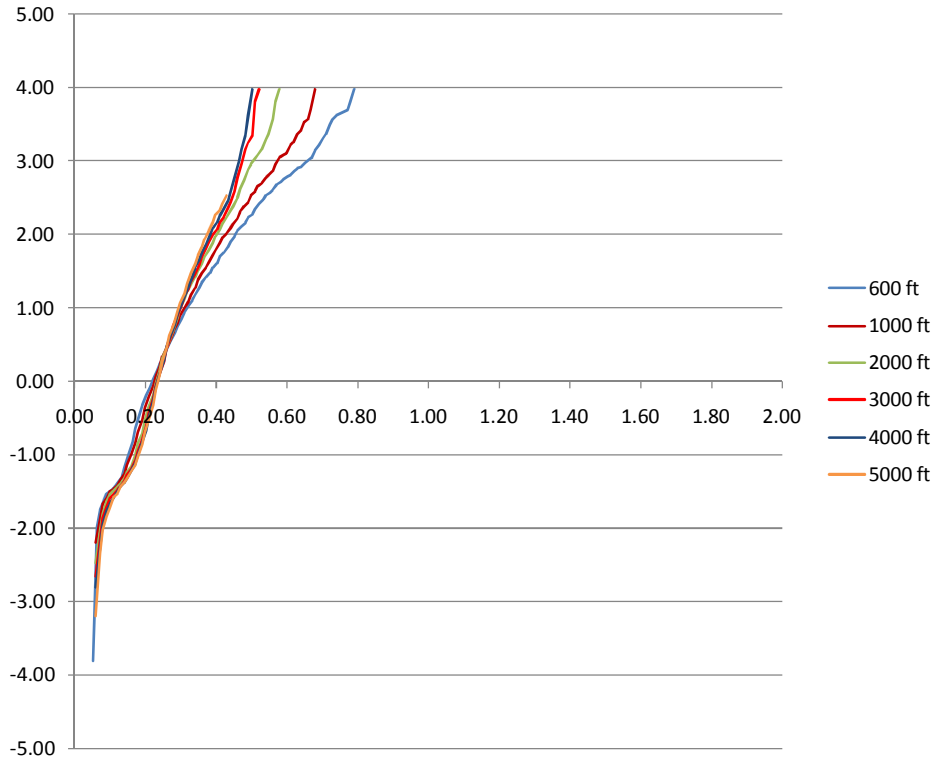
Figure A.12. CDF of UDL for Indiana 9534, lane 3
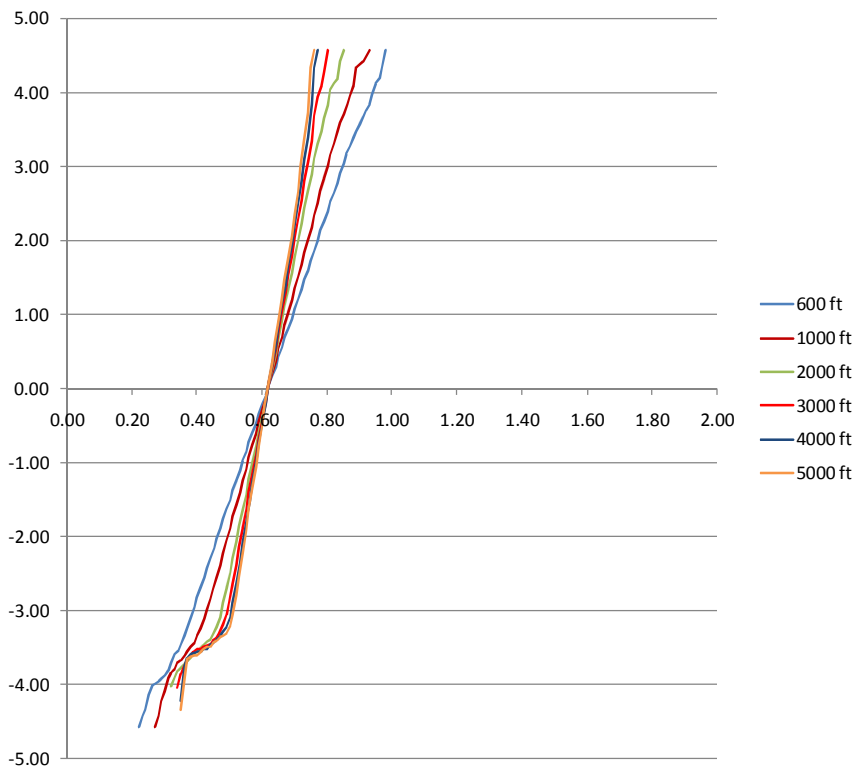
Figure A.13. CDF of UDL for Indiana 9544, lane 1

147
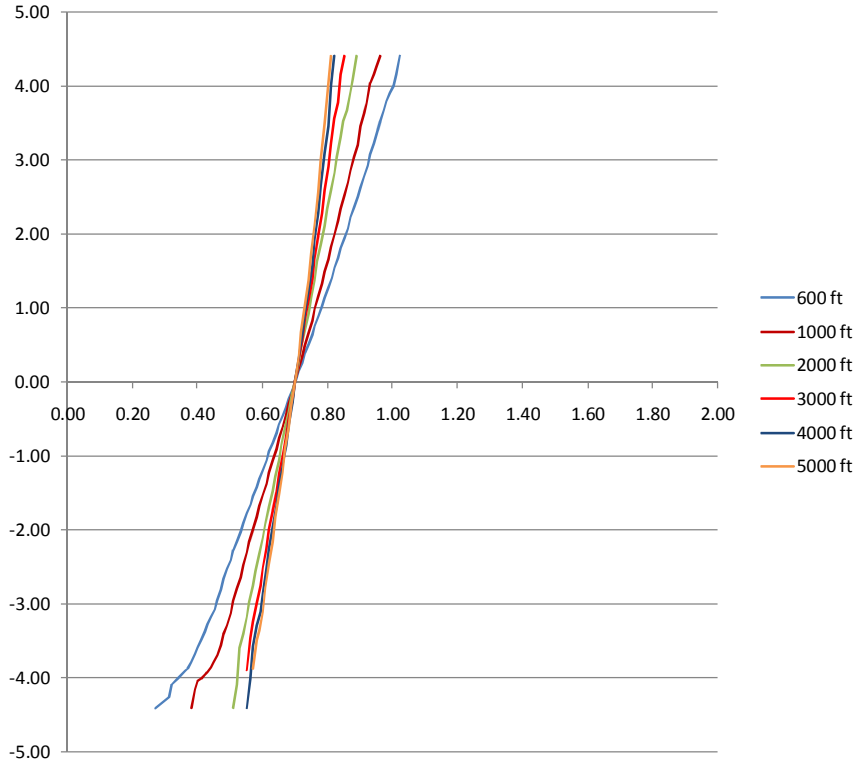
Figure A.14. CDF of UDL for Indiana 9512, lane 1
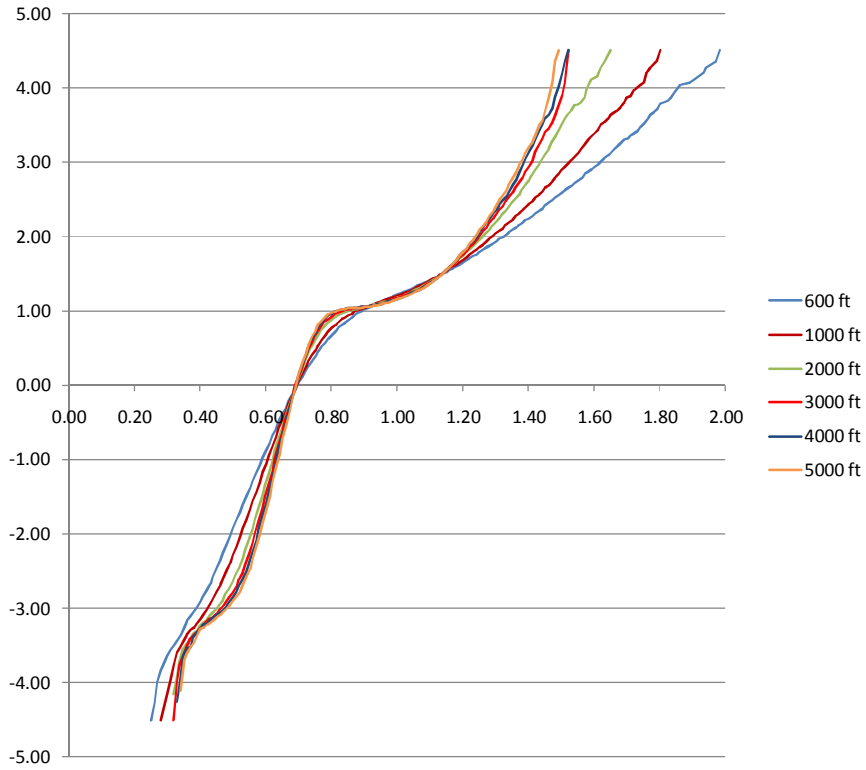
Figure A.15. CDF of UDL for New York 9121, lane 1
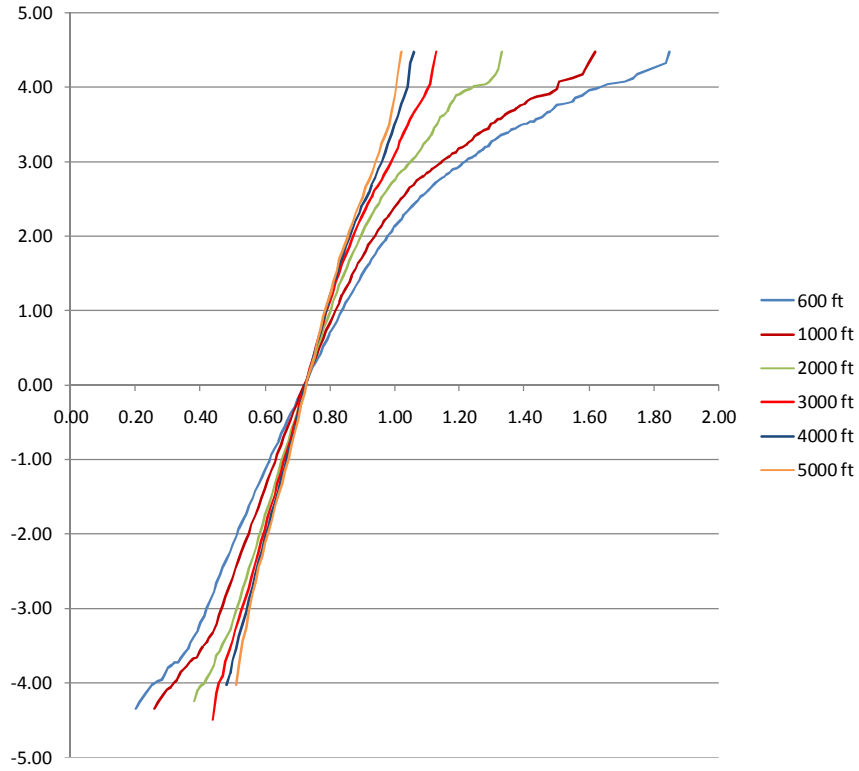
Figure A.16. CDF of UDL for New York 9121, lane 4
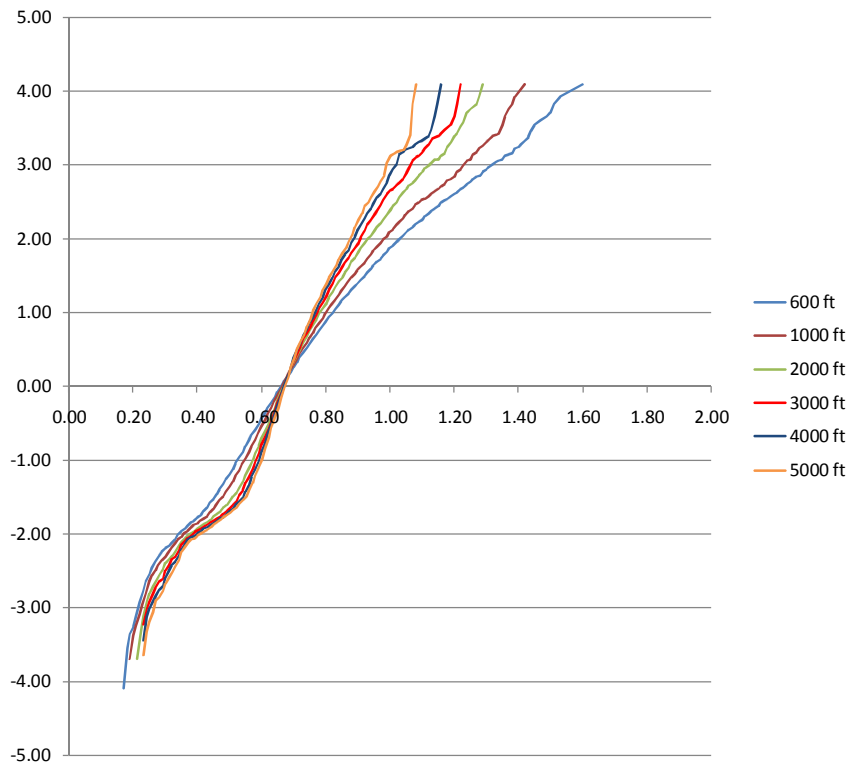
Figure A.17. CDF of UDL for New York 2680, lane 1
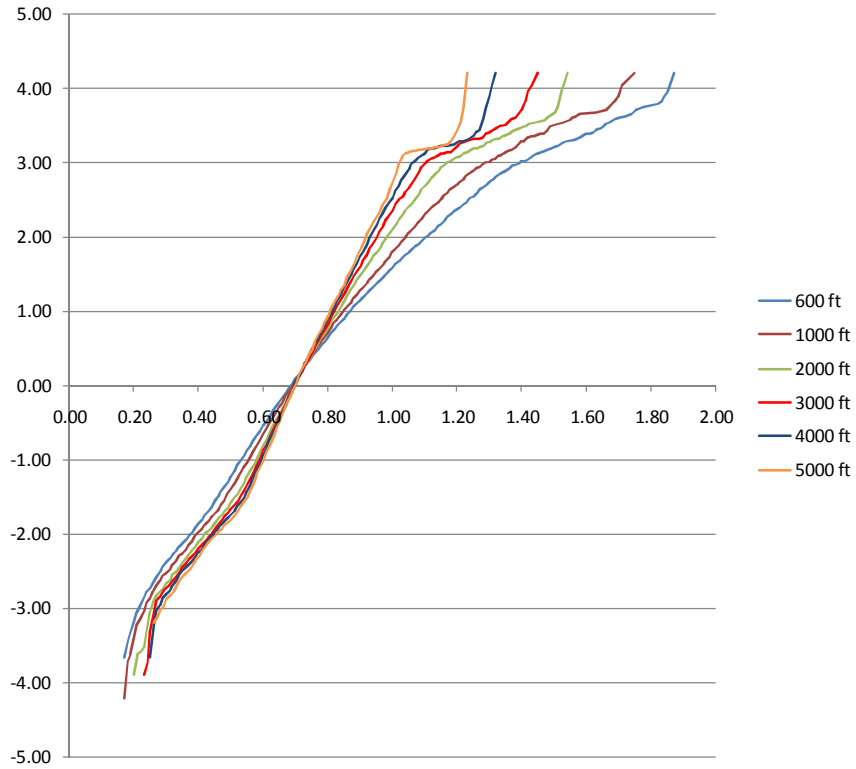
Figure A.18. CDF of UDL for New York 2680, lane 4
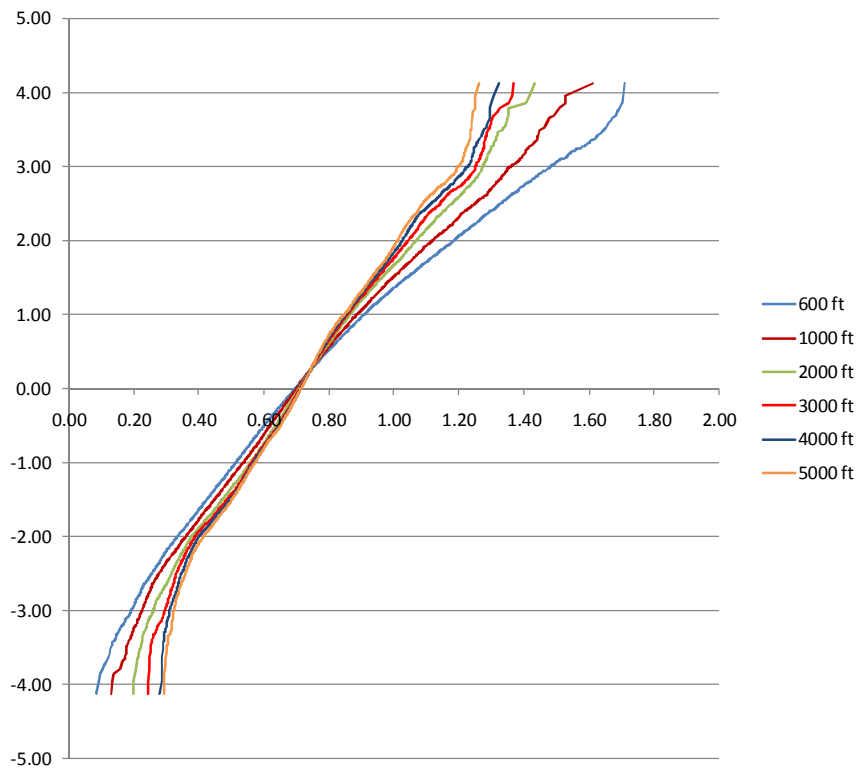
Figure A.19. CDF of UDL for New York I-495 EB, lane 1
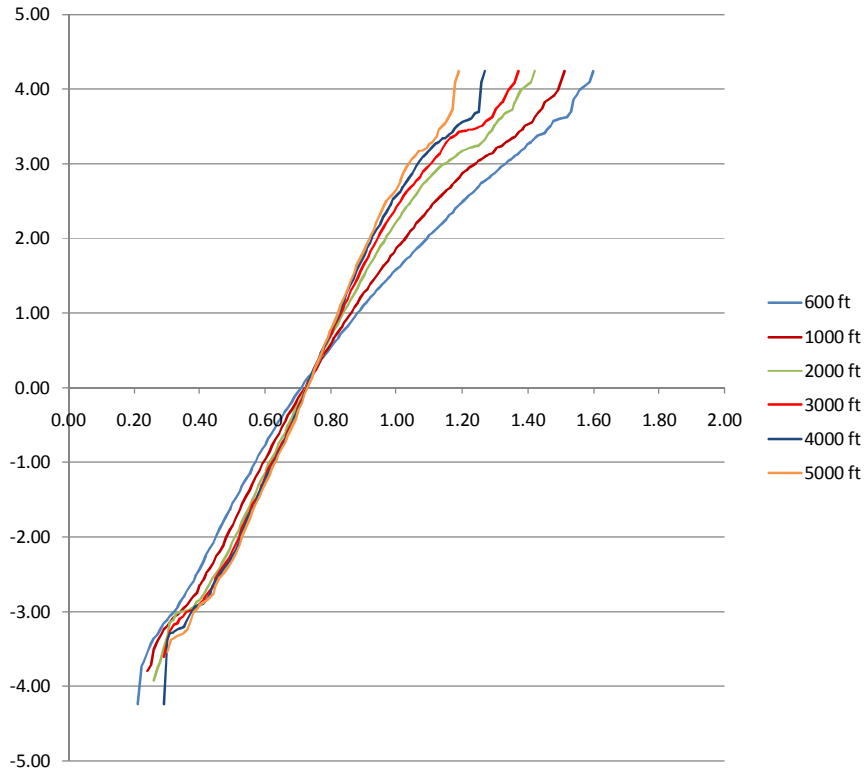
Figure A.20. CDF of UDL for New York I-495 EB, lane 2
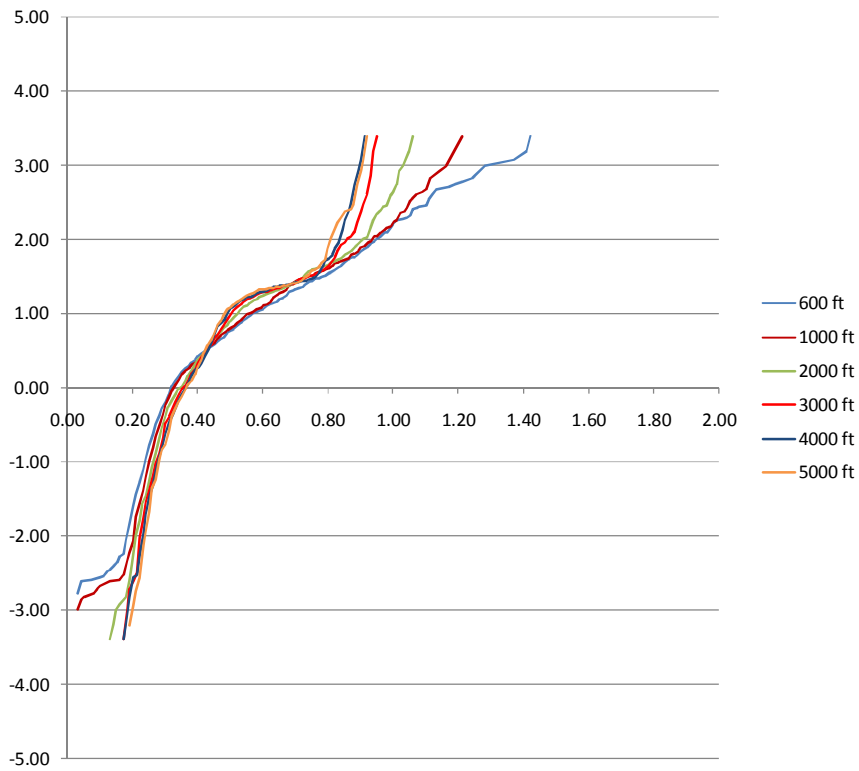
Figure A.21. CDF of UDL for New York I-495 EB, lane 3

151
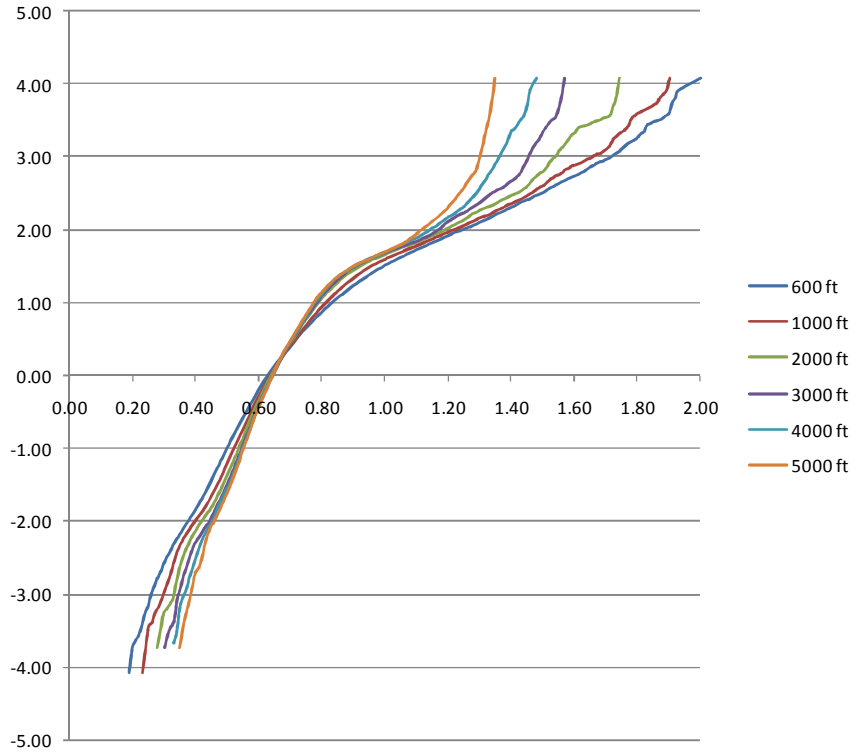
Figure A.22. CDF of UDL for New York I-495 WB, lane 1
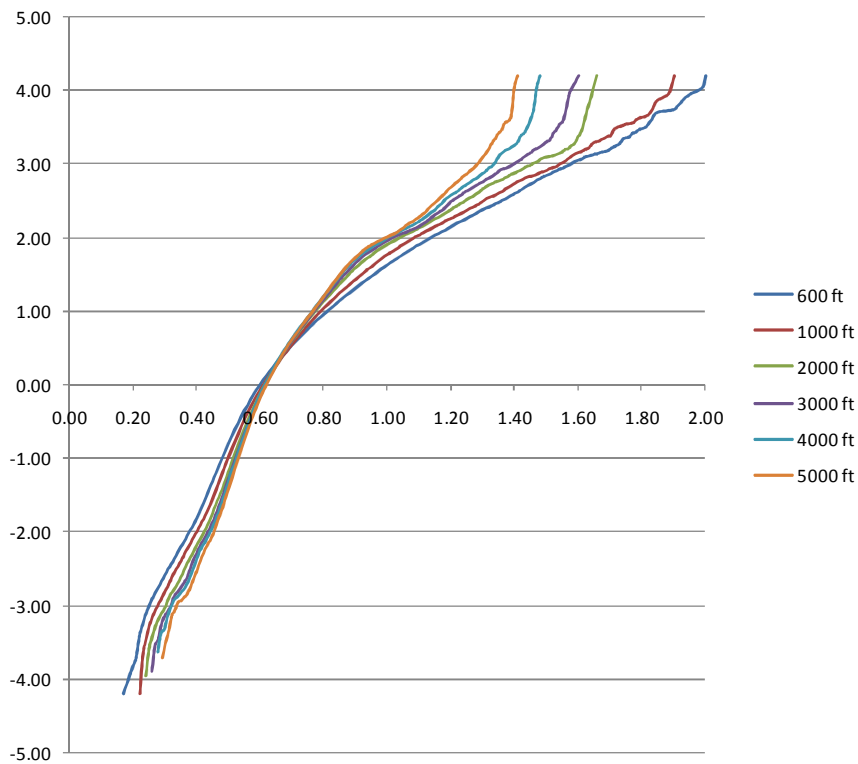
Figure A.23. CDF of UDL for New York I-495 WB, lane 2
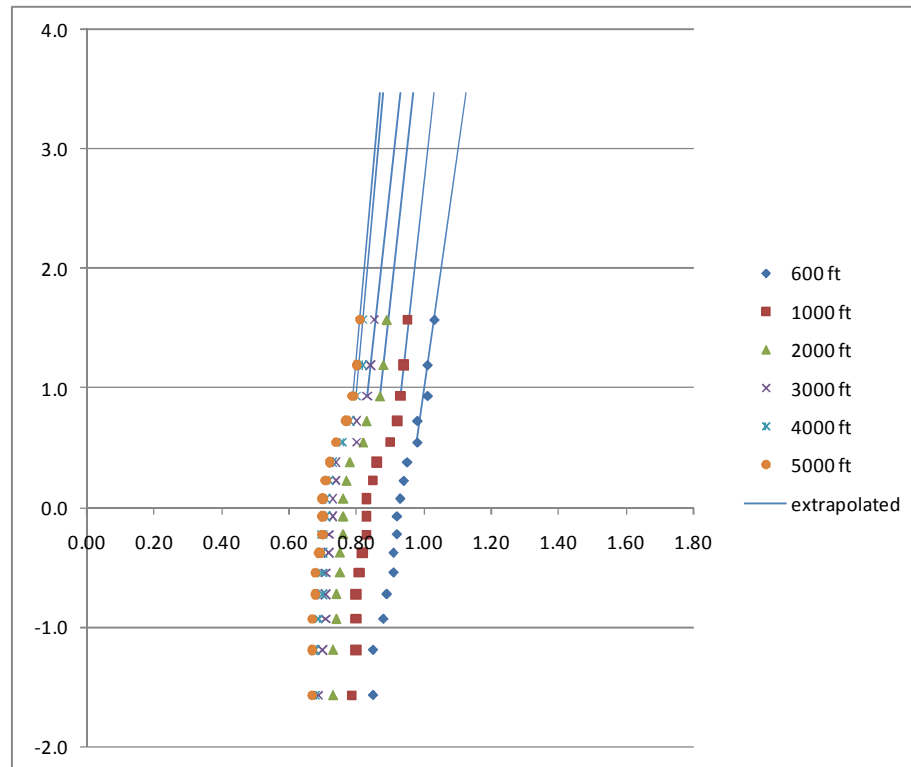
152

APPENDIX B

CDF OF MAXIMUM DAILY UDL
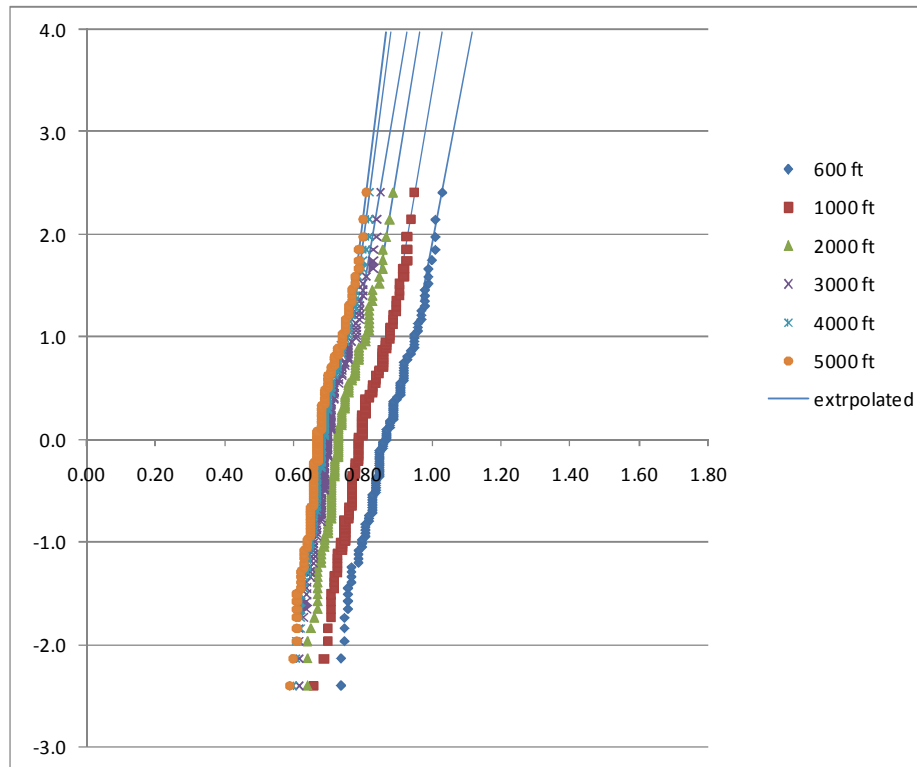
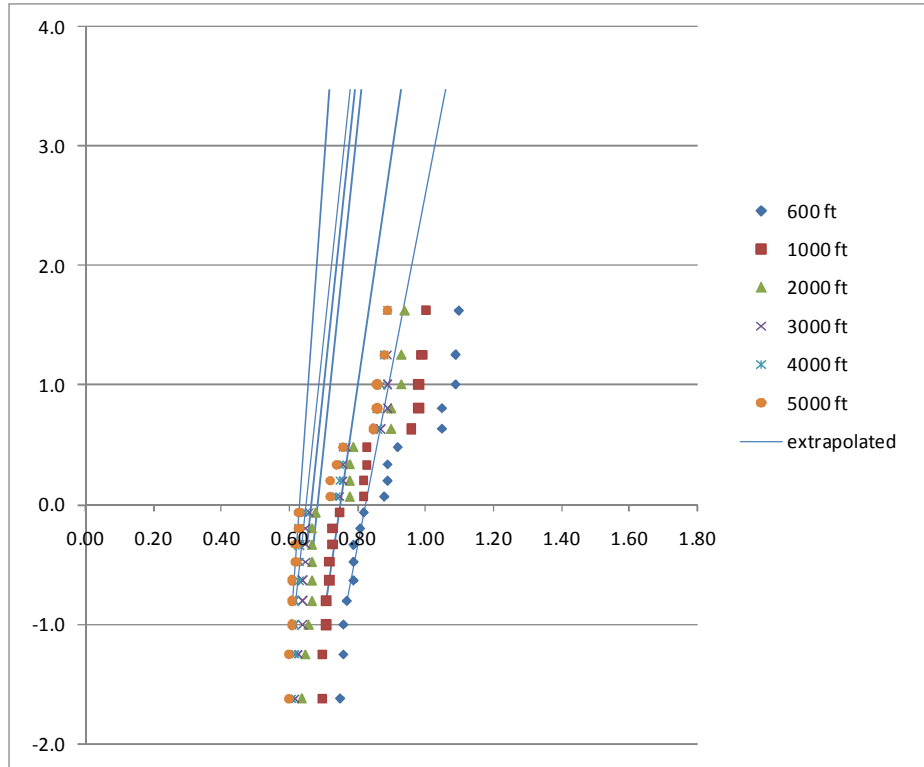Figure B.1. CDF of maximum daily UDL for Oregon I-5 Woodburn, lane 1

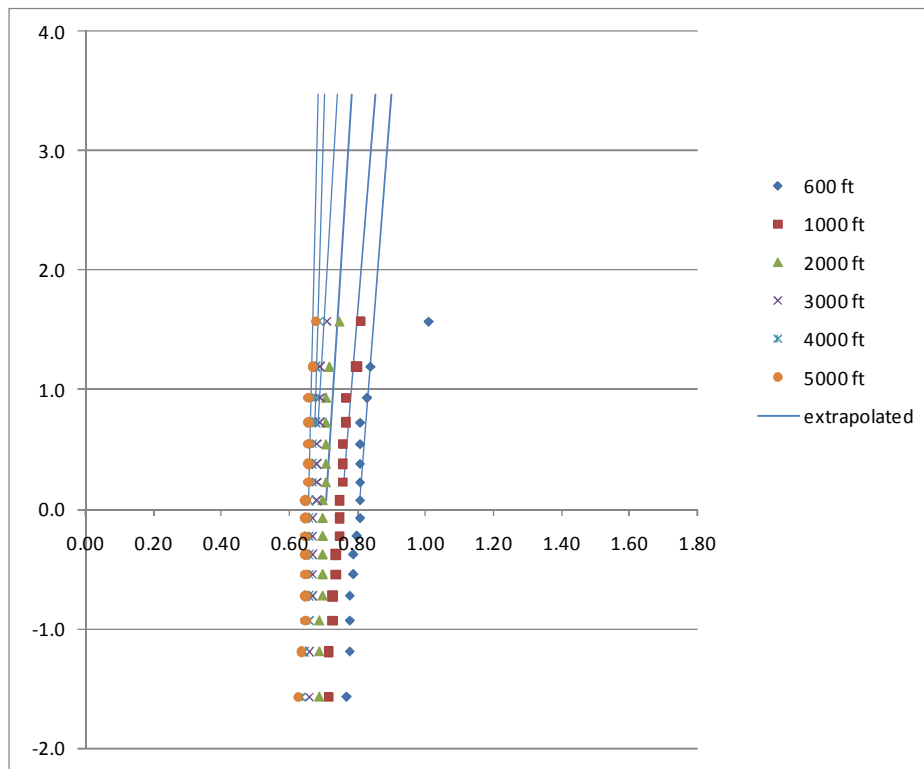Figure B.2. CDF of maximum daily UDL for Oregon I-84 Emigrant Hill, lane 1

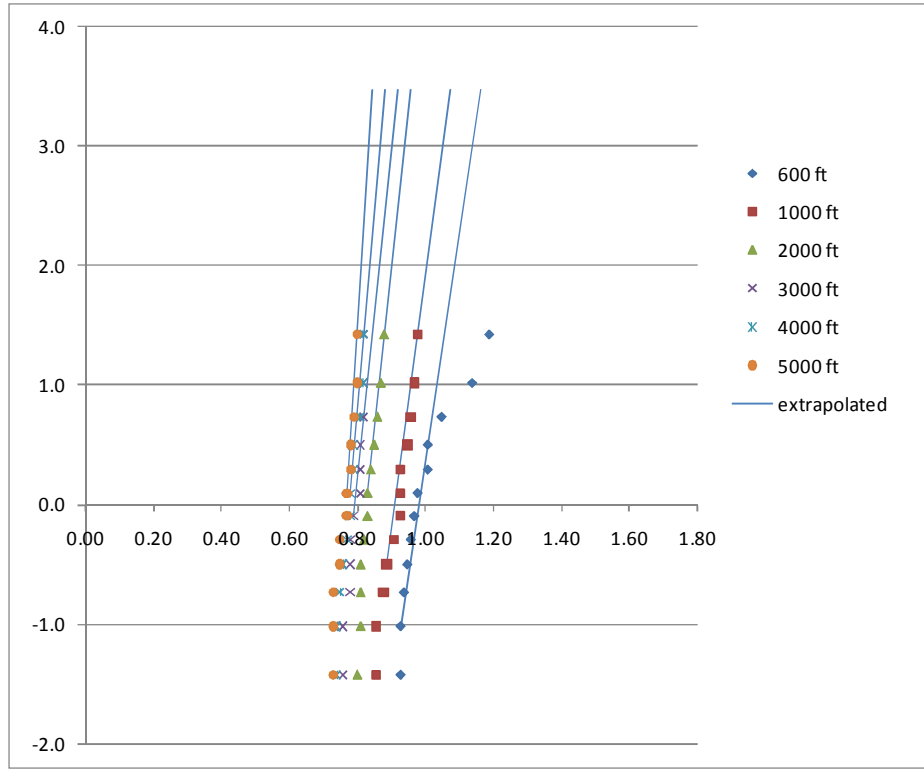Figure B.3. CDF of maximum daily UDL for Oregon OR 58 Lowell, lane 1

154
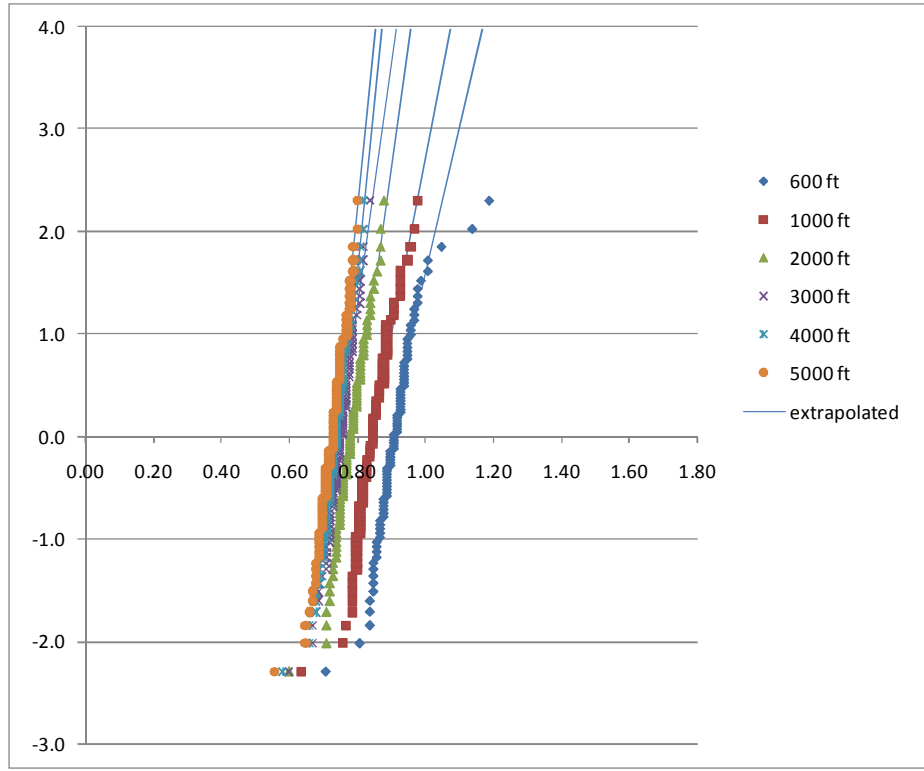
Figure B.4. CDF of maximum daily UDL for Oregon US 97 Bend, lane 1
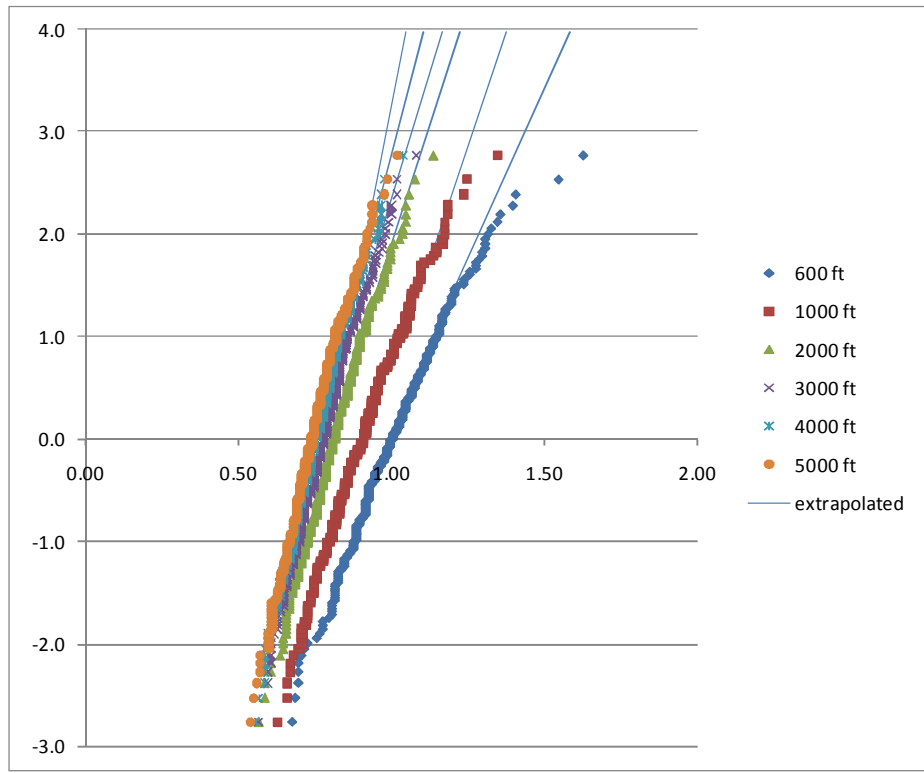
Figure B.5. CDF of maximum daily UDL for Florida 9916, lane 1

155
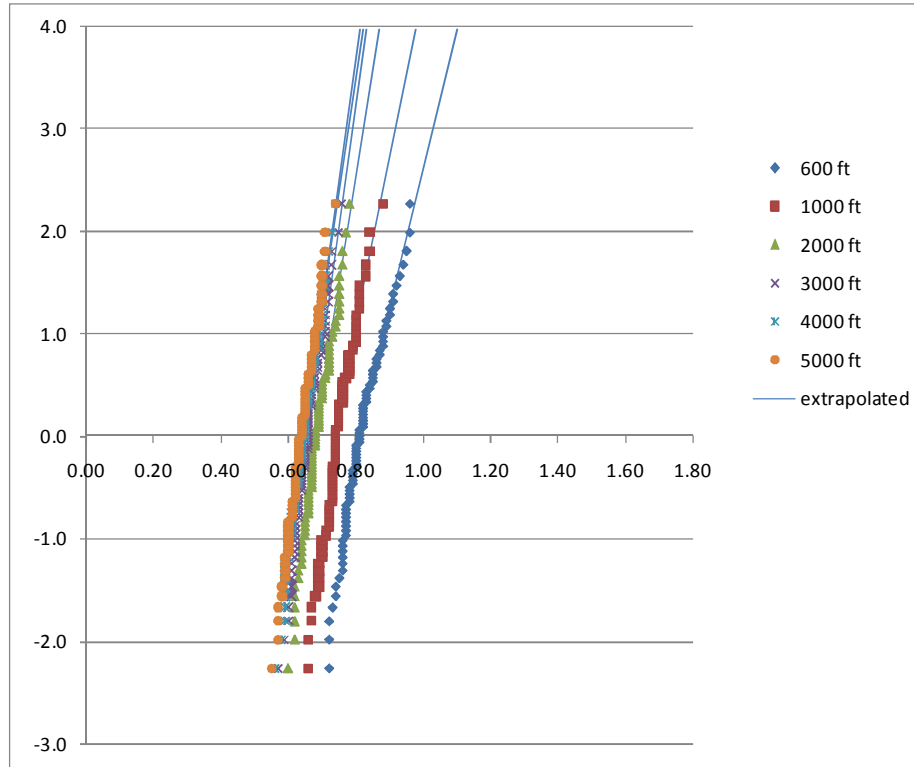
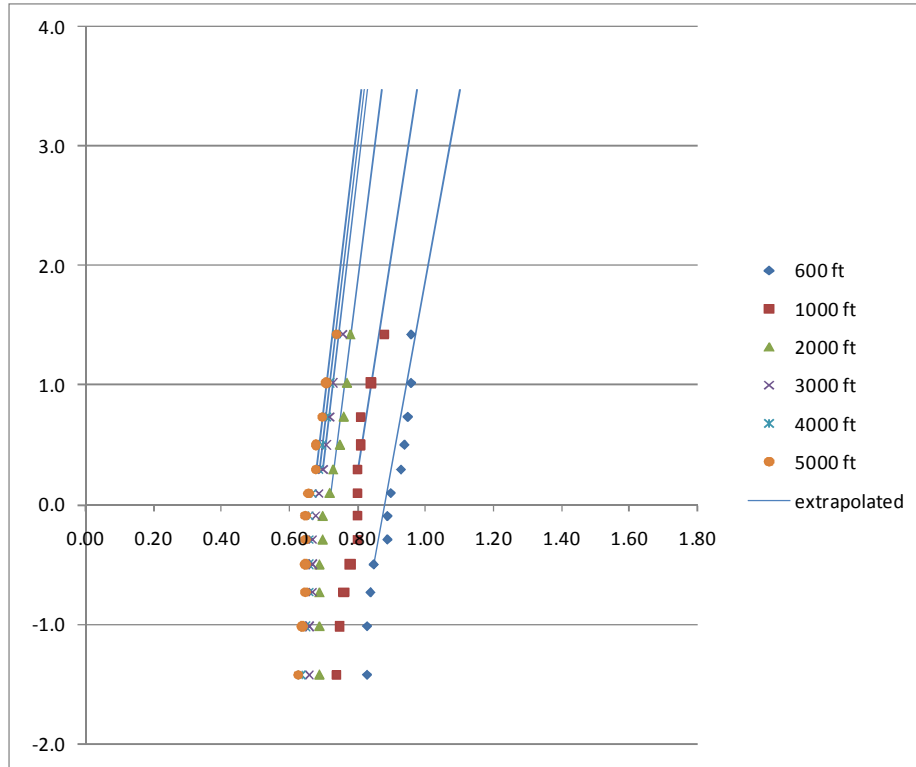Figure B.6. CDF of maximum daily UDL for Florida 9919, lane 1

Figure B.7. CDF of maximum daily UDL for Florida 9927, lane 1

156
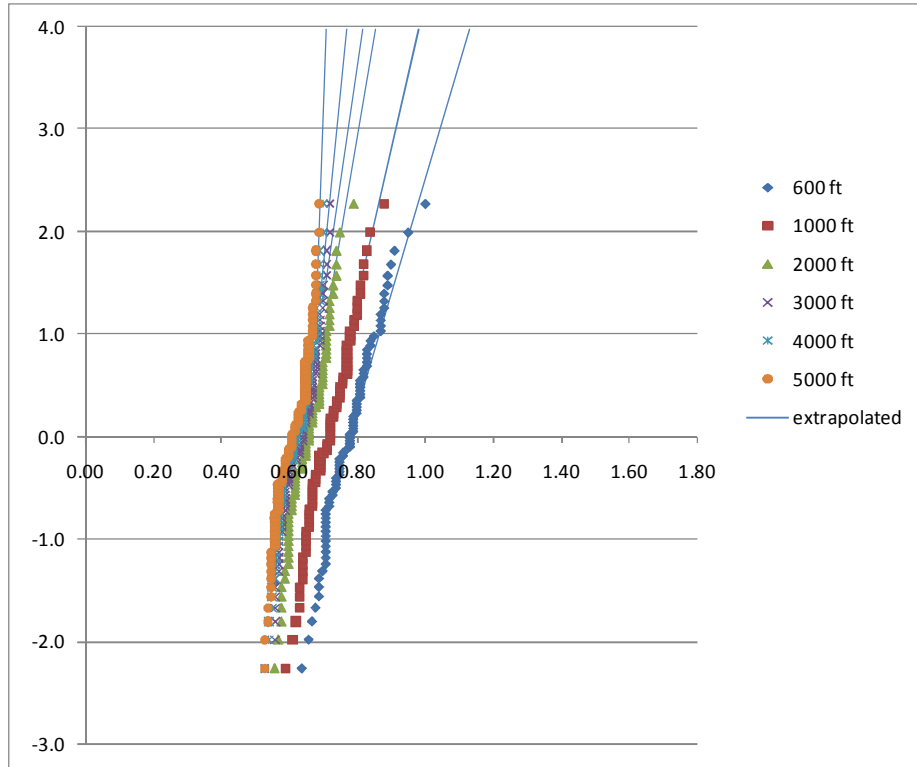
Figure B.8. CDF of maximum daily UDL for Florida 9936, lane 1
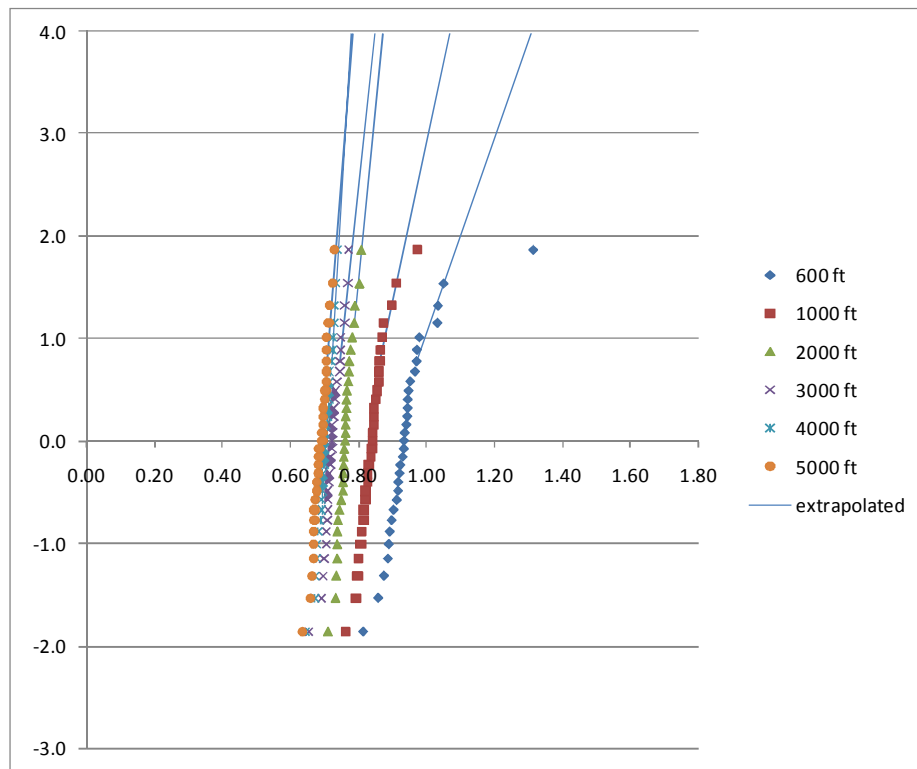
Figure B.9. CDF of maximum daily UDL for Indiana 9534, lane 1

157
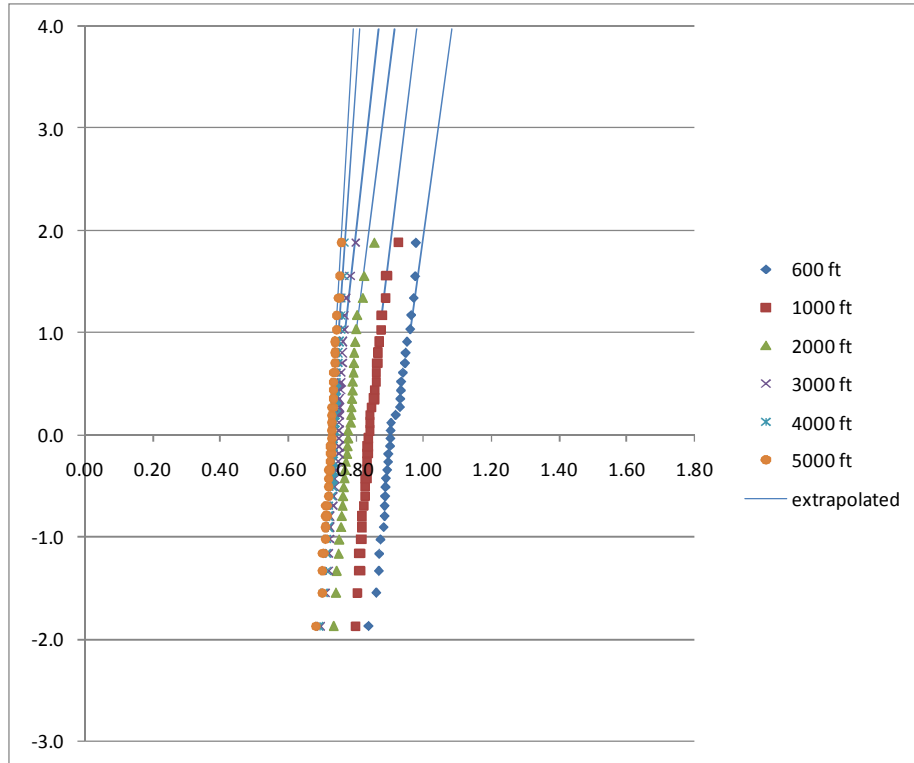
Figure B.10. CDF of maximum daily UDL for Indiana 9544, lane 1
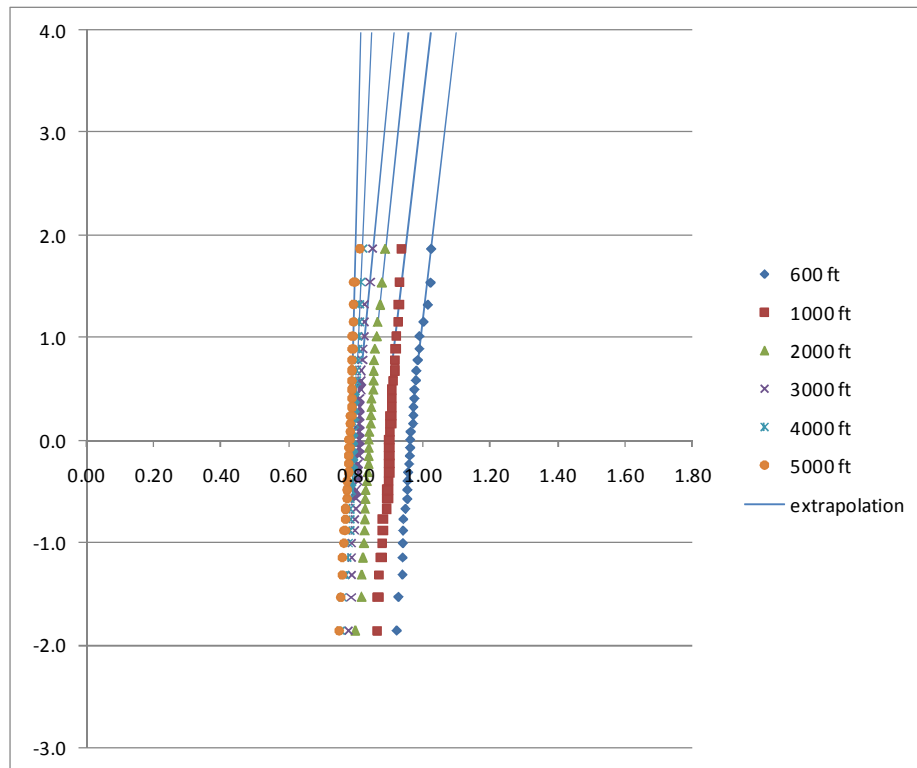
Figure B.11. CDF of maximum daily UDL for Indiana 9512, lane 1

158
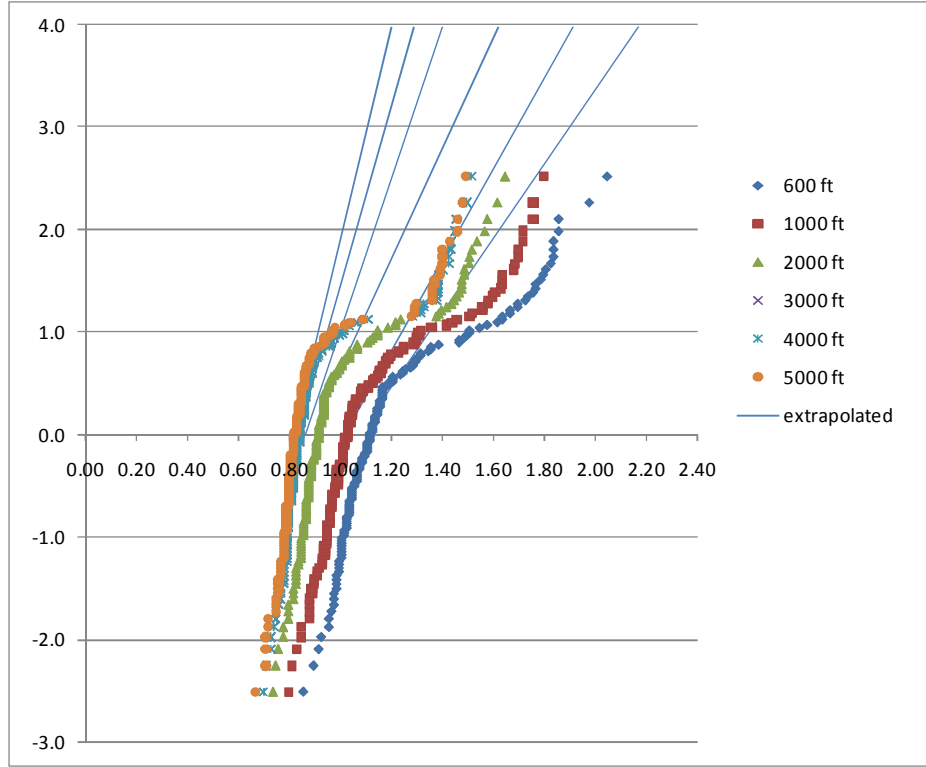
Figure B.12. CDF of maximum daily UDL for New York 9121, lane 1
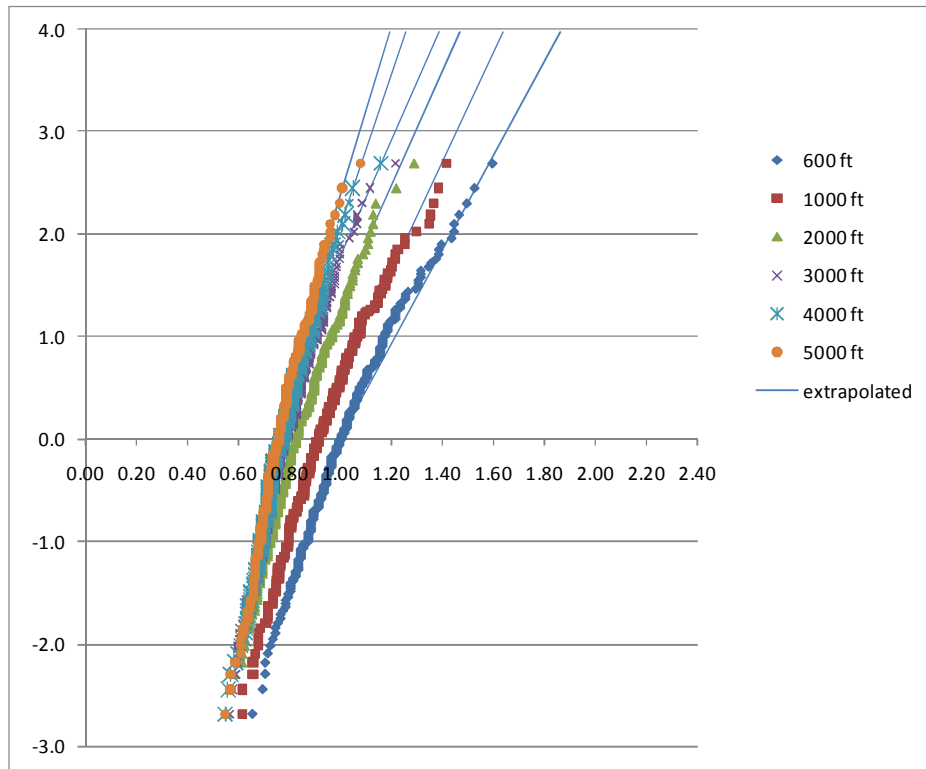
Figure B.13. CDF of maximum daily UDL for New York 2680, lane 1

159
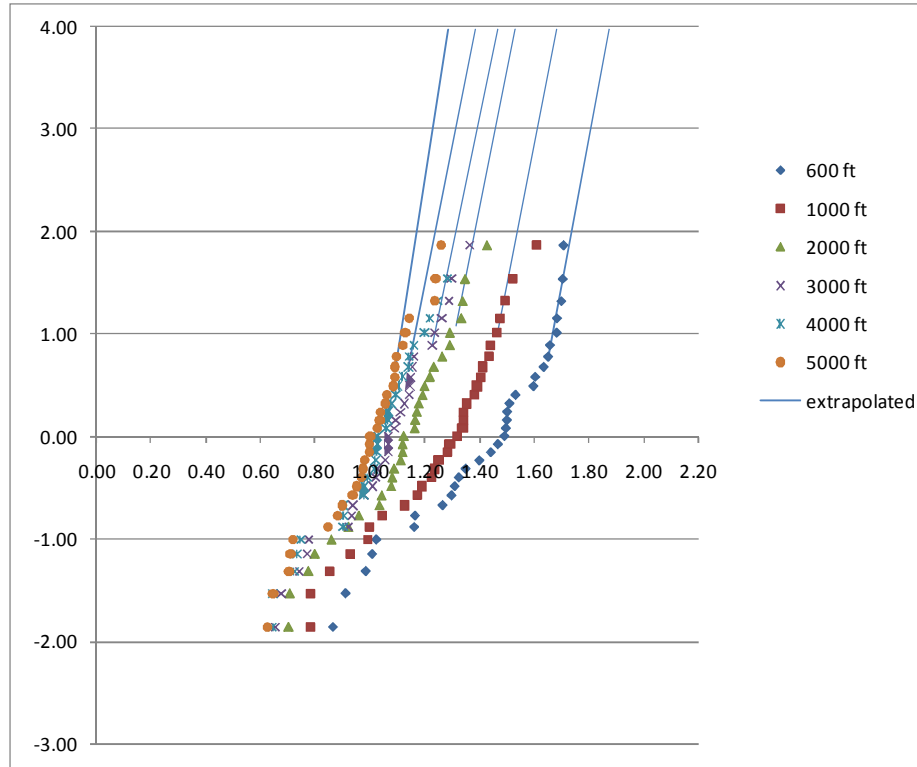
Figure B.14. CDF of maximum daily UDL for New York I-495 EB, lane 1
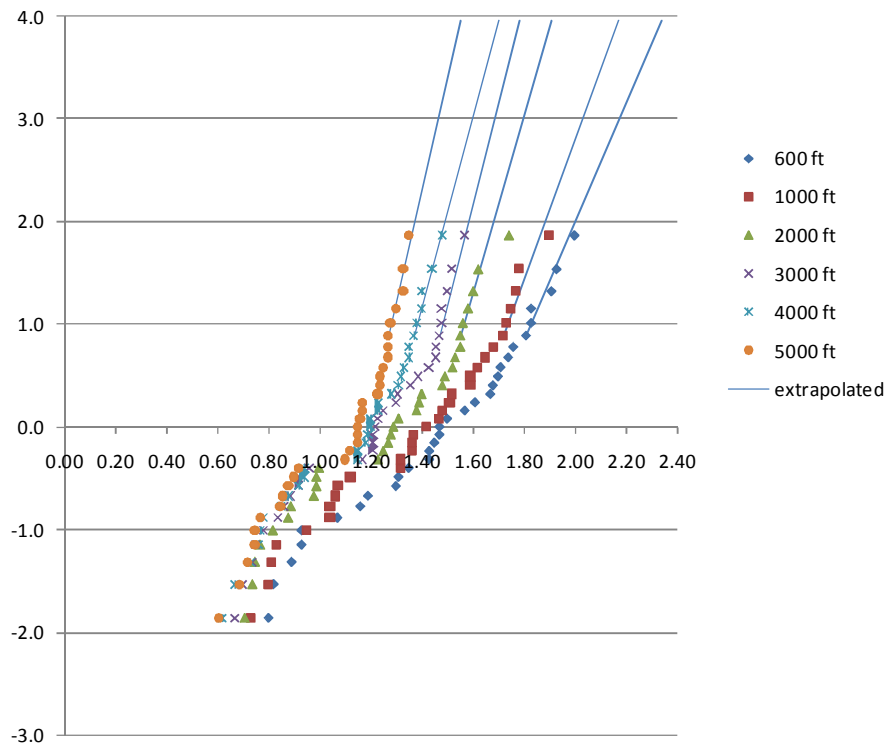
Figure B.15. CDF of maximum daily UDL for New York I-495 WB, lane 1

APPENDIX C

CDF OF MAXIMUM WEEKLY UDL

Figure C.1. CDF of maximum weekly UDL for Oregon I-5 Woodburn, lane 1

Figure C.2. CDF of maximum weekly UDL for Oregon I-84 Emigrant Hill, lane 1

Figure C.3. CDF of maximum weekly UDL for Oregon OR 58 Lowell, lane 1

162

Figure C.4. CDF of maximum weekly UDL for Oregon US 97 Bend, lane 1
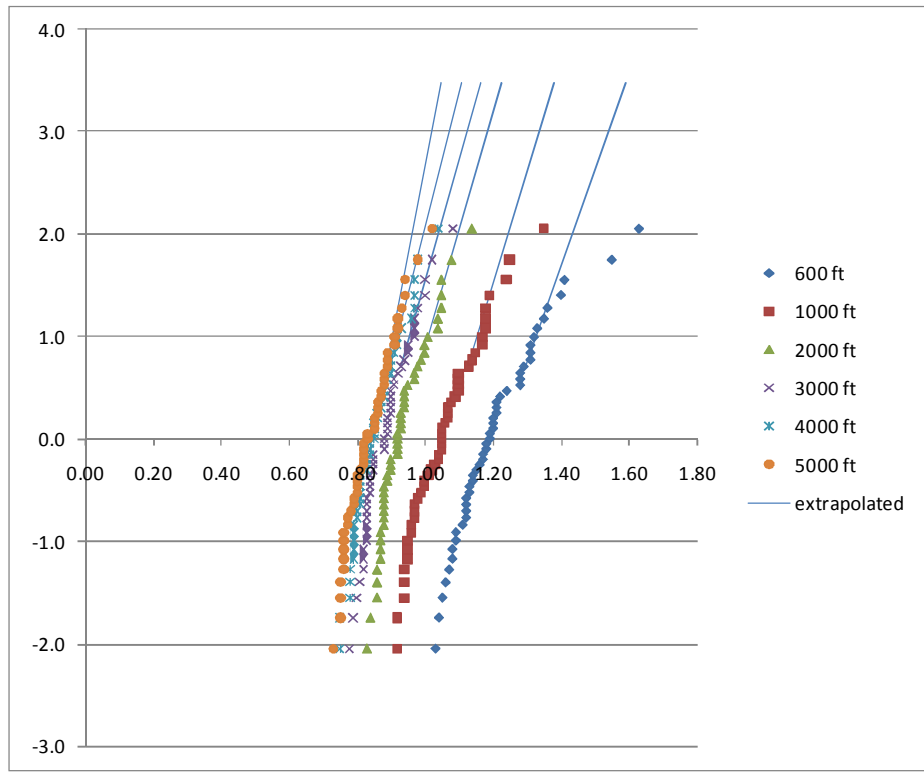
Figure C.5. CDF of maximum weekly UDL for Florida 9916, lane 1

163
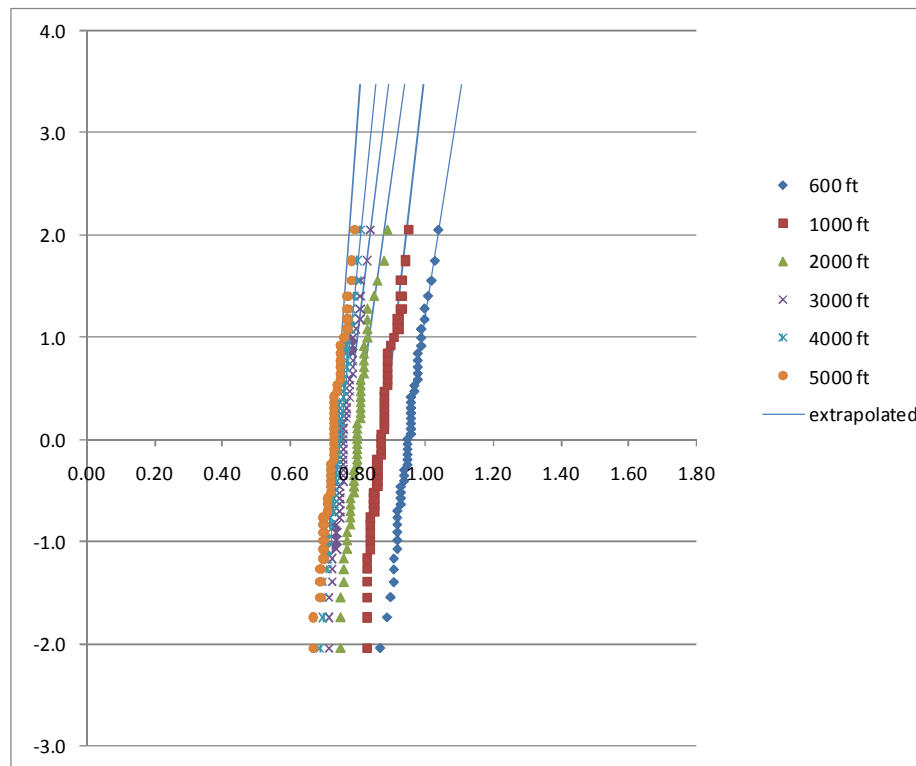
Figure C.6. CDF of maximum weekly UDL for Florida 9919, lane 1

Figure C.7. CDF of maximum weekly UDL for Florida 9927, lane 1
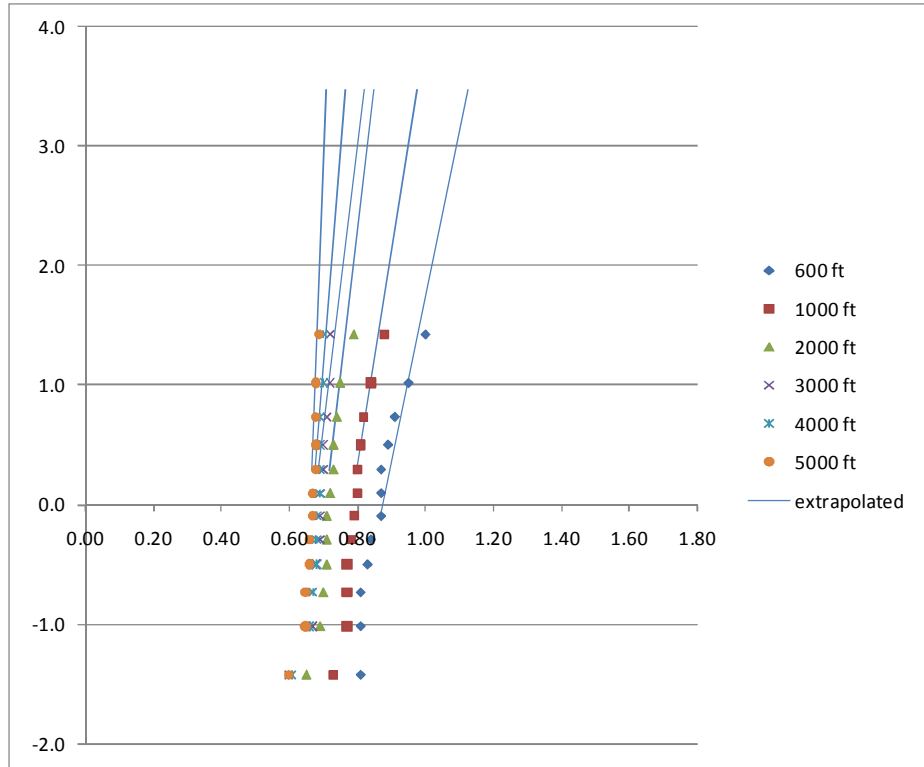
164

www.manaraa.com

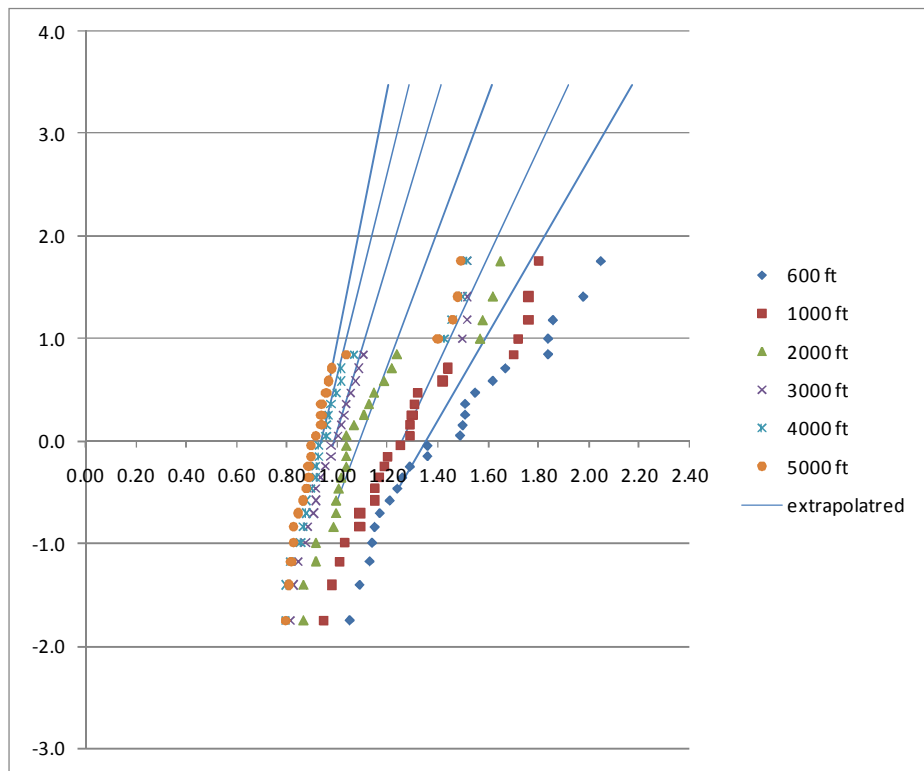Figure C.8. CDF of maximum weekly UDL for Florida 9936, lane 1

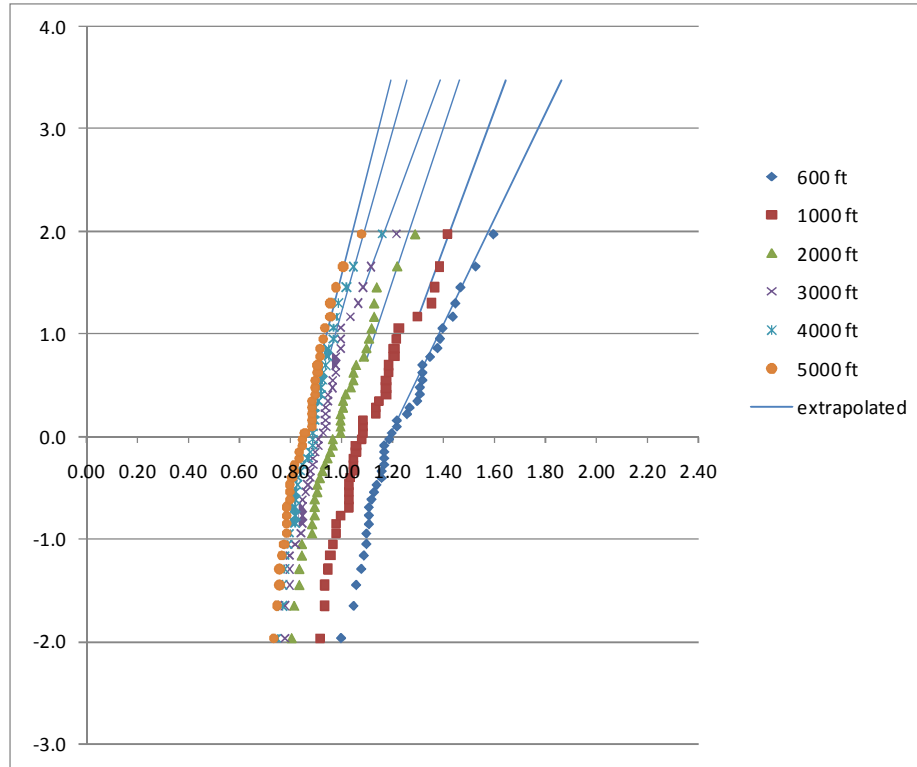Figure C.9.CDF of maximum weekly UDL for New York 9121, lane 1

165

Figure C.10. CDF of maximum weekly UDL for New York 2680, lane 1